NORTHWESTERN UNIVERSITY

Microenvironment Regulation of Proteinase Expression and E-cadherin Ectodomain Generation in Ovarian Cancer

A DISSERTATION

SUBMITTED TO THE GRADUATE SCHOOL
IN PARTIAL FULFILLMENT OF THE REQUIREMENTS

for the degree

DOCTOR OF PHILOSOPHY

Integrated Graduate Program in the Life Sciences (IGP)

By

Jaime Elizabeth Symowicz

EVANSTON, ILLINOIS

June 2007

ABSTRACT

Microenvironment Regulation of Proteinase Expression and E-cadherin Ectodomain Generation in Ovarian Cancer

Jaime Elizabeth Symowicz

Most women diagnosed with epithelial ovarian carcinoma (EOC) initially present with metastases, but little is known about the regulation of ovarian tumor cell dissemination by the tumor microenvironment. Because ovarian cancer cell dissemination is mostly limited to the peritoneal cavity and often results in the accumulation of malignant ascites, the ovarian tumor microenvironment is unique in comparison to other cancers. The ascites maintains constant contact with the primary tumor and peritoneal metastases and contains many factors that foster metastatic spread. Reversible modulation of cell-cell adhesion, cell-matrix adhesion, and proteolytic activity also play a critical role in remodeling of the neoplastic ovarian epithelium, subjecting these processes to microenvironment regulation and implicating collagen-binding integrins and lysophosphatidic acid (LPA) in both E-cadherin and proteinase regulation.

The studies presented in this dissertation now identify and dissect several tumor microenvironment-regulated mechanisms that influence E-cadherin function and proteinase expression to potentially increase the metastatic propensity of ovarian cancer. In contrast to most carcinomas that lose E-cadherin expression with progression, E-cadherin expression is gained during ovarian cancer progression. Mutations in the E-cadherin gene are rare, but other mechanisms likely affect E-cadherin expression and/or function to enhance metastasis. Here, collagen-binding integrin engagement has been shown to regulate two distinct observations

involving E-cadherin function. First, integrin engagement increases E-cadherin internalization and GSK-3β inhibition, resulting in increased β-catenin-mediated transcription and protein expression of known Wnt/β-catenin targets associated with ovarian cancer metastasis (uPA, COX-2, MT1-MMP, MMP-7). Second, integrin engagement enhances MMP-9-dependent E-cadherin cleavage and ectodomain (sE-cad) shedding. sE-cad levels are elevated in EOC patient ascites and incubation of EOC cells with physiologically relevant concentrations of recombinant sE-cad disrupts cell-cell junctions. LPA also promotes the development of a more aggressive phenotype in EOC cells via different mechanisms. MMP-9-dependent E-cadherin ectodomain shedding is increased following LPA treatment and LPA also increases COX-2 expression in EOC cells. COX-2 then functions as a downstream mediator of LPA to increase pro-MMP-2 activation, cell migration, and invasion. Together, these novel results further elucidate mechanisms that may govern ovarian cancer metastasis and identify potential therapy targets for thousands of ovarian cancer patients.

Acknowledgements

Many people helped me get to this stage and I could not have finished this dissertation without them. First, I would like to thank several people who provided valuable reagents and results for the completion of these studies on ovarian cancer metastasis. Dr. Brian Adley prepared and scored the ovarian tumor microarray for this project and provided valuable patient data to compliment the *in vitro* experiments. Dr. Cara Gottardi shared many valuable reagents and provided much needed advice and guidance on the β-catenin project. Dr. Anjen Chenn, his lab members, and the Gottardi lab members let me crash their β-catenin meetings and provided helpful and appreciated feedback on this project. Dr. David Fishman provided the patient ascites samples to make important connections between the patient data and the *in vitro* data. Dr. Rafi Fridman shared the recombinant proMMP-9 and Dr. Nelly Auersperg shared the immortalized borderline ovarian tumor cells lines; both reagents enhanced my investigations. Michelle Woo and Dr. Karen Cowden Dahl allowed me to work on different areas of ovarian cancer research by letting me collaborate with them on their projects.

I would also like to thank and acknowledge the people who helped in the lab on a daily basis. My advisor Dr. Sharon Stack had high expectations, but also made the lab a fun place. I enjoyed working with her over the last five years and feel that her mentoring helped me become a better scientist. The members of Stack Lab, Supurna Ghosh, Yueying Liu, Jeff Johnson, Maria Barbolina, Natalie Moss, Kara Gleason, H.G. Munshi, Edgardo Aritzia, Yi Wu, and Ratna Sen, were also a great group to work with. Their help with experiments and their endless supply of junk food was greatly appreciated, especially the introduction to integrin clustering and bead experiments Supurna provided and the countless hours Kara spent purifying the recombinant

ectodomain. My committee members, Dr. Laurie Hudson, Dr. Jonathan Jones, Dr. Teresa Woodruff, and Dr. Kathy Green, also provided helpful advice and guidance over the last five years. My undergraduate advisor Dr. Linda Schuler and my former boss Dr. Benette Phillips provided an early foundation in cancer research, which better prepared me to take on the rigors of a PhD project.

Finally, I would like to thank my family and friends for their continued support. My Mom and Dad always supported my decision to pursue a PhD and always reassured me that something good would come from the bad luck lab phases. My brother Jay kept me motivated to finish in a more timely manner since we had a friendly competition to see who could be the first doctor in the family and he regularly pointed out his DO degree was taking less time to complete than my PhD. My boyfriend Steve had to listen to a lot of science talk and complaints, but he always supported me and never broke up with me during those times when science was frustrating. Lastly, my friends were always available for lab breaks, support, and commiseration. I greatly appreciated everyone's help in the completion of this dissertation.

List of Frequently Used Abbreviations

2D	Two Dimensional
3D	Three Dimensional
ADAM	A Disintegrin and Metalloproteinase
COX-2	Cyclooxygenase-2
ECM	Extracellular Matrix
EGF	Epidermal Growth Factor
EMT	Epithelial-Mesenchymal Transition
EOC	Epithelial Ovarian Carcinoma
ERK	Extracellular Signal Regulated-Kinase
GSK-3β	Glycogen Synthase Kinase-3β
ICAT	Inhibitor of β-catenin and TCF-4
LPA	Lysophosphatidic Acid
MAPK	Mitogen Activated Protein Kinase
MET	Mesenchymal-Epithelial Transition
MMP	Matrix Metalloproteinase
MT-MMP	Membrane-type Metalloproteinase
OSE	Ovarian Surface Epithelium
PBS	Phospho Buffered Saline
PI3K	Phosphatidylinositol Kinase-3
PKC	Protein Kinase C
sE-cad	Soluble E-cadherin

TIMP	Tissue Inhibitor of Matrix-Metalloproteinases
uPA	Urinary-type Plasminogen Activator
VEGF	Vascular Endothelial Growth Factor

Table of Contents

Figures and Tables

Figure

Chapter 1: Introduction and Background

I) Ovarian Cancer

A) Development of Epithelial Ovarian Cancer

According to the American Cancer Society, approximately 16,000 women die from ovarian cancer and 22,000 women are newly diagnosed each year in the United States. Seventy-five percent of these 22,000 women are diagnosed with existing metastases, classifying ovarian cancer as the most lethal form of gynecologic disease. Late diagnosis is common because the subtle symptoms associated with ovarian cancer are often dismissed or misdiagnosed and the anatomical location of the ovaries makes stage I detection difficult (Fishman and Borzorgi 2002). Risk factors for ovarian cancer include increasing age, nulliparity, use of fertility drugs, and a family history of breast and/or ovarian cancer (Lacey and others 2002). Most hereditary forms of ovarian cancer are associated with germline mutations in the BRCA1 and BRCA2 genes. Multiple pregnancies and the use of oral contraceptives are both associated with decreased risk, providing support for two theories currently proposed to explain why ovarian cancer develops. The Incessant Ovulation Theory hypothesizes that mutations accumulate in ovarian surface epithelium (OSE) as a result of the repetitive wounding and cell proliferation needed for postovulatory repair (Ozols and others 2004). Increased ovulation is associated with the formation of inclusion cysts and changes in the ovarian surface (Feeley and Wells 2001). The Gonadotropin Theory claims that ovarian cancer is caused by cellular transformation induced in the OSE cells after a lifetime exposure to pituitary gonadotropins as the pituitary gonadotropins

surge to initiate each ovulation and remain at high levels following menopause (Ozols and others 2004).

Ninety percent of diagnosed ovarian tumors are classified as epithelial ovarian carcinomas (EOC), which are derived from the OSE or cortical inclusion cysts (Feeley and Wells 2001; Wong and Auersperg 2002). The OSE is part of the pelvic mesothelium and is a thin mesothelial monolayer with a mixed epithelio-mesenchymal phenotype that covers the ovarian surface (Auersperg and others 2002; Wong and Auersperg 2002). In adult women, the OSE has a monolayered flat or cuboidal epithelium characterized by apical microvilli, a basal lamina, and keratin types 7, 8, 18, and 19. Cell-cell adhesion is maintained by desmosomes, incomplete tight junctions, and N-cadherin. The OSE is separated from the ovarian stroma by a basement membrane that overlies the tunica albuginea, a collagenous connective tissue layer. Normally, the OSE is involved in cyclical ovulatory rupture and repair, which is likely coordinated with the reproductive cycle and thus hormone dependent. The OSE also secretes and expresses receptors for hormones, growth factors, and cytokines. The extracellular matrix (ECM) influences the OSE, but the OSE also affects ECM synthesis, lysis, and restructuring. With increasing age, the ovary acquires irregular contours to form OSE-lined surface invaginations or clefts and epithelial inclusion cysts in the ovarian cortex. The OSE in the inclusion cysts is more likely to undergo metaplastic changes and to commit to an epithelial phenotype, which includes the acquisition of a columnar cell shape and expression of E-cadherin and CA125 [Reviewed in (Wong and Auersperg 2002)].

The tumors derived from the OSE display variable properties and are similar to fallopian tube epithelium, endometrium endocervix epithelium, colonic epithelium, and urogenital tract

epithelium (Auersperg and others 2002). EOCs are categorized into the four following histotypes: mucinous, endometrioid, clear cell, and serous (DeFrias and others 2002). Seventy-five percent of mucinous tumors are benign (Katsube and others 1982; Koonings and others 1989) and the neoplastic cells resemble endocervical, gastric, or intestinal epithelium (DeFrias and others 2002). Endometrioid tumors are rare, accounting for only 2-4% of all ovarian tumors. These tumors contain both epithelial elements and stroma similar to the normal endometrium (DeFrias and others 2002). Recently, it has been reported in a mouse genetic model that endometriosis is directly linked to the development of endometrioid tumors (Dinulescu and others 2005). Clear cell tumors display variable cell patterns, but are mostly identified by abundant amounts of transparent cytoplasm. Only 6% of all ovarian tumors are classified as clear cell tumors (DeFrias and others 2002; Scully and others 1998). Serous tumors are derived directly from OSE cells or inclusion cysts (Shih and Kurman 2004) and their epithelium display flat, ciliated, cuboidal or columnar structures similar to the peritoneum surrounding the ovary and fallopian tubes (DeFrias and others 2002). Serous carcinomas are the most common ovarian carcinoma and account for about half of all ovarian neoplasms (Shih and Kurman 2004).

B) Ovarian Cancer Metastasis and Tumor Microenvironment

Only 30% of the women diagnosed with advanced stage ovarian cancer survive five years beyond initial diagnosis (Jemal and others 2004). Ovarian cancer metastasis is initiated when cells exfoliate from the primary tumor as single cells or multi-cellular aggregates [**Fig 1.1**]. Unlike other solid tumors, ovarian cancer rarely spreads via the vasculature, although lymphatic spread is possible (Naora and Montell 2005). Instead, cell dissemination is initially limited to

the peritoneal cavity and is mediated by deregulated cell adhesion and intraperitoneal invasion and migration. The cells float in the peritoneal fluid, attach, invade, and grow at new sites, resulting in the "seeding" of the peritoneal cavity (Ghosh and others 2002; Naora and Montell 2005). Metastases of ovarian cancer are often observed in the uterus, fallopian tubes, liver, omentum, and bowels (Schwartz 2002). The disseminated cells further contribute to tumor metastasis by blocking the peritoneal lymphatics, resulting in the accumulation of malignant ascites in the peritoneal cavity to facilitate cell spreading (Ghosh and others 2002; Kohn 1997). Peritoneal microvessel hyperpermeability and angiogenesis also contribute to ascites formation (Kohn 1997) as the production of vascular endothelial growth factor (VEGF) by tumors cells is associated with increased ascites accumulation in ovarian cancer mouse models (Akutagawa and others 2002; Belotti and others 2003). The ascites provides a favorable environment for ovarian cancer progression as it is rich in growth factors, bioactive lipids, ECM components, inflammatory mediators, and proteolytic enzymes (Freedman and others 2004; Mutsaers 2002; Offner and others 1995). As a result, the presence of ascites is very common in stage III and IV ovarian cancer patients and is associated with a significantly reduced five year survival rate (5% versus 45% without ascites) (Puls and others 1996), necessitating an understanding of this unique tumor microenvironment and how it fosters further cell dissemination and metastatic spread.

C) Current Ovarian Cancer Models

Although monolayer tissue culture models are often used for *in vitro* ovarian cancer investigations, these two dimensional (2D) studies are eventually followed up in alternative models that provide a more accurate physiological model of ovarian cancer metastasis. Three

dimensional (3D) tissue culture models have recently been utilized to identify the mechanisms that regulate disaggregation, adhesion, and invasion of ovarian cancer spheroids in the peritoneal cavity (Burleson and others 2006; Burleson and others 2004; Lessan and others 1999). Animal models are also used to study ovarian cancer, but many differences exist between animal OSE and human OSE in the expression of adhesion molecules, the cellular origin of tumors, the response to hormonal stimulation, and the growth regulatory signaling pathways. Currently bovine OSE appears to be the best animal model for human OSE comparison (Auersperg and others 2002). Because rodent OSE cells are more conducive to cellular transformation, a mouse model has recently been generated where human OSE cells containing mutant versions of p53, Retinoblastoma tumor suppressor (RB), human telomerase reverse transcriptase (hTERT), and KRAS were injected into the peritoneal cavity of mice. These four genes are frequently disrupted or mutated in human ovarian tumors, so it is not surprising that these mice develop ascites and undifferentiated carcinomas or malignant mixed Mullerian tumors following injection of transformed human OSE cells (Liu and others 2004). Recently, border cell migration during oogenesis in the ovary of *Drosophila melanogaster* has proven to be a useful model for genetic analysis of processes involved in ovarian cancer metastasis because border cell migration shares some similarities with cancer cell migration (Montell 2003; Naora and Montell 2005; Yoshida and others 2004).

Figure 1.1

Ovarian Cancer Metastasis

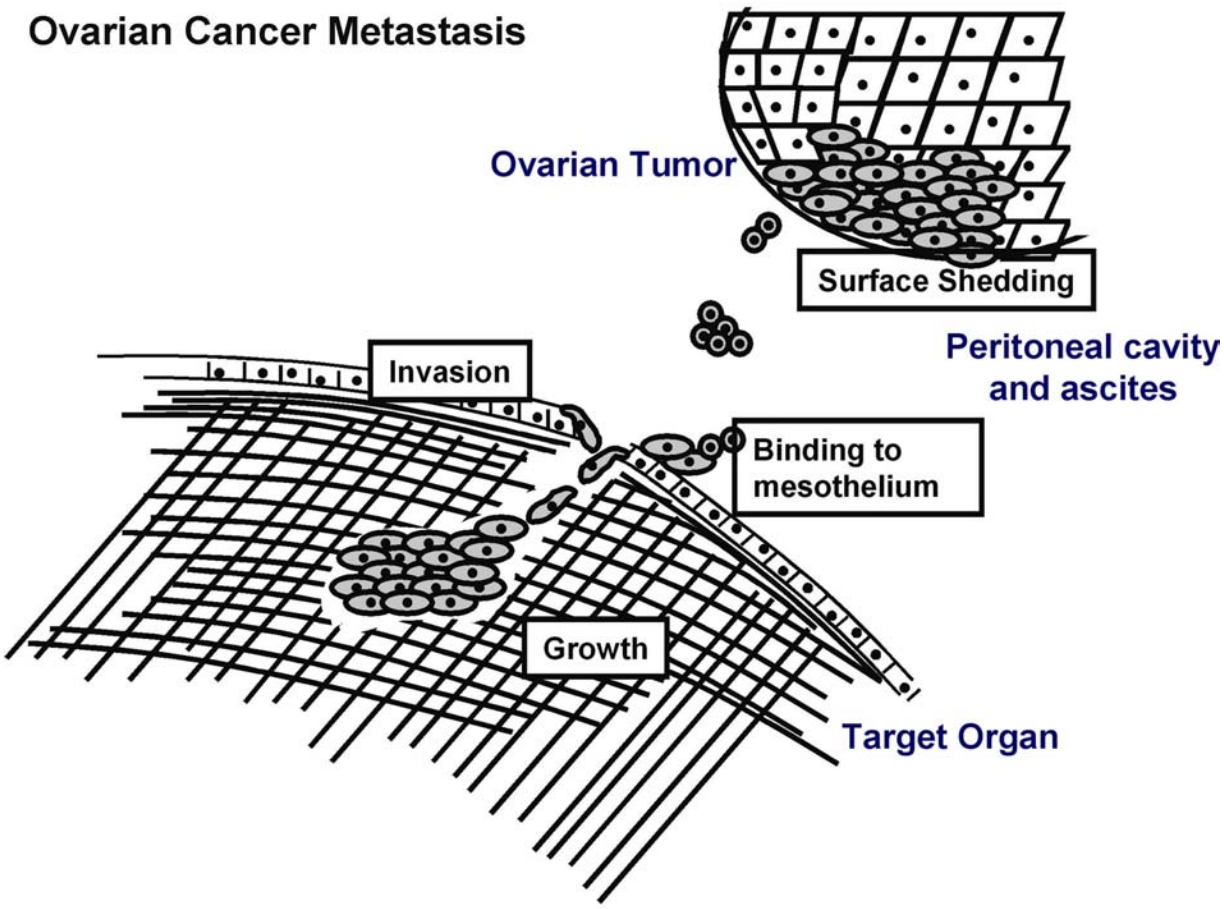

Figure 1.1: Ovarian cancer metastasis

Ovarian tumor cells exfoliate from the primary tumor as single cells and multi-cellular aggregates. Ovarian cancer rarely spreads via the vasculature, limiting cell dissemination to the peritoneal cavity. The cells float in the peritoneal fluid, attach and invade at new sites, resulting in the "seeding" of the peritoneal cavity. Metastases are often reported in the uterus, fallopian tubes, liver, omentum, and bowels. The disseminated cells also block the peritoneal lymphatics, resulting in the accumulation of malignant ascites in the peritoneal cavity. This figure was adapted and used with permission from M. Sharon Stack.

II) E-cadherin

A) Role of E-cadherin in Cell-Cell Adhesion and Cancer Progression

The superfamily of classical cadherins includes epithelial (E)-cadherin and neuronal (N)-cadherin. Classical cadherins are single-span transmembrane-domain glycoproteins that mediate calcium-dependent cell-cell adhesion via homophilic and heterophilic bonds with the extracellular regions of other cadherins on the surface of neighboring cells (Foty 2005; Gumbiner 2000). Classical cadherins associate with intracellular proteins, catenins, to form the cytoplasmic cell-adhesion complex (CCC). β and γ-catenin bind to the C-terminus of classical cadherins while p120-catenin interacts with sites in the cytoplasmic tail. It has originally been proposed that β and γ-catenin then bind to α-catenin and connect the CCC to the actin cytoskeleton [Reviewed in (Cavallaro and Christofori 2004)] [**Fig 1.2**], but this hypothesis is currently under revision after Yamada and colleagues showed that α-catenin does not simultaneously bind to actin filaments and the E-cadherin-β-catenin complex (Yamada and others 2005). They then suggest that this interaction between actin filaments and cadherin-catenin complexes is less static than originally speculated (Yamada and others 2005).

The main functions of E-cadherin include the regulation of cell polarity and the maintenance of epithelial organization (Cavallaro and Christofori 2004). High levels of E-cadherin are observed in normal epithelial cells, but a loss in E-cadherin expression or function often occurs as epithelial cell derived cancers develop and progress and cells adopt a more undifferentiated and invasive phenotype (Okegawa and others 2002; Okegawa and others 2004). It has been suggested that loss of E-cadherin mediated cell-cell adhesion is mandatory for cancer cell invasion and metastasis (Birchmeier and Behrens 1994). Genetic and epigenetic

mechanisms are often responsible for the downregulation of E-cadherin function or expression in tumors. For examples, gene mutations regularly occur in tumors, giving rise to mutant, non-functional versions of E-cadherin. E-cadherin transcription is also reduced by transcription factors Snail, Slug, and SIP1 or by hypermethylation of the gene promoter. Nongenetic mechanisms may also inhibit E-cadherin expression and/or function. For example, matrix metalloproteinase (MMP)-dependent proteolytic degradation of E-cadherin may disrupt cell-cell adhesion or receptor tyrosine kinase- mediated phosphorylation of E-cadherin may promote E-cadherin degradation. When E-cadherin function is lost, *de novo* expression of N-cadherin often occurs and promotes cell motility and migration in cancer cells [Reviewed in (Cavallaro and Christofori 2004)].

Figure 1.2

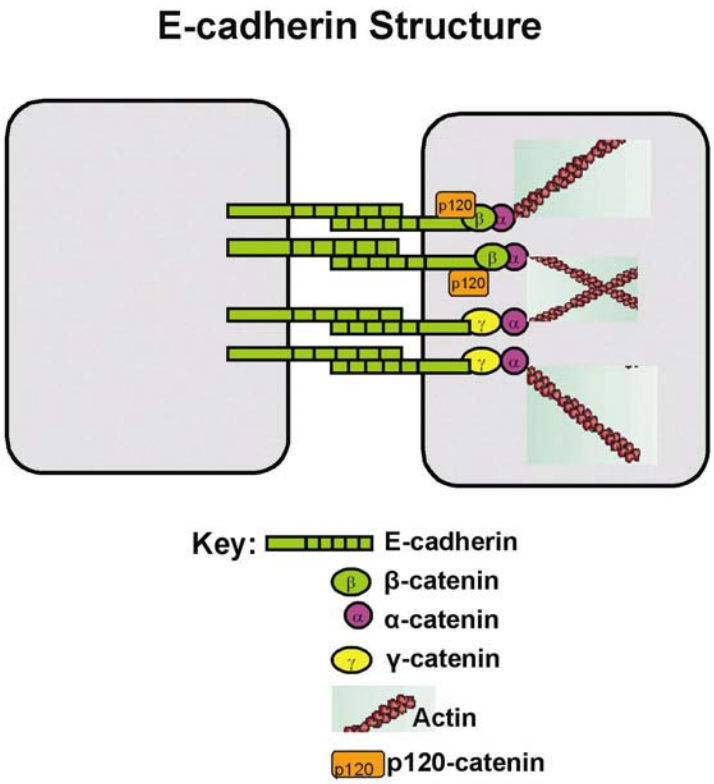
E-cadherin Structure
p120
β
α
β
α
p120
γ
α
γ
α
Key:
E-cadherin
β-catenin
α-catenin
γ-catenin
Actin
p120
p120-catenin

Figure 1.2: E-cadherin structure

Epithelial (E)-cadherin is a member of the superfamily of classical cadherins and mediates calcium-dependent cell-cell adhesion via homophilic and heterophilic protein interactions with cadherins on the surface of neighboring cells. Classical cadherins associate with intracellular proteins, catenins, to form the cytoplasmic cell-adhesion complex (CCC). β- and γ-catenin bind to the C-terminus of classical cadherins while p120-catenin interacts with sites in the cytoplasmic tail. β- and γ-catenin then bind to α-catenin and connect the CCC to the actin cytoskeleton. This figure was adapted from (Cavallaro and Christofori 2004).

B) Role of E-cadherin in Ovarian Cancer Progression

Although most epithelia express abundant E-cadherin, this cadherin is absent in the mesenchymally-derived normal OSE, which instead express N-cadherin. Aberrant epithelial differentiation is an early event in epithelial ovarian carcinogenesis as tumors acquire increasingly complex differentiation similar to the highly specialized epithelia of Mullerian duct origin and undergo an initial mesenchymal epithelial transition (MET) [**Fig 1.3**] (Auersperg and others 1999). In contrast to most carcinomas that lose E-cadherin expression with progression, E-cadherin is abundant in primary differentiated EOCs (Faleiro-Rodrigues and others 2004; Imai and others 2004; Karbova and others 2002; Maines-Bandiera and Auersperg 1997; Marques and others 2004; Patel and others 2003; Sundfeldt and others 1997; Wong and others 1999). E-cadherin expression is observed in peritoneal cell effusions and metastases, but conflicting reports on their E-cadherin expression levels relative to the primary tumor exist. For example, Fujioka and colleagues report that 6 of 10 peritoneal metastases show reduced E-cadherin expression compared to primary tumors in one study (Fujioka and others 2001). In agreement with these findings, a reduction in E-cadherin mRNA expression is observed in metastatic lesions in comparison to primary tumors in a separate study (Fujimoto and others 1997). In contrast, Imai and colleagues note E-cadherin expression is increased in peritoneal lesions when compared to the primary tumors (Imai and others 2004). Similar observations are reported by Davidson and colleagues in effusions although E-cadherin expression is increased in effusions relative to the peritoneal metastases (Davidson and others 2000). Naora and Montell have also suggested based on studies of border cell migration in the *Drosophila melanogaster* ovary that it may be advantageous for ovarian tumor cells to maintain E-cadherin expression. Interestingly,

both border cells and ovarian cancer cells express higher levels of E-cadherin than the epithelia that give rise to them. Border cells require high levels of E-cadherin expression as they depend on E-cadherin-mediated cell-cell adhesion to migrate as a cell cluster on the surface of the nurse cells down the egg chamber towards the oocyte. Decreased E-cadherin surface activity is likely required to facilitate border cell migration; this type of movement parallels integrin-mediated migration on the ECM and ovarian cancer cells may utilize a similar mechanism to maintain attachment of multi-cellular aggregates in the ascites and to adhere to other cells in the peritoneal cavity (Naora and Montell 2005). Regardless of relative E-cadherin expression in metastases, effusions, and primary tumors, E-cadherin deregulation likely plays an unknown role in ovarian cancer cell dissemination.

Mutations in the E-cadherin gene are very rare in ovarian carcinomas (Wong and Auersperg 2002), but other mechanisms may potentially downregulate E-cadherin expression and/or function transiently or permanently, including E-cadherin cleavage and shedding (Covington and others 2006; Dwivedi and others 2006; Lochter and others 1997), epigenetic silencing (Makarla and others 2005; Rathi and others 2002), and defective E-cadherin recycling and trafficking (Bryant and Stow 2004). Decreased E-cadherin expression may result from either epigenetic silencing or increased degradation following endocytosis. Defective trafficking and recycling of E-cadherin upon internalization may encourage increased cytoplasmic localization of E-cadherin. Observations in ovarian tumors support the possibility that modifications in E-cadherin expression or function enhance metastasis. Imai and colleagues show that E-cadherin expression is decreased with advancing tumor stage since E-cadherin expression is reduced in stage III and IV tumors compared to stage I and II tumors (Imai and

others 2004). Marques and colleagues imply that membrane E-cadherin expression is an indicator of a good prognosis as cytoplasmic or absent E-cadherin expression is often associated with increased metastasis and a poor patient outcome (Marques and others 2004). In addition, post-translational modification of E-cadherin function is suggested by data demonstrating the presence of soluble E-cadherin (sE-cad) in ascites and cystic fluids from ovarian cancer patients (Darai and others 1998a; Sundfeldt and others 2001). The next two sections will now describe posttranslational modification of E-cadherin in more detail.

Figure 1.3

Cadherin Expression in Normal and Malignant Ovarian Epithelium

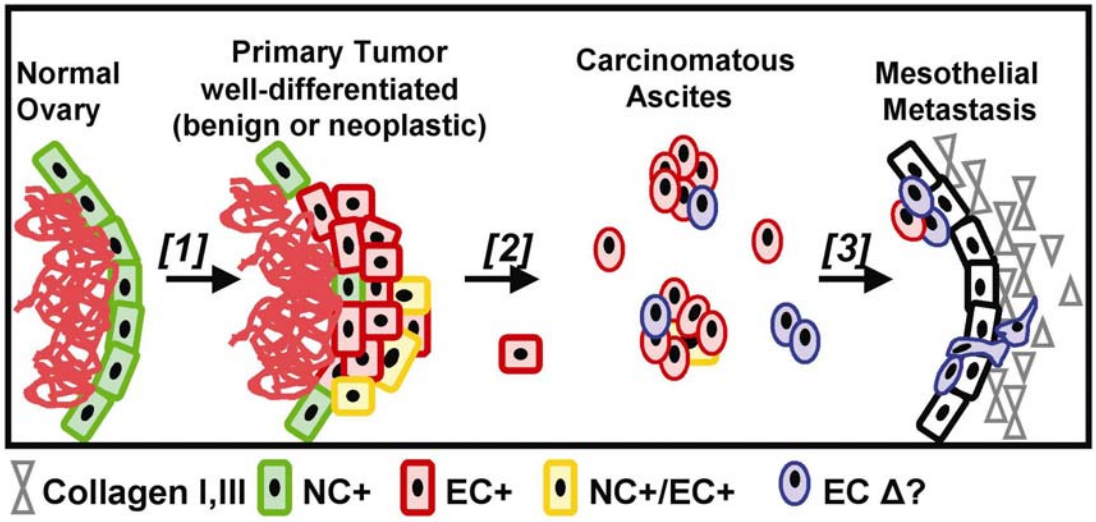

NC=N-cadherin
EC=E-cadherin

Figure 1.3: Cadherin expression in normal and malignant ovarian epithelium

Unlike other normal epithelial cells that express high levels of E-cadherin, this cadherin is absent in the mesenchymally-derived normal OSE, which are connected by N-cadherin. In contrast to other epithelial cell derived cancers that lose E-cadherin with progression, a gain of E-cadherin expression is observed in neoplastic ovarian cells and ovarian tumors. E-cadherin expression is often maintained in peritoneal cell effusions and metastases. This figure was altered and used with permission from M. Sharon Stack.

C) E-cadherin Internalization, Recycling, and Degradation

E-cadherin endocytosis is necessary to regulate E-cadherin availability for junction formation in development, tissue remodeling, and tumorigenesis. Specifically, it has been shown in MDCK cells that surface E-cadherin expression is not limited to cell-cell junction incorporation. Instead a small pool of E-cadherin is always present, but the pool size is increased in preconfluent cells (Le and others 1999). E-cadherin regularly cycles back and forth between adherens junctions and intracellular vesicles and compartments, but the frequency of E-cadherin endocytosis is dependent on cell confluence. In preconfluent cells or non-adherent cells, E-cadherin production is increased and it is trafficked back and forth from the membrane via unregulated pathways before the establishment of cell-cell adhesion. In mature, polarized epithelial cells, most surface E-cadherin is incorporated into adherens junctions and E-cadherin synthesis is decreased, but a small pool is available to continuously cycle to and from the surface. During tumorigenesis or epithelial-to-mesenchymal transitions (EMT), E-cadherin endocytosis may permit its downregulation or degradation in conjunction with a lack of synthesis and replenishment [Reviewed in (Bryant and Stow 2004)].

Several mediators of E-cadherin endocytosis have been previously identified. ARF6 has been reported to regulate E-cadherin endocytosis in two studies (Palacios and others 2002) (Paterson and others 2003). Hakai, an E3 ubiquitin-ligase, also promotes E-cadherin endocytosis. It is speculated that activation of tyrosine kinases, specifically Src, permits interaction between E-cadherin and Hakai. Hakai then ubiquitinates E-cadherin to facilitate endocytosis (Fujita and others 2002). In a cell free assay system, non-trans-interacting E-

cadherin is constitutively endocytosed via a clathrin- dependent pathway, but Rac and Cdc42 are activated by trans-interacting E-cadherin to inhibit E-cadherin endocytosis via IQGAP1 and F-actin (Izumi and others 2004). Clathrin-independent pathways have also been characterized, but the pathway used to internalize E-cadherin is generally dependent on cell type and conditions (Paterson and others 2003). Phorbol esters increase the rate of E-cadherin endocytosis in MDCK cells, but this effect is dependent on protein kinase C (PKC) activity, which may induce changes in the actin cytoskeleton to allow E-cadherin endocytosis (Le and others 2002). Overexpression of a disintegrin and metalloproteinase-9 (ADAM9) is also associated with increased growth factor-mediated recycling of E-cadherin (Hirao and others 2006). Under certain conditions, E-cadherin is also degraded following internalization. v-Src, hepatocyte growth factor-regulated tyrosine kinase substrate (Hrs), and v-Src-induced activation of Rab5 and Rab7 GTPase all promote lysomal degradation of E-cadherin (Palacios and others 2002). Recently, Maeda and colleagues, have reported that expression of an inappropriate cadherin, R-cadherin, in A431 cells leads to increased endocytosis and degradation of endogenous E-cadherin. Degradation of E-cadherin occurs due to competition with R-cadherin for p120ctn binding (Maeda and others 2006). E-cadherin internalization regulates other processes in addition to the breaking and reforming of cell-cell junctions. E-cadherin internalization and trafficking promote the activation of Rap1 and the formation of integrin-based focal adhesions (Balzac and others 2005). E-cadherin endocytosis is also necessary to promote fibroblast growth factor (FGF)-induced internalization and nuclear translocation of the FGF receptor 1 (FGFR1) (Bryant and others 2005). To date, E-cadherin internalization, degradation, and recycling have not been extensively investigated in ovarian cancer. It is interesting to speculate that E-cadherin dynamics play an

important role in the exfoliation of primary ovarian tumors cells, the maintenance of ascitic multi-cellular aggregates, and the adherence to peritonteal mesothelial cells.

D) E-cadherin Cleavage and Ectodomain Shedding

Several proteinases have been previously reported to cleave E-cadherin, releasing its extracellular region or ectodomain. It first has been shown by Damsky and colleagues that proteolytic cleavage of E-cadherin's extracellular domain results in the release of an 80kDa ectodomain fragment (Damsky and others 1983). These proteinases have later been identified as matrix metalloproteinases (MMP) MMP-3 and MMP-7 (Lochter and others 1997; Noe and others 2001). Recently, a disintegrin and metalloproteinase-10 (ADAM10), plasmin, and membrane type I matrix metalloproteinase (MT1-MMP) have also been shown to cleave E-cadherin (Covington and others 2006; Hayashido and others 2005; Maretzky and others 2005). The 80kDa ectodomain is associated with disrupted cell adhesion, increased cell migration, invasion, and proliferation, increased β-catenin-mediated transcription, and elevated MMP-2, MMP-9, and MT1-MMP expression *in vitro* in different cell types (Chunthapong and others 2004; Liu and others 2006; Maretzky and others 2005; Nawrocki-Raby and others 2003; Noe and others 1999; Ryniers and others 2002; Wheelock and others 1987). The effects of the E-cadherin cytoplasmic fragment have not been investigated in these studies since Ito and colleagues have proposed that the E-cadherin cytoplasmic domain is likely rapidly degraded in cells following cleavage of the extracellular region by an MMP (Ito and others 1999), but Steinhausen and colleagues report that caspase-3 cleaves E-cadherin to release 24kDa and 29kDa cytoplasmic regions during apoptosis (Steinhusen and others 2001). In addition, a 100kDa E-cadherin

ectodomain is generated by calpain cleavage following calcium influx or by presenilin-1/secretase-γ cleavage following the induction of apoptosis by staurosporine (Marambaud and others 2002; Rios-Doria and others 2003). When E-cad^{100} is overexpressed in prostate cancer cells, it downregulates endogenous E-cadherin and potentiates PKC-induced cell death (Rios-Doria and Day 2005), but it is unknown which E-cadherin domains other than the extracellular domain constitute this 100kDa fragment. To date, a majority of studies have only focused on the generation and role of the 80kDa ectodomain in disease. Currently, calcium influx, transforming growth factor β (TGF-β), and ischemia are the only known inducers of 80kDa E-cadherin ectodomain shedding (Covington and others 2005; Covington and others 2006; Dwivedi and others 2006; Ito and others 1999). Other potential upstream regulators of the proteinases that cleave E-cadherin to promote ectodomain shedding have not been explored in any cell types.

It is unknown how the shed E-cadherin ectodomain or soluble E-cadherin enhances cancer metastasis. When compared to non-cancer patients, soluble E-cadherin levels are often elevated in the bodily fluids of cancer patients, including serum, urine, and ascites (Billion and others 2006; Chan and others 2005; Darai and others 1998a; Darai and others 1998b; Gadducci and others 1999; Shariat and others 2005; Sundfeldt and others 2001; Syrigos and others 2004). High serum levels of soluble E-cadherin are associated with a poor outcome and the development of metastases in non small cell lung cancer patients (Charalabopoulos and others 2006), a recurrence of gastric cancer (Chan and others 2005), and a poor prognosis in multiple myeloma patients (Syrigos and others 2004). An association between soluble E-cadherin (80kDa) and prostate cancer metastases is observed in both patient tumor and serum samples (Kuefer and others 2003). Soluble E-cadherin levels are elevated in the cystic fluid from

borderline and malignant ovarian tumors when compared to benign cysts and cystadenomas, suggesting this distinction may have diagnostic value preoperatively (Sundfeldt and others 2001). Despite these findings, the mechanism used by the shed ectodomain to enhance metastasis in cancer patients is mostly unknown. *In vitro*, the E-cadherin ectodomain is linked to increased migration, invasion, proliferation, MMP activity, β-catenin-mediated transcription, and disrupted adhesion, but these linkages have not been investigated in more detail in *in vivo* models (Chunthapong and others 2004; Liu and others 2006; Maretzky and others 2005; Nawrocki-Raby and others 2003; Noe and others 2001; Noe and others 1999; Ryniers and others 2002; Wheelock and others 1987). In a murine mammary epithelium model, E-cadherin ectodomain shedding promotes an EMT (Lochter and others 1997). In a rat cataract model, MMP-2/MMP-9-dependent E-cadherin ectodomain shedding is induced by TGF-β and causes an EMT necessary for the formation of anterior subcapsular cataracts (Dwivedi and others 2006). Ischemia also induces E-cadherin ectodomain shedding to contribute to renal failure. It has been speculated that E-cadherin shedding disrupts the cadherin/catenin complex, which is required for renal proximal epithelial cell function (Covington and others 2005; Covington and others 2006). It is currently unknown how the shed E-cadherin ectodomain found in ovarian tumor cystic fluid and ascites will impact ovarian cancer metastasis. Based on others' results in different cancer cell lines, it is hypothesized that the shed ectodomain may promote ovarian cancer dissemination by disrupting cell-cell adhesion, encouraging an EMT, or upregulating migration, invasion, and/or proteinase activity.

Recently, evidence has emerged suggesting that the N-cadherin ectodomain also plays a role in cancer progression. Soluble N-cadherin (90kDa) is elevated in the serum of prostate

cancer patients compared to patients with no signs of disease. A correlation is also observed between high levels of soluble N-cadherin and prostate specific antigen (PSA) (Deryck and others 2006a). Soluble N-cadherin has recently been shown to promote angiogenesis in a rabbit cornea assay and in a chorioallantoic assay. Increased migration of endothelial cells is also observed in a wound closure assay in the presence of soluble N-cadherin in a fibroblast growth factor (FGF) receptor dependent manner (Deryck and others 2006b). The proteinases that cleave N-cadherin have not been identified in these studies, but ADAM10 has been shown to cleave N-cadherin in a separate study (Reiss and others 2005). Reiss and colleagues report that ADAM10-mediated cleavage of N-cadherin results in reduced cell adhesion, redistribution of β-catenin, and increased transcription of Wnt/β-catenin target genes (Reiss and others 2005). Although it is interesting to speculate on the role of N-cadherin ectodomain shedding in the promotion of the initial MET in ovarian cancer progression, this investigation will only focus on the role of E-cadherin ectodomain shedding as there are currently no studies examining the role of both E-cadherin and N-cadherin ectodomain shedding in the same model. In addition, a majority of reports have identified the E-cadherin ectodomain as a possible enhancer of cancer metastasis.

III) β-catenin

A) Roles of β-catenin in Adhesion and Transcription

β-catenin has two main functions: maintenance of cell-cell adhesion and regulation of nuclear gene expression. As described in Section II, at the cell surface β-catenin links the cadherin extracellular region to the actin cytoskeleton by binding to the cytoplasmic region of cadherins and to α-catenin to control cell-cell adhesion (Rimm and others 1995). In contrast,

nuclear and cytoplasmic β-catenin mediate the Wnt signal transduction pathway [**Fig 1.4**]. In the absence of Wnt, cytosolic β-catenin forms a complex with adenomatous polyosis coli (APC), axin/conductin, casein kinases (CK) 1α and 1ε, and glycogen synthase kinase-3β (GSK-3β). β-catenin is then phosphorylated by CK1 at residue 45 and by GSK-3β at residues 41, 37, and 33 to target it for ubiquitination and proteasomal degradation. When Wnt signaling is active, Dishevelled prevents the complex formation and phosphorylation by GSK-3β, permitting β-catenin to translocate to the nucleus, bind with the Tcf/Lef-1 family of transcription factors, and increase transcription of Wnt/β-catenin target genes [Reviewed in (Dihlmann and others 2005; Nelson and Nusse 2004)]. When Wnt signaling is not active, other mechanisms may permit β-catenin translocation to the nucleus. For example, GSK-3β is phosphorylated on residue tyrosine 216 for efficient kinase activity, but its kinase activity is inhibited when it is phosphorylated on residue serine 9. Currently protein kinase A (PKA), protein kinase B (PKB), PKC, Akt/Phosphatidylinositol Kinase-3 (PI3K), Mitogen Activated Protein Kinase (MAPK), and the Src/Extracellular signal regulated-kinase (ERK) signaling cascade have been reported to phosphorylate and inhibit GSK-3β (Almeida and others 2005; Fang and others 2000; Fang and others 2002b; Goode and others 1992; Li and others 2000; Zhou and others 2004).

E-cadherin expression has also been shown to sequester β-catenin at the cell surface, depleting the pool of β-catenin that binds TCF (Gottardi and others 2001). In support of this finding, increased E-cadherin ectodomain shedding or decreased E-cadherin expression both result in the release of β-catenin and increased β-catenin-mediated transcription in two different studies (Koenig and others 2006; Maretzky and others 2005). In contrast, when E-cadherin is introduced into L929 fibroblasts, which lack E-cadherin-mediated cell adhesion and Wnt

signaling, β-catenin is stabilized at cell-cell junctions, but no changes are observed in Wnt target gene expression (Kuphal and Behrens 2006). Based on these observations, the ability of E-cadherin to regulate β-catenin-mediated transcription is likely dependent on cell type and cell conditions.

E-cadherin and GSK-3β are not the only regulators of β-catenin function. Gottardi and Gumbiner have shown that β-catenin exists in the cell in distinct molecular forms with different binding properties, which determine its ability to participate in adhesion or transcription [**Fig 1.5**]. During Wnt signaling, β-catenin is present in a closed conformation and monomeric form that binds TCF, but not the E-cadherin cytoplasmic domain. The closed conformation is created when the COOH terminal of β-catenin is folded back to prevent adhesion to cadherins. When β-catenin dimerizes with α-catenin, binding to cadherins and subsequent adhesion are permitted, but transcription is prevented. If β-catenin is not present in closed conformation or as a β-catenin-α-catenin dimer, then competition between E-cadherin and TCF will occur (Gottardi and Gumbiner 2004a). An endogenous protein named ICAT (inhibitor of β-catenin and TCF-4) also influences β-catenin's ability to regulate transcription. ICAT binds β-catenin and competes its interaction with TCF to prevent its ability to upregulate transcription (Tago and others 2000). *In vitro*, ICAT also competes with E-cadherin for β-catenin binding, but stable expression of ICAT does not appear to alter the stability of the cadherin complex (Gottardi and Gumbiner 2004b). Many other mechanisms including transcriptional repressors and β-catenin nuclear transport affect the ability of β-catenin to regulate transcription, but these factors will not be discussed or considered in this investigation.

Many of the known Wnt/β-catenin target genes regulate cell proliferation, development, and tumorigenesis. Cyclin D1 and cMyc are currently the most investigated Wnt/β-catenin target genes in cancer research. Many of the identified target genes appear to be cell-type specific as their transcription is dependent on the regulation of the Wnt pathway and/or the expression of Wnt proteins in the responding cell. It remains to be determined if any universal Wnt/β-catenin target genes exist (Clevers 2006), but it has been recently suggested that cancer cells express two different sets of Wnt/β-catenin target genes based on their stage. Brabletz and colleagues hypothesized that the “stemness/proliferation group" of target genes is activated early and during tumor progression and the “EMT/dissemination group” of target genes is expressed later and transiently, but mostly at the tumor-host interface, which may explain why variations in Wnt/β-catenin target gene expression occur in different cancer cell line (Brabletz and others 2005).

Figure 1.4

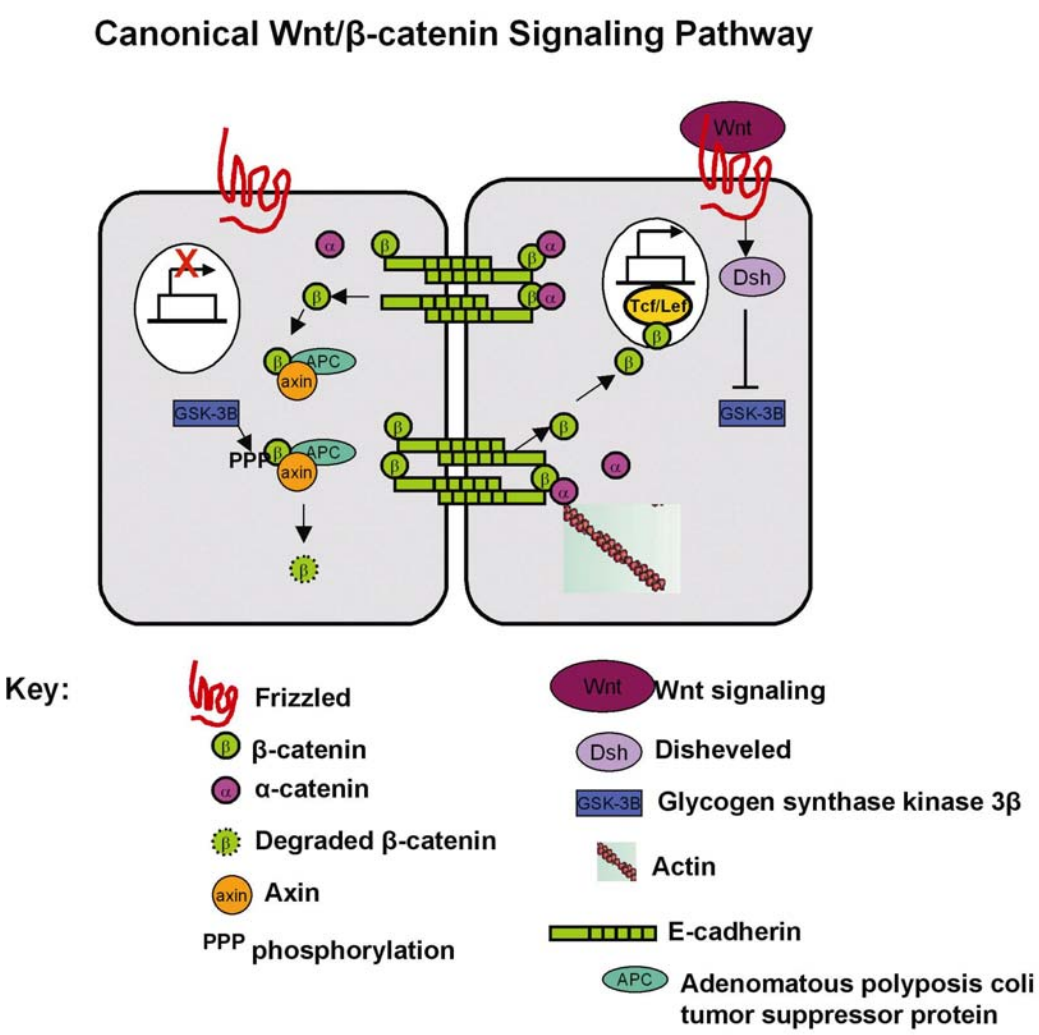
Canonical Wnt/β-catenin Signaling Pathway
Wnt
X
APC
axin
GSK-3B
PPP
Tcf/Lef
Dsh
GSK-3B
Key:
Frizzled
β-catenin
α-catenin
Degraded β-catenin
Axin
PPP phosphorylation
Wnt signaling
Disheveled
Glycogen synthase kinase 3β
Actin
E-cadherin
Adenomatous polyposis coli tumor suppressor protein

Figure 1.4: Canonical Wnt/β-catenin signaling pathway

When β-catenin is not sequestered by cadherins at cell-cell junctions, it translocates to the cytoplasm. In the absence of Wnt signaling, cytosolic β-catenin forms a complex with APC, axin/conductin, CK1α and 1ε, and GSK-3β. β-catenin is then phosphorylated by CK1 and by GSK-3β to target it for ubiquitination and proteasomal degradation. When Wnt signaling is active, Dishevelled prevents complex formation and phosphorylation by GSK-3β, permitting β-catenin to translocate to the nucleus to bind with the Tcf/Lef-1 family of transcription factors to increase transcription of Wnt/β-catenin target genes. Many target genes play a role in tumorigenesis. This figure was adapted from (Cavallaro and Christofori 2004) and (Munshi and Stack 2006).

Figure 1.5

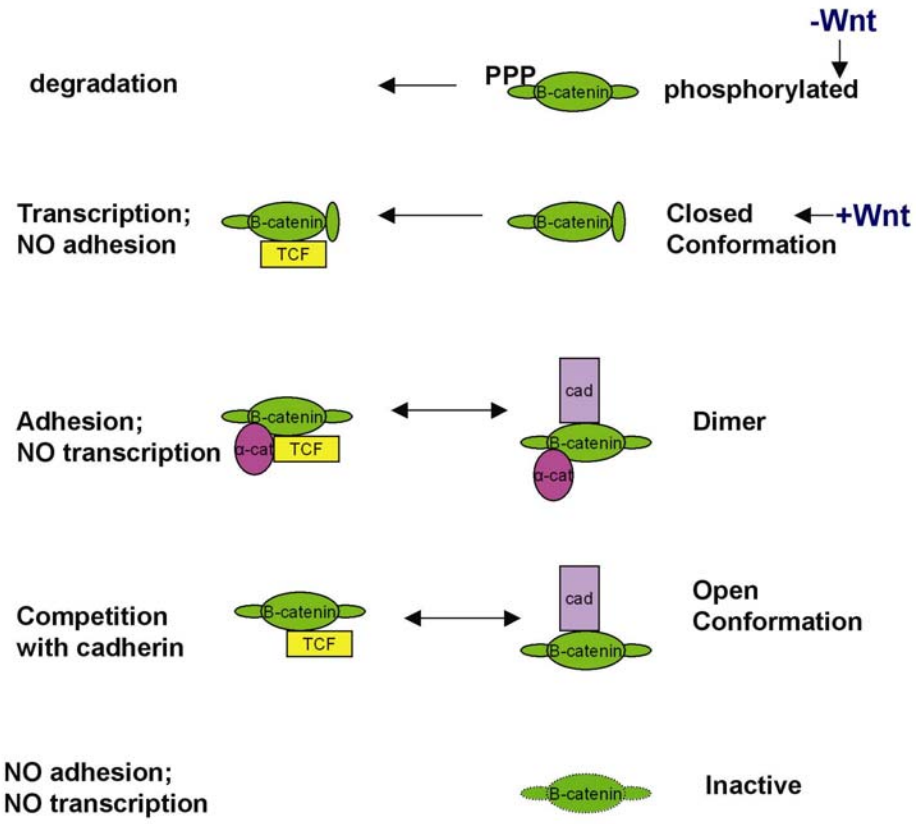
-Wnt
degradation
PPP
β-catenin
phosphorylated
Transcription;
NO adhesion
β-catenin
TCF
β-catenin
Closed
Conformation
+Wnt
Adhesion;
NO transcription
β-catenin
α-cat
TCF
cad
β-catenin
α-cat
Dimer
Competition
with cadherin
β-catenin
TCF
cad
β-catenin
Open
Conformation
NO adhesion;
NO transcription
β-catenin
Inactive

Figure 1.5: β-catenin conformation dictates participation in adhesion or transcription

Gottardi and Gumbiner suggest that β-catenin conformational changes govern its ability to mediate transcription or adhesion. When Wnt signaling is not active, β-catenin exists in a phosphorylated form that is targeted for degradation. Alternatively, when Wnt signaling is active, β-catenin exists in a closed conformation that preferentially associates with TCF to mediate transcription. When β-catenin dimerizes with α-catenin, this form preferentially associates with E-cadherin to mediate cell adhesion. β-catenin also exists in an open conformation where E-cadherin and TCF compete for β-catenin binding. This figure was adapted from (Gottardi and Gumbiner 2004a).

B) Role of β-catenin in Ovarian Cancer Progression

Few mechanisms contributing to increased β-catenin-mediated transcription in ovarian tumors are described in the literature. In colon cancer, mutations are frequently reported in APC, Axin, or β-catenin that prevent degradation of β-catenin (Clevers 2006). Mutations in β-catenin are only common in ovarian endometrioid tumor types and are reported in 16-64% of ovarian endometrioid adenocarcinomas (OEA) (Gamallo and others 1999; Palacios and Gamallo 1998; Saegusa and Okayasu 2001; Sagae and others 1999; Wright and others 1999; Wu and others 2001). These mutations often prevent the binding of GSK-3β to β-catenin (Gamallo and others 1999; Wright and others 1999) and result in the upregulation of previously reported Wnt/β-catenin target genes (Schwartz and others 2003). Misregulated β-catenin signaling governed by a stable and active mutant of β-catenin also promotes ovarian granulosa cell tumor (GCT) development in a mouse model (Boerboom and others 2005), but little is known about unregulated β-catenin signaling in serous tumors. In serous tumors, a statistically significant correlation between nuclear β-catenin localization and ovarian high grade carcinomas has been observed (Lee and others 2003), suggesting mechanisms other than β-catenin mutations potentially increase β-catenin nuclear expression and transcription. Post-translational modification of E-cadherin may be one of these potential mechanisms, as it would limit sequestration of β-catenin. Despite an upregulation of E-cadherin expression in ovarian cancer, Rask and colleagues and Marques and colleagues both show that β-catenin is increased in ovarian adenocarcinoma compared to normal ovarian tissue and benign adenomas, suggesting β-catenin's ability to transactivate transcription of its target genes is maintained as ovarian cancer

progresses (Marques and others 2004; Rask and others 2003). β-catenin expression is also increased in peritoneal metastases and in cell effusions from the ascites/peritoneal fluid when compared to the primary tumor (Davidson and others 2000; Imai and others 2004), suggesting β-catenin signaling is also prevalent in both primary ovarian tumors and disseminated ovarian cancer cells. In addition, GSK-3β inhibition may contribute to increased β-catenin-mediated transcription. GSK-3β is increased in ovarian tumors when compared to normal ovaries (Rask 2003), suggesting downregulation of its activity, not its expression, likely occurs to permit nuclear translocation of β-catenin. Gonadotropins also inactivate GSK-3β via PI3K/Akt, increasing β-catenin/TCF transcriptional activity in OSE cells (Pon and Wong 2006). Three proteinases (matrix metalloproteinase-7, membrane type-1 matrix metalloproteinase, and urinary-type plasminogen activator) elevated in ovarian cancer cell lines and tumors are known to be targets of the β-catenin/Tcf-4 complex in human colorectal cancer (Crawford and others 1999; Hiendlmeyer and others 2004; Takahashi and others 2002), implying misregulated β-catenin signaling may potentially upregulate these proteinases in ovarian cancer cells.

IV) Proteinases

A) The Matrix Metalloproteinase Family

The matrix metalloproteinases (MMP) are a family of proteinases previously associated with cancer development and progression in many different cancer types. MMPs are classified based on their structure into 8 groups: 5 classes are secreted and 3 classes are membrane-type MMPs (MT-MMP) [**Fig 1.6**]. All family members are products of different genes and their expression and secretion are tightly regulated. MMP expression is transcriptionally regulated by

growth factors, hormones, cytokines, and cellular transformation, but MMP proteolytic activity is controlled by the pro-domain, an internal inhibitor of MMP activity. When the pro-domain is cleaved and removed, a conformational change occurs to reveal the active form. Proteolytic activity is also dependent on the catalytic core domain, which contains a metal binding site for a zinc ion (Zn^{+2}). A cysteine residue in the propeptide domain, named the cysteine switch, provides additional regulation of MMP activity by ligating Zn^{+2} to prevent activation. Many MMPs are activated outside the cell by other MMPs or by serine proteinases. With the exception of MMP-7, MMPs also contain a hemopexin domain at the C-terminal end responsible for binding substrates and naturally occurring inhibitors, such as tissue inhibitor of matrix-metalloproteinases (TIMPs), which reversibly inhibit MMPs by binding to them with a 1:1 stoichiometry. Other domain structures exist and contain regions for transmembrane localization, substrate recognition, and additional cleavage required for MMP activation (i.e. the furin domain). In addition to all known components of the ECM, MMPs cleave many different substrates, including latent MMPs, cell-matrix adhesion receptors, cell surface bound ligands, cell-cell adhesion proteins, and growth factor receptors. These actions result in MMP activation, cell-matrix attachment changes, new ECM fragment generation, growth factor release, and growth factors receptor shedding and inactivation [Reviewed in (Egeblad and Werb 2002; McCawley and Matrisian 2000; McCawley and Matrisian 2001a; Nagase and Woessner 1999)].

Figure 1.6

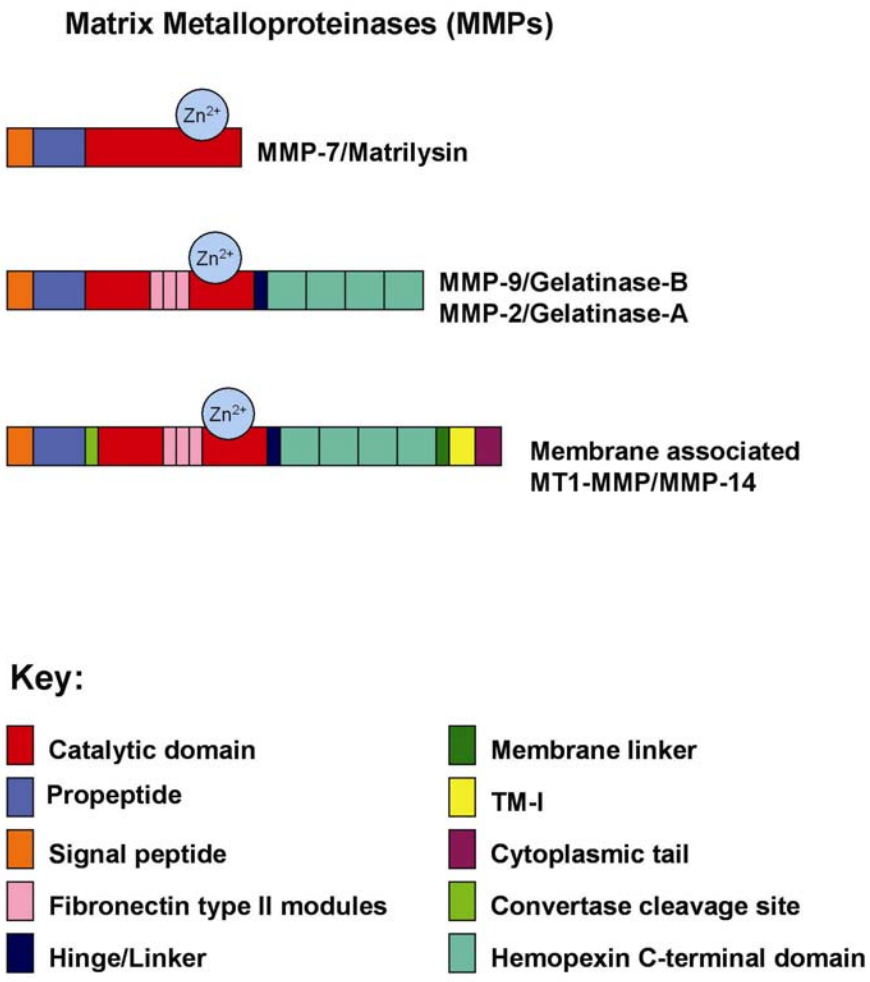
Matrix Metalloproteinases (MMPs)
Zn2+
MMP-7/Matrilysin
Zn2+
MMP-9/Gelatinase-B
MMP-2/Gelatinase-A
Zn2+
Membrane associated
MT1-MMP/MMP-14
Key:
Catalytic domain
Propeptide
Signal peptide
Fibronectin type II modules
Hinge/Linker
Membrane linker
TM-I
Cytoplasmic tail
Convertase cleavage site
Hemopexin C-terminal domain

Figure 1.6: Structure of matrix metalloproteinases

The structures of matrix metalloproteinase-7 (MMP-7), matrix metalloproteinase-2 (MMP-2), matrix metalloproteinase-9 (MMP-9), and membrane type-1 matrix metalloproteinase (MT1-MMP) are shown. This figure was adapted from (Overall and Lopez-Otin 2002).

B) Role of Matrix Metalloproteinases in Cancer Progression

Cancer metastasis development is dependent on excess matrix degradation to encourage destruction of the basement membrane, invasion into the stroma, entry into blood vessels and lymphatics, and establishment of new growths, strongly implicating MMPs in these processes. Different MMPs can be expressed throughout tumorigenesis, but it is also possible that overexpression of one MMP is adequate to promote tumor progression. MMP expression is rarely increased by gene amplification or activating mutations, but likely occurs due to changes in transcriptional regulation. Polymorphisms in MMP promoters are associated with changes in gene transcription and increased cancer susceptibility [Reviewed in (Egeblad and Werb 2002)]. Both tumor cells and stromal cells, including fibroblasts, infiltrating immune cells, and endothelial cells, produce MMPs. Tumor cells may also induce MMP expression in stromal cells by paracrine signaling via the secretion of interleukins, interferons, and growth factors [Reviewed in (McCawley and Matrisian 2000; Sternlicht and Werb 2001)]. MMPs also influence several steps of cancer progression other than invasion and metastasis. MMPs enhance cell growth by activating cell membrane precursor growth factors and by releasing ECM-sequestered growth factors. Apoptosis is induced when MMPs cleave cell adhesion molecules, which may cause apoptotic cell rounding, but apoptosis in inhibited when MMPs release factors that enhance cell survival. MMPs aid angiogenesis by degrading the ECM to permit access of endothelial cells to tumor cells while they inhibit angiogenesis by generating protein fragments that act as angiogenesis inhibitors. MMPs also help tumor cells evade immune surveillance by targeting chemokines and cytokine signaling to diminish infiltration of immune cells into the tumor stroma and proliferation of immune cell populations [Reviewed in (Egeblad and Werb

2002)]. Recently, MMPs have also been reported to induce genetic instability indirectly via cleavage of molecules at the cell surface (Radisky and Bissell 2006). Although MMPs are necessary for normal ovarian function and play a role in ovulation (Hulboy and others 1997), several MMPs, including MMP-1 (collagenase-1), MMP-2 (gelatinase A), MMP-7 (matrilysin), MMP-9 (gelatinase B), MMP-13 (collagenase-3), and MMP-14 (MT1-MMP), are linked to ovarian cancer progression, but currently MMP-2 and MMP-9 are the most studied [Reviewed in (Ghosh and others 2002)]. This investigation will only focus on MMP-9, MMP-2, MT1-MMP, and MMP-7 and on their regulation and actions during ovarian cancer progression.

C) Role of Matrix Metalloproteinase-9 in Ovarian Cancer Progression

MMP-9 (gelatinase B) is one of the most structurally complex members of the MMP family [**Fig 1.6**]. MMP-9 contains three repeats of the fibronectin-type II domain in its catalytic domain, that interact with collagens type I and IV, laminin, and gelatin (Nagase and Woessner 1999; Van den Steen and others 2002). Glycosylation accounts for approximately 15% of the mass of proMMP-9, but the role of these carbohydrate moieties is unknown (Fridman 2003). Keratinocytes, monocytes, tissue macrophages, leukocytes, and malignant cells all produce proMMP-9. ProMMP-9 expression is induced by tumor promoters, growth factors, cytokines, oncogene products, metal ions, reactive oxygen species, and hormones (Van den Steen and others 2002). To activate proMMP-9, the prodomain is removed by MMPs MMP-2, MMP-7, MMP-3, and MMP-13, and by serine proteinases pancreatic trypsin-2, α-chymase, β-chymase, and plasmin. Cell surface association of proMMP-9 with other proteins likely regulates and localizes its activity. For example, proMMP-9/MMP-9 associates with CD44 or surface

associated α_2 (IV) chain of collagen IV at the cell surface. MMP-9 is in the active state when bound to CD44, suggesting this mechanism localizes MMP-9 activity at the cell surface to enhance degradation of substrates in the pericellular space. Although the mechanism remains to be elucidated, MMP-9 also associates with RECK at the cell surface, which facilitates MMP-9 inhibition. Internalization occurs when proMMP-9 binds to LRP, suggesting LRP regulates the levels of latent MMP-9 in the pericellular environment [Reviewed in (Fridman and others 2003)].

In vitro, MMP-9 expression is reported in several ovarian cancer cell lines, but it is not produced by normal OSE. MMP-9 expression is increased in response to many stimuli including growth factors, cytokines, and phorbol myristate acetate (PMA) in ovarian cancer cells (Ghosh and others 2002). Specifically, previous data from Dr. Stack and colleagues show that epidermal growth factor (EGF) induces MMP-9 protein expression in the OVCA429 ovarian cancer cell line and requires the MAPK and PI3K signaling pathways (Ellerbroek and others 2001a; Ellerbroek and others 1998). A separate study also verifies the role of EGF in promoting elevated MMP-9 expression in ovarian cancer cells (Alper and others 2001). EGFR activation and PI3K-mediated signaling also promote cell surface association of proMMP-9 to likely facilitate cellular invasion (Ellerbroek and others 2001b). Gonadotropin-releasing hormone (GnRH) transactivates the MMP-9 promoter and increases its expression and activation in Caov-3 and OVCAR-2 ovarian cancer cell lines. The invasive and migratory behavior induced by GnRH is also MMP-2 and MMP-9-dependent (Cheung and others 2006). In addition to enhancing migration and invasion of ovarian cancer cells, MMP-9 contributes to the release of

biologically active VEGF to increase ascites formation in a mouse ovarian cancer model (Belotti and others 2003).

The source of MMP-9 found in the ovarian tumor microenvironment still remains controversial. Several studies demonstrate that stromal cells are the sole contributors of MMP-9 to the tumor microenvironment, while other studies show ovarian tumors also produce MMP-9. For example, Huang and colleagues show that stromal MMP-9, which is most likely derived from tumor infiltrating macrophages, is critical in enhancing angiogenesis and proliferation of human ovarian tumors in a mouse model (Huang and others 2002). MMP-9 is also produced by epithelial cells, fibroblasts, and endothelial cells in the tumor microenvironment (McCawley and Matrisian 2001b). In addition, two separate studies report that although MMP-9 is expressed at high levels in a majority of both ovarian tumors and their surrounding stromal compartments, only stromal MMP-9 expression is associated with poor patient survival and the presence of ascites (Kamat and others 2006; Ozalp and others 2003). In contrast to these findings, several studies report that MMP-9 is produced by ovarian tumor cells. According to the results of three separate studies, MMP-9 mRNA is expressed in ovarian tumors (Davidson and others 1999; Huang and others 2000; Naylor and others 1994). Ovarian tumor MMP-9 expression is also demonstrated using immunohistochemistry (Kamat and others 2006; Ozalp and others 2003) and gelatin zymography (Lengyel and others 2001; Naylor and others 1994). Epithelial MMP-9 immunoreactivity is elevated in malignant ovarian tumors when compared borderline ovarian tumors (Ozalp and others 2003). In addition, short term primary culture of ovarian cancer cells from primary tumors, metastatic lesions, and ascites produce MMP-9, which is decreased with increasing passage in culture (Fishman and others 1997). MMP-9 expression is elevated in

ovarian cancer cells from the peritoneal fluid when compared to mesothelial cells (Sakata and others 2002). Interestingly, a moderate increase in MMP-9 gene expression occurs in macrophages cocultured with the IGROV1 ovarian cancer cell line, suggesting cancer cells polarize macrophages towards a tumor associated phenotype (Hagemann and others 2006). Regardless of its source, high MMP-9 levels in ovarian tumor tissues and ascites are associated with disease recurrence and poor patient survival (Demeter and others 2005), but due to these conflicting reports, it is important to re-establish the observation that ovarian tumor cells also produce MMP-9 to enhance ovarian cancer metastasis.

D) Role of Matrix Metalloproteinase-7 in Ovarian Cancer Progression

MMP-7 (matrilysin) is also secreted as a proenzyme, but it differs from the other MMPs as it lacks a hemopexin domain and has a markedly smaller molecular weight (proMMP-7=28kDa) **[Fig 1.6]**. MMP-7 cleaves ECM components elastin, type IV collagen, fibronectin, vitronectin, aggrecan, and proteoglycans, but it is also known for its ability to cleave cell surface molecules including tumor necrosis factor-α (TNF-α) precursor, Fas ligand (FasL), heparin binding epidermal growth factor (HB-EGF), E-cadherin, and β4-integrin. Interestingly, MMP-7 is one of the few MMPs with expression limited to tumor cells; stromal cells in the tumor microenvironment do not secrete MMP-7. Early in tumorigenesis, MMP-7 modifies insulin growth factor (IGF) and HB-EGF to increase cell proliferation. Invasion is enhanced when MMP-7 degrades ECM components or cleaves E-cadherin to promote shedding of its ectodomain. Apoptosis is also aided when MMP-7 cleavage results in FasL shedding and TNF-α shedding [Reviewed in (Ii and others 2006)].

Few studies have examined the role of MMP-7 in ovarian cancer. MMP-7 is overexpressed in EOC tumor specimens and in ovarian cancer cell lines (Wang and others 2005) and overexpression of MMP-7 is associated with increased invasion *in vitro* (Wang and others 2006a). In a separate study, intense MMP-7 staining and a greater number of tumor areas showing MMP-7 expression are both significantly correlated with nuclear localization of β-catenin in endometrioid tumors only (Sillanpaa and others 2006). Mutations in the β-catenin gene that stabilize β-catenin are fairly common in endometrioid ovarian tumors (Gamallo and others 1999; Palacios and Gamallo 1998; Saegusa and others 2001; Sagae and others 1999; Wright and others 1999; Wu and others 2001). In all ovarian tumor types, tumors displaying a low number of areas with MMP-7 staining are associated with a higher histological tumor grade and a more advanced tumor stage. Interestingly, patients with a high number of tumor areas expressing MMP-7 experience a significantly greater disease related recurrence-free survival rate (Sillanpaa and others 2006). *In vitro*, lysophosphatidic acid (LPA), VEGF, and interleukin-8 (IL-8) increase MMP-7 secretion in the DOV13 ovarian cancer cell line and recombinant human MMP-7 increases proMMP-2 activation (Wang and others 2006a; Wang and others 2005). Incubation of recombinant human MMP-7 with conditioned media from IOSE-29 (immortalized ovarian surface epithelium) cells results in the activation of both proMMP-2 and proMMP-9 (Wang and others 2005). The limited information on the role MMP-7 in ovarian cancer necessitate the identification of additional regulators of MMP-7 expression in ovarian cancer models.

E) Role of Membrane Type-1 Matrix Metalloproteinase and Matrix Metalloproteinase-2 in Ovarian Cancer Progression

MT1-MMP (MMP-14) is a type I transmembrane proteinase involved in pericellular proteolysis of the ECM **[Fig 1.6]**. MT1-MMP degrades collagens type I, II, and III, gelatin, laminins 1 and 5, fibronectin, vitronectin, aggrecan, fibrin, and lumican. The propeptide domain of MT1-MMP is cleaved by furin or propeptide convertases in the Golgi, which allows MT1-MMP to exist as an active enzyme on the cell surface. The catalytic domain of the 60kDa active form of MT1-MMP can be removed to inactivate and downregulate MT1-MMP (size=45kDa). In addition, MT1-MMP is inhibited by TIMP-2, 3, and 4, but not TIMP-1. A GPI-anchored glycoprotein named RECK (reversion-inducing-cysteine rich protein with Kazal motifs) also inhibits MT1-MMP's proteolytic activity. MT1-MMP is necessary for cancer invasion, cell growth, and angiogenesis. Specifically, it enhances cell migration and invasion by pericellular ECM degradation, CD44 and syndecan 1 shedding, and ERK activation, but MT1-MMP is most known for its participation in proMMP-2 activation to further enhance cell migration and invasion [Reviewed in (Itoh and Seiki 2006)].

MMP-2 (gelatinase A) is a secreted MMP necessary for the degradation of the basement membrane as it degrades collagens and gelatin [**Fig 1.6**]. Similar to MMP-9, MMP-2 contains three repeats of the fibronectin-type II domain in its catalytic domain, which interact with collagens and gelatins (Nagase and Woessner 1999); MMP-2 is also secreted by many human tissue cell types, circulating leukocytes, and tumor cells (Van den Steen and others 2002). ProMMP-2 expression is increased in response to many stimuli including growth factors, LPA, cytokines, and phorbol myristate acetate (PMA) (Ghosh and others 2002). ProMMP-2 activation

only occurs upon association with MT1-MMP and TIMP-2. When MT1-MMP is on the cell surface, it forms an enzyme-inhibitor complex by binding the N-terminal inhibitory domain of TIMP-2 via its catalytic domain. An MT1-MMP-TIMP-2-proMMP-2 ternary complex is formed when the exposed C-terminal domain of TIMP-2 binds to the hemopexin domain of proMMP-2. ProMMP-2 activation does not occur without TIMP-2. A second unbound MT1-MMP then activates proMMP-2 when it forms a homo-oligomer complex with the bound MT1-MMP in the ternary complex through their hemopexin domains and/or transmembrane domains [Reviewed in (Itoh and others 2006; Nagase and Woessner 1999)].

Although MMP-2 is not produced by normal OSE, it is expressed as both latent and active forms in ovarian cancer cell lines (Moser and others 1994). MT1-MMP is also expressed in ovarian cancer ascites, cancer cell lines, and ovarian tumor samples (de Nictolis and others 1996; Ellerbroek and others 1999; Stack and others 1998). It has been speculated that MT1-MMP is produced by ovarian cancer cells to initiate cell surface activation of proMMP-2 derived from either tumor cells or stromal cells to permit cell migration, invasion, and metastasis (Afzal and others 1998; Ellerbroek and others 1999; Fishman and others 1996). Davidson and colleagues also speculate that high MMP-2 is necessary to establish peritoneal metastases as MMP-2 expression is increased in ovarian cancer cells in effusions relative to mesothelial cells while primary tumor MMP-2 expression is decreased compared to stromal cells (Davidson and others 2001). In agreement with this hypothesis, Torng and colleagues suggest that stromal MMP-2 is expressed early and promotes early EOC invasion (Torng and others 2004). Ovarian cancer cells also induce increased MMP-2 production by tumor stromal cells (Boyd and Balkwill 1999; Drew and others 2004). Regardless of their source, increased MMP-2 and MT1-MMP

expression in ovarian tumor cells and/or stromal cells are associated with advanced stage ovarian carcinomas and short term survival (Davidson and others 1999; Kamat and others 2006), necessitating a better understanding of the regulation of MMP-2 and MT1-MMP expression and activation in ovarian cancer.

F) Role of Urinary-type Plasminogen Activator in Ovarian Cancer Progression

The plasminogen activation system also plays an important role in tumor invasion and metastasis. The proenzyme plasminogen is converted to plasmin by urinary-type plasminogen activator (uPA) and its conversion is further enhanced by the binding of uPA to its cell surface specific receptor uPAR. Once converted, plasmin degrades fibrin and components of the ECM and basement membrane. uPA also degrades ECM proteins and activates other matrix degrading enzymes, including MMP-2 and MMP-9. Plasminogen activator inhibitor-1 (PAI-1) inhibits uPA even when uPA is bound to uPAR [Reviewed in (Reuning and others 1998)].

uPA also contributes to the progression of ovarian cancer. Malignant ovarian epithelial cells display greater uPA binding activity and 17 to 38 fold higher uPA expression compared to normal ovarian epithelium (Casslen and others 1991; Young and others 1994). Activated Ras, PMA, PKC, LPA, and integrin clustering all increase uPA production (Ghosh and others 2002). Increased uPAR immunoreactivity is also observed at the invasive front in ovarian tumors (Young and others 1994). When uPA synthesis is inhibited, *in vitro* invasion and *in vivo* colonization of intra-peritoneally injected ovarian cancer cells is reduced in a mouse model (Wilhelm and others 1995). These observations all imply that increased proteolysis occurs in the

tumor microenvironment when tumor or stroma derived uPA binds uPAR on tumor cell surfaces (Ghosh and others 2002).

V) Integrins

A) Integrin Function and Rationale for Model

Integrins are glycoproteins that form heterodimeric receptors consisting of an alpha (α) subunit and a beta (β) subunit. The α and β subunits are covalently linked and each subunit has a large extracellular domain, a single membrane spanning domain, and a short, non-catalytic cytoplasmic tail. Currently 25 different integrin pairings resulting from 18 α subunits and 8 β subunits have been observed [Reviewed in (Hood and Cheresh 2002)]. Most integrins bind to ECM ligands, but they also bind to ADAMs, immunoglobulin-type receptors, and vascular cell adhesion molecules (VCAMs) on other cells, and to bacterial polysaccharides and viruses. Known cellular functions mediated by integrins include adhesion to basement membranes, migration on ECM components, formation of platelet aggregates, establishment of intercellular junctions in the immune system, and support of bacterial and viral cellular entry [Reviewed in (Danen 2005)]. In addition, the integrin cytoplasmic tails transactivate signaling pathways via the recruitment and activation of focal adhesion kinase (FAK) and/or the Src family kinases (SFKs) among other effectors (Guo and Giancotti 2004). This phenomenon is known as outside-in signaling and regulates the pathways governing cell migration, invasion, gene transcription, and survival. Inside-out signaling occurs when cytoplasmic tail-mediated signaling promotes alterations in the conformation of integrin extracellular domains, affecting their affinity and adhesive capacity. (Danen 2005; Hood and Cheresh 2002). Integrins control cellular responses

via the formation of signal transduction complexes on a cytoskeletal framework and this integration of signaling and cytoskeletal events is regulated by the physical nature of the integrin-ligand interaction [**Fig 1.7**]. For example, integrin ligation or low valency integrin occupancy is induced by matrix protein fragments and the integrin is then redirected to focal adhesions, but activation of tyrosine kinases or the accumulation of cytoskeleton components does not occur. This situation is modeled using soluble antibodies specific to integrin subunits. In contrast, integrin aggregation or clustering is stimulated by an intact matrix and results in the activation of numerous downstream cell signaling pathways and the accumulation of cytoskeletal factors at the integrin cytoplasmic tails. Experimentally, this state is mimicked using integrin subunit-specific antibodies immobilized on latex beads (Miyamoto and others 1995a; Miyamoto and others 1995b; Munshi and Stack 2006; Yamada and Miyamoto 1995). This model is advantageous as it allows for the characterization of the early events following integrin activation, which cannot be observed when cells must first be plated on an intact matrix. It also permits a more physiologically relevant examination of integrin-mediated signaling events governing ovarian cancer cell dissemination as integrins are likely aggregated by the exposed submesothelial ECM and by collagen fragments in the ascites.

Figure 1.7

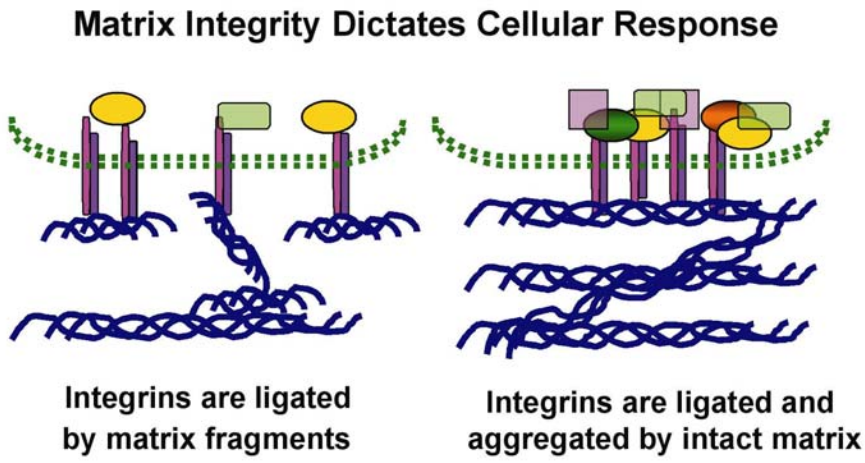
Matrix Integrity Dictates Cellular Response
Integrins are ligated by matrix fragments
Integrins are ligated and aggregated by intact matrix

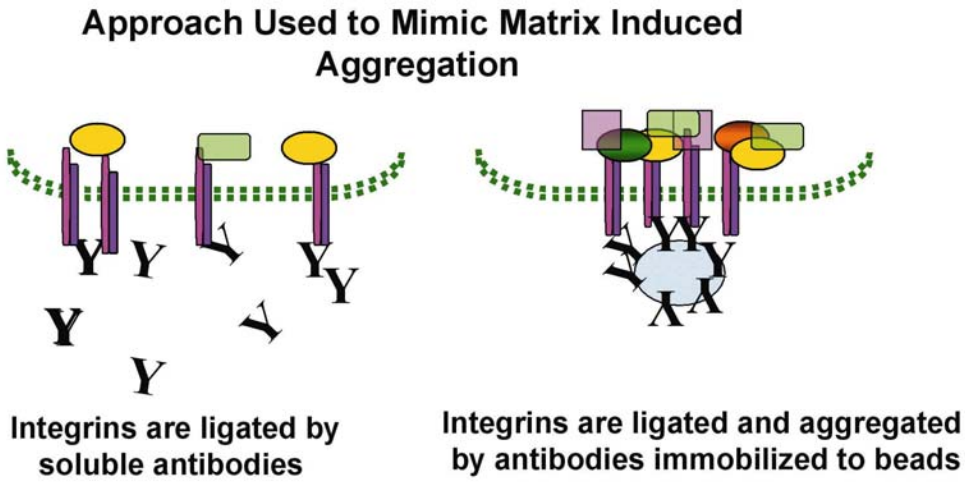
Approach Used to Mimic Matrix Induced Aggregation
Integrins are ligated by soluble antibodies
Integrins are ligated and aggregated by antibodies immobilized to beads

Figure 1.7: Models of integrin ligation and aggregation

Integrins control cellular responses via the formation of signal transduction complexes on a cytoskeletal framework and this integration of signaling and cytoskeletal events is regulated by the physical nature of the integrin-ligand interaction. Integrin ligation or low valency integrin occupancy is induced by matrix protein fragments and the integrin is then redirected to focal adhesions, but robust activation of tyrosine kinases or the accumulation of cytoskeleton components does not occur. This situation is modeled *in vitro* using soluble antibodies specific to integrin subunits. Integrin aggregation or clustering is stimulated by an intact matrix and results in the robust activation of numerous cell signaling pathways and the accumulation of cytoskeletal factors at the integrin cytoplasmic tails. Experimentally, this state is mimicked *in vitro* using integrin subunit-specific antibodies immobilized on beads. This figure was adapted from (Munshi and Stack 2006).

B) Role of Collagen-Binding Integrins in Ovarian Cancer Metastasis

Integrins are implicated in many steps of cancer metastasis, including degradation and penetration of the basement membrane, intravasation into blood vessels and lymphatic vessels, attachment to leukocytes, platelets, and endothelial cells, and extravasation and growth in the target organ. Changes in integrin expression levels are often observed as cancers develop and progress. Cancer cells often switch integrin expression to a profile that is most beneficial to their stage of progression. For example, upregulated integrin expression promotes adhesion to the basement membrane and early tumor growth, but downregulated integrin expression promotes detachment from the basement membrane and prevents anoikis as the cancer begins to metastasize. Because integrin signaling is dependent on the cell type and the oncogenic mutations of each tumor, it is difficult to determine which integrins are associated with enhancing or inhibiting cancer progression [Reviewed in (Danen 2005; Guo and Giancotti 2004)].

Although ovarian cancer does not spread via the vasculature, reversible modulation of cell-matrix adhesion plays a critical role in remodeling of the neoplastic ovarian epithelium during metastasis, implicating integrins in intra-peritoneal dissemination. As with other cancer types, ovarian tumor cells alter their integrin profile to foster metastatic spread. Normal OSE cells express integrins α2, α3, α6, β1, and β4. In contrast, ascitic ovarian cancer cells display low expression of α6 and β4 integrins, suggesting integrin expression is downregulated to facilitate release from the laminin-rich basement membrane under the OSE and exfoliation from the primary tumor [Reviewed in (Skubitz 2002)]. Exfoliated tumor cells then adhere to peritoneal

mesothelial cells, and disrupt the mesothelial monolayer, exposing the type I/III collagen-rich submesothelial ECM. Ovarian carcinoma cells adhere to this exposed submesothelial ECM more strongly than to the mesothelial monolayer and exhibit preferential adhesion to interstitial collagen type I (Fishman and others 1998; Ghosh and others 2002; Harvey and Amlot 1983; Moser and others 1994; Niedbala and others 1987). In agreement with this observation, high expression of collagen-binding integrins α2, α3, and β1 integrins is reported in many ascites derived ovarian cancer cell lines in several studies (Skubitz 2002). Ascites derived spheroids also display moderate adhesion to collagen type I, which is partially dependent on β1 integrin (Burleson and others 2004). Attachment of ovarian tumor cells to the peritoneal mesothelial cells is required prior to disruption of the mesothelial monolayer. The LP9 mesothelial cell line displays surface expression of fibronectin, laminin, and collagens type I, III, and IV (Lessan and others 1999; Lessan and Skubitz 1998) and β1 integrin partially mediates adhesion of SKOV3 ovarian carcinoma cells and patient derived spheroids to LP9 mesothelial cell monolayers *in vitro* (Burleson and others 2004; Lessan and others 1999). In addition to mediating cell-matrix adhesion, clustering of collagen-binding integrins likely regulates signaling events that enhance ovarian cancer metastasis.

C) Regulation of Matrix Metalloproteinases and Urinary-type Plasminogen Activator by Collagen-Binding Integrins

Several reports, including studies carried out by Dr. Stack and colleagues, have linked integrin aggregation and increased proteinase expression and activation in different cell types (Azzam and Thompson 1992; DiPersio and others 2000; Ellerbroek and others 1999; Ellerbroek

and others 2001b; Fishman and others 1998; Ghosh and others 2000; Gilles and others 1997; Haas and others 1998; Seltzer and others 1994). Ellerbroek and colleagues show that multivalent aggregation of β1 integrins promotes proMMP-2 activation and increases MT1-MMP expression and processing in DOV13 ovarian cancer cells (Ellerbroek and others 1999; Ellerbroek and others 2001b). Similar observations regarding proMMP-2 activation are reported in fibroblasts, fibrosarcoma cells, and invasive breast cancer cell lines cultured on 3D collagen matrices (Azzam and Thompson 1992; Gilles and others 1997). Integrin engagement is also speculated to promote active MT1-MMP localization to sites of cell-matrix contact (Ellerbroek and others 2001b; Galvez and others 2002; Wolf and others 2003). Few studies report an association between uPA activity and integrin engagement in ovarian cancer cells, with the exception of Hapke and colleagues showing that OV-MZ-6 human ovarian cancer cells cultured on collagen type IV display increased expression of uPA, uPAR, and PAI-1 (Hapke and others 2001), but Ghosh and colleagues show that clustering of α3 and β1 integrins increases uPA secretion in premalignant oral keratinocytes PP126, which also requires ERK1/2 activation. PAI-1 expression and localization of uPAR are also affected, but the net increase in proteolytic activity is greater (Ghosh and others 2000). Little evidence also exists linking increased MMP-9 secretion to collagen-binding integrin engagement in ovarian cancer cell lines, but in immortalized mouse keratinocytes, α3β1 integrin expression is necessary for the induction of MMP-9 expression (DiPersio and others 2000) because α3β1 integrin expression regulates MAPK-dependent MMP-9 expression by enhancing MMP-9 mRNA stability (Iyer and others 2005). α3β1 is also associated with increased invasion and MMP-9 activity in breast cancer cells (Morini and others 2000). No reports of β1 integrin involvement in MMP-7 expression or

activation currently exist in the literature. Other than MAPK pathway components and tyrosine kinase signaling (Ellerbroek and others 1999; Ghosh and others 2000), many of the effectors connecting collagen-binding integrin engagement and proteinase expression and/or activation are mostly unexplored, especially in ovarian cancer models.

D) Regulation of E-cadherin and Cell-Cell Adhesion by Collagen-Binding Integrins

Integrin-mediated signaling regulates a variety of different effects on cadherins and cell-cell adhesion. For example, culturing pancreatic cancer cells on collagen type I and III leads to a downregulation of E-cadherin expression (Menke and others 2001). Increased integrin surface expression and adhesion to laminin-1 and collagens type I and IV are associated with decreased cell-cell adhesion in transformed human keratinocytes (Zhang and others 2006). Integrin signaling molecules Fak and paxillin regulate N-cadherin-based cell-cell adhesion in HeLa cells (Yano and others 2004). Increased Src phosphorylation following integrin engagement is also reported in many different cell types (Arias-Salgado and others 2003; Guo and Giancotti 2004), suggesting Src acts as a downstream mediator of integrin aggregation to regulate cell-cell adhesion. The Src family kinases (SFKs) include Src, Yes, and Fyn and they often colocalize at sites of cell-cell adhesion (Avizienyte and Frame 2005). Irby and Yeatman demonstrate that activated Src disrupts cadherin-catenin complexes in human colon cancer cell lines (Irby and Yeatman 2002). Src-induced disruption of E-cadherin localization is dependent on β1 integrin signaling in a colon cancer cell line (Avizienyte and others 2002). Engagement of fibronectin integrins induces Src-dependent disruption of VE-cadherin-containing adherens junctions in bovine endothelial aortic cell monolayers (Wang and others 2006b). Caveolin-1 indirectly

increases cell-cell adhesion in ovarian cancer cells via inhibition of Src kinases (Miotti and others 2005). Src is also identified as a regulator of E-cadherin internalization (Fujita and others 2002; Palacios and others 2005). These finding imply Src may act as important effector of integrin-mediated signaling to modify E-cadherin expression and/or function in ovarian cancer cells.

VI) Lysophosphatidic acid

A) Functions of Lysophosphatidic Acid

Lysophosphatidic acid (LPA) is a bioactive water-soluble phospholipid consisting of a single fatty acid chain, a glycerol backbone, and a free phosphate group and is a major component in serum. LPA mediates a variety of physiological functions including differentiation inhibition or reversion, smooth muscle contraction, increased endothelial permeability, gap-junctional communication inhibition, and cellular rounding and spreading. LPA also plays a role in cancer progression by regulating cell proliferation, survival, migration, *in vitro* invasion, and *in vitro* wound healing. These actions are mediated via the LPA receptors, formerly known as the endothelial differentiation gene (EDG) family of G protein coupled receptors (GPCR). LPA1 (EDG2) is the most commonly expressed receptor and is observed in the colon, small intestine, placenta, brain, heart, pancreas, ovary and prostate. LPA2 (EDG4) and LPA3 (EDG7) are not as widely as expressed as LPA1, but are often expressed in cancer cells, including ovarian cancer cells. The LPA receptors couple with three different G proteins to regulate distinct cellular pathways via PI3K/Akt, Ras-ERK, Rho and Rac GTPases, or phospholipase C. Crosstalk between LPA receptors and receptor tyrosine kinases also transmits

LPA-mediated signals and LPA has previously been reported to phosphorylate and transactivate members of the human epidermal growth factor receptor (HER) family in several different cells types, including head and neck squamous carcinoma cell lines, PC12 cells, keratinocytes, COS-7 cells, Rat-1 fibroblasts, and ovarian cancer cells (Daub and others 1997; Daub and others 1996; Gshwind and others 2002; Kim and others 2000; Xu and others 1995a). In addition, LPA promotes GPCR-regulated transmembrane MMP cleavage and subsequent release of growth factor precursors to activate the epidermal growth factor receptor (EGFR) [Reviewed in (Mills and Moolenaar 2003)].

B) Role of Lysophosphatidic Acid in Ovarian Cancer Progression

LPA contributes to the development, progression, and metastasis of ovarian cancer. LPA is increased in both the plasma and ascites of ovarian cancer patients and is detected at concentrations up to 80μM (Fang and others 2002a; Westermann and others 1998; Xu and others 1995b). Ovarian tumor cells and peritoneal mesothelial cells both produce LPA, thereby maintaining an LPA rich microenvironment (Fishman and others 2001; Mills and others 2002b; Ren and others 2006; Xiao and others 2001; Xu and others 1995b; Xu and others 1998). Expression of the LPA2 and LPA3 receptors is elevated in several ovarian cancer cell lines, but expression of LPA1 is variable (Mills and others 2002b; Mills and Moolenaar 2003). Elevated LPA levels are detectable in 98% of patients with ovarian cancer, including 90% of patients with stage I disease, suggesting that LPA promotes early events in ovarian carcinoma dissemination. This is supported by studies demonstrating that treatment of ovarian tumor cells with LPA *in vitro* results in an enhanced metastatic phenotype, characterized by increased proteolytic activity,

stimulation of motility and more aggressive invasive behavior (Fishman and Borzorgi 2002; Fishman and others 2001; Li and others 2005; Pustilnik and other 1999; Ren and others 2006; So and others 2004). Specifically, LPA treatment results in increased activation of MMP-2, MMP-7, and uPA in ovarian cancer cell lines (Fishman and others 2001; Pustilnik and others 1999; So and others 2004). LPA also increases adhesion of ovarian cancer cells to type I collagen *in vitro* (Fishman and others 2001; Ren and others 2006), suggesting it may have a similar effect when ovarian cancer cells disrupt the mesothelial monolayer. In addition to its roles in enhancing cell-matrix adhesion and proteolytic activity, LPA induces the expression of additional genes that contribute to proliferation, survival, or metastasis, including c-myc, VEGF, interleukin-8 (IL-8), and cyclooxgenase-2 (COX-2) (Fishman and Borzorgi 2002; Hu and others 2001; Mills and Moolenaar 2003; Moolenaar and others 1986; Reiser and others 1998; Schwartz and others 2001; Xu and others 1998). Despite several associations between LPA and migratory and invasive cell behavior, the influence of LPA on cell-cell adhesion is largely unexamined, which is surprising as decreased cell-cell adhesion often permits migration and invasion. Only two studies investigating the effect of LPA on cell-cell adhesion exist in the literature. LPA is associated with enhancing adherens junction dissolution and colony dispersal (Jourquin and others 2006) and with indirectly promoting an EMT via phosphorylation of Stat5a in a Rho-dependent manner (Benitah and others 2003). As LPA levels are often elevated in stage I to IV ovarian cancer patients, LPA likely plays a role in the downregulation of cell-cell adhesion to promote cell dissemination at all stages of metastasis.

VII) Cyclooxygenase-2

A) Functions of Cyclooxygenase Isoforms

The main function of cyclooxygenases (COX) is the catalysis of the rate-limiting step in prostaglandin (PG) synthesis from arachidonic acid, generating prostaglandin H_2 (PGH_2) that is subsequently converted to prostaglandin E_2 (PGE_2) and other prostaglandins. Prostaglandins are involved in many physiological functions including blood clotting, ovulation, labor, bone metabolism, nerve growth and development, wound healing, kidney function, blood vessel tone, and immune responses. Two cyclooxygenase isoforms, cyclooxygenase-1 (COX-1) and cyclooxygenase-2 (COX-2), catalyze prostaglandin synthesis and are inhibited by nonsteroidal anti-inflammatory drugs (NSAIDs). COX-1 is expressed constitutively in most normal human tissues. It is speculated to play a housekeeping function by maintaining prostaglandin levels and is most known for promoting vasodilatation and maintaining gastrointestinal integrity. Although not constitutively expressed, COX-2 expression is induced by growth factors, cytokines, and tumor promoters and is inducible in most cell and tissue types often at sites of inflammation. Several normal physiological functions are associated with COX-2 and include kidney function, neural development and response, ovulation, embryo implantation, and bone remodeling. COX-2 is also associated with the following pathological conditions: inflammatory arthritis, Alzheimer's Disease, and cancer [Reviewed in (Dempke and others 2001; DuBois and others 1998; Katori and Majima 2000)].

B) Role of Cyclooxygenase-2 in Ovarian Cancer Progression

COX-2 contributes to tumorigenesis by changing the levels of pro- and anti-apoptotic factors to inhibit apoptosis, by increasing growth factor expression to promote angiogenesis, and by increasing MMP expression to enhance invasiveness (Dempke and others 2001). Data supporting a role for COX-2 in ovarian physiology and pathobiology are complex, with opposing reports of COX-2 prevalence in normal human ovarian tissue (Denkert and others 2002; Landen and others 2003; Li and others 2004; Matsumoto and others 2001). COX-2 expression was only observed in the corpus luteum during menstruation (Matsumoto and others 2001), but COX-2 inhibition delays and blocks ovulation in humans (Norman 2001; Pall and others 2001) and mice genetically deficient in COX-2 also fail to ovulate (Lim and others 1997), suggesting COX-2 activity is essential for normal ovarian function. COX-2 induction is thought to be necessary for the rupture of the preovulatory follicle and subsequent release of oocytes during ovulation. It has been speculated that COX-2 or prostaglandins may increase collagenase and proteolytic activity and decrease synthesis of basement membrane components in ovarian granulosa and surface epithelial cells, permitting ovulation (Butler and others 1991; Tsafriri 1995). In addition, COX-2 expression is reported in benign, borderline and malignant ovarian tumors (Ali-Fehmi and others 2003; Denkert and others 2002; Klimp and others 2001; Landen and others 2003; Li and others 2004) where it is associated with chemotherapy resistance and a poor survival rate (Ferrandina and others 2002a). Ascites from ovarian cancer patients contains elevated levels of PGE_2 compared to nonmalignant ascites or ascites from other carcinomas (Denkert and others 2002), further supporting a role for COX-2 in ovarian pathobiology. A specific role for COX-2 in regulating ovarian cancer metastasis has not been reported, although COX-2 staining is

significantly higher in metastatic ovarian tumors (Li and others 2004). Due to LPA's association with increased COX-2 expression (Reiser and others 1998) and proMMP-2 activation (Fishman 2001) in two separate studies, it is now essential to determine if COX-2 is a potential drug target that may potentially limit LPA-induced invasive behavior in ovarian cancer cells.

VIII) Thesis Proposal and Central Hypothesis

Due to the high number of women presenting with peritoneal metastases at initial diagnosis, it is necessary to fully understand the processes that regulate ovarian cancer metastasis. Ovarian cancer metastasis is facilitated by three sequential processes: the exfoliation of cells from the primary tumor, the maintenance of ascitic multi-cellular aggregates, and the adherence and invasion of tumor cell in the peritoneal cavity [**Fig 1.1, page 19**]. Investigation of these processes is further complicated by the complexity of the ovarian tumor microenvironment as the primary tumor and peritoneal metastases remain in constant contact with a variety of factors that enhance cell dissemination and invasion.

This dissertation examines the hypothesis that reversible modulation of cell-cell adhesion, cell-matrix adhesion, and proteolytic activity play a critical role in the remodeling of the neoplastic ovarian epithelium during metastasis. The following model has been proposed, implicating collagen-binding integrins and LPA in the regulation of intra-peritoneal dissemination. Integrin engagement occurs when integrins are aggregated by collagen fragments in the ascites or by the collagen-rich submesothelial ECM; therefore, the effects on integrin engagement and cell dissemination and invasion are limited to these steps. In contrast, ovarian tumor cells are exposed to LPA very early in ovarian cancer progression as LPA levels are often

elevated in stage I patients, so LPA likely plays a role in enhancing cell dissemination and invasion during all three steps of ovarian cancer metastasis. The following aims have been proposed to test the role of these two prevalent factors, collagen and LPA, in the tumor microenvironment in the regulation of cell-cell adhesion and proteolytic expression and activity. Due to the rarity of E-cadherin gene mutations in ovarian tumors, Aims 1, 2, and 4 propose to identify alternative mechanisms that downregulate E-cadherin expression and/or function to facilitate ovarian cancer cell dissemination while Aims 1 and 3 consider the regulation of proteolytic activity and *in vitro* metastatic behavior.

Aim 1 (Chapter 2): Evaluate the initial effects of integrin activation on junctional localization of E-cadherin and β-catenin

Aim 2 (Chapter 3): Examine the intermediate temporal effects (within 24 hours) of integrin activation on E-cadherin regulation

Aim 3 (Chapter 4): Determine the role of COX-2 in LPA-induced proMMP-2 activation and subsequent migration and invasion of ovarian cancer cells

Aim 4 (Chapter 5): Examine the intermediate temporal effects (within 24 hours) of LPA on MMP-9 expression and E-cadherin regulation

Chapter 2: Engagement of collagen-binding integrins increases E-cadherin internalization and β-catenin-mediated transcription in ovarian cancer cells

Introduction and Rationale

Seventy-five percent of ovarian cancer patients present at initial diagnosis with disseminated intraperitoneal metastases with poor prognosis (Fishman and Borzorgi 2002), necessitating an understanding of the mechanisms that promote ovarian cancer metastasis. In contrast to other epithelial cell-derived cancers, the OSE undergoes an initial MET (Auersperg and others 1999) and E-cadherin expression is abundant in both primary tumors and peritoneal metastases (Davidson and others 2000; Fujimoto and others 1997; Fujioka and others 2001; Imai and others 2004; Maines-Bandiera and Auersperg 1997; Marques and others 2004; Wong and others 1999). Mutations in the E-cadherin gene are rare in ovarian carcinomas (Wong and Auersperg 2002), but other mechanisms may potentially downregulate E-cadherin expression and/or function, including defective E-cadherin recycling and trafficking (Bryant and Stow 2004).

Integrin-mediated signaling has been linked to modulation of cadherin function, localization, and/or expression (Avizienyte and others 2002; Menke and others 2001; Wang and others 2006b; Yano and others 2004; Zhang and others 2006), in addition to the regulation of proteolytic activity (Azzam and Thompson 1992; DiPersio and others 2000; Ellerbroek and others 1999; Ellerbroek and others 2001b; Fishman and others 1998; Ghosh and others 2000; Gilles and others 1997; Haas and others 1998; Seltzer and others 1994; Tomesek and others 1997), suggesting alterations in these processes can enhance ovarian cancer metastasis. As previously described in Chapter 1 (section II-C), E-cadherin endocytosis is necessary to regulate

the availability of E-cadherin for junction formation in development, tissue remodeling, and tumorigenesis. A small pool of E-cadherin cycling back and forth from the cell surface may mediate these processes (Bryant and Stow 2004). E-cadherin internalization also influences the amounts of free β-catenin that can translocate to the nucleus (Gottardi and others 2001). As previously mentioned in Chapter 1 (section III-B), β-catenin expression is increased in ovarian adenocarcinoma compared to normal ovarian tissue and benign adenomas, suggesting β-catenin's ability to transactivate transcription of its target genes is maintained as ovarian cancer development progresses and E-cadherin expression is upregulated (Rask and others 2003). The current study has been proposed to test the hypothesis that integrin signaling influences E-cadherin localization, function, and/or expression to upregulate the transcription of known Wnt/β-catenin target genes necessary for ovarian cancer metastasis. This dissertation now reports that aggregation of collagen-binding integrins increases E-cadherin internalization, GSK-3β inhibition, and β-catenin-mediated transcription, resulting in increased expression of proteinases important for ovarian cancer invasion. These studies describe a novel mechanism where ovarian cancer cell invasion is increased via an upregulation of proteinase expression despite maintenance of net E-cadherin expression.

Results

Effects of integrin aggregation on E-cadherin expression and localization.

As a consequence of intraperitoneal metastasis, clustering of collagen-binding integrins α2β1 and α3β1 occurs when disseminated ovarian tumor cells attach to the collagen-rich submesothelial ECM (Ghosh and others 2002) and the resulting metastases may exhibit reduced

E-cadherin expression when compared to the primary tumor (Fujimoto and others 1997; Fujioka and others 2001; Maines-Bandiera and Auersperg 1997; Marques and others 2004; Wong and others 1999). To determine if long-term integrin engagement downregulates net E-cadherin expression, OVCA433 cells were cultured on thin layer type I collagen matrix for 5 days. Whole cell lysates were prepared for western blot analysis of E-cadherin levels. Cells cultured on plastic served as a control. No changes in net E-cadherin expression were observed in cells cultured on type I collagen for 2,3, or 5 days [**Fig 2.1A**]. OVCA433 cells were repeatedly passaged back onto type I collagen for a total of one month and no permanent changes were observed in net E-cadherin expression or surface E-cadherin expression [**Fig 2.1B**]. E-cadherin expression was also evaluated using immunofluorescence microscopy. Interestingly, although no alterations in net E-cadherin expression were observed, E-cadherin was no longer localized to the cell periphery following cell growth on type I collagen, but instead displayed a more diffuse staining pattern [**Fig 2.1C**]. Upon further examination, this appeared to be a temporary or dynamic effect, as it was observed at two different time points (5 days and 5 weeks) (data not shown).

Unfortunately, it could not be determined based on the data in Figure 2.1B if E-cadherin redistribution was limited to the cell surface or if E-cadherin was internalized. In order to first determine if E-cadherin redistribution was due to changes in E-cadherin surface expression, OVCA433 cells were treated with bead-immobilized subunit-specific antibodies to α2, α3, or β1 integrin or control IgG to rapidly aggregate their integrins at earlier time points. After 1 hour, cells were surface labeled with cell-impermeable biotin and lysed [**Fig 2.2A**]. The resulting lysates were incubated with NeutrAvidin Protein to isolate the labeled proteins, which represents

the proteins remaining on the cell surface following short-term integrin engagement [**Fig 2.2B**]. As shown by western blotting, E-cadherin surface expression was rapidly decreased following engagement of integrins α2, α3, and β1. To verify that E-cadherin is internalized, OVCA433 cells were first labeled with a cleavable and cell-permeable form of biotin to detect E-cadherin that was internalized following aggregation of β1 integrins [**Fig 2.2C**]. After 1 hour of integrin aggregation, cells were then treated with MESNA to remove any biotin remaining on the cell surface. Internalized proteins were protected from MESNA-mediated biotin cleavage. As shown by western blotting, E-cadherin internalization was increased following short-term β1 integrin engagement [**Fig 2.2D**]. Because long-term integrin engagement did not permanently downregulate E-cadherin surface expression or net E-cadherin expression [**Fig 2.1**], internalized E-cadherin was either recycled back to the cell surface or degraded and resynthesized. Due to a lack of cell viability after several temperature shifts, it could not be determined using the internalization protocol described above if E-cadherin was recycled back to the cell surface. Instead, integrins were engaged in the presence of proteasome inhibitor MG-132 to determine if internalized E-cadherin was degraded [**Fig 2.2E**]. Increased E-cadherin expression was not observed in the presence of MG-132, suggesting E-cadherin was not proteasomally degraded upon internalization at this time point. This experiment will later be conducted in the presence of lysosomal inhibitors and recyling inhibitors to determine internalized E-cadherin's fate.

Figure 2.1

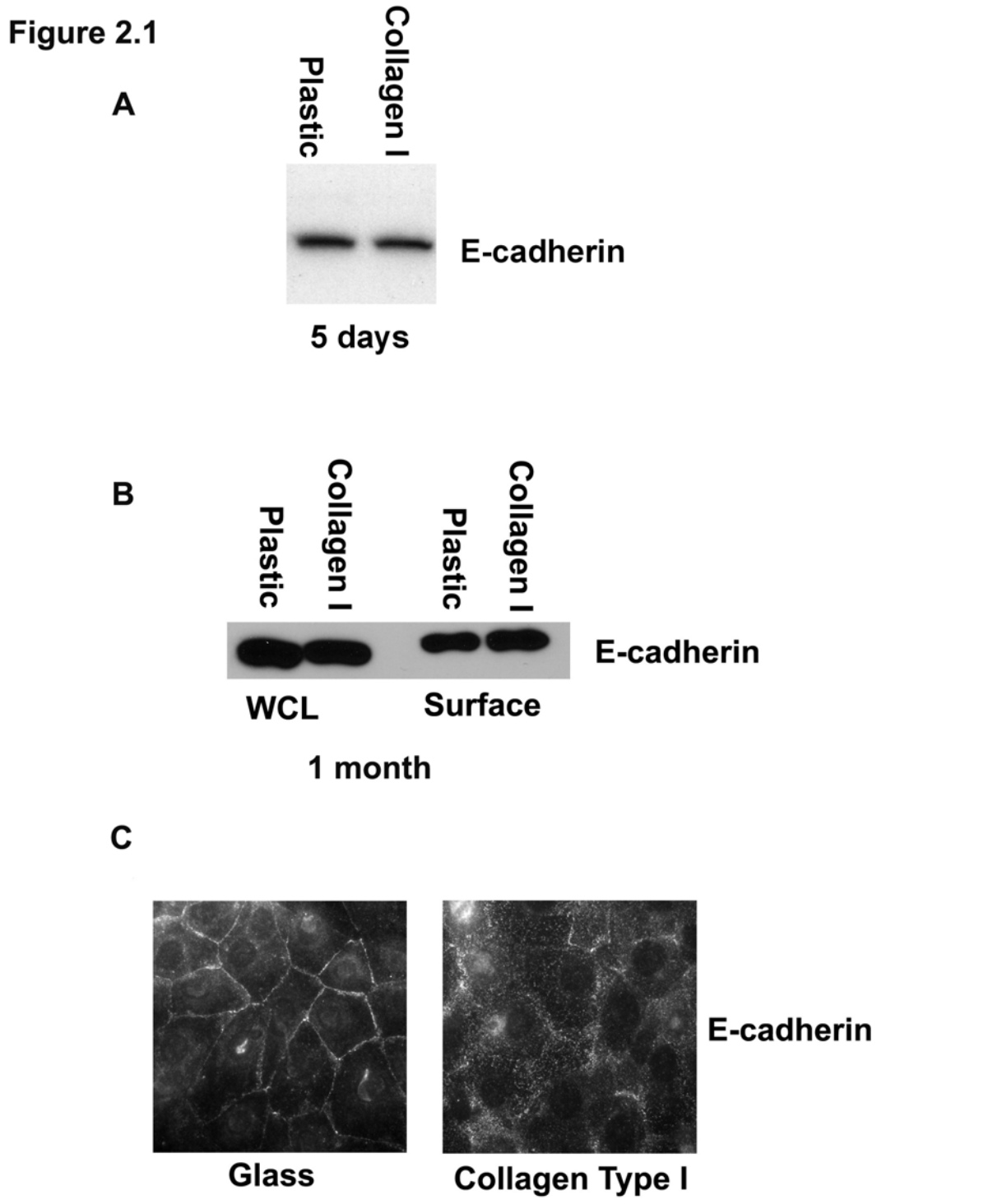
A
Plastic
Collagen I
E-cadherin
5 days
B
Plastic
Collagen I
Plastic
Collagen I
E-cadherin
WCL
Surface
1 month
C
Glass
Collagen Type I
E-cadherin

Figure 2.1: Engagement of collagen-binding integrins promotes E-cadherin redistribution, but no change in net E-cadherin expression.

A) OVCA433 cells were cultured on thin layer collagen type I collagen coated tissue culture dishes or plastic dishes for 5 days. Whole cell lysates (25μg) were electrophoresed on a 9% SDS-PAGE gel, transferred to a PVDF membrane, and immunoblotted with anti-E-cadherin (HECD-1) (1:4000), followed by peroxidase-conjugated secondary antibody (1:5000) and enhanced chemiluminescence detection.

B) OVCA433 cells were repeatedly passaged back onto plastic or type I collagen coated tissue culture dishes for a total of 1 month. Cells were processed for analysis of whole cell lysates and surface proteins, as indicated. Whole cell lysates (20μg) were electrophoresed on a 9% SDS-PAGE gel, transferred to a PVDF membrane, and immunoblotted with anti-E-cadherin (HECD-1) (1:4000), followed by peroxidase-conjugated secondary antibody (1:5000) and enhanced chemiluminescence detection. Full length E-cadherin (120kDa) was detected. To evaluate the amount of E-cadherin present on the cell surface, cells were surface-biotinylated, lysed, and lysates (45μg) incubated with NeutrAvidin. Following incubation, the NeutrAvidin-conjugated lysates and resulting supernatant were electrophoresed on a 9% SDS-PAGE gel, transferred to a PVDF membrane, and immunoblotted with anti-E-cadherin (HECD-1) (1:4000), followed by peroxidase-conjugated secondary antibody (1:5000) and enhanced chemiluminescence detection to examine the surface E-cadherin expression. An appropriate surface expression loading control was not available since integrin engagement also promoted internalization of the transferrin receptor.

C) OVCA433 cells were cultured on type I collagen coated coverslips or on glass coverslips as a control for a total of 5 weeks. Cells were then processed for immunofluorescence using anti-E-cadherin (HECD-1) (1:300 dilution) and FITC-conjugated IgG, as described in Chapter 7 (20X magnification).

Figure 2.2A

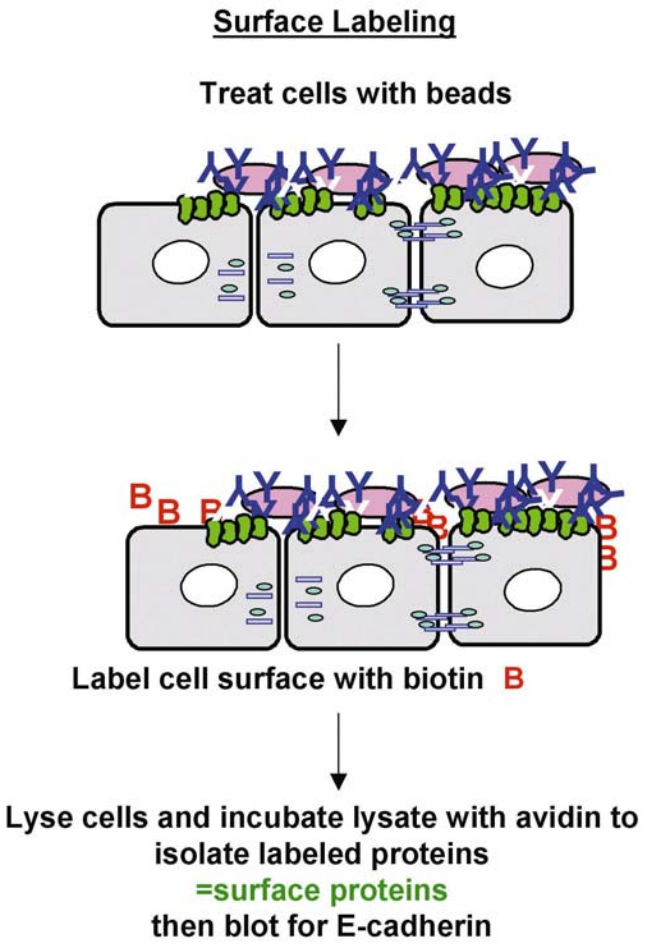
Surface Labeling
Treat cells with beads
Label cell surface with biotin B
Lyse cells and incubate lysate with avidin to isolate labeled proteins
=surface proteins
then blot for E-cadherin

Figure 2.2B

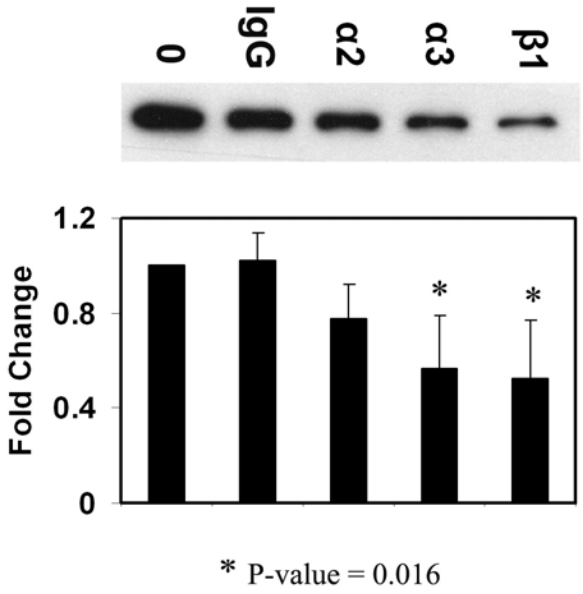

* P-value = 0.016

Figure 2.2C

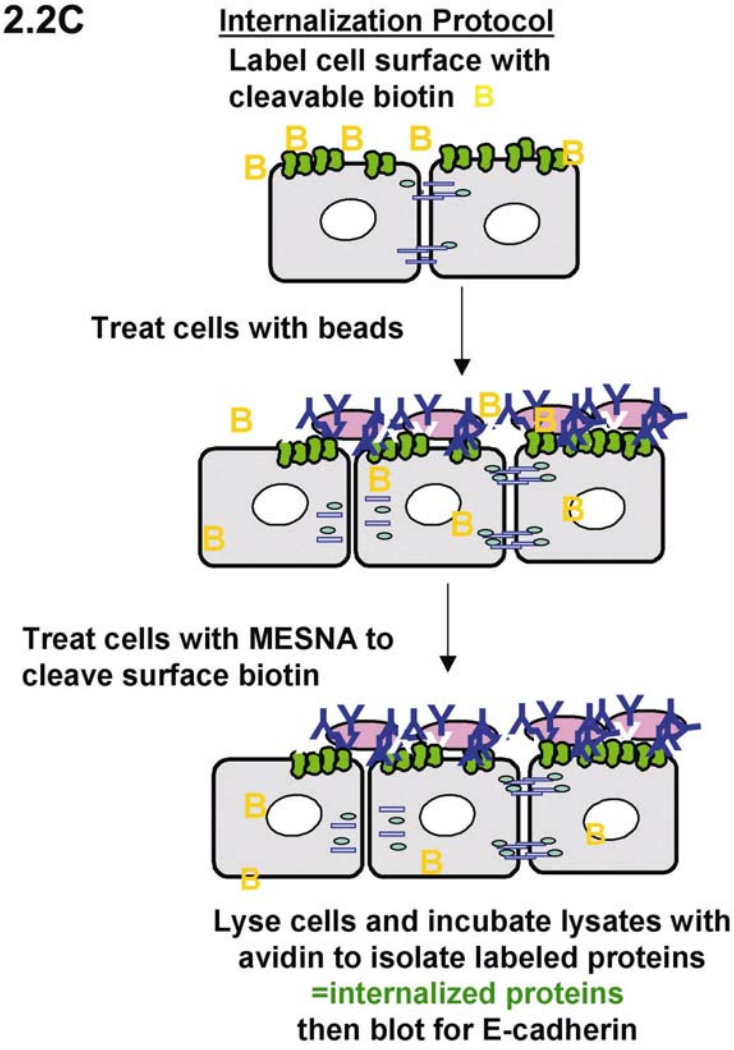
Internalization Protocol
Label cell surface with cleavable biotin B
Treat cells with beads
Treat cells with MESNA to cleave surface biotin
Lyse cells and incubate lysates with avidin to isolate labeled proteins
=internalized proteins
then blot for E-cadherin

Figure 2.2D

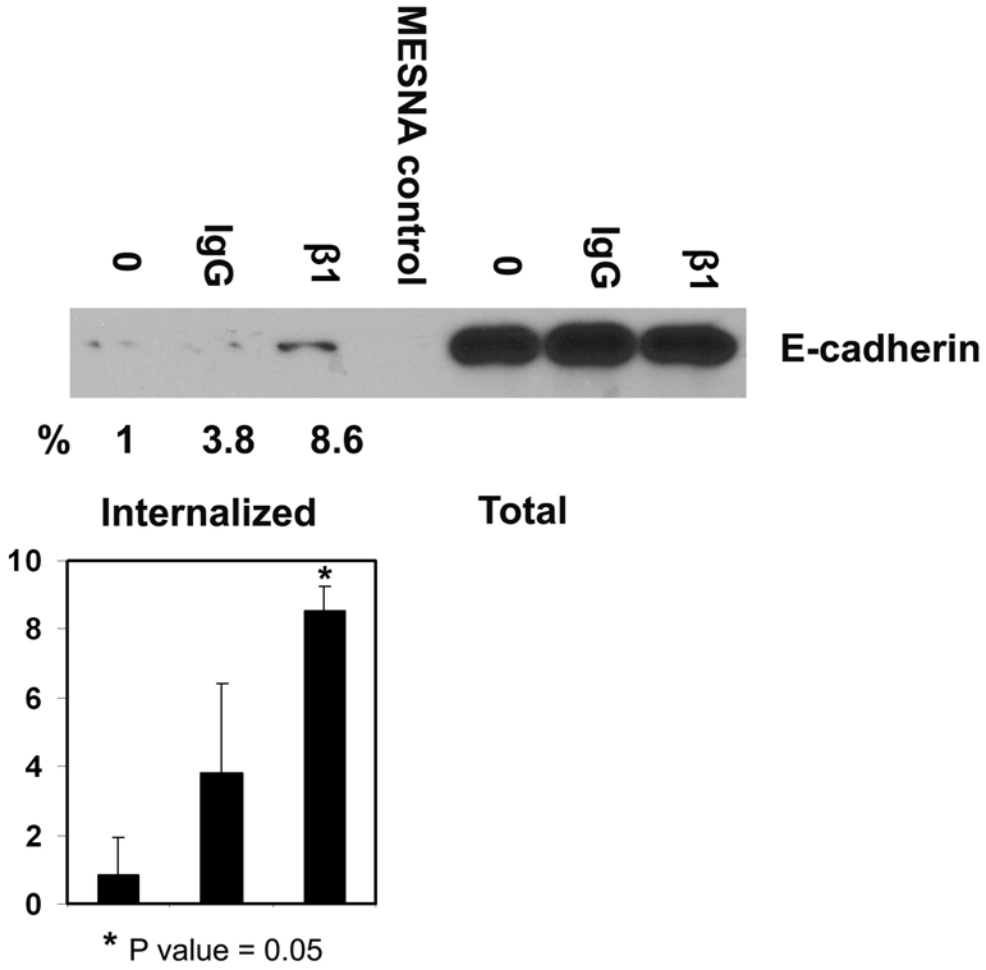
MESNA control
0
IgG
β1
0
IgG
β1
E-cadherin
% 1 3.8 8.6
Internalized
Total
10
8
6
4
2
0
*
* P value = 0.05

Figure 2.2E

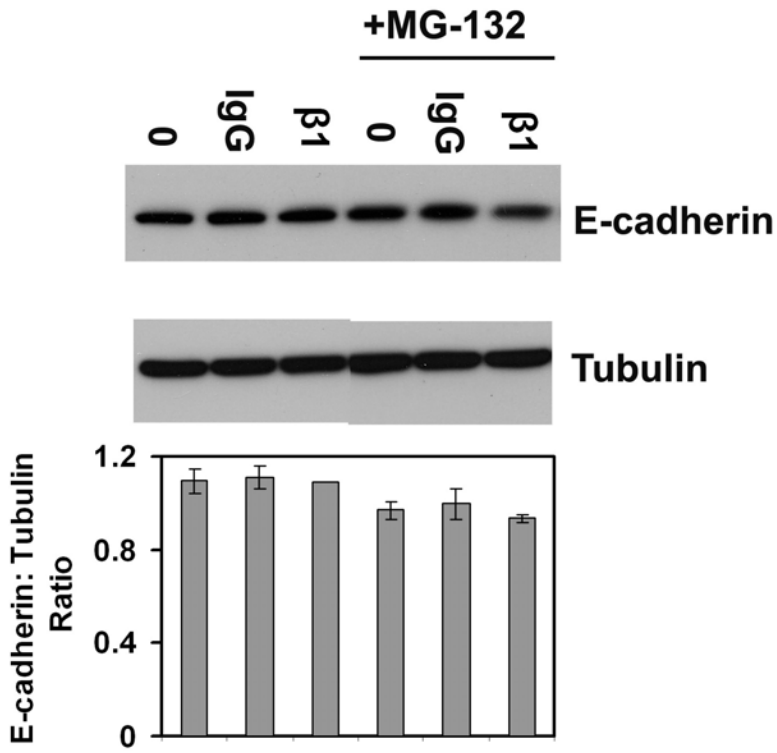
+MG-132
0
IgG
β1
0
IgG
β1
E-cadherin
Tubulin
E-cadherin: Tubulin Ratio
1.2
0.8
0.4
0

Figure 2.2: Engagement of collagen-binding integrins increases E-cadherin internalization

A) The method used to surface label OVCA433 cells with biotin following integrin aggregation was described in the following diagram. Cells were first treated with latex beads at 37°C to induce integrin engagement for 1 hour. After 1 hour, cells were placed on ice and surface labeled with cell-impermable biotin. The cells were then lysed and the resulting lusates were incubated overnight with NeutrAvidin to isolate proteins remaining on the cell surface following integrin engagement. These isolated proteins were then examined for changes in E-cadherin surface expression using western blotting. This protocol was also described in more detail in Chapter 7.

B) OVCA433 cells were treated with control IgG, anti-integrin α2, anti-integrin α3, or anti-integrin β1 immobilized to latex beads (as indicated) for 1 hour. To evaluate the amount of E-cadherin present on the cell surface, cells were surface-biotinylated, lysed, and lysates (60-100μg) were incubated with NeutrAvidin. Following incubation, the NeutrAvidin-conjugated lysates and resulting supernatant were electrophoresed on a 9% SDS-PAGE gel, transferred to a PVDF membrane, and immunoblotted with anti-E-cadherin (HECD-1) (1:4000), followed by peroxidase-conjugated secondary antibody (1:5000) and enhanced chemiluminescence detection to examine the surface E-cadherin expression. A representative western blot and densitometric quantification of E-cadherin were shown. Results were normalized against the densitometric reading for untreated cells (first lane) and represent four independent experiments, with the exception of results for cells treated with α2 beads, which represent two independent

experiments. An appropriate surface expression loading control was not available since integrin engagement also promoted internalization of the transferrin receptor.

C) The method used to isolate internalized E-cadherin following integrin was described in the following diagram. Cells were first surface labeled on ice with a cleavable form of biotin. The cells were then treated with magnetic beads to induce integrin aggregation for 1 hour at 37°C. After 1 hour, the cells were treated with MESNA at room temperature to cleave any biotin still remaining on the cell surface; internalized biotin was protected from MESNA-mediated cleavage. The cells were then lysed and the lysates were incubated with NeutrAvidin to isolate any proteins that were internalized from the cell surface in response to integrin engagement. These isolated proteins were then examined for changes in internalized E-cadherin expression using western blotting. This protocol was also described in more detail in Chapter 7.

D) OVCA433 cells were labeled with a cleavable form of biotin on ice. Warm cell culture media (37ºC) was added to the cells with 20µl of magnetic beads coated with β1 integrin antibody. After a 1 hour incubation at 37ºC, cells were treated with MESNA and iodoacetamide at room temperature to strip off any biotin remaining on the cell surface. The cells were then lysed and lysates (50-100µg) were incubated with NeutrAvidin to isolate the labeled surface proteins that were internalized following integrin engagement. In control experiments, the MESNA step was not included to allow analysis of total labeled protein (internalized and cell surface pool). Cells were also kept on ice during the course of the experiment to determine the efficiency of surface stripping with MESNA (MESNA control). A representative western blot and densitometric

quantification of internalized E-cadherin were shown. Results were normalized against the densitometric reading for the MESNA control and the corresponding densitometric reading for total labeled E-cadherin expression. These results represent the percentage of internalized E-cadherin relative to total E-cadherin and include three independent experiments.

E) OVCA433 cells were pretreated with MG-132 (20μg/ml) or equivalent DMSO prior to treatment with control IgG or anti-integrin β1 immobilized to latex beads (as indicated) for 90 minutes. Whole cell lysates (40-50μg) were electrophoresed on a 9% SDS-PAGE gel, transferred to a PVDF membrane, and immunoblotted with anti-E-cadherin (HECD-1) (1:4000), followed by peroxidase-conjugated secondary antibody (1:5000) and enhanced chemiluminescence detection. Full length E-cadherin (120kDa) was detected. Tubulin was used as a loading control. A representative western blot and densitometric quantification of E-cadherin were shown. Results were normalized against the corresponding densitometric reading for tubulin and represent two independent experiments.

Effect of integrin aggregation on β-catenin localization and function

β-catenin is often sequestered by E-cadherin at cell-cell junctions (Gottardi and others 2001). To determine the fate of β-catenin following E-cadherin internalization, the western blot in Figure 2.2A was stripped and reprobed for β-catenin [**Fig 2.3A**]. As expected, as surface E-cadherin levels diminished, surface E-cadherin associated β-catenin levels were also decreased, but it remained unclear if β-catenin was released from E-cadherin. To determine if β-catenin remained bound to internalized E-cadherin, the western blot in Figure 2.2D was stripped and reprobed for β-catenin [**Fig 2.3B**]. A very small amount of β-catenin remained associated with internalized E-cadherin, suggesting a portion of β-catenin may be released from internalized E-cadherin. To further verify this observation, future experiments will examine the disruption of the E-cadherin-β-catenin complex following integrin aggregation. It could still not be determined if β-catenin translocated to the nucleus or was targeted for degradation in the cytoplasm following integrin aggregation, so whole cell lysates were examined for the presence of active β-catenin following short-term engagement of β1 integrins [**Fig 2.3C**]. The active form of β-catenin is dephosphorylated at residue Ser37 or Thr4, which targets it for degradation when phosphorylated (van Noort and others 2002). Active β-catenin expression was increased following integrin engagement. To further verify that active β-catenin was translocating to the nucleus, cells were transfected with the TOPflash luciferase reporter construct to measure β-catenin-mediated transcription following 32 hours of integrin engagement [**Fig 2.3D**]. The ratios represent the TOPflash reading normalized to the corresponding control FOPflash reading. Both readings were also normalized to a Renilla luciferase signal to account for transfection efficiency. TOPflash activity was significantly increased almost 2-fold following engagement of

β1 integrins when compared to control cells, suggesting that β-catenin transcriptionally activates Tcf/Lef-regulated genes in response to integrin engagement.

GSK-3β phosphorylates β-catenin when it is complexed with APC and Axin and targets it for ubiquitination and degradation, preventing the translocation of β-catenin to the nucleus (Dihlmann and others 2005; Nelson and Nusse 2004). The ability to target β-catenin for degradation is inhibited when GSK-3β is phosphorylated on serine residue 9 (Srivastava and Pandey 1998). To determine if integrin-mediated signaling enhances phosphorylation and inhibition of GSK-3β, whole cell lysates were examined following 3 to 4 hours of integrin aggregation. GSK-3β phosphorylation was increased when β1 integrins were clustered [**Fig 2.3E**]. Additional experiments are currently in progress to explore preliminary evidence suggesting a Src family kinase phosphorylates GSK-3β to partially decrease it ability to target β-catenin for degradation.

Several known β-catenin/Wnt target genes are upregulated in ovarian tumors (Schwartz 2003) and potentially enhance invasion and subsequent metastasis. Protein levels of Wnt/β-catenin target genes COX-2 (Araki and others 2003)[**Fig 2.4B**], MMP-7 (Crawford and others 1999) [**Fig 2.5A, black bars (Flag)**], and MT1-MMP (Takahashi and others 2002) [**Fig 2.4C**] were increased following integrin engagement, as shown by western blotting. In addition, the activity of another Wnt/β-catenin target gene, uPA (Hiendlmeyer and others 2004), was increased as determined by a coupled colorimetric assay [**Fig 2.4D**]. Expression of cyclin D1 [**Fig 2.4A**] remained constant despite integrin engagement. To verify that integrin engagement increased target gene expression via a β-catenin-mediated signaling mechanism, cells were transiently transfected with ICAT, an endogenous inhibitor that binds β-catenin to compete with

its interaction with TCF (Gottardi and Gumbiner 2004b), and integrins were aggregated using antibody coated beads. Currently, only the effects on uPA and MMP-7 were examined. uPA activity was reduced approximately 15-20% in cells transfected with ICAT when compared to cells transfected with the control vector (Flag) [**Fig 2.5B**]. ProMMP-7 protein levels were reduced approximately 40-50% when cells were transfected with ICAT [**Fig 2.5A**]. These experiments need to be repeated to verify these results. Together, these studies involving β-catenin-mediated transcription provide evidence for a mechanism that may promote ovarian cancer invasion and metastasis via the upregulation of proteinases and without the downregulation of E-cadherin expression.

Figure 2.3

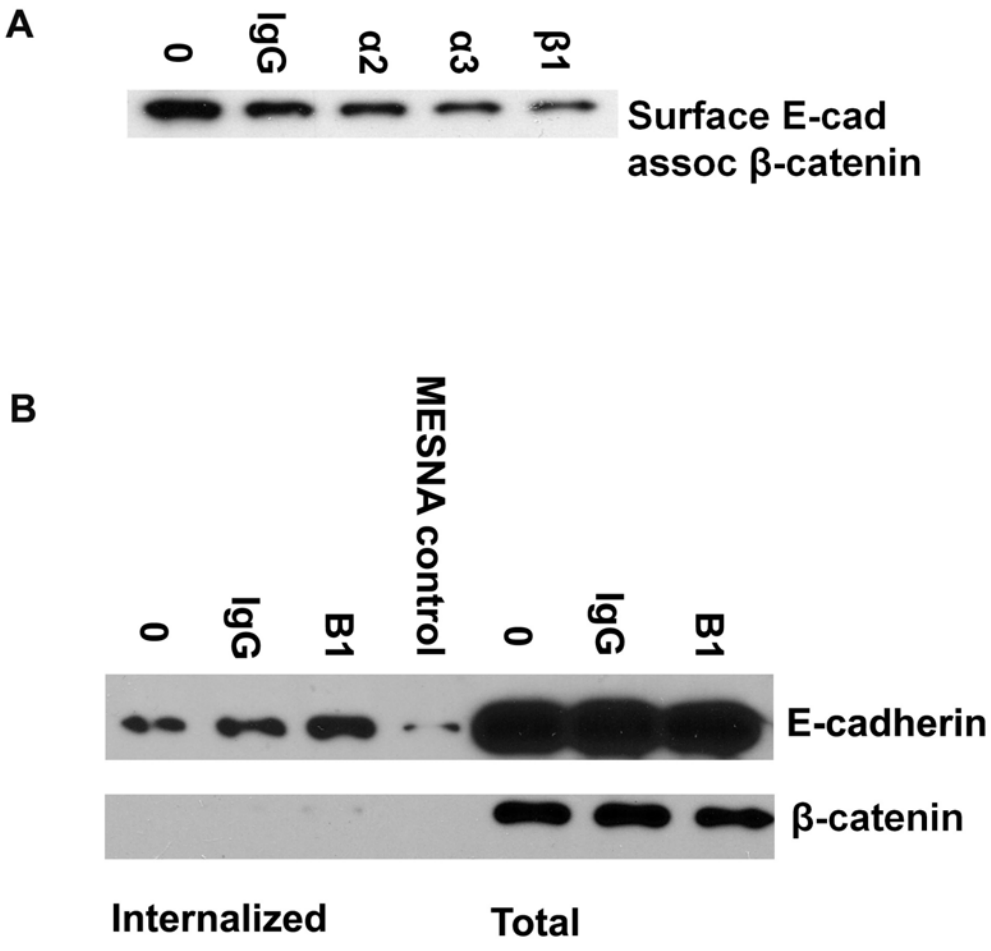
A
0
IgG
α2
α3
β1
Surface E-cad
assoc β-catenin
B
MESNA control
0
IgG
B1
0
IgG
B1
E-cadherin
β-catenin
Internalized
Total

Figure 2.3

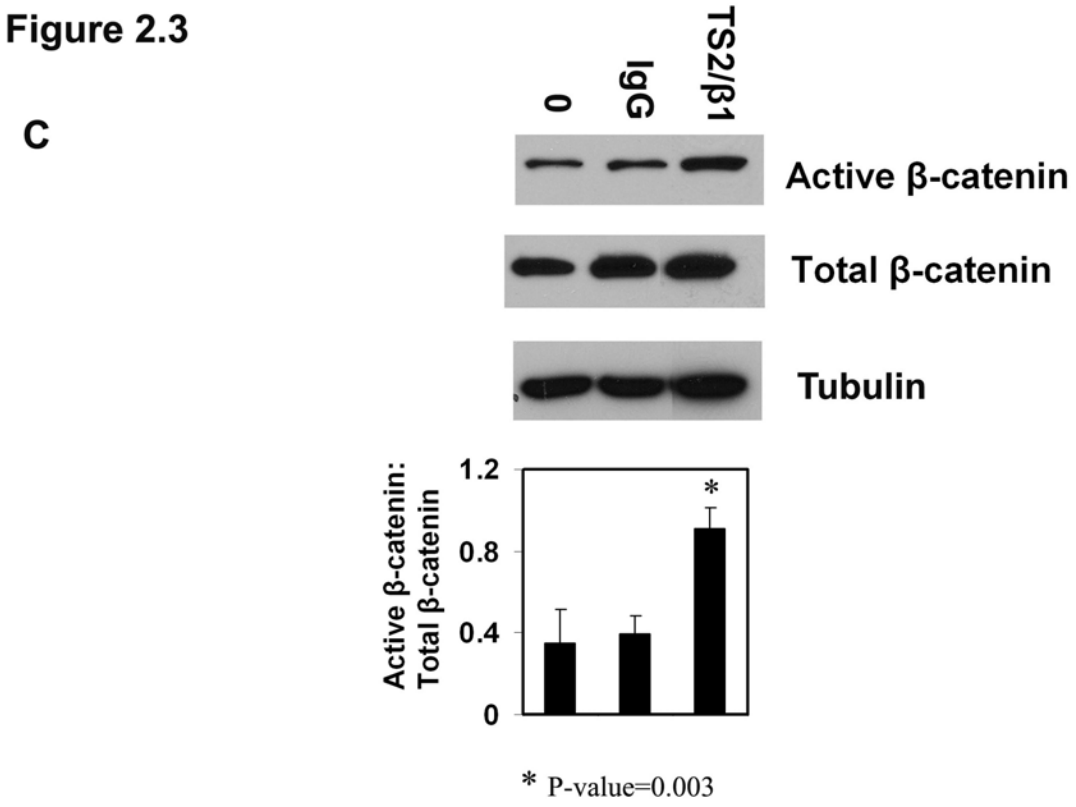
C
0
IgG
TS2/β1
Active β-catenin
Total β-catenin
Tubulin
Active β-catenin:
Total β-catenin
1.2
0.8
0.4
0
*
* P-value=0.003
D
Topflash Activity
topflash/FOP ratio
2.5
2
1.5
1
0.5
0
P-value = 0.022
1.538
0.886
IgG
TS2/β1

Figure 2.3E

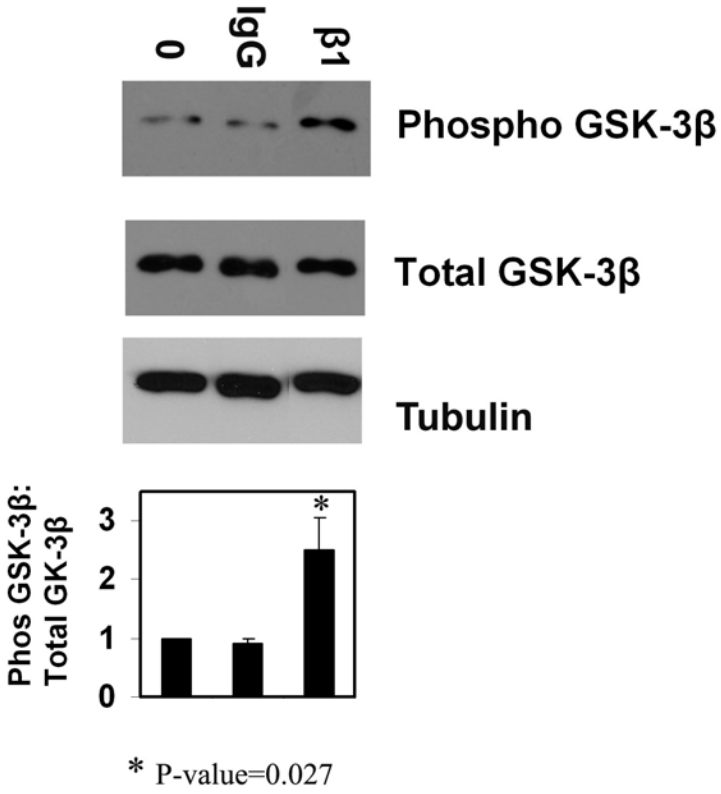

* P-value=0.027

Figure 2.3: Integrin engagement and subsequent E-cadherin internalization results in increased β-catenin-mediated transcription.

A) The western blot shown in Figure 2.2B was stripped and immunoblotted with anti-β-catenin (1:1000), followed by peroxidase-conjugated secondary antibody (1:5000) and enhanced chemiluminescence detection to examine changes surface E-cadherin associated β-catenin expression.

B) The western blot shown in Figure 2.2D was stripped and immunoblotted with anti-β-catenin (1:1000), followed by peroxidase-conjugated secondary antibody (1:5000) and enhanced chemiluminescence detection to examine changes in internalized E-cadherin associated β-catenin expression (bottom panel). The western blot for E-cadherin was also shown at a later exposure time (top panel) compared to the original blot in Figure 2.2D to better examine internalized E-cadherin associated β-catenin levels. Both E-cadherin and β-catenin western blots in this figure were exposed for the same amount of time.

C) OVCA433 cells were cultured in low calcium (0.1mM $CaCl_2$) serum containing media for 1 hour prior to treatment with control IgG or anti-integrin β1/TS2 immobilized to latex beads (as indicated) for 90 minutes. Whole cell lysates (15-40μg) were electrophoresed on a 9% SDS-PAGE gel, transferred to a PVDF membrane, and immunoblotted with anti-active β-catenin (dephospho form) (1:1000), anti- β-catenin , or anti-tubulin followed by peroxidase-conjugated secondary antibody (1:5000) and enhanced chemiluminescence detection. A representative western blot and densitometric quantification of active β-catenin were shown. Results were normalized against the corresponding densitometric readings for total β-catenin and represent three independent experiments.

D) OVCA433 cells were transiently cotransfected with a Renilla luciferase reporter construct (pRL-CMV) and either the firefly luciferase TOPflash TCF Reporter Plasmid or FOPflash TCF mutant Reporter Plasmid. Cells were cultured in low calcium (0.1mM $CaCl_2$) serum containing media for 1 hour prior to treatment with control IgG or anti-integrin β1/TS2 immobilized to latex beads for 30 hours. Firefly luciferase readings were first normalized to the reading for the corresponding Renilla luciferase reading to account for transfection efficiency. The adjusted TOPflash reading was then normalized to the corresponding adjusted FOPflash reading to account for background reading of the TOPflash construct. The results are representative of 5 separate experiments.

E) OVCA433 cells were cultured in serum-free media prior to treatment with control IgG or anti-integrin β1 immobilized to latex beads (as indicated) for 3 to 4 hours. Whole cell lysates (20-40μg) were electrophoresed on a 9% SDS-PAGE gel, transferred to a PVDF membrane, and immunoblotted with anti-phospho GSK-3β (Ser9), anti-GSK-3β, or anti-tubulin (1:1000) followed by peroxidase-conjugated secondary antibody (1:5000) and enhanced chemiluminescence detection. A representative western blot and densitometric quantification of phospho GSK-3β were shown. Results were normalized against the corresponding densitometric readings for total GSK-3β and represent three independent experiments.

Figure 2.4

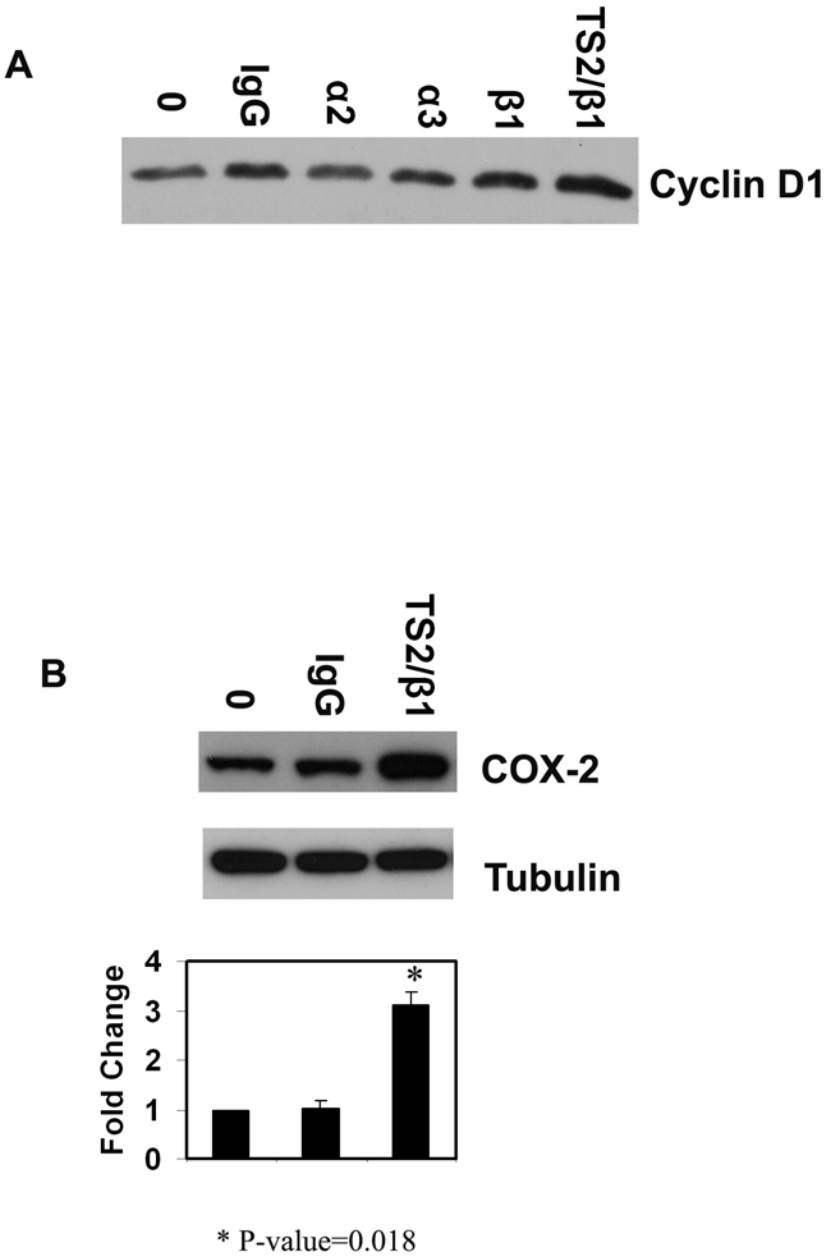

* P-value=0.018

Figure 2.4

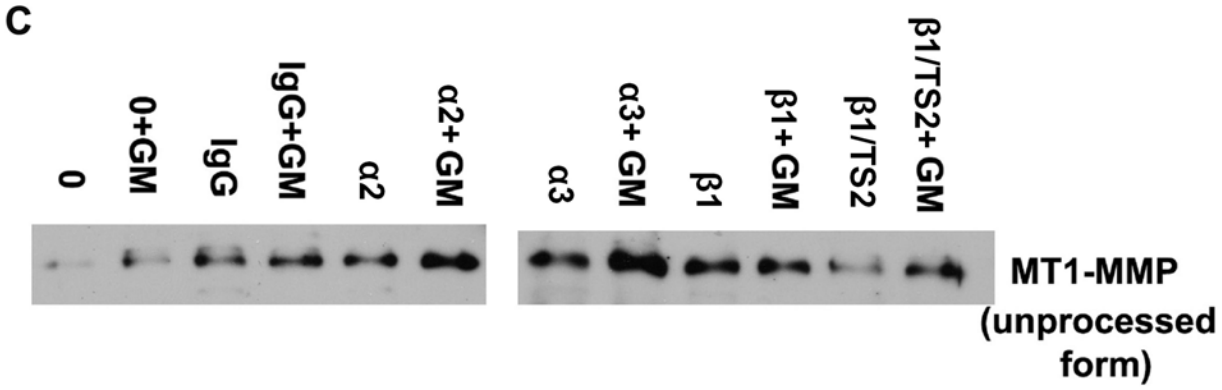
C
0
0+GM
IgG
IgG+GM
α2
α2+ GM
α3
α3+ GM
β1
β1+ GM
β1/TS2
β1/TS2+ GM
MT1-MMP
(unprocessed
form)

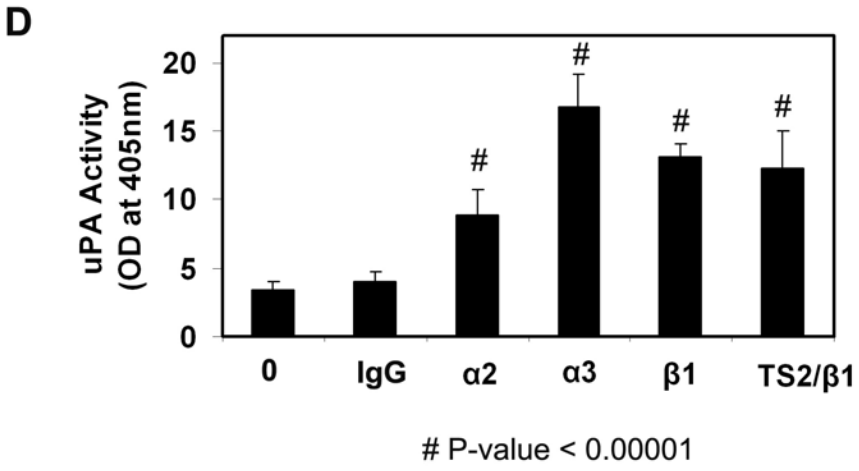
D
uPA Activity
(OD at 405nm)
20
15
10
5
0
#
#
#
#
0
IgG
α2
α3
β1
TS2/β1
P-value < 0.00001

Figure 2.4: Engagement of collagen-binding integrins increases protein expression of known Wnt/β-catenin target genes

A) OVCA433 cells were serum starved overnight and incubated in serum-free low calcium (0.1mM $CaCl_2$) MEM for 1 hour. Cells were then treated with control IgG, anti-integrin α2, anti-integrin α3, anti-integrin β1, or anti-integrin β1/TS2 immobilized to latex beads (as indicated) for 4 hours in serum-free low calcium MEM. Whole cell lysates (40μg) were electrophoresed on a 9% SDS-PAGE gel, transferred to a PVDF membrane, and immunoblotted with anti-cyclin D1 followed by peroxidase-conjugated secondary antibody (1:5000) and enhanced chemiluminescence detection. Results represent one experiment.

B) OVCA433 cells were serum starved overnight and prior to treatment with control IgG, or anti-integrin β1/TS2 immobilized to latex beads (as indicated) for 4 hours. Whole cell lysates (40μg) were electrophoresed on a 9% SDS-PAGE gel, transferred to a PVDF membrane, and immunoblotted with anti-COX-2 or anti-tubulin (1:1000) followed by peroxidase-conjugated secondary antibody (1:5000) and enhanced chemiluminescence detection. A representative western blot and densitometric quantification of COX-2 were shown. Tubulin was used as a loading control. Results were normalized against the corresponding densitometric readings for untreated cells (first lane) and represent two independent experiments. One experiment was conducted in serum-free low calcium MEM while the other experiment was conducted in serum-free MEM.

C) OVCA433 cells were pretreated with GM6001 (50μM) or DMSO and incubated in low calcium (0.1mM $CaCl_2$) MEM prior to treatment with control IgG, anti-integrin α2, anti-integrin α3, anti-integrin β1, or anti-integrin β1/TS2. Cells were surface-biotinylated, lysed, and lysates

(80μg) were incubated with NeutrAvidin. Following incubation, the NeutrAvidin-conjugated lysates and resulting supernatant were electrophoresed on a 12% SDS-PAGE gel, transferred to a PVDF membrane, and immunoblotted with anti-MT1-MMP (1:1000), followed by peroxidase-conjugated secondary antibody (1:5000) and enhanced chemiluminescence detection. An appropriate surface expression loading control was not available since integrin engagement also promoted internalization of the transferrin receptor. Results represent one experiment.

D) OVCA433 cells were serum starved overnight and prior to treatment with control IgG, anti-integrin α2, anti-integrin α3, anti-integrin β1, or anti-integrin β1/TS2 immobilized to latex beads (as indicated) for 36 hours. Net plasminogen activity was evaluated in conditioned media using a coupled assay to monitor plasminogen activation and the resulting plasmin hydrolysis of a colored substrate. The results were normalized against the reading for untreated cells and represent three independent experiments done in triplicate.

Figure 2.5A

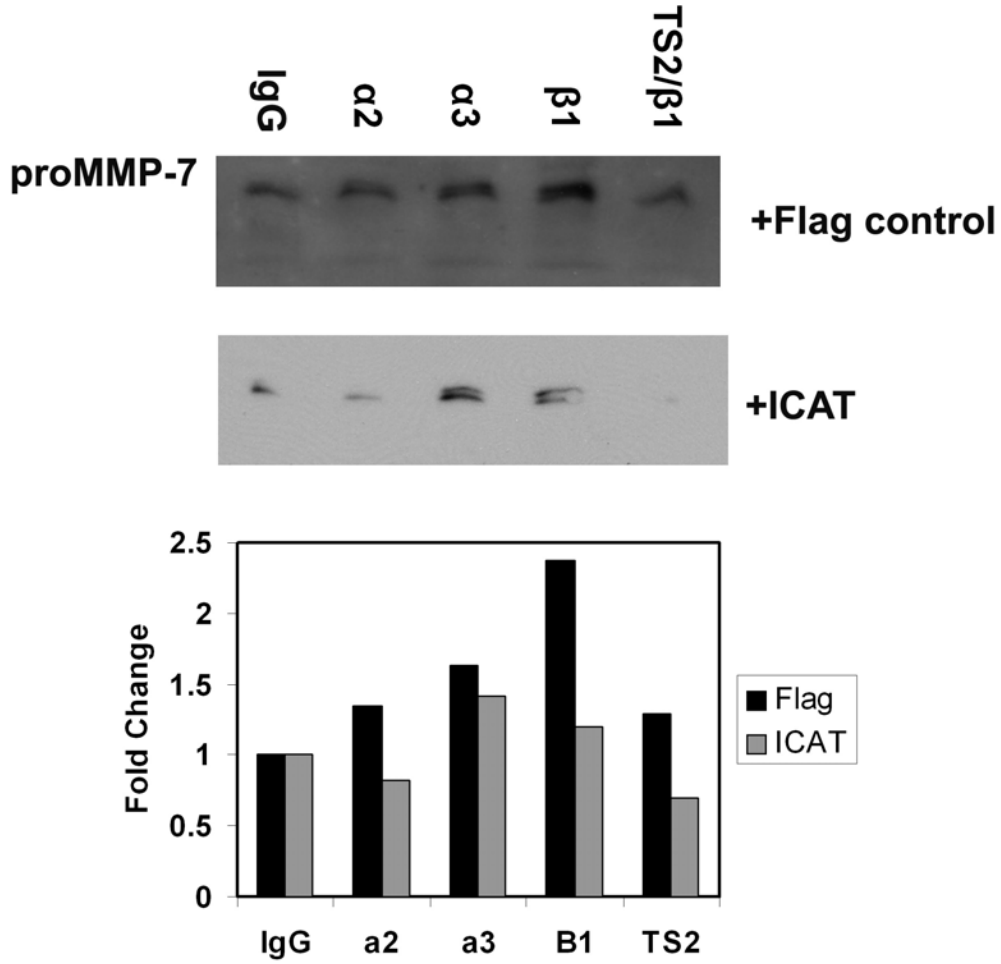

Reduction in proMMP-7 expression with ICAT

α2	39%
α3	13%
β1	50%
TS2/β1	46%

Figure 2.5B

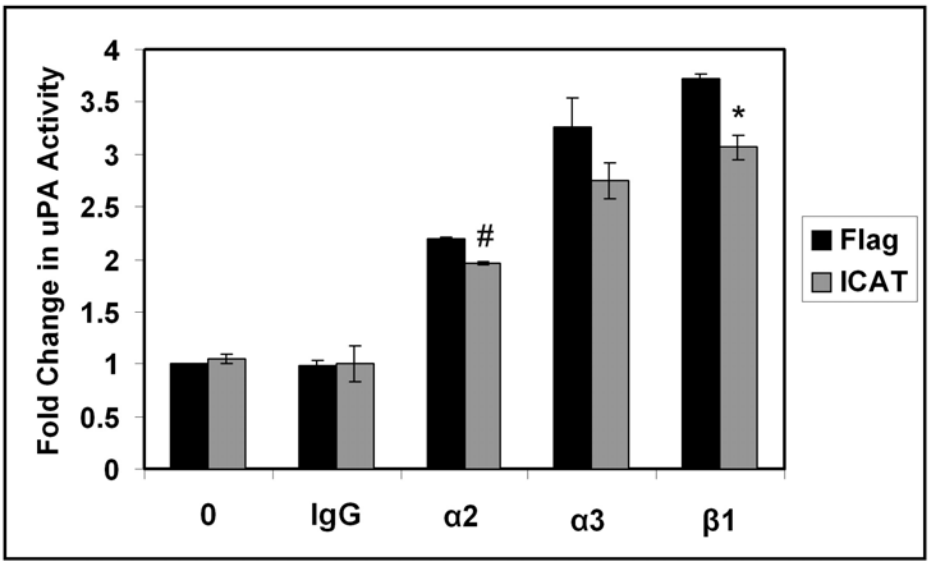

Reduction in uPA activity with ICAT	
0	0%
IgG	0%
α2	11%
α3	16%
β1	18%

P-value = 0.007

* P-value = 0.03

Figure 2.5: ICAT expression reduces protein expression of β-catenin target genes MMP-7 and uPA.

A) OVCA433 cells were transiently transfected using Fugene 6 with ICAT or a control Flag-tagged vector (Flag) and then replated at $0.75x10^5$ cells/ml. Cells were then serum starved overnight prior to treatment with control IgG, anti-integrin α2, anti-integrin α3, or anti-integrin β1 immobilized to latex beads (as indicated) for 36 hours. The resulting conditioned media was concentrated using a YM-10 microcon concentrator and electrophoresed on a 12% SDS-PAGE gel, transferred to a PVDF membrane, and immunoblotted with anti-MMP-7 (total) (1:500) followed by peroxidase-conjugated secondary antibody (1:5000) and enhanced chemiluminescence detection. A densitometric quantification of proMMP-7 was shown. Results were normalized against the corresponding densitometric readings for IgG treated cells (first lane) and represent one experiment. The reduction in proMMP-7 expression due to ICAT transfection was indicated below the quantification.

B) OVCA433 cells were transiently transfected using Fugene 6 with ICAT or a control Flag-tagged vector (Flag) and then replated at $0.75x10^5$ cells/ml. Cells were then serum starved overnight prior to treatment with control IgG, anti-integrin α2, anti-integrin α3, or anti-integrin β1 immobilized to latex beads (as indicated) for 36 hours. Conditioned media was evaluated for uPA activity using a coupled assay to monitor plasminogen activation and the resulting plasmin hydrolysis of a colored substrate. Results were normalized against the densitometric readings for untreated Flag transfected cells and the reduction in uPA activity due to ICAT transfection was indicated below the quantification. The results represent two independent experiments done in triplicate.

Functional effect of inhibition of β-catenin signaling on cell invasion

To determine the effect of β-catenin signaling on cell invasion *in vitro*, OVCA433 cells were transiently transfected with ICAT or the control Flag-tagged vector (Flag) and then seeded in Boyden chambers overlaid with Matrigel. Serum-containing cell culture medium was used a chemoattractant. After 24 hours, invasive activity was reduced in the OVCA433 cells transiently expressing ICAT [**Fig 2.6**], suggesting that upregulation of proteinases that are also Wnt/β-catenin target genes play a role in ovarian cancer cell invasion. This experiment will also be repeated using Boyden chambers overlaid with collagen to better model ovarian cancer cells adhering to the exposed collagen-rich submesothelial ECM.

Figure 2.6

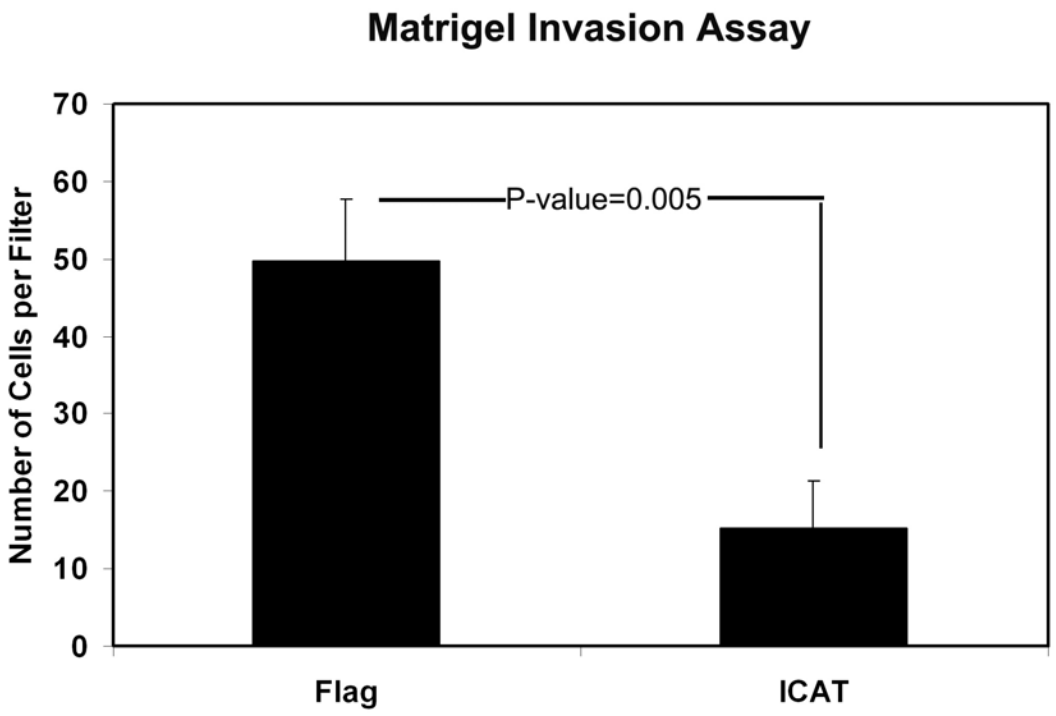
Matrigel Invasion Assay
Number of Cells per Filter
70
60
50
40
30
20
10
0
P-value=0.005
Flag
ICAT

Figure 2.6: Effect of ICAT on cell invasive activity

OVCA433 cells were transiently transfected with either ICAT or a control Flag-tagged vector (Flag) and $2.5x10^5$ cells were added to each porous polycarbonate filters (8μm pore) coated with Matrigel. Serum-containing cell culture medium was added to the bottom well to serve as a chemoattractant. After 24 hours, the filters were collected and stained and cells were counted. Data represent the total number of cells per filter for three experiments done in triplicate.

Discussion

Previous data from Dr. Stack and colleagues demonstrating integrin-regulated proteinase expression in EOC cells suggest a potential functional link between integrin engagement, enhanced proteolytic activity, and modulation of E-cadherin function (Chapter 3)(Ellerbroek 1999 and others; Ellerbroek and others 2001b). Although integrin signaling is linked to modulating β-catenin-mediated transcription (Koenig and others 2006; Oloumi and others 2004) and altering E-cadherin localization (Avizienyte and others 2002), the ability of integrins to regulate E-cadherin internalization to increase proteinase activity is mostly unexplored. The new results presented in this dissertation now show that engagement of collagen-binding integrins increases E-cadherin internalization and GSK-3β inhibition, allowing β-catenin to translocate to the nucleus to upregulate the transcription of proteinases relevant for ovarian cancer metastasis [**Fig 2.7**].

Due to the gain of E-cadherin expression as ovarian cancers develop (Auersperg and others 1999), it is difficult to predict how β-catenin-mediated transcription may be affected in these tumors. It has been suggested that E-cadherin acts as a tumor suppressor by sequestering β-catenin, blocking its translocation to the nucleus, and subsequent upregulation of Wnt target genes (Gottardi and others 2001); therefore, it is predicted that β-catenin-mediated transcription would be decreased as ovarian tumors develop, but mechanisms of β-catenin regulation have recently proven to be more complex. For example, as discussed in Chapter 1 (section III-A), Gottardi and Gumbiner show that β-catenin exists in the cell in distinct molecular forms with different binding properties, which determine its ability to participate in adhesion or Wnt

signaling [**Fig 1.5**] (Gottardi and Gumbiner 2004a). Another study has also shown that a gain of E-cadherin expression does not suppress invasion by downregulating β-catenin-mediated transcription. E-cadherin adhesion inhibits invasion in cancer cell lines, but invasion suppression is actually mediated by the β-catenin binding domain on E-cadherin's cytoplasmic tail or by depletion of β-catenin. Changes in the expression of β-catenin/TCF target genes are not needed to facilitate E-cadherin's invasion suppressor activity (Wong and Gumbiner 2003), suggesting a gain of E-cadherin expression will not always inhibit β-catenin-mediated transcription.

In support of the findings presented in this dissertation, two studies report that β-catenin is increased in ovarian adenocarcinoma compared to normal ovarian tissue and benign adenomas, suggesting β-catenin's ability to transactivate transcription of Wnt/β-catenin target genes is maintained as ovarian cancer development progresses and E-cadherin expression is upregulated (Marques and others 2004; Rask and others 2003). β-catenin nuclear expression is considered an indicator of good prognosis where membranous expression of β-catenin was an indicator of a poor outcome, but this study only examines stage I and II ovarian tumors (Gamallo and others 1999). In contrast to these findings, Lee and colleagues report a statistically significant correlation between nuclear β-catenin localization and ovarian high grade carcinomas in serous tumors (Lee and others 2003). The OVCA433 cell line used in this investigation is derived from a serous tumor. The same group also notes a tendency for poor survival in these patients, although this observation is not statistically significant due to a small sample size (Lee and others 2003). β-catenin expression is also increased in peritoneal metastases and in cell effusions from the ascites/peritoneal fluid when compared to the primary tumor (Davidson and others 2000; Imai and others 2004), suggesting β-catenin signaling is also prevalent in both

primary ovarian tumors and disseminated ovarian cancer cells. Mutations in CTNNB1, the gene encoding β-catenin, are common only in ovarian endometrioid tumor types (Gamallo and others 1999; Palacios and Gamallo 1998; Saegusa and others 2001; Sagae and others 1999; Wright and others 1999; Wu and others 2001) and often prevent the binding of GSK-3β to β-catenin (Gamallo and others 1999; Wright and others 1999), resulting in the upregulation of previously reported β-catenin/Wnt target genes (Schwartz and others 2003), but this dissertation identifies a different mechanism involving β-catenin and GSK-3β to upregulate transcription of Wnt/β-catenin target genes.

GSK-3β also plays an important role in the regulation of β-catenin and subsequent transcription of Wnt/β-catenin target genes. GSK-3β expression is increased in ovarian tumors when compared to normal ovaries (Rask and others 2003), suggesting a greater inhibition of β-catenin-mediated transcription will occur in ovarian tumors; however, our results show that GSK-3β inhibition is increased following integrin aggregation, suggesting an alternative mechanism is employed by integrin signaling to enhance β-catenin-mediated transcription. GSK-3β regulation is dual; residue tyrosine 216 must be phosphorylated for efficient kinase activity and residue serine 9 is phosphorylated by PKA, PKB, PKC, Akt/PI3K, and MAPK to inhibit GSK-3β (Almeida and others 2005; Fang and others 2000; Fang and others 2002b; Goode and others 1992; Li and others 2000; Zhou and others 2004). Although not fully investigated yet, the preliminary results presented in this chapter suggest that Src activity partially regulates GSK-3β activity. Increased Src phosphorylation following integrin engagement has been reported in many different cell types (Arias-Salgado and others 2003; Guo and Giancotti 2004). Coluccia and colleagues showed that treatment of colorectal cancer cells with a new Src family

tyrosine kinase inhibitor (SKI-606) prevented Src dependent activation of β-catenin and its ability to bind to TCF4. Membranous/cytoplasmic localization of β-catenin and decreased motility was also reported (Coluccia and others 2006), but it is unlikely that Src is the sole regulator of GSK-3β inhibition in OVCA433 cells. It has been reported that activation of the Src/ERK signaling cascade via Wnts and phosphorylated ERKs are required to inhibit GSK-3β in osteoblasts (Almeida and others 2005), suggesting other effectors activated downstream of integrin engagement may act in conjunction with Src to inhibit GSK-3β if this preliminary evidence proves valid in future experiments.

It has been suggested recently that Wnt/β-catenin target genes can be divided into two groups: a "stemness/proliferation group" that is activated early and during tumor progression and a "EMT/dissemination group" that is expressed later and transiently, but mostly at the tumor-host interface (Brabletz and others 2005). An argument can then be made that the ovarian cancer cells during integrin engagement represent disseminating and migratory cancer cells interacting with the peritoneal mesothelial cells; therefore, only Wnt target genes associated with EMT or dissemination, such as proteinases, will be upregulated, and Wnt target genes associated with proliferation, such as cyclin D1, will remain unchanged following integrin aggregation. Recently, a collagen-binding integrin-regulated model involving E-cadherin and increased β-catenin mediated transcription has been described in pancreatic cancer cells (Koenig and others 2006). Pancreatic cancer cells produce collagens type I and III, but it is unknown if the collagen present in their microenvironment promotes or prevents invasion (Koenig and others 2006). In contrast to the findings presented in this dissertation, Koenig and colleagues find that via Src and FAK, collagen-binding integrins promote a disruption of cadherin-catenin complexes, which

releases β-catenin to upregulate Wnt/β-catenin target genes cyclin D1 and c-myc at earlier time points (Koenig and others 2006) and eventually promotes reduced E-cadherin expression at later time points (Menke and others 2001). No changes in GSK-3β phosphorylation occur when pancreatic cancer cell line Panc-1 is cultured on collagen type I (Koenig and others 2006). Observed increases in cell proliferation and in cyclin D1 and c-myc expression suggest the pancreatic cancer cells in this model are in a proliferation phase (Koenig and others 2006), not in a more migratory phase like this model of ovarian cancer cells adhering to new sites in the peritoneal cavity via collagen-binding integrins.

Activity of uPA and expression of proMMP-7 is likely not restored to basal levels in all cases upon ICAT transfection for two possible reasons. First, both gene promoters are regulated by multiple transcription factors, which still likely bind to the promoter and increase transcription to some extent despite decreased binding of β-catenin (Crawford and others 1999; Hiendlmeyer and others 2004). For example, MMP-7 transcription is upregulated by combined activation of transcription factors PEA3, c-JUN, β-catenin, and LEF-1 (Crawford and others 2001). Second, OVCA433 cells have a low transfection efficiency. At best, the Fugene transfection method only yields a transfection efficiency of 50%, so ICAT expression is not global throughout the cell population. These results can be verified using lithium chloride to inhibit GSK-3β since it is now known that integrin engagement increases GSK-3β inhibition to promote translocation of β-catenin to the nucleus. These experiments will also be repeated to determine that the integrin-mediated increase in MT1-MMP expression is dependent on β-catenin-regulated transcription.

Metastases eventually resemble the organization of their primary tumors, suggesting that a temporary EMT or transient loss of membranous E-cadherin expression occurs to facilitate cancer cell migration and invasion (Brabletz and others 2005). Although integrin aggregation does not promote a loss in net E-cadherin expression, increased E-cadherin internalization may be necessary to encourage cell dissemination from the primary tumor. E-cadherin is not permanently downregulated because cells must maintain adhesion of ascitic cellular aggregates and then form new adhesive contacts with peritoneal mesothelial cells (Naora and Montell 2005); therefore, E-cadherin internalization likely plays an important role in the breaking and reforming of cell-cell junctions during ovarian cancer cell dissemination. As a result of E-cadherin internalization, β-catenin-mediated transcription and proteinase expression are increased, suggesting this integrin-mediated mechanism promotes ovarian cancer metastasis without inducing a loss in E-cadherin expression.

Figure 2.7

Chapter 2: Summary of Results

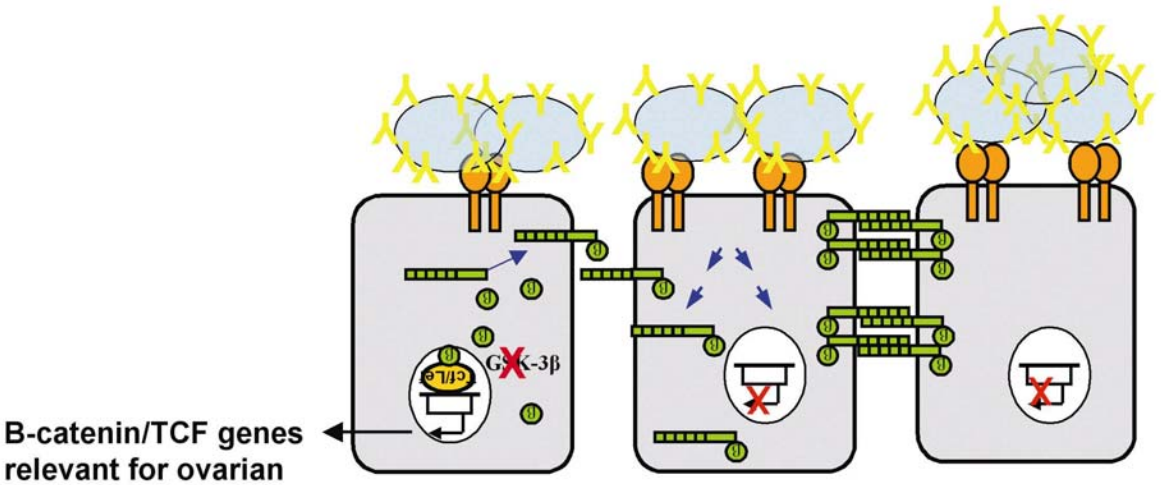

B-catenin/TCF genes relevant for ovarian cancer metastasis

- **uPA**
- **COX-2**
- **MT1-MMP**
- **MMP-7**

Figure 2.7: Chapter 2 summary of results

The results presented in Chapter 2 show that engagement of collagen-binding integrins results in the rapid internalization of E-cadherin and inhibition of GSK-3β, which then permits increased β-catenin-mediated transcription. As a result, protein expression of known Wnt/β-catenin target genes, COX-2, uPA, MT1-MMP, and MMP-7 is increased. Cell invasion is also increased and likely due to increased proteinase expression.

Chapter 3: Engagement of collagen-binding integrins promotes matrix-metalloproteinase-9-dependent E-cadherin ectodomain shedding

Results presented in this chapter were previously published in Cancer Research (Symowicz and others 2007).

Introduction and Rationale

Reversible modulation of cell-cell adhesion, cell-matrix adhesion, and proteolytic activity plays a critical role in remodeling of the neoplastic ovarian epithelium during metastasis, implicating cadherins, integrins, and proteinases in intra-peritoneal dissemination. While mutations in the E-cadherin gene are rare in ovarian carcinomas (Wong and Auersperg 2002), post-translational modification of E-cadherin function via an unknown mechanism is suggested by data demonstrating soluble E-cadherin (sE-cad) in ascites and cystic fluids from ovarian cancer patients (Darai and others 1998a; Sundfeldt and others 2001). As described in Chapter 1 (section II-D), several studies have reported that MMPs mediate E-cadherin cleavage and ectodomain shedding, but additional upstream regulators of this process are still largely unknown. Previous data from Dr. Stack and colleagues and other laboratories demonstrate that proteinase expression and activity are regulated by integrin signaling, functionally coupling cell-matrix adhesion and proteinase-dependent invasion (Azzam and Thompson 1992; DiPersio and others 2000; Ellerbroek and others 1999; Ellerbroek and others 2001b; Fishman and others 1998; Ghosh and others 2000; Gilles and others 1997; Haas and others 1998; Seltzer and others 1994; Tomesek and others 1997). As MMPs have been implicated in E-cadherin ectodomain shedding (Covington and others 2006; Damsky and others 1983; Lochter and others 1997; Maretzky and others 2005; Noe and others 2001) and cell-matrix adhesion has been linked to MMP expression

(Ellerbroek and others 1999; Ellerbroek and others 2001b), the current study has been proposed to evaluate a potential functional link between the interaction of cellular integrins with submesothelial interstitial collagens and decreased E-cadherin function. This dissertation now reports that aggregation of collagen-binding integrins promotes E-cadherin ectodomain shedding in an MMP- and Src kinase-dependent manner. Integrin-mediated E-cadherin ectodomain shedding is reduced by an MMP-9 function-blocking antibody and the shed ectodomain is generated upon incubation of cells with exogenous active MMP-9. Furthermore, incubation of cells with physiologically relevant concentrations of recombinant E-cadherin ectodomain disrupts adherens junctions, suggesting that sE-cad at levels present in ovarian cancer ascites may play an active functional role in tumor dissemination. These studies provide a novel mechanism for post-translational modification of E-cadherin function induced by cell-matrix contact.

Results

E-cadherin expression and processing in the ovarian tumor microenvironment.

Aberrant epithelial differentiation is an early event in ovarian carcinogenesis; therefore, in contrast to most carcinomas that lose E-cadherin expression with progression (Auersperg and others 1999), E-cadherin is abundant in primary ovarian carcinomas [**Fig. 3.1A**] (Imai and others 2004; Maines-Bandiera and Auersperg 1997; Marques and others 2004; Wong and others 1999). Samples of primary ovarian tumors from 137 patients (70 serous carcinoma, 42 endometrioid carcinoma, 16 clear cell carcinoma, 9 mucinous carcinoma) were examined for E-cadherin immunoreactivity. The vast majority of ovarian tumors (86%) displayed positive E-cadherin

immunoreactivity and E-cadherin expression was high (3+ or 2+) in 72% of patients overall (70% of serous, 62% of endometrioid, 94% of clear cell, 100% of mucinous). A representative example of each histotype stained for E-cadherin and a serial H&E section is shown in **Fig. 3.1A**. E-cadherin expression was maintained in the majority of tumor samples regardless of tumor histotype or Federation Internationale des Gynaecologistes et Obstetristes (FIGO) stage, consistent with the observation that genetic mutations in the E-cadherin gene that result in loss of expression are rare in ovarian tumors (Wong and Auersperg 2002).

Single cells and multi-cellular aggregates are shed from primary ovarian tumors and adhere via integrins to submesothelial collagens, suggesting that post-translational modulation of E-cadherin may occur to alter adhesive function and promote intraperitoneal dissemination. Indeed, a soluble E-cadherin ectodomain fragment (sE-cad) of unreported size was detected in the serum of patients with gastric cancer, multiple myeloma, and melanoma (Billion and others 2006; Chan and others 2005; Syrigos and others 2004). Cystic fluid from patients with benign or malignant cystic ovarian masses also contained elevated sE-cad (Darai and others 1998a; Sundfeldt and others 2001), although no significant differences were observed in sera (Darai and others 1998a; Sundfeldt and others 2001). ELISA and immunoblot analysis were used to detect sE-cad in a total of 47 ascites samples from women with benign ovarian cysts, Meig's Syndrome, ovarian hyperstimulation syndrome (OHSS) or stage I, III, and IV ovarian cancer. sE-cad levels were significantly elevated (6-fold, $p<.005$) in ascites from women with ovarian cancer compared to ascites from women with OHSS or benign ovarian cysts [**Fig. 3.1B**]. Immunoblot analysis was then used to evaluate the integrity of the sE-cad fragment(s) detected by ELISA using an antibody to the E-cadherin extracellular region (HECD-1). A major 80kDa

E-cadherin ectodomain species was detected in the majority of ovarian cancer ascites samples, but was not present in non-malignant ascites [**Fig. 3.1C**]. Full length E-cadherin, fragments containing the cytoplasmic domain, and degraded E-cadherin ectodomain fragments <80 kDa were not detected (data not shown).

Figure 3.1A

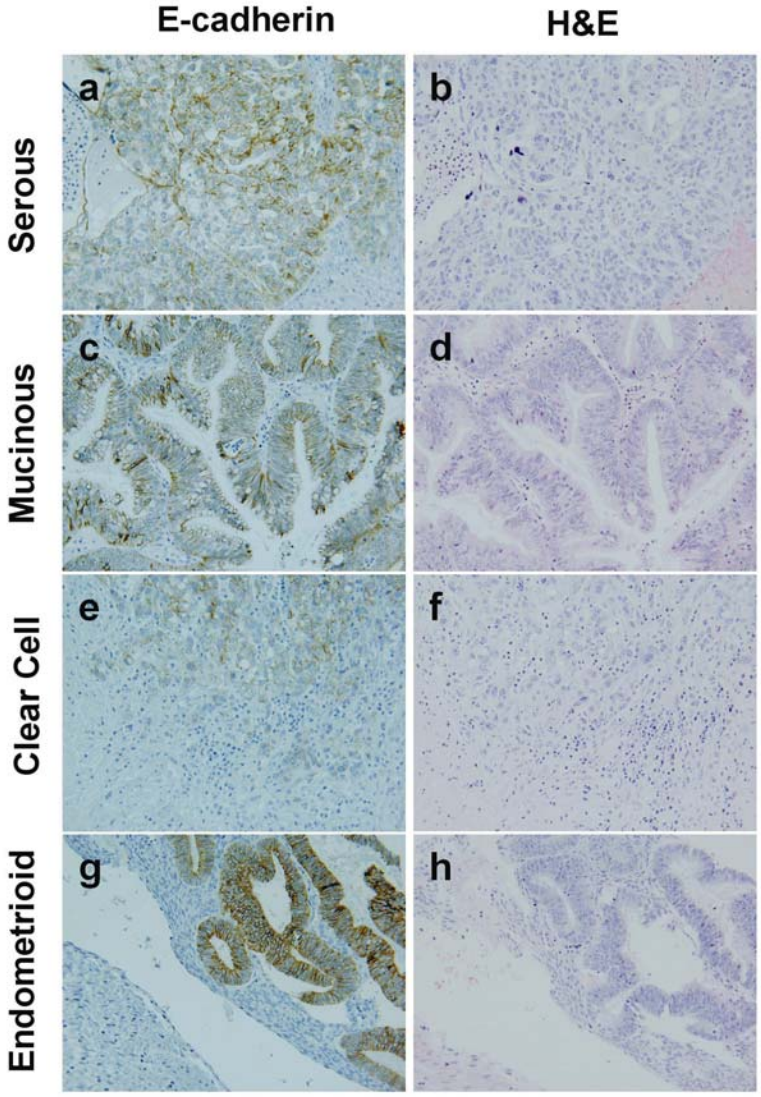
E-cadherin
H&E
Serous
Mucinous
Clear Cell
Endometrioid
a
b
c
d
e
f
g
h

Figure 3.1B

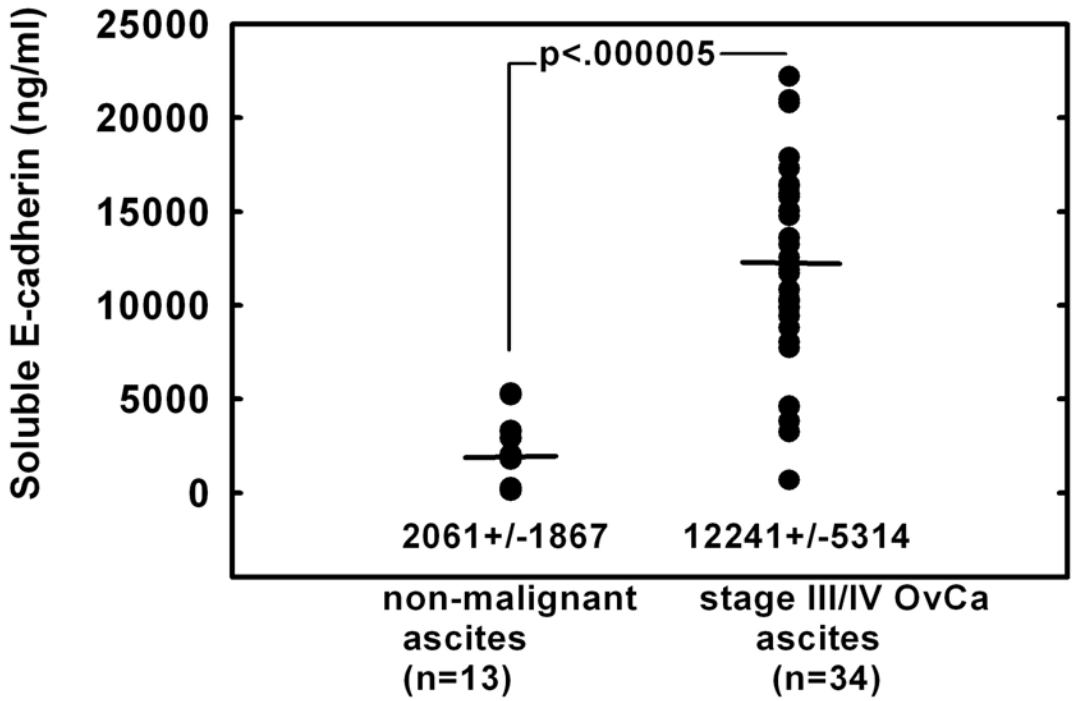
Soluble E-cadherin (ng/ml)
25000
20000
15000
10000
5000
0
p<.000005
2061+/-1867
12241+/-5314
non-malignant ascites (n=13)
stage III/IV OvCa ascites (n=34)

Figure 3.1C

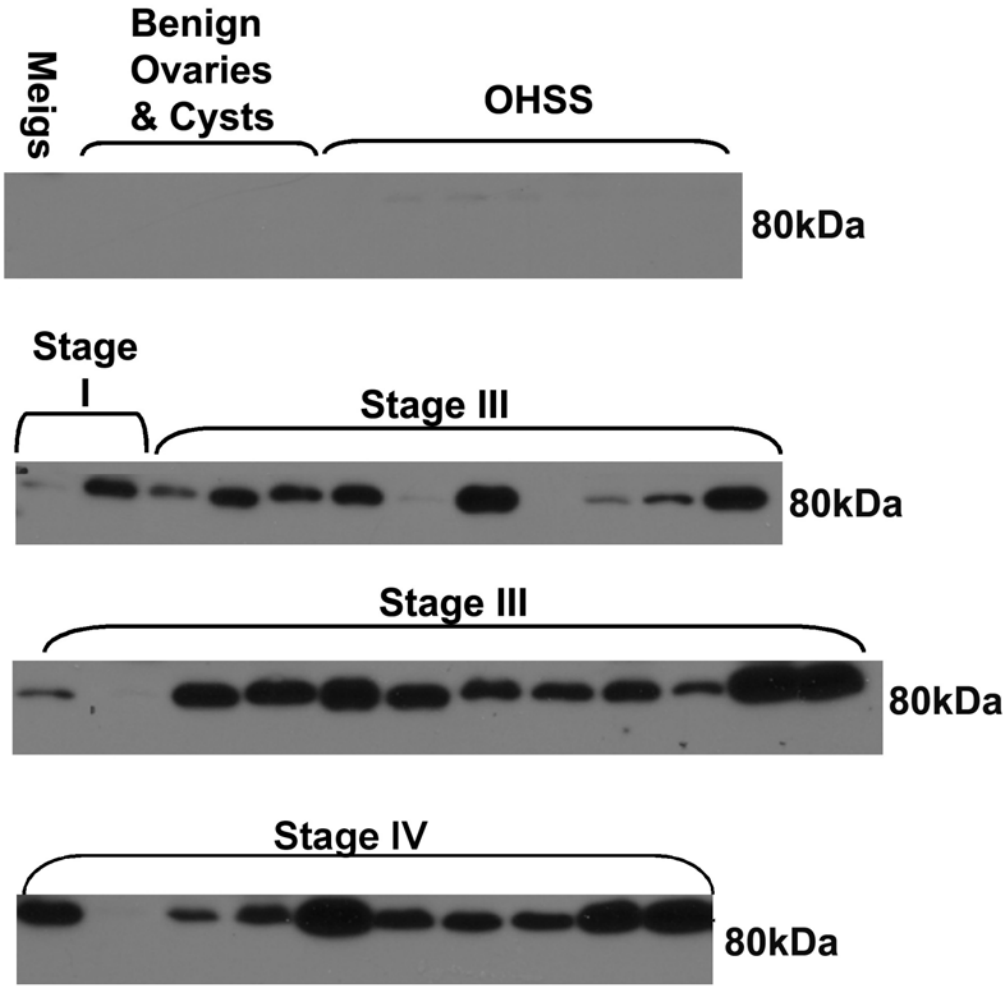
Meigs
Benign Ovaries & Cysts
OHSS
80kDa
Stage I
Stage III
80kDa
Stage III
80kDa
Stage IV
80kDa

Figure 3.1: E-cadherin expression in ascites and tumor samples from ovarian cancer patients.

A) Samples were stained with antibodies to E-cadherin (1:200) (a,c,e,g) or H&E (b,d,f,h) as described in Chapter 7. a-b, serous carcinoma; c-d, mucinous carcinoma; e-f, clear cell carcinoma; g-h, endometrioid carcinoma.

B,C) Non-malignant ascites samples (n=13) were obtained from women diagnosed with benign ovarian cysts, ovarian hyperstimulation syndrome (OHSS), or Meigs Syndrome (Meigs). Malignant ascites samples (n=34) were obtained from women diagnosed with ovarian cancer at either Stage I, III, or IV. **B)** Patient ascites samples were analyzed using ELISA according to manufacturer's specifications to determine the levels of soluble E-cadherin (sE-cad).

C) Ascites samples (1µl) were diluted in PBS, electrophoresed on 9% SDS-PAGE gels, transferred to PVDF membranes, and immunoblotted with anti-E-cadherin (HECD-1) (1:4000), followed by peroxidase-conjugated secondary antibody (1:5000) and enhanced chemiluminescence detection. Whole cell lysates from the OVCA433 cell lines served as a positive control for full length (120kDa) E-cadherin (E-cad) (not shown).

Integrin clustering increases E-cadherin ectodomain shedding.

The 80kDa E-cadherin ectodomain is shed following proteolytic cleavage in several different cell types *in vitro* (Covington and others 2006; Damsky and others 1983; Lochter and others 1997; Maretzky and others 2005; Noe and others 2001); however, the cellular events that regulate this process are not well-characterized. As a consequence of intraperitoneal metastasis, clustering of collagen-binding integrins α2β1 and α3β1 occurs when aggregates of cells attach to the collagen-rich submesothelial ECM (Ghosh and others 2002). To evaluate the effect of integrin clustering on E-cadherin status, OVCA429 and OVCA433 cells were treated with bead-immobilized subunit-specific antibodies to α3 or β1 integrin or control IgG. E-cadherin ectodomain shedding was then evaluated by immunoprecipitation of conditioned media using E-cadherin ectodomain-specific antibodies followed by western blotting. Additional controls are presented in **Fig 3.2C**. Increased shedding of the E-cadherin ectodomain was observed following aggregation of collagen-binding integrins in two ovarian cancer cell lines [**Fig. 3.2A,B]**, but further characterization of integrin-mediated E-cadherin ectodomain shedding in the OVCA433 cell line was required. Previous studies showed that Src activity is necessary for the disruption of cadherin-mediated cell adhesion in cancer cells (Avizienyte and others 2002; Irby and Yeatman 2002), and integrin signaling was linked to Src-induced junction disruption (Avizienyte and others 2002). Integrin aggregation in the presence of the Src family kinase inhibitor PP2 decreased E-cadherin ectodomain shedding [**Fig. 3.2D**], suggesting Src kinase activity is also needed to promote E-cadherin ectodomain shedding. It was also reported that integrin clustering induces phosphorylation and transactivation of the epidermal growth factor receptor (EGFR) in the absence of EGF (Yu and others 2000). To determine if EGFR activity

was also necessary to promote E-cadherin ectodomain shedding, integrins were aggregated in the presence of AG1478, an inhibitor of EGFR phosphorylation [**Fig 3.2E**]. E-cadherin ectodomain shedding was not decreased by AG1478 cotreatment, suggesting EGFR activity was not required. COX-2 was previously shown to regulate proteinase activity in cancer cells (chapter 4)(Ishizaki and others 2006; Shishodia and others 2004; Wu and others 2005), implicating COX-2 in integrin-mediated cleavage of E-cadherin. In addition, integrin engagement increased COX-2 expression [**Fig 2.4B**]. Integrin aggregation was induced in the presence of COX-2 specific inhibitor NS-398 [**Fig 3.2F**], but E-cadherin ectodomain shedding was not reduced, suggesting COX-2 was not necessary.

To investigate whether E-cadherin ectodomain shedding resulted in a net loss of cellular E-cadherin protein, whole cell lysates were evaluated following integrin aggregation. No net change in total full length (120kDa) E-cadherin expression was observed in whole cell lysates following integrin aggregation [**Fig. 3.3A**]. This was confirmed by surface biotinylation to distinguish cell surface and cytoplasmic pools of E-cadherin. Despite increased ectodomain shedding observed at 20 hours, surface and cytoplasmic expression of full length E-cadherin was not modulated at this time point [**Fig. 3.3B**]. Long term culture (1 month) of OVCA433 cells on thin layer collagen also did not induce a permanent reduction in net or surface E-cadherin expression [**Fig 2.1B**]. As these results suggested that new protein synthesis replenishes the shed E-cadherin, aggregation of β1 integrins was induced in the presence of the protein synthesis inhibitor cycloheximide (CHX) to test this hypothesis and the resulting conditioned media were analyzed for the E-cadherin ectodomain. Integrin-induced E-cadherin ectodomain shedding was reduced by CHX treatment [**Fig. 3.3C**]. Together, these results support the hypothesis that

integrins act as upstream modulators of E-cadherin ectodomain shedding that is dependent on new protein synthesis.

Figure 3.2

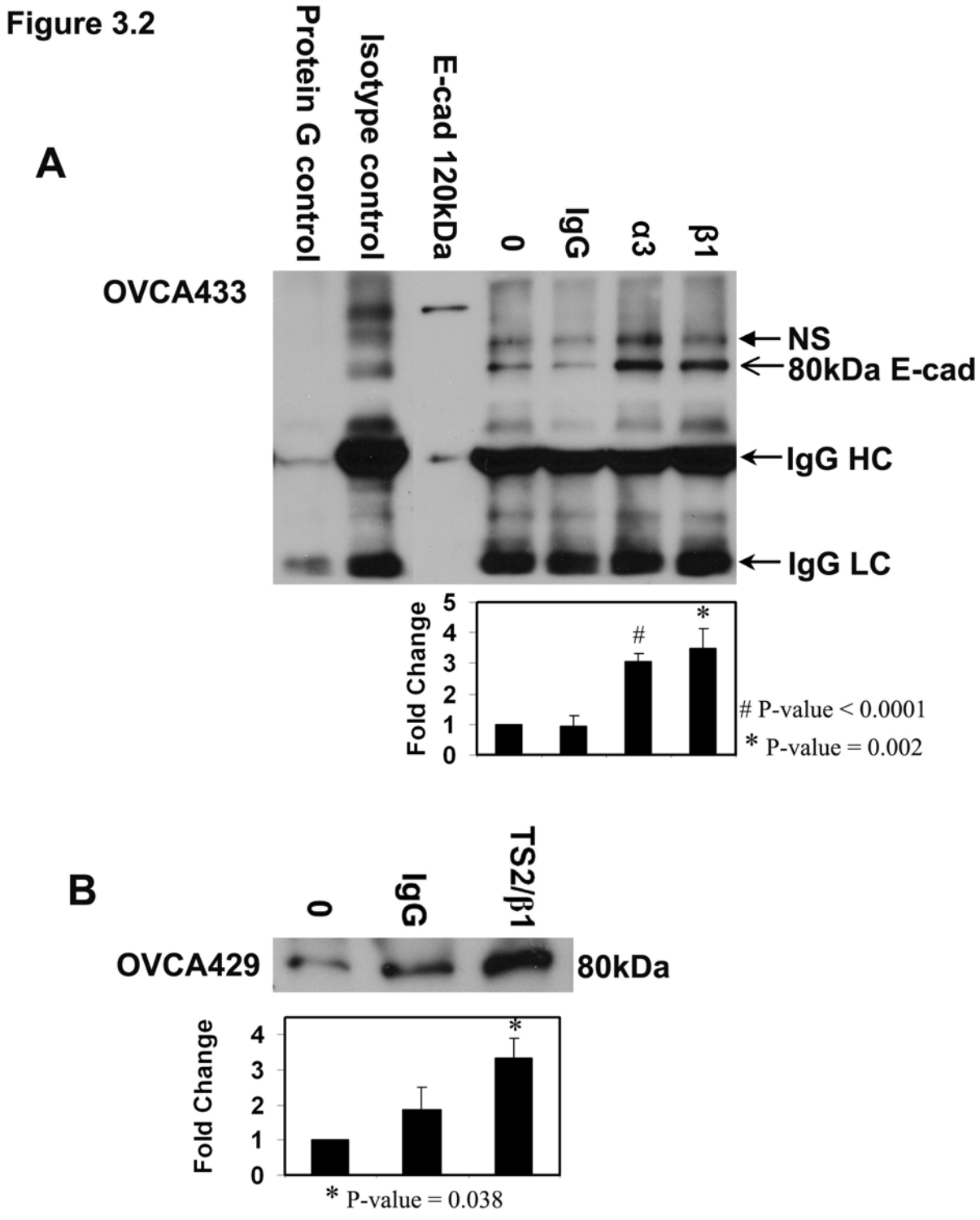
A
Protein G control
Isotype control
E-cad 120kDa
0
IgG
α3
β1
OVCA433
NS
80kDa E-cad
IgG HC
IgG LC
Fold Change
5
4
3
2
1
0
#
*
P-value < 0.0001
* P-value = 0.002
B
0
IgG
TS2/β1
OVCA429
80kDa
Fold Change
4
3
2
1
0
*
* P-value = 0.038

Figure 3.2C

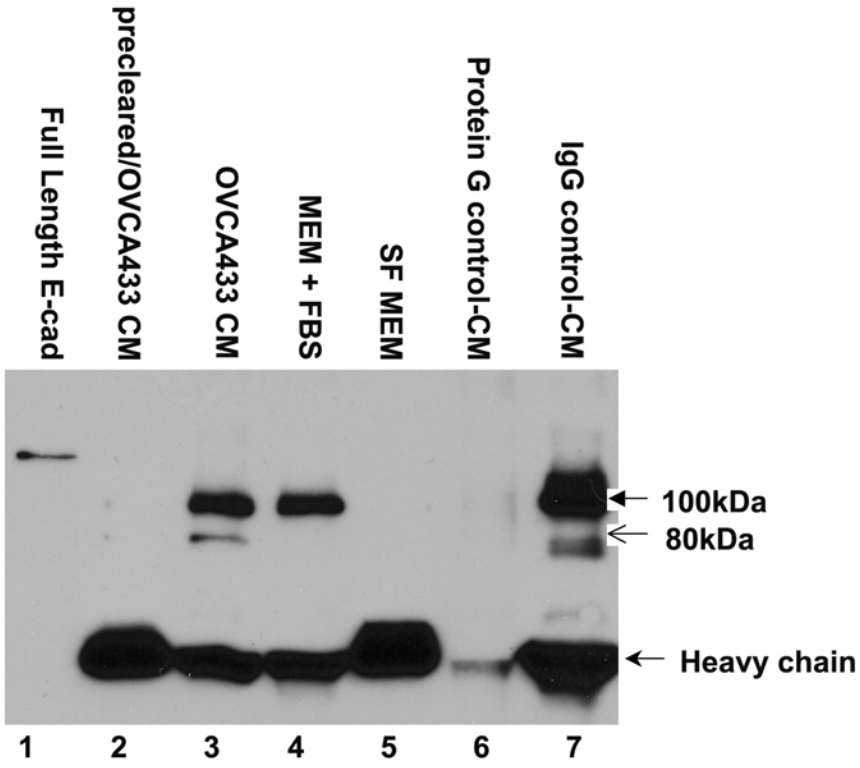
Full Length E-cad
precleared/OVCA433 CM
OVCA433 CM
MEM + FBS
SF MEM
Protein G control-CM
IgG control-CM
100kDa
80kDa
Heavy chain
1
2
3
4
5
6
7

Figure 3.2D

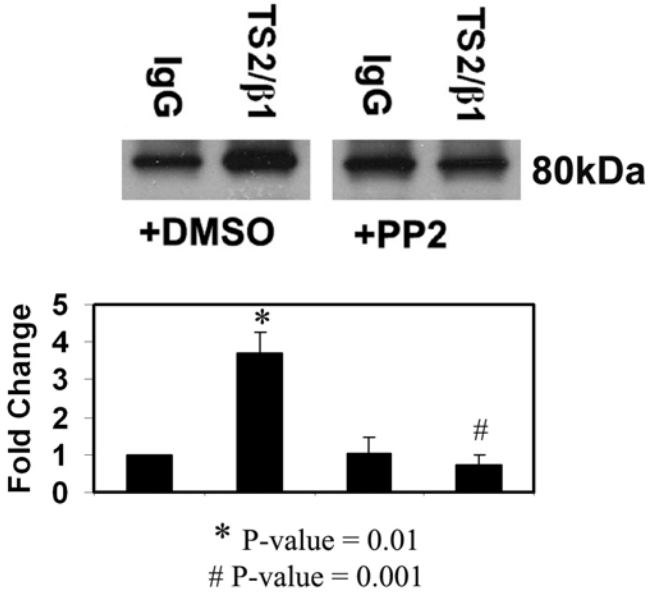

* P-value = 0.01
# P-value = 0.001

Figure 3.2

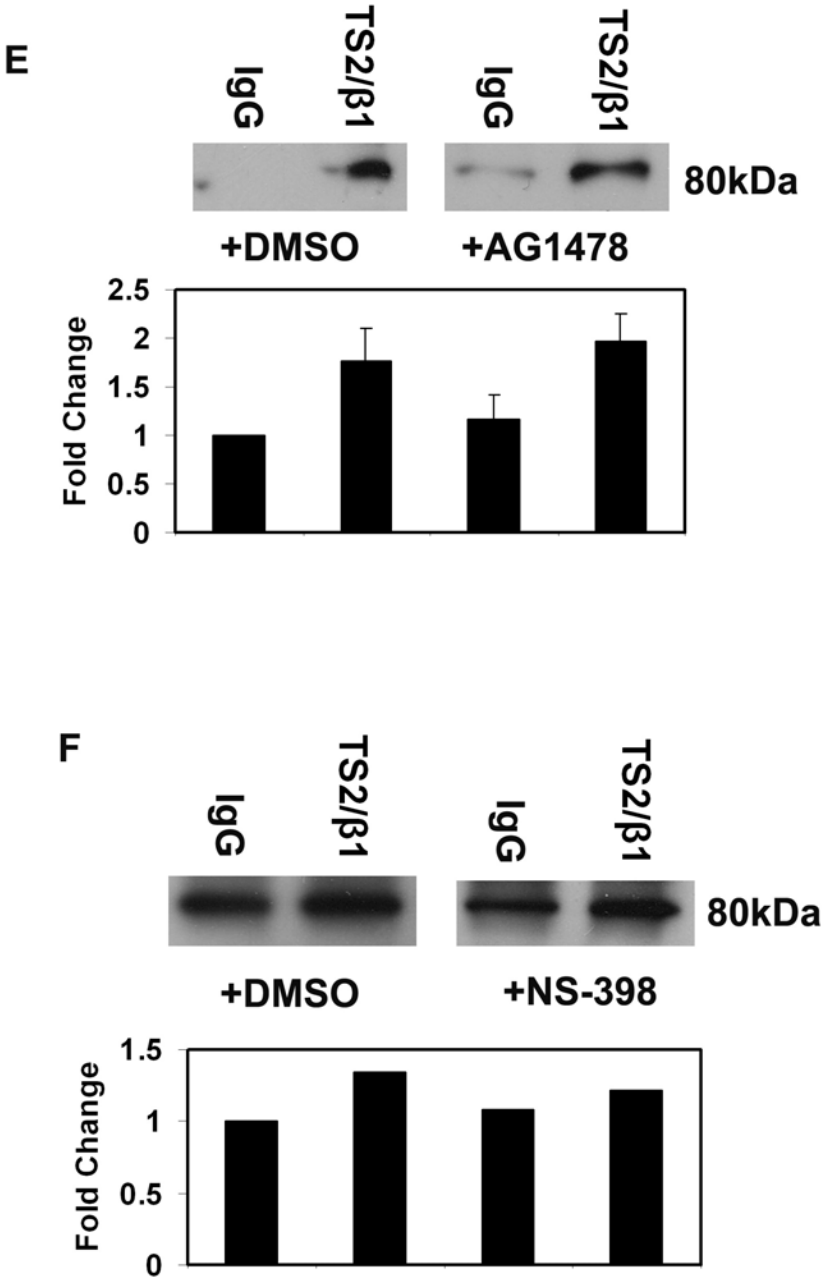
E
IgG
TS2/β1
IgG
TS2/β1
80kDa
+DMSO
+AG1478
Fold Change
2.5
2
1.5
1
0.5
0
F
IgG
TS2/β1
IgG
TS2/β1
80kDa
+DMSO
+NS-398
Fold Change
1.5
1
0.5
0

Figure 3.2: Engagement of collagen-binding integrins promotes E-cadherin ectodomain shedding.

A) OVCA433 cells were treated with control IgG, anti-integrin α3, or anti-integrin β1 immobilized to latex beads (as indicated) for 20 hours. The 80kDa E-cadherin ectodomain was immunoprecipitated from the conditioned media, as described in Chapter 7. Controls included conditioned media incubated with protein G sepharose beads alone to verify specificity of the E-cadherin antibody (first lane) and conditioned media subjected to immunoprecipitation with mouse IgG to show isotype specificity (second lane). Immunoprecipitates were electrophoresed on a 9% SDS-PAGE gel, transferred to a PVDF membrane, and immunoblotted with anti-E-cadherin (HECD-1) (1:4000), followed by peroxidase-conjugated secondary antibody (1:5000) and enhanced chemiluminescence detection. OVCA433 whole cell lysates were used a positive control for full length E-cadherin (third lane) and the IgG heavy and light chains are shown as loading controls (lanes 4-7). A representative western blot and densitometric quantification of the 80kDa ectodomain were shown. Results were normalized against the densitometric reading for untreated cells (fourth lane) and represent four independent experiments. NS=non-specific band; IgG HC=IgG heavy chain; IgG LC=IgG light chain

B) OVCA429 cells were treated with control IgG or anti-integrin β1/TS2 immobilized to latex beads (as indicated) for 20 hours. The 80kDa E-cadherin ectodomain was immunoprecipitated from the conditioned media, as described in Chapter 7. Immunoprecipitates were electrophoresed on a 9% SDS-PAGE gel, transferred to a PVDF membrane, and immunoblotted with anti-E-cadherin (HECD-1) (1:4000), followed by peroxidase-conjugated secondary antibody (1:5000) and enhanced chemiluminescence detection. A representative western blot

and densitometric quantification of the 80kDa ectodomain were shown. Results were normalized against the densitometric reading for untreated cells (first lane) and represent three independent experiments.

C) Additional immunoprecipitation controls were also included to demonstrate the specificity of the E-cadherin HECD-1 antibody for the 80kDa ectodomain. Whole cell lysates from OVCA433 cells served as a western blot control for full length E-cadherin (1st lane). Conditioned media from OVCA433 cells contained the 80kDa E-cadherin ectodomain and a 100kDa band (3rd lane). A 100kDa protein was also isolated from serum containing culture media used to culture OVCA433 cells (4th lane) and was likely a non-specific protein found in serum that cross reacts with the HECD-1 antibody as it was not isolated from serum-free culture media (5th lane). Conditioned media was also incubated with protein G sepharose beads alone to verify specificity of the E-cadherin antibody (6th lane). Conditioned media was subjected to immunoprecipitation with mouse IgG to show isotype specificity (7th lane) and a band running below 80kDa was detected.

D) OVCA433 cells were preincubated with PP2 (10μM) or DMSO prior to treatment with either control IgG or TS2/β1 antibody immobilized on latex beads (as indicated) for 20 hours. The 80kDa E-cadherin ectodomain was immunoprecipitated from the conditioned media, as described in Chapter 7. Immunoprecipitates were electrophoresed on a 9% SDS-PAGE gel, transferred to a PVDF membrane, and immunoblotted with anti-E-cadherin (HECD-1) (1:4000), followed by peroxidase-conjugated secondary antibody (1:5000) and enhanced chemiluminescence detection. A representative western blot and densitometric quantification of

the 80kDa ectodomain were shown. Results were normalized against the densitometric reading for cells treated with control IgG beads (first lane) and represent three independent experiments.

E) OVCA433 cells were preincubated with AG1478 (10μM) or DMSO prior to treatment with either control IgG or TS2/β1 antibody immobilized on latex beads (as indicated) for 20 hours. The 80kDa E-cadherin ectodomain was immunoprecipitated from the conditioned media, as described in Chapter 7. Immunoprecipitates were electrophoresed on a 9% SDS-PAGE gel, transferred to a PVDF membrane, and immunoblotted with anti-E-cadherin (HECD-1) (1:4000), followed by peroxidase-conjugated secondary antibody (1:5000) and enhanced chemiluminescence detection. A representative western blot and densitometric quantification of the 80kDa ectodomain were shown. Results were normalized against the densitometric reading for cells treated with control IgG beads (first lane) and represent three independent experiments.

F) OVCA433 cells were preincubated with NS-398 (50μM) or DMSO prior to treatment with either control IgG or TS2/β1 antibody immobilized on latex beads (as indicated) for 20 hours. The 80kDa E-cadherin ectodomain was immunoprecipitated from the conditioned media, as described in Chapter 7. Immunoprecipitates were electrophoresed on a 9% SDS-PAGE gel, transferred to a PVDF membrane, and immunoblotted with anti-E-cadherin (HECD-1) (1:4000), followed by peroxidase-conjugated secondary antibody (1:5000) and enhanced chemiluminescence detection. A representative western blot and densitometric quantification of the 80kDa ectodomain were shown. Results were normalized against the densitometric reading for cells treated with control IgG beads (first lane) and represent one experiment.

Figure 3.3

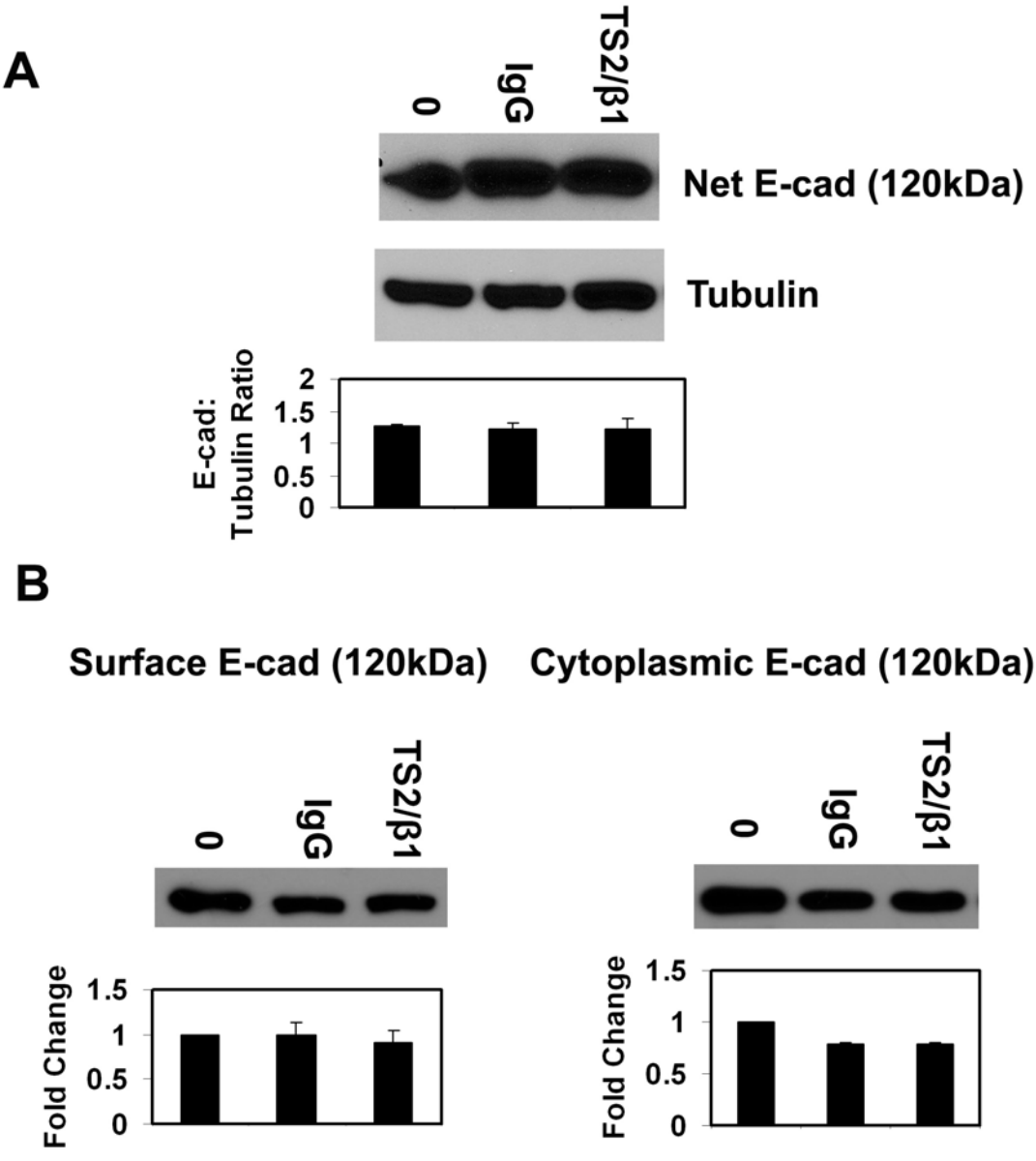
A
0
IgG
TS2/β1
Net E-cad (120kDa)
Tubulin
E-cad:
Tubulin Ratio
2
1.5
1
0.5
0
B
Surface E-cad (120kDa)
Cytoplasmic E-cad (120kDa)
0
IgG
TS2/β1
Fold Change
1.5
1
0.5
0

Figure 3.3C

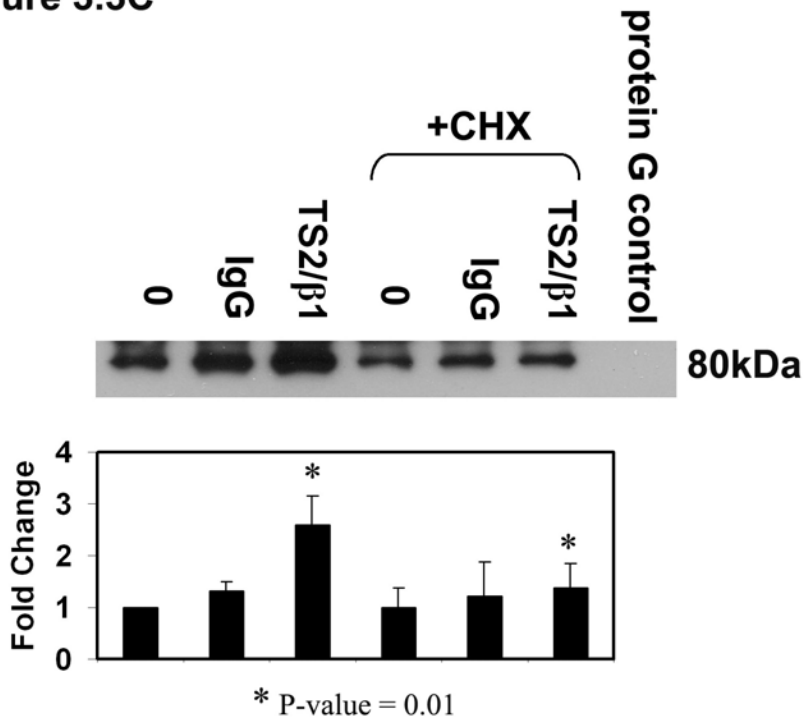
protein G control
+CHX
TS2/β1
IgG
0
TS2/β1
IgG
0
80kDa
Fold Change
4
3
2
1
0
*
*
* P-value = 0.01

Figure 3.3: Net E-cadherin levels are not changed despite increased ectodomain shedding.

A) OVCA433 cells were treated with either control IgG or TS2/β1 antibody immobilized on latex beads (as indicated) for 20 hours. Whole cell lysates (20μg) were electrophoresed on a 9% SDS-PAGE gel, transferred to a PVDF membrane, and immunoblotted with anti-E-cadherin (HECD-1) (1:4000), followed by peroxidase-conjugated secondary antibody (1:5000) and enhanced chemiluminescence detection. Full length E-cadherin (120kDa) was detected. Tubulin was used as a loading control. A representative western blot and densitometric quantification of full length E-cadherin were shown. Results were normalized against the densitometric reading for tubulin and represent three independent experiments.

B) To evaluate the amount of E-cadherin present on the cell surface, cells were surface-biotinylated, lysed, and lysates (50μg) incubated with NeutrAvidin. Following incubation, the NeutrAvidin-conjugated lysates and resulting supernatant were electrophoresed on a 9% SDS-PAGE gel, transferred to a PVDF membrane, and immunoblotted with anti-E-cadherin (HECD-1) (1:4000), followed by peroxidase-conjugated secondary antibody (1:5000) and enhanced chemiluminescence detection to examine the surface E-cadherin expression and cytoplasmic E-cadherin expression, respectively. Full length E-cadherin (120kDa) was detected in both populations. A representative western blot and densitometric quantification of full length E-cadherin were shown. Results were normalized against the densitometric reading for untreated cells (first lane). Surface and cytoplasmic E-cadherin results represent three and two independent experiments, respectively.

C) OVCA433 cells were preincubated with cycloheximide (20μM, CHX) or DMSO prior to treatment with either control IgG or TS2/β1 antibody immobilized on latex beads (as indicated) for 20 hours. The 80kDa E-cadherin ectodomain was immunoprecipitated from the conditioned media, as described in Chapter 7. Immunoprecipitates were electrophoresed on a 9% SDS-PAGE gel, transferred to a PVDF membrane, and immunoblotted with anti-E-cadherin (HECD-1) (1:4000), followed by peroxidase-conjugated secondary antibody (1:5000) and enhanced chemiluminescence detection. Conditioned media was also incubated with Protein G sepharose only (Protein G control) to demonstrate the specificity of the E-cadherin immunoprecipitation. A representative western blot and densitometric quantification of the 80kDa ectodomain were shown. Results were normalized against the densitometric reading for untreated cells (first lane) and represent four independent experiments.

MMP-9-dependent generation of E-cadherin ectodomain following integrin aggregation.

MMP-dependent E-cadherin ectodomain shedding was observed in various cell types; however the cellular events that regulate this process are not well-characterized (Covington and others 2006; Damsky and others 1983; Lochter and others 1997; Maretzky and others 2005; Noe and others 2001). Dr. Stack and colleagues previously demonstrated that multi-valent aggregation of collagen binding integrins regulates MMP expression by ovarian cancer cells (Ellerbroek and others 1999; Ellerbroek and others 2001b). Aggregation of collagen-binding integrins in the presence of the broad spectrum MMP inhibitor GM6001 reduced E-cadherin ectodomain shedding, implicating integrin-regulated MMP activity in this process [**Fig. 3.4A**]. Integrin clustering increased expression of MMP-9 [**Figs. 3.4B&C**] and MMP-9 immunoreactivity was prevalent in the majority of human ovarian tumors analyzed **[Fig. 3.4D]**. While MMP-9 is commonly expressed by stromal elements in many tumors (DeClerck 2000), *in situ* hybridization analyses provided definitive evidence for robust expression of MMP-9 by malignant ovarian epithelium (Davidson and others 1999; Huang and others 2000; Naylor and others 1994). This is supported by immunohistochemical analysis of 141 primary ovarian tumors (71 serous tumors, 43 endometrioid tumors, 18 clear cell tumors, 9 mucinous tumors), which demonstrates MMP-9 expression in 74% of specimens (representative examples shown in **Fig. 3.4D)**. MMP-9 expression was high (2+ or 3+) in 28% of serous tumors, 21% of endometrioid tumors, 11% clear cell tumors, and 22% of mucinous tumors. Furthermore, as determined by ELISA, total MMP-9 expression was elevated approximately 2-fold in the ascites of ovarian cancer patients when compared to the ascites from women with benign ovarian cysts

[**Fig 3.4E**]. These findings suggest that MMP-9 may be an important factor in the ovarian tumor microenvironment that contributes to E-cadherin ectodomain shedding.

To evaluate the potential contribution of MMP-9 to E-cadherin cleavage, integrin aggregation was induced in the presence of an MMP-9 function-blocking antibody. Specific blocking of MMP-9 activity abolished the integrin-mediated increase in shed E-cadherin ectodomain with little impact on basal ectodomain shedding [**Fig. 3.5A**]. Because the MMP-9 blocking antibody inhibits extracellular MMP-9 activity, these data demonstrate MMP-9-dependent cleavage of surface-associated, rather than intracellular, E-cadherin. To further verify MMP-9-catalyzed E-cadherin ectodomain shedding, cells were incubated with recombinant activated exogenous MMP-9 at 100 ng/ml, which was found to be the approximate average concentration of MMP-9 in ovarian cancer ascites using ELISA [**Fig 3.4E**]. A substantial increase in the shed E-cadherin ectodomain was catalyzed by MMP-9 and the generation of the ectodomain was inhibited by the MMP inhibitor GM6001 [**Fig. 3.5B**]. Changes in E-cadherin expression and localization were also evaluated using immunofluorescence following exogenous MMP-9 treatment in OVCA429 cells [**Fig 3.5C**]. Alterations in E-cadherin expression and localization were restricted to the edges of cell clusters. These data support a role for both endogenous and exogenous MMP-9 in promoting E-cadherin ectodomain shedding. Additional comparison of tumors with high levels of MMP-9 immunoreactivity (scored 2+ or 3+ in the analysis above, n=68) and serial sections stained with anti-E-cadherin antibodies support these *in vitro* data. While a statistically significant negative correlation was not shown overall in tumor samples, evaluation of serial sections demonstrated that 51% of tumors with high MMP-9 expression exhibit low or absent E-cadherin staining (0 or 1+) and all MMP-9 positive tumors

exhibited focal areas of high MMP-9 positivity co-localized with low E-cadherin staining [**Fig. 3.5D**]. Together these findings support the hypothesis that MMP-9 is a regulator of E-cadherin ectodomain shedding in the ovarian tumor microenvironment.

Figure 3.4

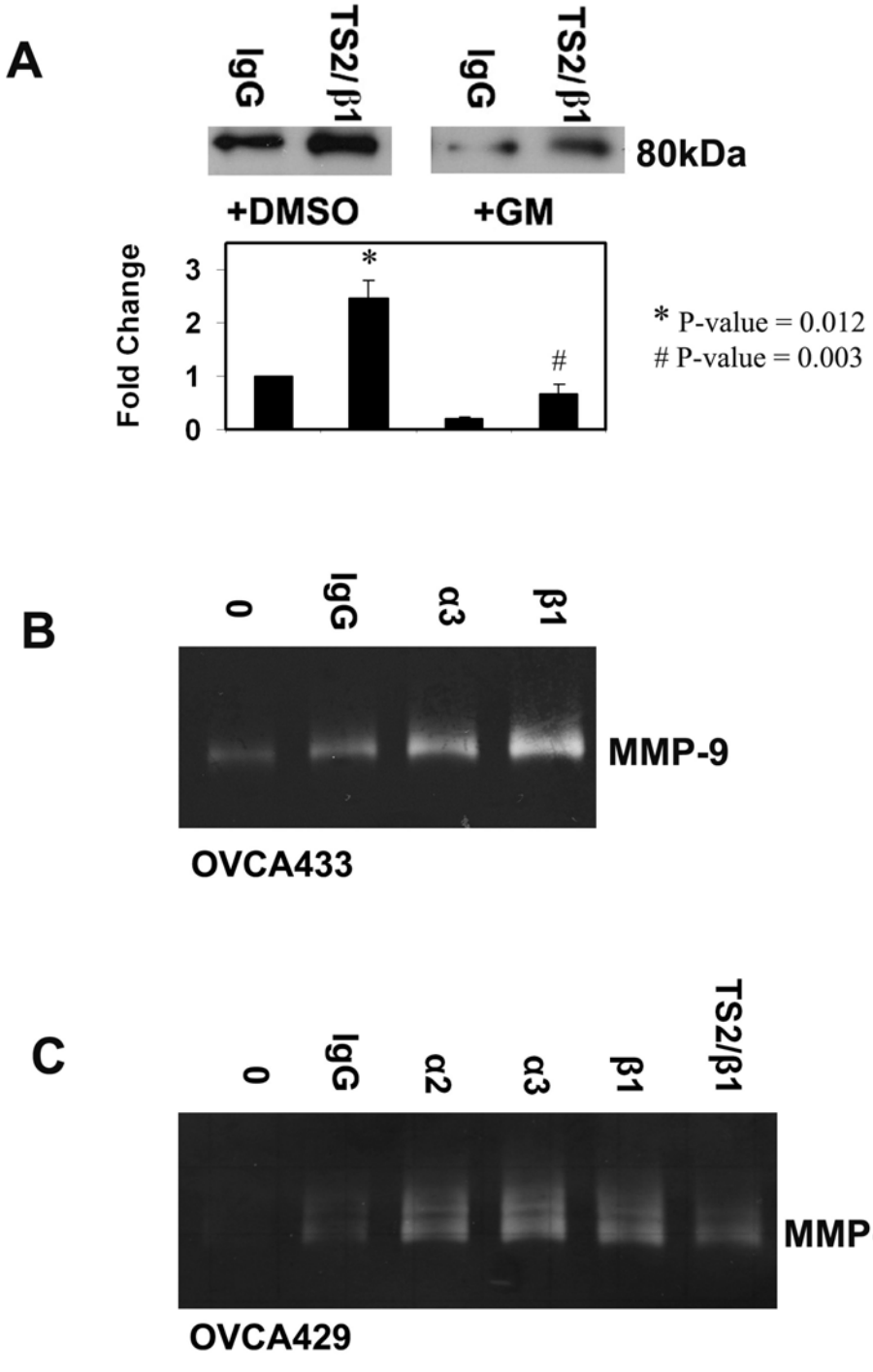
A
IgG
TS2/β1
IgG
TS2/β1
80kDa
+DMSO
+GM
Fold Change
3
2
1
0
*
#
* P-value = 0.012
# P-value = 0.003
B
0
IgG
α3
β1
MMP-9
OVCA433
C
0
IgG
α2
α3
β1
TS2/β1
MMP-9
OVCA429

Figure 3.4D

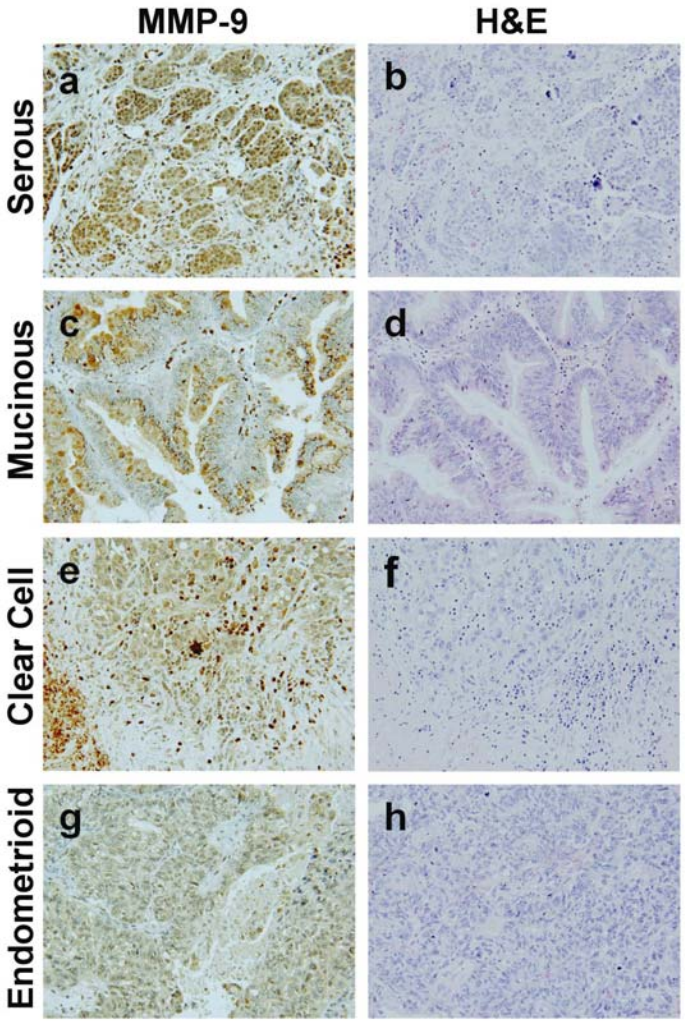

Figure 3.4E

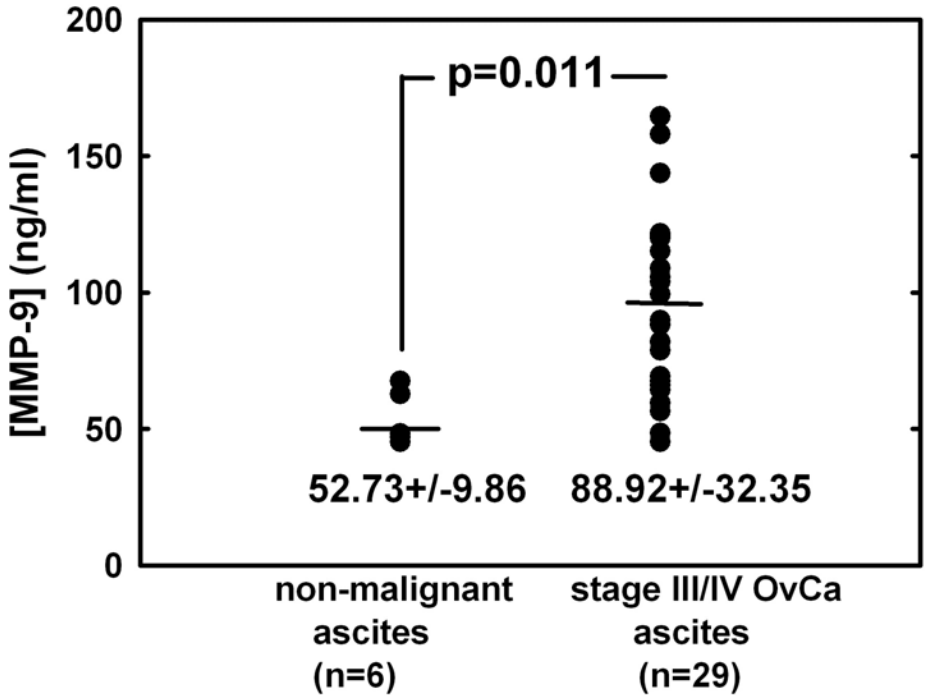
200
150
100
50
0
[MMP-9] (ng/ml)
p=0.011
52.73+/-9.86
88.92+/-32.35
non-malignant ascites (n=6)
stage III/IV OvCa ascites (n=29)

Figure 3.4: MMP-9 expression in ovarian cancer cell lines, tumor samples, and ascites samples

A) OVCA433 cells were preincubated with GM6001 (50μM) or DMSO prior to treatment with either control IgG or TS2/β1 antibody immobilized on latex beads (as indicated) for 20 hours. The 80kDa E-cadherin ectodomain was immunoprecipitated from the conditioned media, as described in Chapter 7. Immunoprecipitates were electrophoresed on a 9% SDS-PAGE gel, transferred to a PVDF membrane, and immunoblotted with anti-E-cadherin (HECD-1) (1:4000), followed by peroxidase-conjugated secondary antibody (1:5000) and enhanced chemiluminescence detection. A representative western blot and densitometric quantification of the 80kDa ectodomain were shown. Results were normalized against the densitometric reading for cells treated with control IgG beads (first lane) and represent three independent experiments.

B) OVCA433 cells were treated with control IgG, anti-integrin α3, or anti-integrin β1 immobilized to latex beads (as indicated) for 40 hours. **C)** OVCA429 cells were treated with control IgG, anti-integrin α2, anti-integrin α3, anti-integrin β1, or anti-integrin β1/TS2 immobilized to latex beads (as indicated) for 36 hours. **B, C)** The resulting conditioned media (30μl) were analyzed for MMP-9 expression using gelatin zymography. Under serum-free conditions, the proenzyme form of MMP-9 was detected.

D) Tumor samples were stained with antibodies to MMP-9 (1:200) (a,c,e,g) or H&E (b,d,f,h) as described in Chapter 7. a-b, serous carcinoma; c-d, mucinous carcinoma; e-f, clear cell carcinoma; g-h, endometrioid carcinoma.

E) Patient ascites samples were analyzed using ELISA according to manufacturer's specifications to determine the levels of total MMP-9. 29 samples were obtained from stage III or IV ovarian cancer patients and 6 non-malignant samples were obtained women with benign ovarian cysts.

Figure 3.5

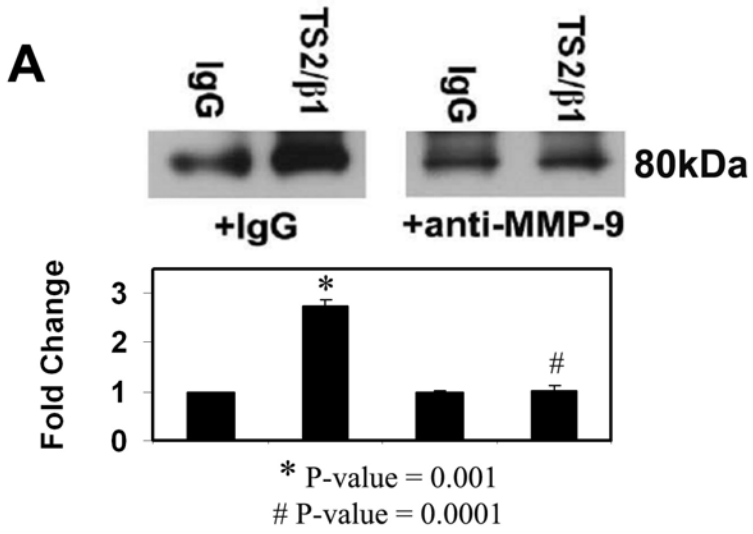
A
IgG
TS2/β1
IgG
TS2/β1
80kDa
+IgG
+anti-MMP-9
Fold Change
3
2
1
0
*
#
* P-value = 0.001
# P-value = 0.0001

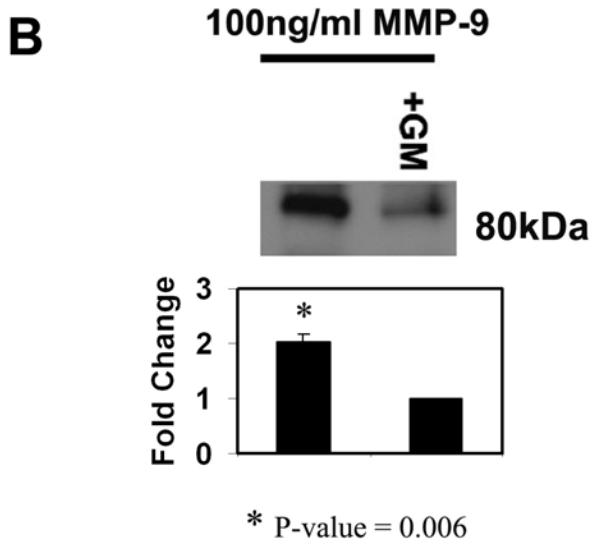
B
100ng/ml MMP-9
+GM
80kDa
Fold Change
3
2
1
0
*
* P-value = 0.006

Figure 3.5C

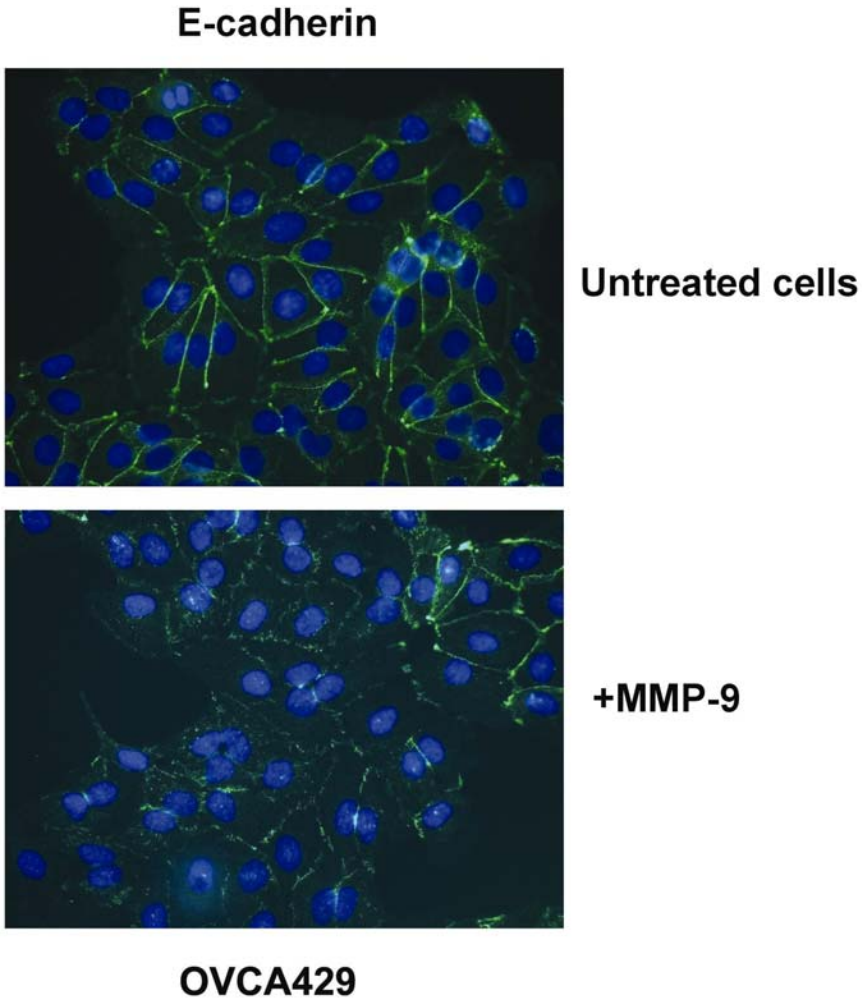

Figure 3.5D

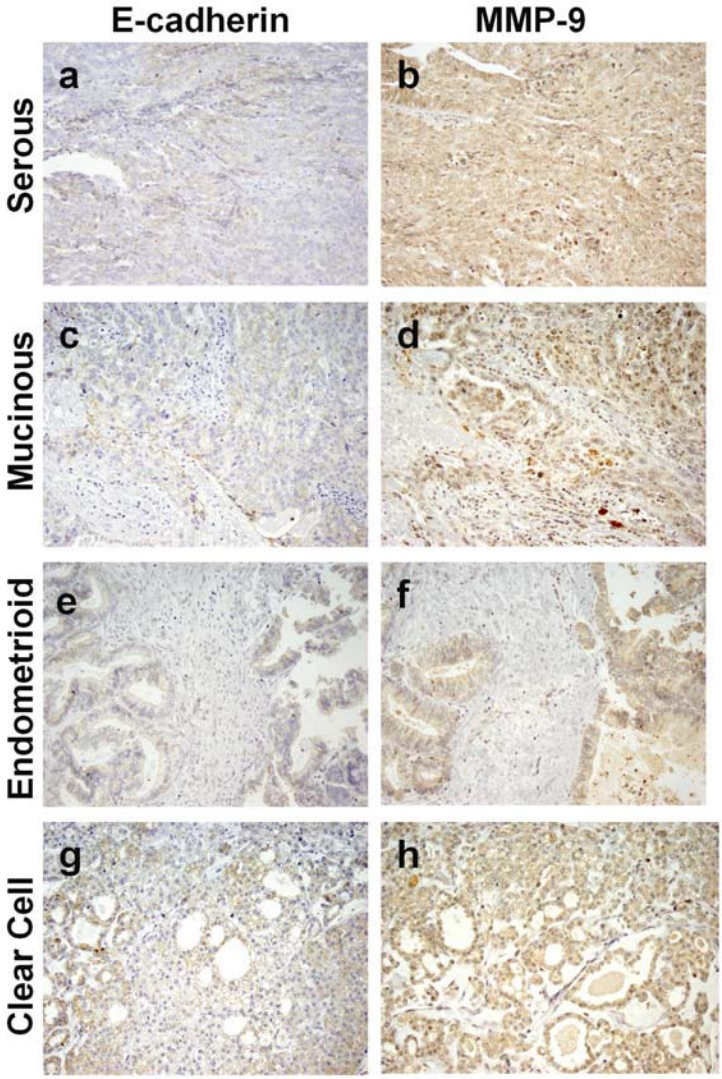
E-cadherin
MMP-9
Serous
Mucinous
Endometrioid
Clear Cell
a
b
c
d
e
f
g
h

Figure 3.5: MMP-9 promotes integrin-mediated E-cadherin ectodomain shedding.

A) OVCA433 cells were preincubated with anti-MMP-9 (10μg/ml) or control IgG prior to treatment with either control IgG or TS2/β1 antibody immobilized on latex beads (as indicated) for 20 hours. The 80kDa E-cadherin ectodomain was immunoprecipitated from the conditioned media, as described in Chapter 7. Immunoprecipitates were electrophoresed on a 9% SDS-PAGE gel, transferred to a PVDF membrane, and immunoblotted with anti-E-cadherin (HECD-1) (1:4000), followed by peroxidase-conjugated secondary antibody (1:5000) and enhanced chemiluminescence detection. A representative western blot and densitometric quantification of the 80kDa ectodomain were shown. Results were normalized against the densitometric reading for cells treated with control IgG beads (first lane) and represent three independent experiments.

B) OVCA433 cells were preincubated with GM6001 (50μM) or DMSO prior to treatment with recombinant activated MMP-9 (100 ng/ml) for 24 hours. A protease inhibitor was added to each sample and then the 80kDa E-cadherin ectodomain was immunoprecipitated from the conditioned media, as described in Chapter 7. Immunoprecipitates were electrophoresed on a 9% SDS-PAGE gel, transferred to a PVDF membrane, and immunoblotted with anti-E-cadherin (HECD-1) (1:4000), followed by peroxidase-conjugated secondary antibody (1:5000) and enhanced chemiluminescence detection. A representative western blot and densitometric quantification of the 80kDa ectodomain are shown. Results were normalized against the densitometric reading for cells treated with MMP-9 and GM (second lane) and represent three independent experiments.

C) OVCA429 cells were plated on glass coverslips at approximately 60% confluence. The next day, cells were incubated in serum-free media overnight prior to treatment with recombinant activated MMP-9 (100ng/ml) for 48 hours. Cells were then processed for immunofluorescence using anti-E-cadherin (HECD-1) (1:300 dilution) and FITC-conjugated IgG, as described in Chapter 7 (40X magnification).

D) Serial sections of ovarian tumor samples were stained with antibodies to E-cadherin (1:200) (a,c,e,g) or MMP-9 (1:200) (b,d,f,h) as described in Chapter 7. a-b, serous carcinoma; c-d, mucinous carcinoma;; e-f, endometrioid carcinoma g-h, clear cell carcinoma.

The shed ectodomain disrupts preformed adherens junctions.

In contrast to other tumors where the shed E-cadherin ectodomain is released into the circulation, primary ovarian tumors maintain direct contact with sE-cad-rich ascites at high concentration (average 12 μg/ml, **Fig. 3.1B**). This unique microenvironment provides a physiologically relevant model system to assess the potential functional contribution of the E-cadherin ectodomain to ovarian cancer pathobiology. To test the hypothesis that the ectodomain may interact with endogenous cellular E-cadherin, cells were treated with a recombinant form of the human E-cadherin ectodomain (designated hEcad-Fc) and changes in junctional integrity were evaluated using immunofluorescence microscopy. Preformed junctions were disrupted by hEcad-Fc [**Fig. 3.6Abd & fh**] at concentrations representing the average value detected in ovarian cancer patient ascites (12 μg/ml, **Fig. 3.1B**). Morphological changes were also apparent at 48 hours, with evidence of increased cell dispersion relative to more compact colonies maintained by control cells [**Fig. 3.6Ad**]. β-catenin localization was also evaluated using immunofluorescence microscopy. No changes in β-catenin localization were observed at 24 and 48 hours [**Fig 3.6Ci-l**]. Changes in active β-catenin expression in whole cell lysates were also evaluated via western blotting following short-term treatment with hEcad-Fc. The levels of active β-catenin were rapidly decreased at 4 hours [**Fig 3.6D**]. Expression of active β-catenin at later time points and the effects of hEcad-Fc on β-catenin-mediated transcription will need to be investigated further using the TOPflash assay to fully understand the effects of the shed ectodomain on β-catenin. These data suggest that, although integrin-mediated E-cadherin ectodomain shedding does not result in a net loss of cellular E-cadherin [**Fig. 3.4A,B**], the

ectodomain remaining in the ovarian tumor microenvironment promotes cell-cell junction disruption, thereby potentially enhancing intraperitoneal dissemination.

Figure 3.6

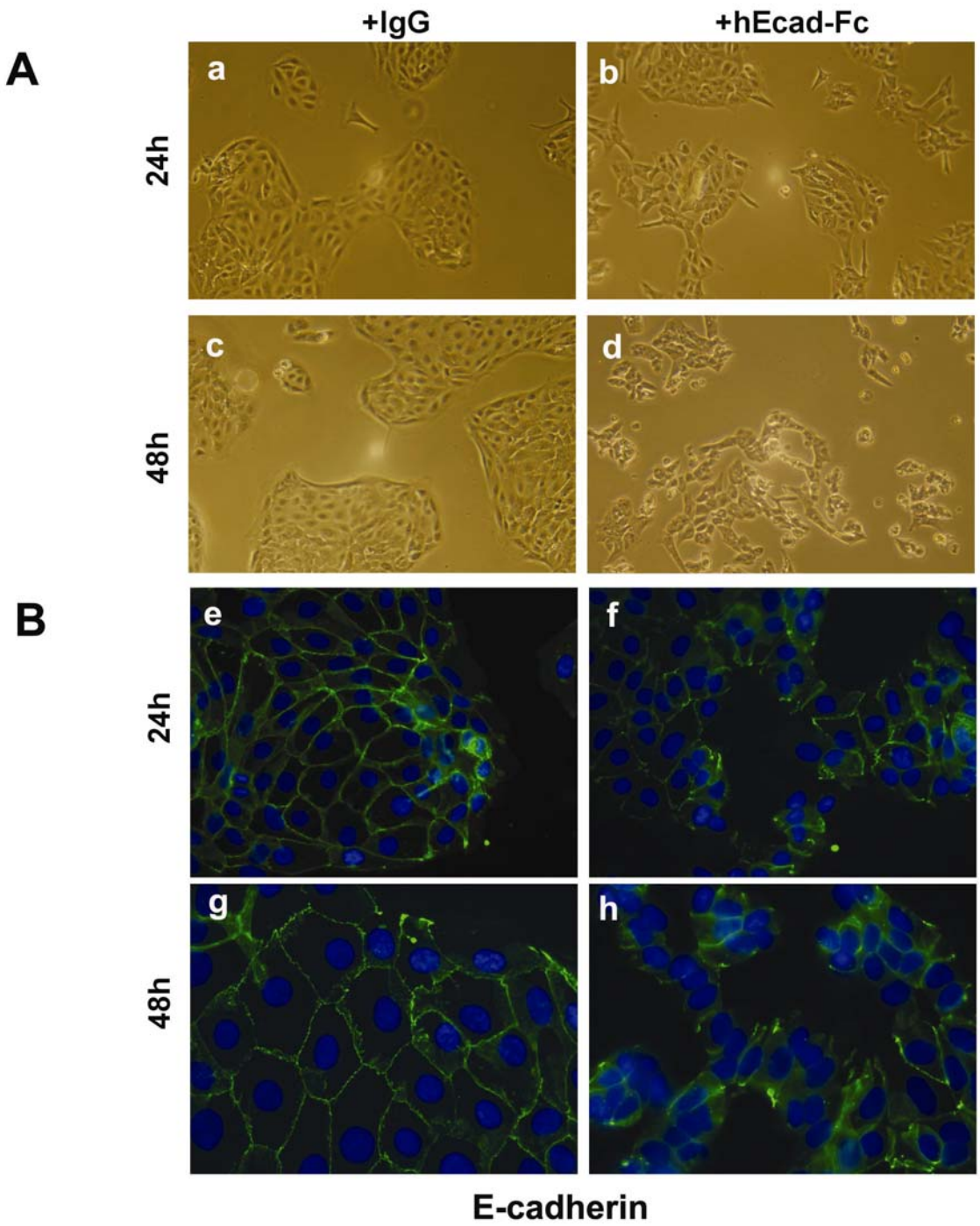

Figure 3.6C

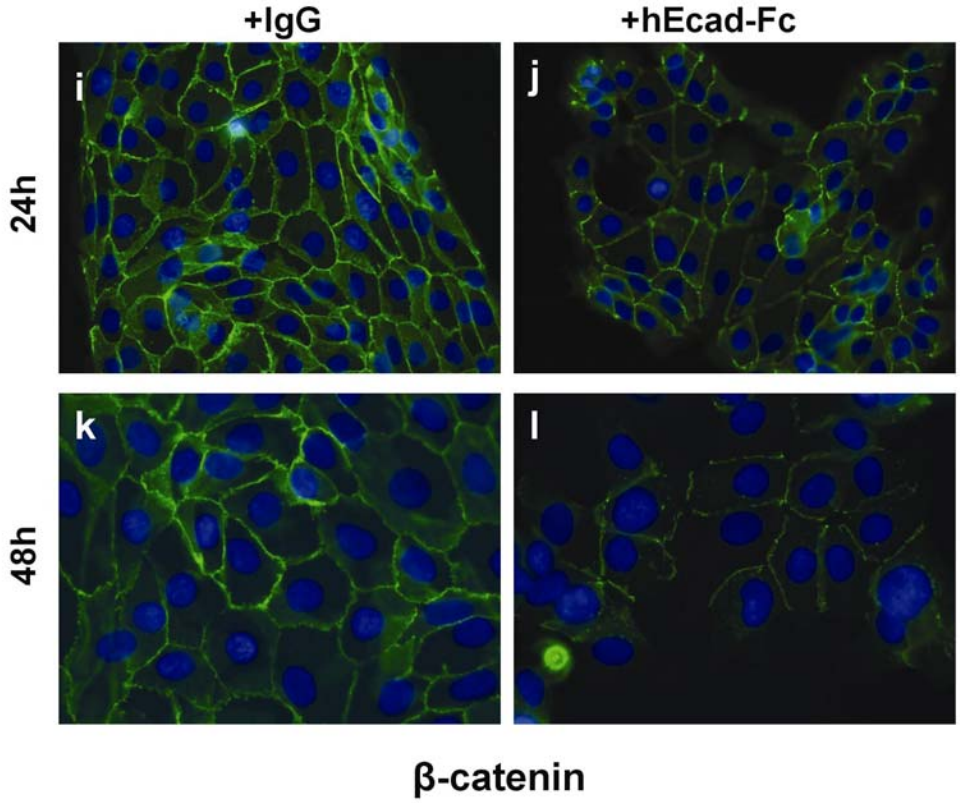

Figure 3.6D

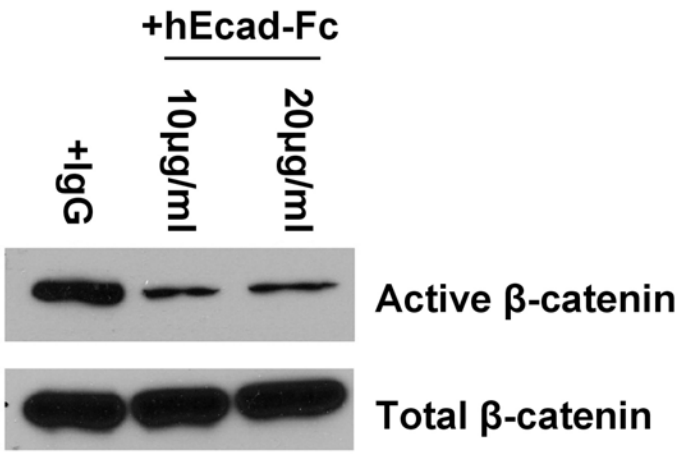

Figure 3.6: The shed E-cadherin ectodomain promotes cell junction disruption and cell dissemination

OVCA433 cells were plated on glass coverslips at approximately 60% confluence. The next day, cells were incubated in serum-free media overnight prior to treatment with hEcad-Fc (12μg/ml) or control IgG for 24 and 48 hours as indicated. **A)** Phase contrast images of cells were taken at 24 (a,b) and 48 hours (c,d) (10X magnification). **B, C)** Cells were then processed for immunofluorescence using anti-cytoplasmic E-cadherin (1:300 dilution) or anti-β-catenin and FITC-conjugated IgG, as described in Chapter 7, at 24 (e,f,i,j) and 48 (g,h,k,l) hours (40X magnification).

D) OVCA433 cells were plated at approximately 60% confluence and cultured in low calcium serum-containing MEM (0.1mM $CaCl_2$) for 1 hour prior to treatment with hEcad-Fc (10 and 20μg/ml) or control IgG (20μg/ml) for 4 hours. The resulting whole cell lysates (25μg) were electrophoresed on a 9% SDS-PAGE gel, transferred to a PVDF membrane, and immunoblotted with anti-active β-catenin (8E7) (1:1000) or anti-β-catenin, as indicated, followed by peroxidase-conjugated secondary antibody (1:5000) and enhanced chemiluminescence detection.

Preliminary Data

Effects of the shed E-cadherin ectodomain on *in vitro* wound closure

The E-cadherin ectodomain was also previously associated with increased cell migration in other cell types (Chunthapong and others 2004; Maretzky and others 2005; Noe and others 2001; Ryniers and others 2002). To determine the effects of the shed ectodomain on cell motility after disseminated cells have attached to sites in the peritoneal cavity, disrupted the mesothelial monolayer, and exposed the collagen-rich submesothelial matrix, OVCA433 cells were plated on thin layer type I collagen and an artificial wound was created in confluent monolayer cultures. Cells were treated with control IgG or hEcad-Fc at a concentration of 12μg/ml and wound closure was measured at 0, 24, and 48 hours [**Fig 3.7A,B**]. Very little effect was observed on wound closure at 24 hours, but a decrease in wound closure was seen in the presence of hEcad-Fc at 48 hours. Similar results were also observed when cells were cultured on plastic (data not shown). As the shed ectodomain was previously associated with increased cell migration and invasion in other cell types (Chunthapong and others 2004; Maretzky and others 2005; Noe and others 2001; Ryniers and others 2002), these preliminary results showing an inhibition of wound closure in OVCA433 on type I collagen were very surprising. Results in Figure 3.6 show that hEcad-Fc disrupted preformed cell-cell junctions in OVCA433 cells, so it is interesting to speculate that decreased cell adhesion is responsible for reduced wound closure, but further investigation of the mechanism utilized by the ectodomain to downregulate cell-cell adhesion is necessary.

After determining that the shed ectodomain inhibited wound closure in OVCA433 cells, its effects were also evaluated in the LP9 mesothelial cell line to determine if it also prevented

wound closure after disseminated ovarian cancer cells disrupt the mesothelial monolayer. LP9 cells express N-cadherin and P-cadherin, but lack E-cadherin expression (Kara Gleason, personal communication). Although LP9 cells did not express E-cadherin, cadherin binding was shown to be more promiscuous that originally predicted, suggesting hEcad-Fc may bind to other cadherin extracellular regions (Niessen and Gumbiner 2002; Prakasam and others 2006). LP9 cells were cultured on thin layer type I collagen for several days to achieve confluence (approximately 90% confluence). Cells were serum starved overnight and an artificial wound was made in the monolayer. The cells appeared to retract slightly in serum-free conditions. LP9 cells did not fill the wound as uniformly as the OVCA433 cells did, but instead elongated and attempted to stretch over the wound [**Fig 3.8A**]. Although this assay was difficult to measure, hEcad-Fc slightly inhibited wound closure in LP9 cells at 24 hours, but these results were not statistically significant [**Fig 3.8B**]. All wounds were closed at 48 hours and could not be measured [**Fig 3.8A**]. These preliminary results are intriguing and worth pursuing due to their physiological relevance as they provide evidence of another mechanism used by the shed ectodomain to enhance ovarian cancer metastasis. Similar results were observed in LP9 cells cultured on plastic (data not shown), although cells did not adhere as well to plastic as to collagen type I. Due to rapid wound closure by these cells, an effect mediated by hEcad-Fc may be more apparent at a time point prior to 24 hours. In addition, as later determined, the culture media and serum-free media used in this experiment was not optimal for LP9 cell growth, suggesting LP9 cells may behave differently if this assay were repeated in the appropriate media.

Figure 3.7

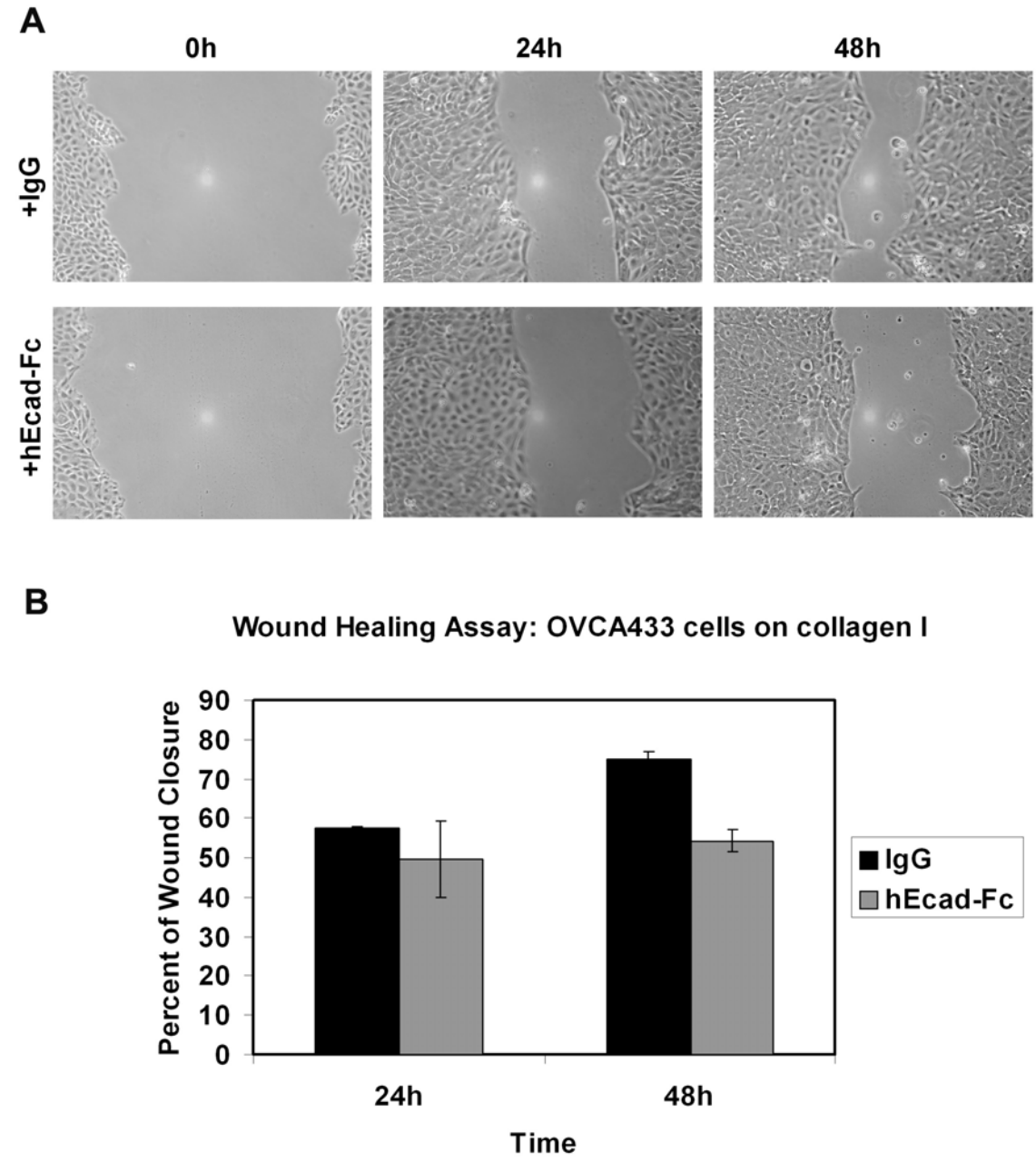
A
0h
24h
48h
+IgG
+hEcad-Fc
B
Wound Healing Assay: OVCA433 cells on collagen I
Percent of Wound Closure
90
80
70
60
50
40
30
20
10
0
24h
48h
Time
IgG
hEcad-Fc

Figure 3.7: Effects of the shed E-cadherin ectodomain on OVCA433 cell wound closure.

Scratch wounds were introduced into confluent cultures of OVCA433 cells on thin layer type I collagen as indicated in Chapter 7 prior to treatment with hEcad-Fc or control IgG (12μg/ml), as indicated. At pre-selected points, cultures were photographed using a digital camera and the relative scratch width was measured. The data included results from 1 assay done in duplicate. Representative images were shown for the 0, 24, and 48 hour time points in **A** and quantitative data were shown for both time points in **B**.

Figure 3.8

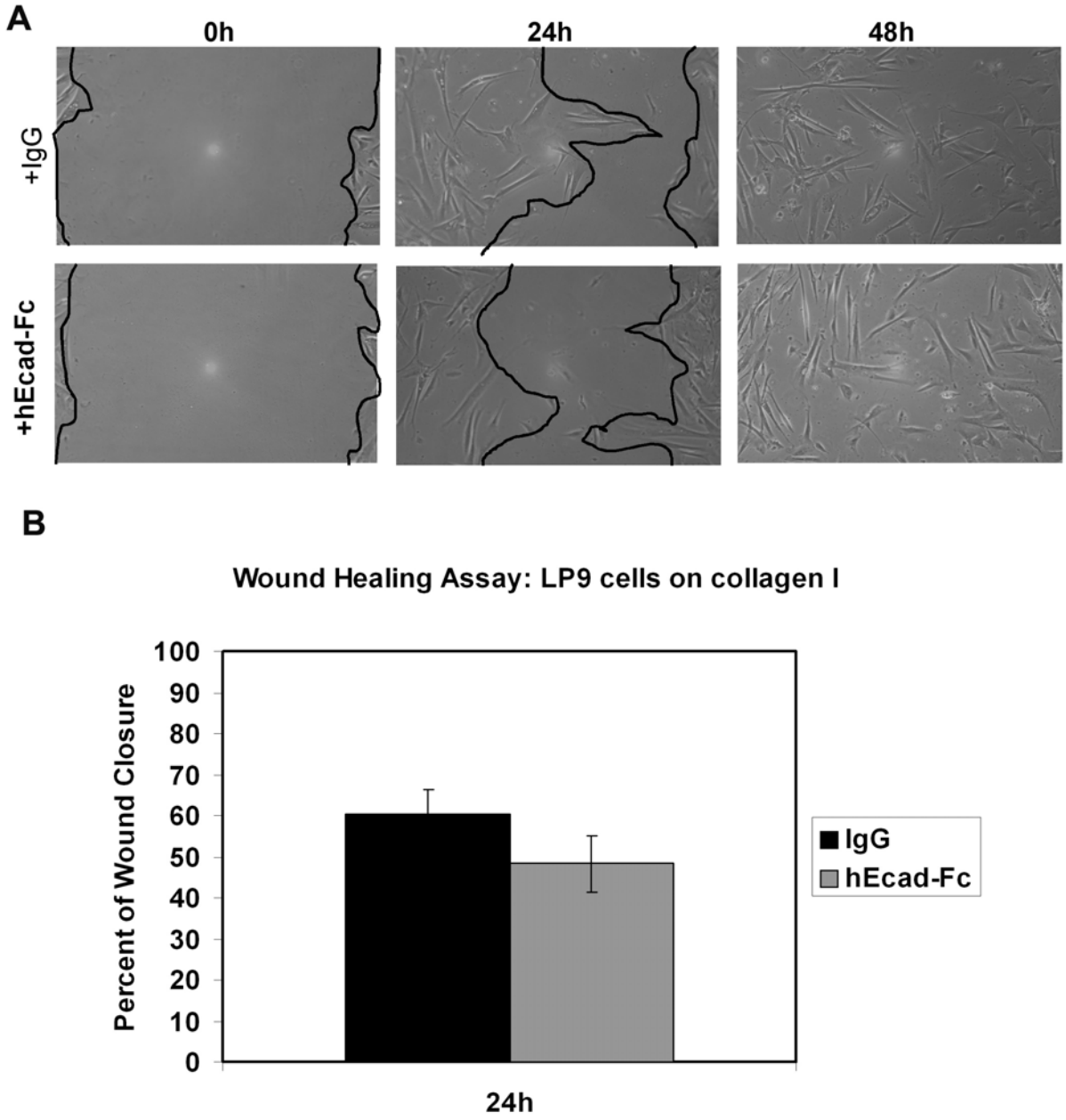
A
0h
24h
48h
+IgG
+hEcad-Fc
B
Wound Healing Assay: LP9 cells on collagen I
Percent of Wound Closure
100
90
80
70
60
50
40
30
20
10
0
24h
IgG
hEcad-Fc

Figure 3.8: Effects of the shed E-cadherin ectodomain on LP9 mesothelial cell wound closure.

Scratch wounds were introduced into confluent cultures of LP9 cells cultured on thin layer type I collagen as indicated in Chapter 7 prior to treatment with hEcad-Fc or control IgG (12μg/ml), as indicated. At pre-selected points, cultures were photographed using a digital camera and the relative scratch width was measured. The data included results from 1 assay done in duplicate. Representative images were shown for the 0, 24, and 48 hour time points in **A** and quantitative data were shown for the 24h time point in **B**.

Discussion

The majority of women with ovarian cancer present at diagnosis with established metastases throughout the peritoneal cavity (Fishman and Borzorgi 2002), suggesting that a more detailed understanding of factors that promote intraperitoneal dissemination may result in therapeutic strategies that target metastasis. Reversible modulation of cell-matrix adhesion, cell-cell adhesion, and proteolytic activity are key events in ovarian cancer metastasis. Shedding of single cells and multi-cellular aggregates from the primary tumor requires junction disruption, while intraperitoneal adhesion and localized invasion are necessary to establish metastases (Ghosh and others 2002). Following disruption of the mesothelial monolayer, disseminated ovarian tumor cells preferentially adhere to the exposed submesothelial ECM via collagen-binding integrins α2β1 and α3β1 and subsequently anchor at these new sites to establish metastases throughout the peritoneal cavity (Ghosh and others 2002). As ovarian cancer induces a fibroproliferative response characterized by enhanced synthesis of interstitial collagens in the peritoneal cavity, EOC cells or multi-cellular aggregates in ascites also encounter collagen species that engage cellular integrins (Zhu and others 1993). Previous data from Dr. Stack and colleagues demonstrating integrin-regulated proteinase expression in EOC cells (Ellerbroek and others 1999; Ellerbroek and others 2001b) suggest a potential functional link between integrin engagement, enhanced proteolytic activity and modulation of E-cadherin function. Although several proteinases have been reported to cleave E-cadherin (Covington and others 2006; Damsky and others 1983; Lochter and others 1997; Maretzky and others 2005; Noe and others 2001), upstream regulators of the proteinase(s) that promote ectodomain shedding are largely unexplored. The current data in this dissertation support the hypothesis that integrin-regulated

MMP-9-catalyzed E-cadherin ectodomain shedding may potentiate metastatic dissemination of EOC [**Fig 3.9**].

While the current data demonstrate a role for MMP-9 expressed by EOC cells in E-cadherin ectodomain shedding, multiple cell types may contribute to MMP-9 expression in the ovarian tumor microenvironment. MMP-9 is produced by epithelial cells, fibroblasts, endothelial cells, and peritoneal mesothelial cells (Martin and others 2000; McCawley and Matrisian 2001b). Similar to murine model studies of squamous cell carcinogenesis demonstrating that inflammatory cells in the stroma are the primary MMP-9 source (Coussens and others 2000), stromal MMP-9 from tumor infiltrating macrophages is also shown to promote angiogenesis and proliferation of ovarian tumors in a murine xenograft model (Huang and others 2002), although extensive macrophage infiltration is not apparent in the human tumors evaluated in the current study [**Fig 3.4D**]. In human ovarian tumors, MMP-9 immunoreactivity is observed in both the epithelial and stromal compartments (Kamat and others 2006; Ozalp and others 2003) and MMP-9 activity is detected by gelatin zymography (Lengyel and others 2001; Naylor 1994). Epithelial MMP-9 immunoreactivity was increased in malignant ovarian tumors relative to borderline ovarian tumors (Ozalp and others 2003). Three distinct studies also demonstrate MMP-9 mRNA expression in the epithelial compartment of human EOC tumors by *in situ* hybridization analysis. (Davidson and others 1999; Huang and others 2000; Naylor and others 1994). These data are supported by studies using short-term primary cultures of EOC cells obtained from primary tumors, ascites, and peritoneal metastases, demonstrating MMP-9 expression in early passage tumor epithelial cells decreases with increasing passage in culture, indicative of regulation by a component(s) of the *in vivo* tumor microenvironment (Fishman and

others 1997). Regardless of the cellular source of the secreted proteinase, high MMP-9 levels in ovarian tumor tissues and ascites are associated with disease recurrence and poor patient survival (Demeter and others 2005). Further, the data in this chapter demonstrate that both EOC-expressed and exogenous MMP-9 effectively catalyze E-cadherin ectodomain shedding.

c-Src and Src-family kinases participate in integrin-mediated transmission of signals from the extracellular microenvironment, either via focal adhesion kinase (FAK) activation (Guo and Giancotti 2004) or by a FAK-independent direct interaction between Src and the β integrin cytoplasmic tail that induces Src activation and stabilizes the activated kinase following integrin clustering (Arias-Salgado and others 2003). Activated Src has been shown to disrupt cadherin-catenin complexes in human colon cancer cells (Irby and Yeatman 2002) and recent studies demonstrate Src-mediated disruption of cell-cell junctions in colon cancer cells that is dependent on integrin signaling (Avizienyte and others 2002). As the current data demonstrate that inhibition of Src activity blocked integrin-induced E-cadherin ectodomain shedding, it is interesting to speculate that Src activity functions to initiate junction dissolution, thereby facilitating access of MMP-9 to the E-cadherin cleavage site at the cell surface.

Integrin-induced E-cadherin ectodomain shedding does not result in a net loss of E-cadherin, as new protein synthesis occurs to replace the shed adhesion molecule. However, other factors prevalent in ascites including LPA and EGF enhance MMP-9 expression in ovarian cancer cells (Ellerbroek and others 2001a)[Chapter 5] and may contribute to E-cadherin ectodomain shedding, resulting in further modulation of E-cadherin function. Although an overall negative correlation between MMP-9 and E-cadherin immunoreactivity was not observed in tumor samples, evaluation of serial sections demonstrated staining heterogeneity such that all

MMP-9 positive tumors exhibited focal areas of high MMP-9 positivity co-localized with low or absent E-cadherin staining. Similar results are observed in OVCA429 cells when exogenous MMP-9 treatment induces changes in E-cadherin localization and expression that are limited to the edges of cell clusters. These results support the hypothesis that MMP-9 is a regulator of E-cadherin ectodomain shedding in the ovarian tumor microenvironment although its influence on E-cadherin expression may be transient or heterogeneous.

It has been proposed that the gain of E-cadherin expression observed during ovarian tumorigenesis is advantageous for metastatic progression by enabling survival of multi-cellular aggregates in suspension (ascites), inducing attachment to other cells in the peritoneal cavity, and promoting cohort migration that facilitates metastatic implantation (Naora and Montell 2005). Results from a recent study have reported that human ovarian carcinomas without metastasis exhibit E-cadherin membrane expression while E-cadherin staining is either cytoplasmic or absent in metastatic ovarian carcinomas (Marques and others 2004), suggesting that sustained E-cadherin expression and/or function is not necessary following tumor cell attachment and anchoring at new sites. Although immunofluorescence images are not provided, it is interesting to note that this study utilizes the HECD-1 antibody, which detects the E-cadherin extracellular domain, and the results are thereby indicative of either a defect in membrane trafficking or, alternatively, enhanced E-cadherin internalization in metastatic lesions that retain E-cadherin positivity (Marques and others 2004). E-cadherin-negative samples in the study from Marques and colleagues (Marques and others 2004) could result from epigenetic silencing of E-cadherin expression (Makarla and others 2005; Rathi and others 2002) and/or may represent lesions with levels of E-cadherin ectodomain shedding that exceed rates of replenishment. Together with the

current data in Figure 3.1 showing high levels of shed E-cadherin ectodomain in ascites from women with ovarian cancer, these combined results indicate multiple complex mechanisms of E-cadherin regulation in ovarian tumors.

The shed E-cadherin ectodomain, at concentrations found in human carcinomatous ascites, induces characteristics of a phenotypic EMT in ovarian cancer cells, such as junction disruption and morphological alteration to a migratory phenotype. Similarly, in both murine mammary epithelium and in a rat cataract model, E-cadherin ectodomain shedding promotes an EMT (Dwivedi and others 2006; Lochter and others 1997). Although the association between EMT and E-cadherin ectodomain shedding has not been evaluated in human cancer models, sE-cad is elevated in the bodily fluids of cancer patients and is associated with poor prognosis or the development of metastasis (Billion and others 2006; Chan and others 2005; Darai and others 1998a; Sundfeldt and others 2001; Syrigos and others 2004). *In vitro*, the E-cadherin ectodomain is linked with increased migration, invasion, proliferation, MMP activity and disrupted adhesion in various cell lines (Chunthapong and others 2004; Liu and others 2006; Nawrocki-Raby and others 2003; Noe and others 2001; Wheelock and others 1987). sE-cad levels are elevated in the cystic fluid from borderline and malignant ovarian tumors when compared to benign cysts and cystadenomas (Sundfeldt and others 2001), suggesting this distinction may have diagnostic value preoperatively.

It is unknown if the 80kDa E-cadherin ectodomain detected in ovarian cancer ascites is a monomer or dimer, as the samples were analyzed in western blots under reducing conditions. hEcad-Fc is currently the best tool available to determine the effects of shed ectodomain and has been used in other investigations (Chunthapong and others 2004; Liu and others 2006). Due to

anticipated technical difficulties, determination of the E-cadherin ectodomain conformation in ascites was never attempted. The ectodomain could potentially be isolated from ascites samples for experimental use, but it is uncertain if denaturation would occur during the low pH elution step, rendering the ectodomain non-functional. Unpurified ascites samples cannot be used since growth factors and proteinases are also present and influence migration, cell junction disruption, and proliferation. Despite a lack of knowledge on the form the E-cadherin ectodomain adopts in the ascites, the results of other studies imply the E-cadherin ectodomain may exist as a dimer. For example, although Pokutta and colleagues have previously reported that the E-cadherin ectodomain exists as a monomer in the presence and absence of calcium (Pokutta and others 1994), Nagar and colleagues have later shown that the E-cadherin ectodomain forms lateral dimers that are held together by calcium ions (Nagar and others 1996), suggesting that the dimerization of shed E-cadherin ectodomain will be induced by calcium present in human serum and ascites. In addition, Brieher and colleagues report that the C-cadherin ectodomain forms dimers in the presence and absence of calcium and does not bind to cells expressing C-cadherin in the absence of calcium (Brieher and others 1996). In support of the results in this dissertation, a monomeric form of the E-cadherin ectodomain expressed in baculovirus did not inhibit cell aggregation of cells expressing E-cadherin (Herrenknecht and Kemler 1993); therefore, calcium may be necessary to mediate disruption of cell-cell junctions as observed in Figure 3.6, especially if this effect is mediated via hEcad-Fc binding to ovarian cancer cells.

The current data provide additional evidence for high levels of sE-cad in the ovarian tumor microenvironment and demonstrate that, in contrast to other tumors where the shed E-

cadherin ectodomain is released into the circulation, primary ovarian tumors maintain direct contact with sE-cad-rich ascites at high concentration. This dissertation supports a model for increased E-cadherin ectodomain shedding as tumor cells disseminate from the primary tumor, adhere to the exposed collagen-rich submesothelial matrix, and upregulate MMP-9 activity as a consequence of integrin clustering [**Fig 3.9**]. As the primary tumor and both suspended and anchored metastatic cells maintain contact with sE-cad-rich ascites, high levels of sE-cad in the ovarian tumor microenvironment may encourage further disaggregation of cells from the primary tumor or ascitic cancer cell spheroids, thereby enhancing metastatic dissemination.

Figure 3.9

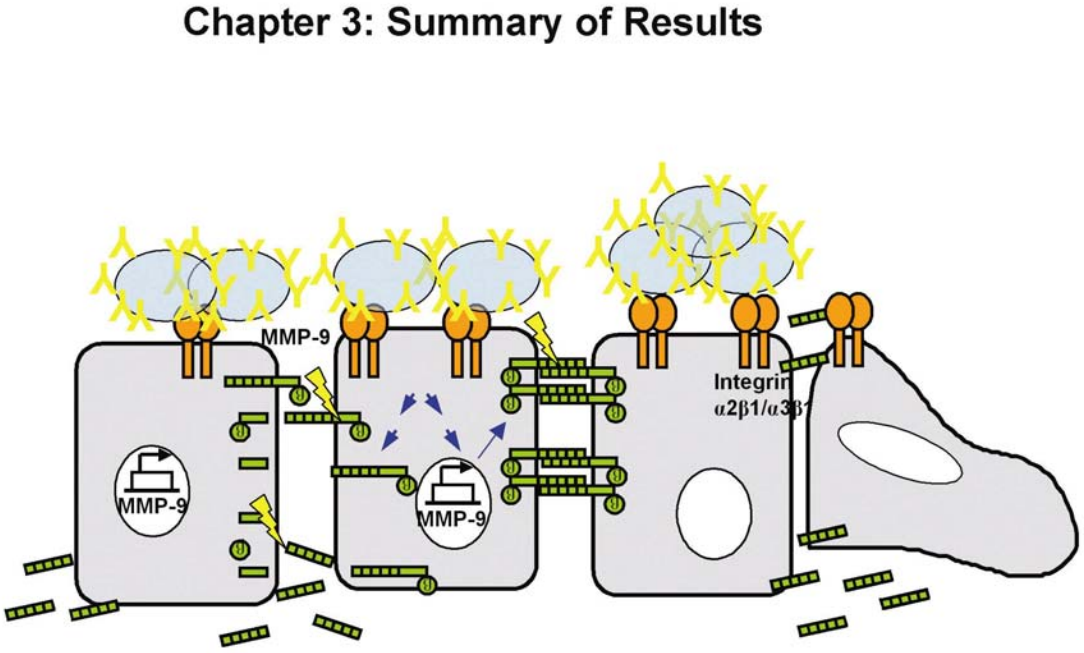
Chapter 3: Summary of Results
MMP-9
MMP-9
MMP-9
Integrin
α2β1/α3β1

Figure 3.9: Chapter 3 summary of results

The data presented in Chapter 3 show that engagement of collagen-binding integrins results in increased MMP-9 expression and MMP-9-dependent E-cadherin ectodomain shedding. The shed ectodomain then disrupts preformed cell-cell junctions, suggesting it may enhance ovarian tumor cell dissemination in patients.

Chapter 4: Cyclooxygenase-2 functions as a mediator of lysophosphatidic acid to promote aggressive behavior in ovarian carcinoma cells.

Results presented in this chapter were previously published in Cancer Research (Symowicz and others 2005).

Introduction and Rationale

As mentioned in Chapter 1 (section VI-B), LPA contributes to the development, progression, and metastasis of ovarian cancer and is increased in both the plasma and ascites of ovarian cancer patients at concentrations up to 80μM (Fang and others 2002a; Westermann and others 1998; Xu and others 1995a). Treatment of ovarian tumor cells with LPA *in vitro* results in an enhanced metastatic phenotype, characterized by increased proteolytic activity, stimulation of motility and more aggressive invasive behavior (Fishman and Borzorgi 2002; Fishman and others 2001). LPA also induces the expression of additional genes that contribute to proliferation, survival, or metastasis, including COX-2 (Fishman and others 2002; Hu and others 2001; Mills and Moolenaar 2003; Moolenaar and others 1986; Reiser and others 1998; Schwartz and others 2001; Xu and others 1998).

A specific role for COX-2 in regulating ovarian cancer metastasis has not been reported, although it has been shown that COX-2 staining is significantly higher in metastatic ovarian tumors (Li and others 2004). COX-2 expression is reported in benign, borderline and malignant ovarian tumors (Ali-Fehmi and others 2003; Denkert and others 2002; Klimp and others 2001; Landen and others 2003; Li and others 2004) where it is associated with chemotherapy resistance and a poor survival rate (Ferrandina and others 2002a). Ascites from ovarian cancer patients contains elevated levels of PGE_2 compared to nonmalignant ascites or ascites from other

carcinomas (Denkert and others 2002), further supporting a role for COX-2 in ovarian pathobiology.

The current study has been undertaken to test the hypothesis that LPA promotes a metastatic phenotype in ovarian cancer cells via a COX-2-dependent mechanism. Evaluation of human ovarian tumors demonstrates positive COX-2 immunoreactivity in 98% of cases, with 70% displaying moderate to high-level expression, including 50% of borderline ovarian tumors. Treatment of ovarian tumor cells with LPA *in vitro* induces COX-2 protein expression in a time and concentration-dependent manner, while COX-1 expression is not affected. In addition to signaling via EDG/LPA receptors, LPA-induced transactivation of EGFR increases COX-2 expression via the Ras/MAPK pathway. Inhibition of COX-2 activity decreases proMMP-2 expression and LPA-induced proMMP-2 activation and reduces MMP-dependent motility and invasion. These data demonstrate that COX-2 functions as a downstream mediator of LPA to potentiate aggressive cellular behavior in ovarian carcinoma cells.

Results

Analysis of COX-2 expression in human ovarian cells and tissues.

Samples from 173 patients were examined for COX-2, COX-1, and cytokeratin-7 immunoreactivity. Of these samples, 77 (45%) were serous carcinoma, 45 (26%) were endometrioid carcinoma, 18 (10%) were clear cell carcinomas, 9 (5%) were mucinous carcinomas, and 24 (14%) were borderline tumors. The vast majority of ovarian tumors (98%) displayed positive COX-2 immunoreactivity. COX-2 expression was high (3+ or 2+) in 63% of patients, compared to 39% with high COX-1 staining [**Table 4.1**]. A representative example of a

serous ovarian tumor with intense COX-2 immunoreactivity is shown relative to COX-1 and keratin 7 in **Figure 4.1 [A-D]**. Of note, 8 of 9 mucinous tumors (89%) displayed high COX-2 expression [**Fig 4.1E-H**]. COX-2 expression was also elevated in borderline ovarian tumors (50%), relative to 29% displaying high COX-1 staining (**Fig 4.1I-L, Table 4.1**). Significant differences in high (3+ or 2+) COX-2 expression between borderline and other tumors were not observed. No significant COX-2 staining was observed in the stromal compartment. Strong COX-2 positivity (3+ or 2+) was not differentially distributed according to FIGO stage or histotype.

Table 4.1. Immunohistochemical expression of COX-1 and COX-2 in borderline and malignant ovarian epithelial tumors.

	COX-2				COX-1			
Histotype	**3+**	**2+**	**1+**	**0**	**3+**	**2+**	**1+**	**0**
Serous (77)	30 (39%)	25 (32%)	19 (25%)	3 (4%)	10 (13%)	35 (45%)	20 (26%)	12 (16%)
Endometrioid (45)	25 (56%)	11 (24%)	9 (20%)	0 (0%)	6 (13%)	6 (13%)	15 (34%)	18 (40%)
Clear Cell (18)	7 (39%)	3 (17%)	7 (39%)	1 (5%)	0 (0%)	1 (5%)	3 (17%)	14 (78%)
Mucinous (9)	5 (56%)	3 (33%)	1 (11%)	0 (0%)	2 (22%)	1 (11%)	0 (0%)	6 (67%)
Borderline (24)	6 (25%)	6 (25%)	12 (50%)	0 (0%)	3 (12%)	4 (17%)	7 (29%)	10 (42%)

Figure 4.1

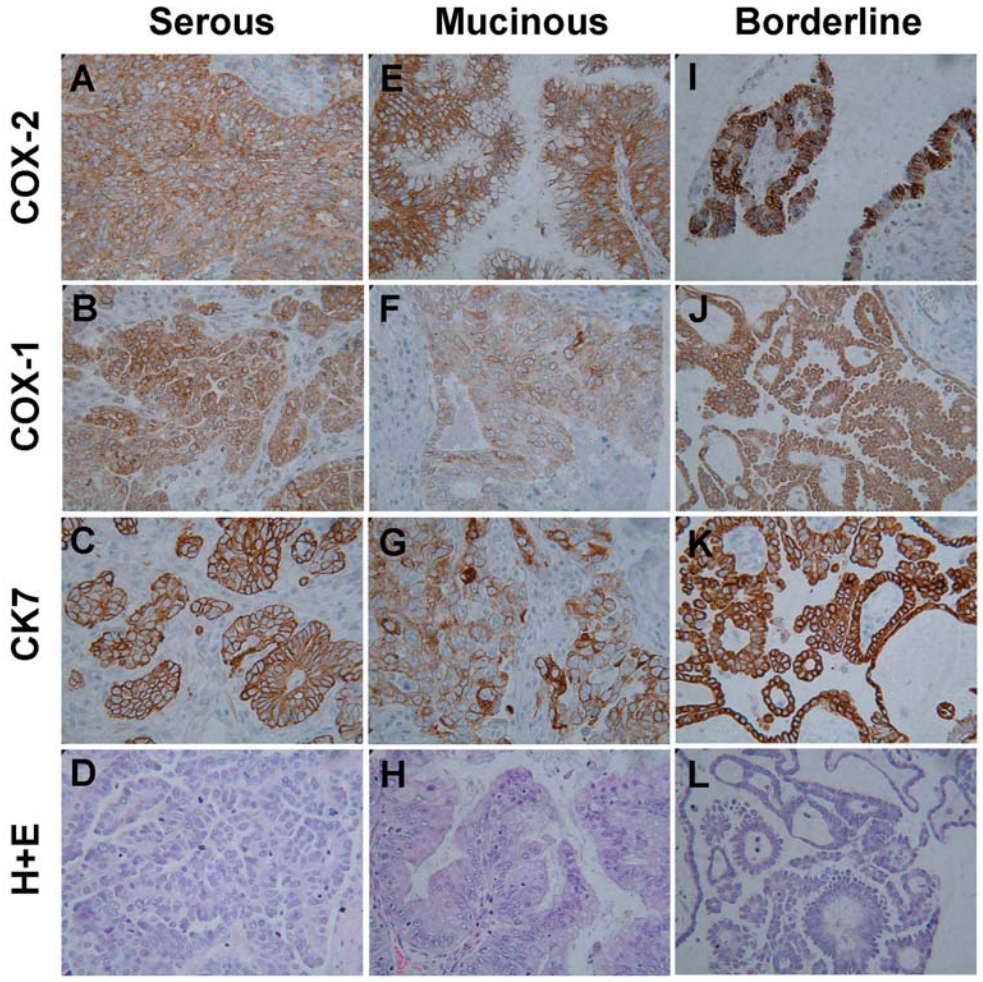

Figure 4.1: Immunohistochemical expression of COX-1, COX-2, and cytokeratin-7 in ovarian tumor samples.

Samples were stained with antibodies to COX-2 (1:200; A, E, I), COX-1 (1:50; B, F, J), cytokeratin-7 (CK7, 1:200; C, G, K) or hematoxylin and eosin (H+E; D, H, L) as detailed in Chapter 7. (A-D) serous carcinoma; (E-H) mucinous carcinoma; (I-L) borderline tumor.

LPA-induced COX-2 expression in ovarian cancer cell lines

LPA levels were often elevated in both the plasma and ascites of ovarian cancer patients where it was reported to contribute to ovarian cancer development, progression and metastasis (Fang and others 2002a; Westermann and others 1998; Xu and others 1995a). As plasma and ascites LPA levels were not available from the patient population above, the effect of LPA on COX-2 expression was instead examined in several ovarian cell lines, including immortalized borderline ovarian carcinoma cells (HuIOSBT-1.5, HuIOSBT-2.2, HuIOSBT-3.3), and several malignant ovarian carcinoma cell lines (OVCA 429, OVCA 433, CaOV-3, OVCAR3, SKOV3, DOV13). With the exception of the CaOV-3 cells, all ovarian carcinoma cell lines were known to be isolated from the ascites of distinct patients. Cells were treated with 30μM LPA for 3 hours and the basal and induced levels of COX-2 protein were analyzed by western blotting relative to a COX-2 standard [**Fig 4.2**]. In borderline ovarian carcinoma cells, HuIOSBT-1.5 and HuIOSBT-3.3 cells expressed low basal levels of COX-2 that were greatly increased with LPA treatment, while HuIOSBT-2.2 cells expressed high basal levels of COX-2 that were unchanged with the addition of LPA. Differential responses were observed in the six malignant ovarian carcinoma cell lines, with 4 of the 6 cell lines responding to LPA treatment by induction of COX-2 (**Fig. 4.2**; OVCA429, OVCA433, CaOV-3, DOV13). Neither SKOV-3 nor OVCAR3 cells expressed detectable constitutive or LPA-inducible COX-2. As shown in a representative example using DOV13 cells, induction of COX-2 was time-dependent, reaching a maximum at 2 to 4 hours following LPA treatment [**Fig 4.3A**]. Induction was observed at low LPA concentrations (10 μM) and was positively regulated by increasing LPA concentration [**Fig**

4.3B]. No constitutive or LPA-inducible COX-1 expression was observed in the DOV13 cells under these conditions [**Fig 4.3C**].

LPA transduces signals via the endothelial differentiation gene EDG/LPA subfamily of G protein-coupled receptors leading to changes in adenylate cyclase activity, activation of the Ras-Raf-Erk pathway, and stimulation of phospholipases C and D (Mills and Moolenaar 2003; Xu and others 1998). With the exception of OVCAR3 and SKOV3, expression of EDG/LPA receptor family members was not previously characterized in these cell lines. Treatment of cells with LPA in the presence of pertussis toxin (PTX) decreased COX-2 induction [**Fig 4.4A, top panel, lane 3**], implicating LPA-dependent signaling through G_i protein-coupled receptors in this process (Westermann and others 1998). Activation of EGFR family members was also reported to induce COX-2 expression (Coffey and others 1997; Vadlamudi and others 1999). Further, recent studies implicated LPA in EGFR transactivation via both PTX-sensitive and –insensitive pathways (Daub and others 1997; Daub and others 1996; Gshwind and others 2002; Kim and others 2000; Laffargue and others 1999). Treatment of DOV13 cells with LPA under serum-free conditions induced phosphorylation of EGFR [**Fig 4.4A, middle panel**], showing that LPA can transactivate EGFR in DOV13 cells. LPA-mediated transactivation of EGFR was PTX insensitive [**Fig 4.4A, middle panel, lane 3**]. Co-treatment with LPA and the EGFR-specific tyrosine kinase inhibitor AG1478 also abrogated the ability of LPA to induce COX-2 expression [**Fig 4.4A, top panel, lane 4**]. Similar results were obtained following inhibition of the Ras/MAPK pathway using the MEK inhibitor PD98059 [**Fig 4.4B**]. Combined treatment of DOV13 cells with LPA, PTX, and AG1478, resulted in a greater reduction in COX-2 protein induction relative to treatment with each inhibitor individually [**Fig 4.4A, top panel, lane 5**],

suggesting that distinct signaling pathways promote COX-2 expression. To provide further support for this hypothesis, DOV13 cells were treated with LPA and EGF. Both EGF [**Fig 4.4C, lane 2**] and LPA [**Fig 4.4C, lane 3**] individually induced COX-2 protein expression, while co-treatment with both EGF and LPA further enhanced COX-2 expression [**Fig 4.4C, lane 4**]. Together these data support a major role for LPA-mediated EGFR transactivation in COX-2 induction and suggest both EDG/LPA receptors and EGFR contribute to optimal LPA-mediated COX-2 induction DOV13 cells.

Figure 4.2

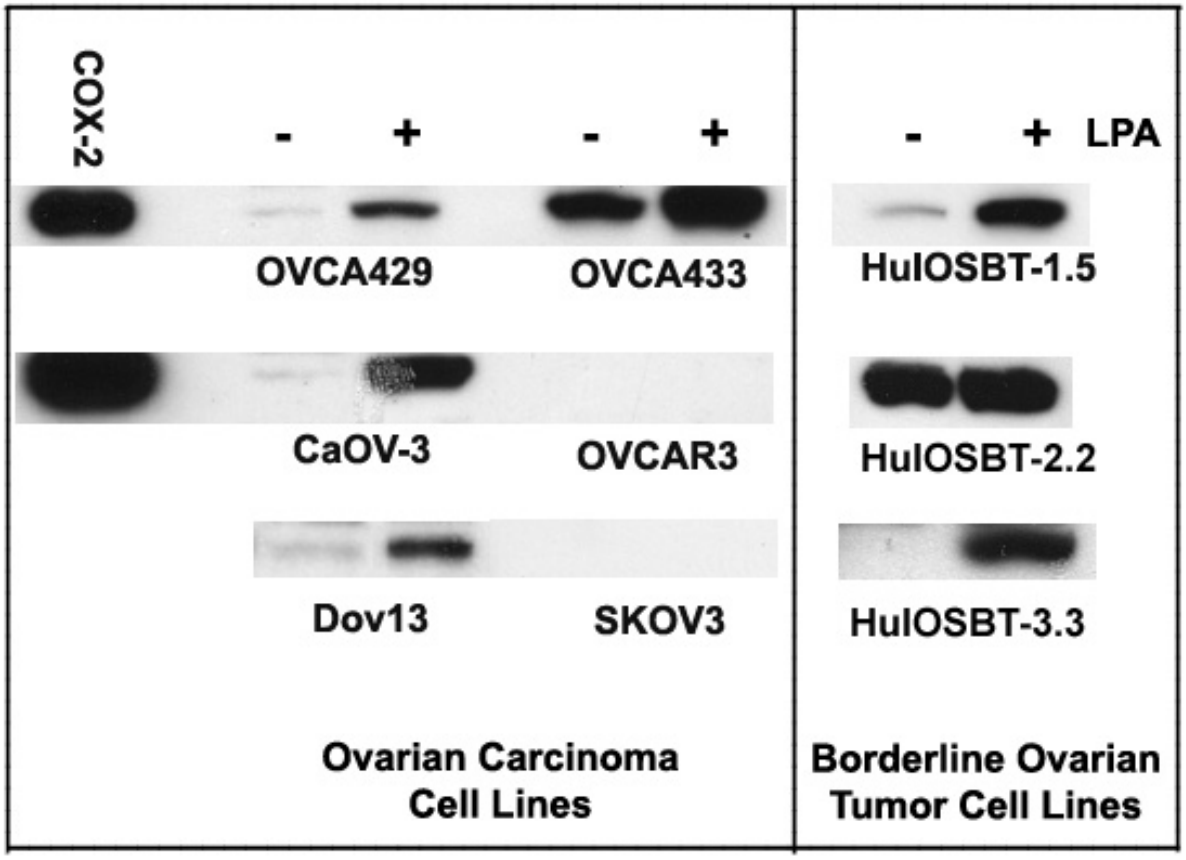
COX-2
- + - +
OVCA429
OVCA433
CaOV-3
OVCAR3
Dov13
SKOV3
Ovarian Carcinoma Cell Lines
- + LPA
HulOSBT-1.5
HulOSBT-2.2
HulOSBT-3.3
Borderline Ovarian Tumor Cell Lines

Figure 4.2: Effect of LPA on COX-2 expression in ovarian cells.

Cells were cultured as indicated in Chapter 7, serum starved overnight, and cultured in the presence or absence of 30μM LPA for 3 hours. Cells lysates (50μg for all cell lines except OVCAR3 - 30μg) were electrophoresed on an 8% SDS-polyacrylamide gel, electroblotted to PVDF membrane, and probed with anti-COX-2 (1:1000 dilution) followed by peroxidase-conjugated secondary antibody (1:5000) and enhanced chemiluminescence detection. A COX-2 standard (50ng) was included as a control.

Figure 4.3

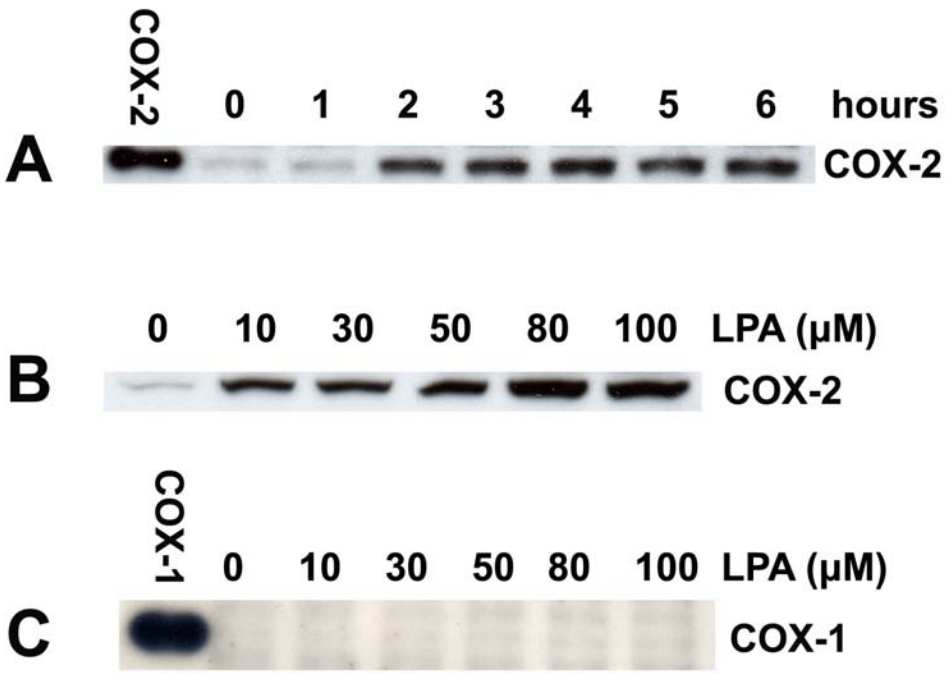
COX-2
0
1
2
3
4
5
6
hours
A
COX-2
0
10
30
50
80
100
LPA (μM)
B
COX-2
COX-1
0
10
30
50
80
100
LPA (μM)
C
COX-1

Figure 4.3: LPA induces COX-2 expression in a time and concentration-dependent manner.

A) DOV13 cells were cultured in the presence of 30μM LPA for time points indicated. Lysates (65μg) were electrophoresed on an 8% SDS-polyacrylamide gel, electroblotted to PVDF membrane, and immunoblotted with anti-COX-2 (1:1000), followed by peroxidase-conjugated secondary antibody (1:5000) and enhanced chemiluminescence detection. A COX-2 standard (50ng) was included as a control.

B) DOV13 cells were cultured for 3 hours in the presence of increasing concentrations of LPA as indicated. Lysates (80μg) were electrophoresed on an 8% SDS-polyacrylamide gel, electroblotted to PVDF membrane and immunoblotted with anti-COX-2 (1:1000), followed by peroxidase-conjugated secondary antibody (1:5000) and enhanced chemiluminescence detection. A COX-2 standard (50ng) was included as a control (not shown).

C) DOV13 cells were cultured for 3 hours in the presence of increasing concentrations of LPA, as indicated. Lysates (65μg) were electrophoresed on an 8% SDS-polyacrylamide gel, electroblotted to PVDF membrane and immunoblotted with anti-COX-1 (1:1000), followed by peroxidase-conjugated secondary antibody (1:5000) and enhanced chemiluminescence detection. A COX-1 standard (50ng) was included as a control.

Figure 4.4

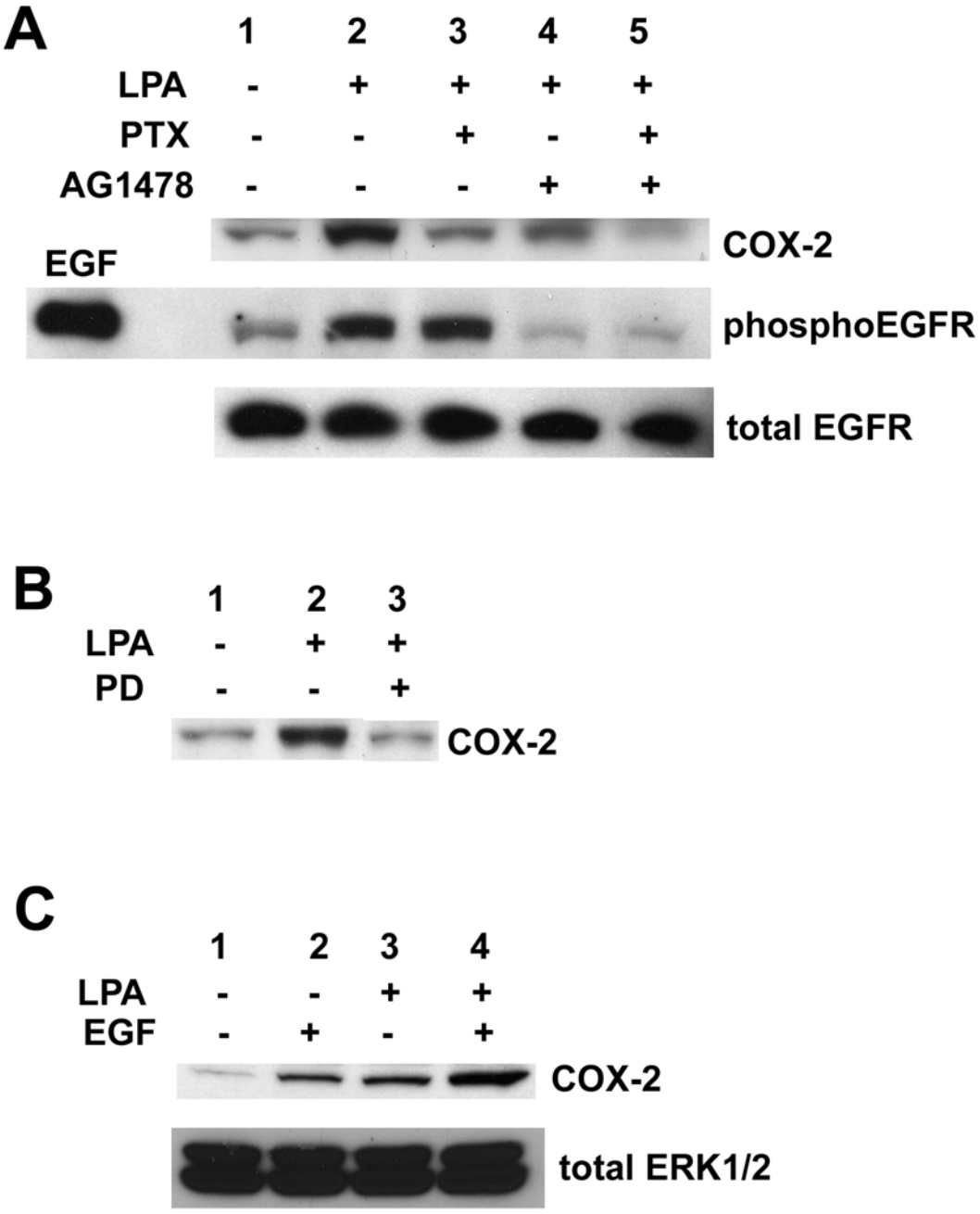
A
1 2 3 4 5
LPA - + + + +
PTX - - + - +
AG1478 - - - + +
EGF
COX-2
phosphoEGFR
total EGFR
B
1 2 3
LPA - + +
PD - - +
COX-2
C
1 2 3 4
LPA - - + +
EGF - + - +
COX-2
total ERK1/2

Figure 4.4: LPA induces COX-2 expression via EDG/LPA receptor and EGFR transactivation.

A) DOV13 cells were pretreated with PTX (100ng/ml) in the presence or absence of the EGFR tyrosine kinase inhibitor AG1478 (10μM) for 2 hours prior to addition of LPA (30μM) for 3 hours. Lysates (50μg) were electrophoresed on an 8% SDS-polyacrylamide gel, electroblotted to PVDF membrane, and immunoblotted with anti-COX-2 (1:1000), anti-phosphoEGFR mixture (1:1000) or anti-total EGFR (1:1000) as indicated, followed by peroxidase-conjugated secondary antibody (1:5000) and enhanced chemiluminescence detection. OVCA433 cells treated with EGF (20ng/ml) served as a positive control for EGFR phosphorylation (center panel).

B) DOV13 cells were pretreated with the MEK inhibitor PD98059 (50μM) prior to the addition of LPA (30μM) for 3 hours. Lysates (75μg) were electrophoresed on an 8% SDS-polyacrylamide gel, electroblotted to PVDF membrane, and immunoblotted with anti-COX-2 (1:1000), followed by peroxidase-conjugated secondary antibody (1:5000) and enhanced chemiluminescence detection. A COX-2 standard (50ng) was included as a control (not shown).

C) DOV13 cells were treated with EGF (30ng/ml) and/or LPA (30μM) for 4 hours. Lysates (70μg) were electrophoresed on an 8% SDS-polyacrylamide gel, electroblotted to PVDF membrane, and immunoblotted with anti-COX-2 (1:1000), followed by peroxidase-conjugated secondary antibody (1:5000) and enhanced chemiluminescence detection. A COX-2 standard (50ng) was included as a control (not shown). The blot was stripped and reprobed with anti-total ERK 1/2 (1:2000) to verify equal loading.

Functional effect of COX-2 inhibition on LPA-induced aggressive behavior

Separate studies implicated either LPA or COX-2 in expression and activation of proMMP-2 (Attiga and others 2000; Fishman and others 2001; Pan and others 2001; Tsujii and others 1997). To evaluate whether COX-2 activity is necessary for LPA-induced proMMP-2 activation, DOV13 cells were pretreated with increasing concentrations of the specific COX-2 inhibitor NS-398 followed by LPA for an additional 24 hours and changes in proMMP-2 processing were evaluated via gelatin zymography. As previously reported using LPA concentrations as low as 2.5-5μM (Fishman and others 2001), LPA stimulates activation of proMMP-2, as indicated by the appearance of a lower molecular weight band representative of the activated form of the enzyme [**Fig 4.5, lane 2, arrow**]. Treatment with NS-398 blocked the ability of LPA to induce proMMP-2 activation in a dose dependent manner [**Fig 4.5A, lanes 3-5**], implicating COX-2 as a mediator of LPA-induced MMP-2 activation. At higher concentrations (100μM), downregulation of proMMP-2 protein expression was also observed [**Fig 4.5, lane 5**], although no effect on cell viability was evident. This was confirmed by an MMP-2 ELISA, showing a decrease in total MMP-2 (pro and active) expression in the presence of NS-398 (**Fig 4.5B**, *$p<.05$, #$p<.005$), indicating that COX-2 modulates pericellular proteolytic potential via regulation of both proMMP-2 expression and activation. No change in MT1-MMP or TIMP-2 were observed (data not shown).

LPA was previously reported to potentiate the motility and invasiveness of ovarian cancer cells (Fishman and others 2001; Pustilnik and others 1999; Sawada and others 2002). Similarly, COX-2 activity is necessary for enhanced migration and spreading of cancer cells and endothelial cells (Dormond and others 2002; Dormond and others 2001; Eibl and others 2003;

Timoshenko and others 2003), and overexpression of COX-2 enhances invasiveness of colon carcinoma cells (Tsujii and others 1997). To determine whether the LPA-induced increase in motility and invasiveness in ovarian cancer cells requires COX-2 activity, an artificial wound was created in confluent cultures of DOV13 cells and the effect of COX-2 inhibition on LPA-stimulated wound closure was evaluated. Inhibition of COX-2 activity blocked LPA-stimulated wound closure in a dose dependent manner at both 24 hours and 48 hours [**Fig 4.6A,B**, $p<.05$]. Dr. Stack and colleagues previously reported that LPA stimulates the MMP-dependent invasive activity of DOV13 cells (Fishman and others 2001). To evaluate the requirement for COX-2 activity in this process, cells were seeded into HTS Fluoroblok inserts overlaid with Matrigel and incubated for 48 hours prior to labeling followed by quantification of the invasive cells. Inhibition of COX-2 activity abrogated the stimulatory effect of LPA on ovarian cancer cell invasive activity [**Fig.4.6C**, $p<.005$].

Figure 4.5

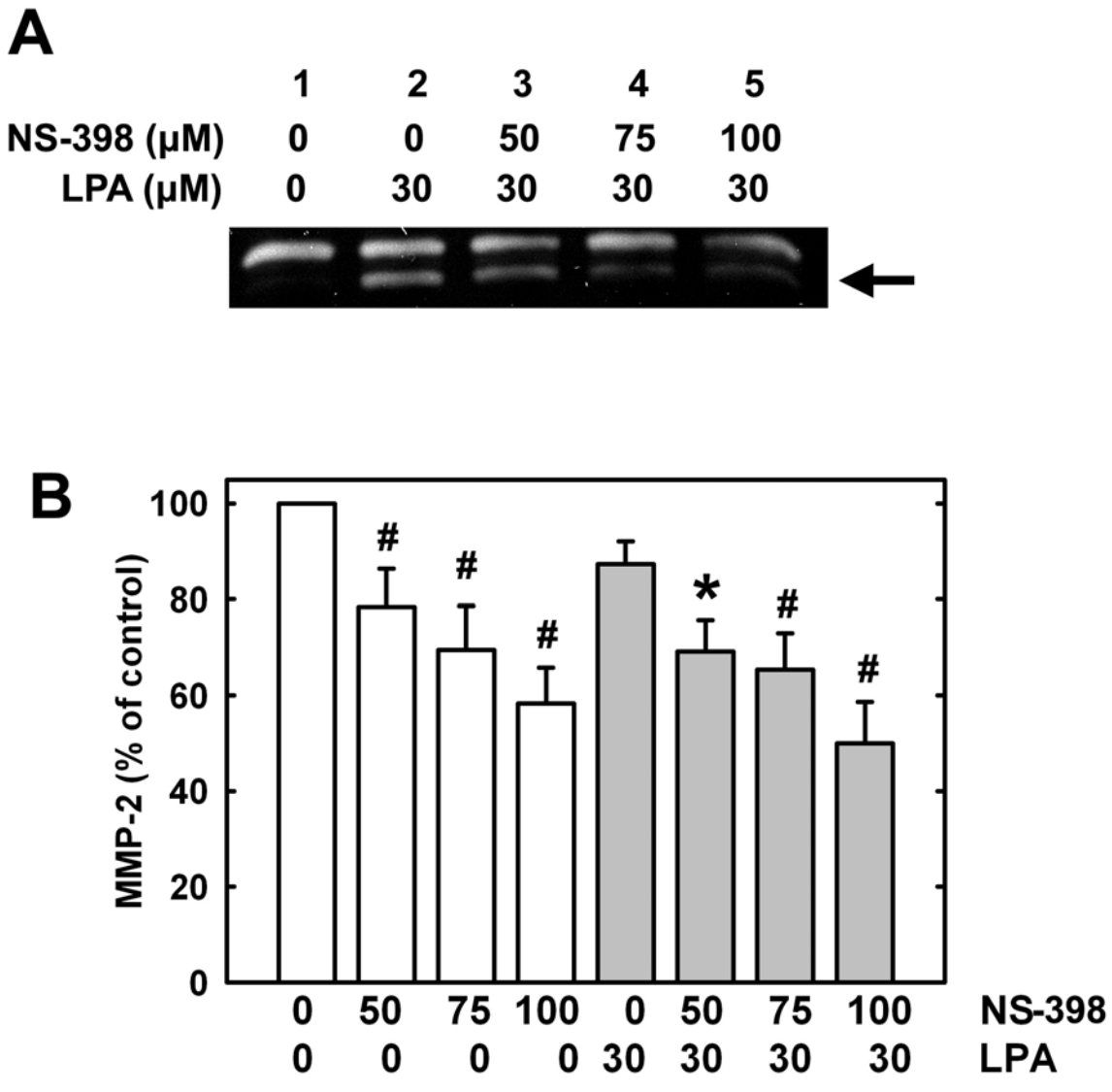
A
1 2 3 4 5
NS-398 (μM) 0 0 50 75 100
LPA (μM) 0 30 30 30 30
B
MMP-2 (% of control)
100
80
60
40
20
0
#
#
#
*
#
#
0 50 75 100 0 50 75 100 NS-398
0 0 0 0 30 30 30 30 LPA

Figure 4.5: COX-2 inhibitor NS-398 decreases LPA-induced proMMP2 activation and proMMP-2 expression.

A) DOV13 cells were pretreated with NS-398 as indicated for 3 hours prior to culture in the presence of LPA (30μM) for 24 hours. Conditioned media was analyzed by gelatin zymography. Arrow: migration position of active MMP-2.

B) Conditioned media was also analyzed using ELISA to detect total MMP-2 expression. The data include results from 4 separate experiments. (#$p<.005$; *$p<.05$)

Figure 4.6

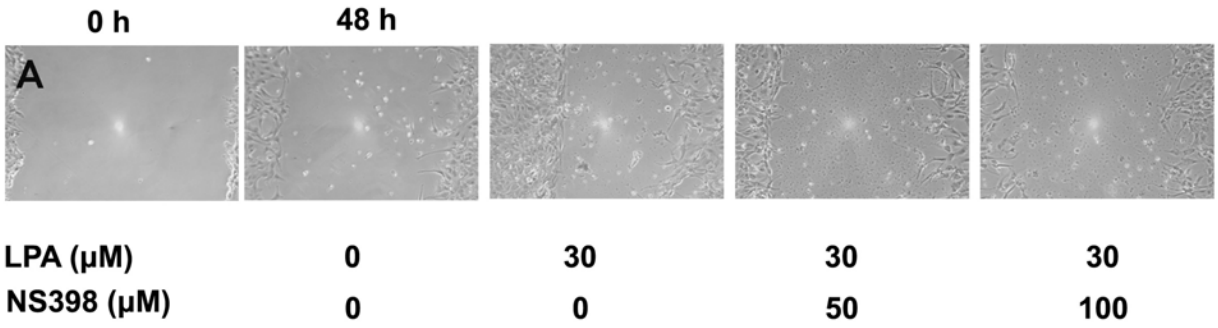
0 h
48 h
A
LPA (μM) 0 30 30 30
NS398 (μM) 0 0 50 100

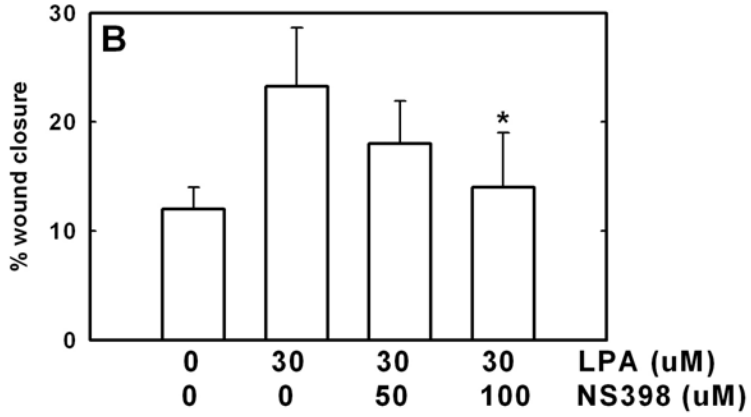
B
% wound closure
30
20
10
0
*
0 30 30 30 LPA (uM)
0 0 50 100 NS398 (uM)

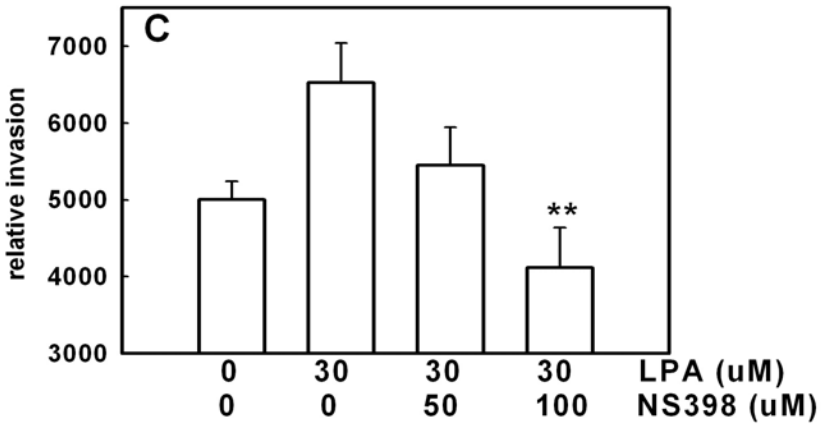
C
relative invasion
7000
6000
5000
4000
3000
**
0 30 30 30 LPA (uM)
0 0 50 100 NS398 (uM)

Figure 4.6: COX-2 inhibitor NS-398 decreases LPA-induced motility and invasion.

A,B) Scratch wounds were introduced into confluent cultures of DOV13 cells as indicated in Chapter 7 prior to treatment with NS-398 in the presence or absence of LPA, as indicated. At pre-selected points, cultures were photographed using a digital camera and the relative scratch width determined using the MetaMorph Imaging System. The data include results from 3 separate assays. Representative images are shown for the 48 hour time point in A and quantitative data are shown for the 24 hour time point in B (*$p<.05$).

C) DOV13 cells were added to the Matrigel coated top chamber of the HTS Fluoroblok Insert System and pre-incubated for 1 hour in the presence or absence of NS-398 as indicated. LPA (30μM) was added and cells were allowed to invade for 48 hours prior to staining with calcein AM and quantitation of fluorescence as indicated in Chapter 7. Data represent the average of three separate experiments (**$p<.005$).

Discussion

In ovarian cancer patients, LPA concentrations are elevated in the ascites and range from 1 to 80μM, providing an LPA-rich microenvironment for ovarian tumors (Fang and others 2002a; Fishman and Borzorgi 2002; Mills and others 2002b; Xiao and others 2001; Xu and others 1995a; Xu and others 1998). LPA promotes the proliferation, survival, and metastasis of ovarian cancer by inducing the expression of key regulatory genes (Hu and others 2001; Moolenaar and others 1986; Schwartz and others 2001; Xu and others 1998). Proteinase regulation is also modulated by LPA in ovarian cancer cells, leading to LPA-dependent changes in motility and invasive behavior (Fishman and Borzorgi 2002; Fishman and others 2001). The current data demonstrate that LPA also induces COX-2 expression in premalignant and malignant ovarian epithelium, indicating a role for COX-2 as a downstream mediator of LPA. This is supported by analysis of human ovarian tumors, the majority of which exhibit strong COX-2 immunoreactivity (Ali-Fehmi and others 2003; Denkert and others 2002; Ferrandina and others 2002a; Klimp and others 2001; Landen and others 2003)[**Fig 4.1 and Table 4.1**].

While data regarding COX-2 expression in the normal ovary suggest a functional link to ovulation (Denkert and others 2002; Landen and others 2003; Lim and others 1997; Matsumoto and others 2001), COX-2 expression is observed in benign, borderline and malignant ovarian tumors (Ali-Fehmi and others 2003; Denkert and others 2002; Klimp and others 2001; Landen and others 2003; Li and others 2004). The data in this chapter are in agreement with the published results. Although the majority of studies report lack of correlation between COX-2 immunoreactivity and tumor stage, grade or histological type, COX-2 positivity has been proposed as an independent prognostic indicator (Ali-Fehmi and others 2003; Denkert and others

2002; Ferrandina and others 2002a). Although the data in this dissertation also show a lack of correlation between COX-2 immunoreactivity and tumor stage, it is interesting to note that 8 of 9 cases with a mucinous histotype were strongly COX-2 positive (2+ or 3+), as previously reported for two mucinous ovarian tumors in a separate study (Ferrandina and others 2002a).

The current data support a role for LPA in the induction of COX-2 expression in ovarian carcinoma cells and tumors. This is consistent with the observation that expression of both LPA and COX-2 is detectable in ovarian cancer patients with early stage disease (Ali-Fehmi and others 2003; Denkert and others 2002; Ferrandina and others 2002a; Sutphen and others 2004; Westermann and others 1998). The magnitude of LPA-induced COX-2 expression varied among the immortalized borderline and malignant ovarian carcinoma cell lines. These cell lines are derived from distinct patients, accounting for their varying physiological characteristics, and likely differentially express members of the EDG/LPA receptor family (Mills and others 2002b). COX-2 induction is blocked by pertussis toxin, implicating LPA signaling through G_i protein coupled receptors in the EDG/LPA receptor family (Xu and others 1998). The data in this dissertation also further support a mechanism in which LPA transactivates EGFR and demonstrate that EGFR tyrosine kinase activity is also necessary for maximal LPA-induced COX-2 expression. EGFR family members (EGFR, ErbB2, and ErbB3) are frequently overexpressed in ovarian tumors (Ferrandina and others 2002b) and EGFR overexpression is associated with a more invasive and malignant phenotype in ovarian cancer cells (Alper and others 2001; Alper and others 2000; Brader and others 1998). In addition, EGFR signaling mediates COX-2 induction in other cancer cell lines (Kulkarni and others 2001; Ohno and others 2001; Sheng and others 2001; Vadlamudi and others 1999). Crosstalk between EGFR and G_i

protein coupled receptors promotes EGFR transactivation in the absence of EGF (Gshwind and others 2001). LPA has previously been reported to transactivate EGFR in several different cells types, including head and neck squamous carcinoma cell lines (Gshwind and others 2002), PC12 cells (Kim and others 2000), keratinocytes (Daub and others 1997), COS-7 cells (Daub and others 1997), and Rat-1 fibroblasts (Daub and others 1996). In addition, ErbB-2 has been reported to associate with a specific sequence in the COX-2 promoter to increase COX-2 gene expression (Wang and others 2004). Together these data support a mechanism where both LPA-induced transactivation of EGFR and activation of the EDG/LPA receptor results in upregulated COX-2 expression in ovarian tumors [**Fig 4.7**]. It should be noted that in two recent studies, COX-2 immunoreactivity did not correlate with EGFR expression in ovarian tumors (Ali-Fehmi and others 2003; Ferrandina and others 2002b). However, the presence of LPA in the ascites or serum of these patients may lead to amplification of EGFR signaling without altering EGFR expression status. Analysis of a potential relationship between EGFR activation (i.e., phosphorylation) and COX-2 expression was not yet reported.

LPA-induced expression of COX-2 may contribute to ovarian cancer progression via multiple mechanisms. COX-2 expression was recently correlated with tumor angiogenesis in patients with high-grade, advanced stage serous ovarian carcinoma (Ali-Fehmi and others 2003) and other reported functions of COX-2 include inhibition of apoptosis and promotion of proliferation and angiogenesis (Dempke and others 2001). Treatment with COX-2 inhibitors such as NS-398 may block these pathways through COX-2-dependent and –independent mechanisms (Denkert and others 2003; Grosch and others 2001; Rodriguez-Burford and others 2002). The current data demonstrate that inhibition of COX-2 activity decreases proMMP-2

expression and LPA-induced proMMP-2 activation and subsequently inhibits LPA-induced motility and invasive activity [**Fig 4.7**]. In support of this observation, COX-2-overexpressing colon carcinoma cells exhibit enhanced proMMP-2 activation and invasiveness that is blocked by treatment with a COX inhibitor (Tsujii and others 1997) and COX-2 inhibition in lung and prostate cancer cells leads to decreased MMP-2 expression (Attiga and others 2000; Pan and others 2001). Currently very little is known about the mechanisms by which COX-2 or prostaglandins increase MMP activity and cell invasiveness, but it has previously been shown that the COX-2 inhibitor NS-398 decreases the transcription of MMP-2, reducing both its expression and activity (Pan and others 2001). The data in this chapter showing that NS-398 treatment decreases expression of proMMP-2 suggests that MMP-2 activity is decreased in a similar manner in ovarian carcinoma. A slight increase in COX-2 protein levels is observed following long term treatment with high concentrations of NS-398 (data not shown), however LPA-induced COX-2 expression clearly predominates in this system. Further, the decrease in pro- and active MMP-2 following NS-398 treatment for 24 hours indicates that COX-2 activity remains inhibited by NS-398 at this time point. Altered COX-2 protein in response to NS-398 was observed in colorectal cancer cell lines at 72 and 96 hours (Elder and others 2000; Elder and others 2002) and in pancreatic cancer cell lines at 48 hours (Molina and others 1999).

Many reports examining the clinical benefits of COX-2 inhibitors and NSAIDs in ovarian cancer address the role of these compounds in chemoprevention (Akhmendkhanov and others 2001; Mills 2002a; Smith and others 2004; Tavani and others 2001), but their therapeutic efficacy at modulating progression is yet to be determined. It is possible that COX-2 inhibitors may have a detrimental effect when administered with other chemotherapeutic agents, as

demonstrated in an *in vitro* study showing reduced apoptotic effects of paclitaxel on two ovarian cancer cell lines co-treated with NS-398 (Munkarah and others 2003). However, COX-2 inhibitor therapy is promising in the treatment of other cancers and recent data suggest that celecoxib may actually improve the preoperative response to paclitaxel and carboplatin in patients with non-small cell lung cancer (Altorki and others 2003). Another recent study suggests that rofecoxib, a specific COX-2 inhibitor, may negatively regulate angiogenesis in human colorectal cancer liver metastases (Fenwick and others 2003). As of 2005, many clinical trials investigating the efficacy of celecoxib in breast, cervical, pancreatic, non-small cell lung, colon, and prostate cancer are underway (www.cancer.gov). Based on the results of the current study and other published data, it is reasonable to speculate that COX-2 inhibitor therapy may also prove efficacious for ovarian cancer patients. However many questions regarding the therapeutic use of COX-2 inhibitors remain, such as the stage(s) of tumor development when treatment will be most effective and the combination of therapies that can be administered with COX-2 inhibitors for the greatest benefit. COX-2 overexpression was observed in ovaries experiencing early preneoplastic changes, leading to speculation that COX-2 may mimic ovulation by promoting the loss of the basement membrane of the ovarian surface epithelium, increasing the risk of ovarian tumorigencity (Roland and others 2003; Smith and others 2004); therefore, COX-2 inhibitors may be more beneficial in the early stages of cancer or as chemopreventive agents. In addition, preclinical data using the *Min* mouse model of colon cancer demonstrated that combination therapy comprised of both a COX-2 and an MMP inhibitor is more efficacious than either agent alone (Wagenaar-Miller and others 2003), suggesting combination therapy may be more beneficial in treating stage III and IV ovarian

cancer. Based on our results, future development of molecular diagnostic techniques that allow individual characterization of multiple parameters such as the presence and concentration of LPA in serum or ascites, the expression and activity of EGFR and COX-2, and the presence of active proteinases such as MMP-2 may allow for the development of more effective ovarian cancer patient-targeted combination therapies.

Following the publication of the results presented in Chapter 4, a later study has suggested that COX-1 is a better therapeutic target for EOC treatment (Daikoku and others 2005). This study relies on use of a mouse model where murine OSE containing minimal tumor-inducing genetic alterations have been used to generate ovarian tumors. The OSE cells and resulting tumors express high levels of COX-1. Tumor growth is reduced with a specific COX-1 inhibitor, but treatment with a COX-2 inhibitor has no effect. Unfortunately, murine OSE cells are used to generate EOC models in this study (Daikoku and others 2005). Rodent OSE cells are more conducive to cellular transformation than human OSE cells (Liu and others 2004). Even though COX-1 is expressed in many ovarian tumor samples [**Table 4.1**] (Gupta and others 2003), it is unknown if the same observations would occur in a mouse model using human OSE cells to generate EOC. In addition, Daikoku and colleagues did not consider the ovarian tumor microenvironment, which can alter COX-2 expression in ovarian cancer cell lines as demonstrated in this chapter. As DOV13 ovarian cancer cells lack COX-1 expression [**Fig 4.3**], the effects of the tumor microenvironment on COX-1 expression could not be determined, but since many ovarian tumors express both COX-1 and COX-2, it would be beneficial to now consider NSAID treatment for ovarian cancer patients to inhibit both cyclooxygenase isoforms.

Figure 4.7

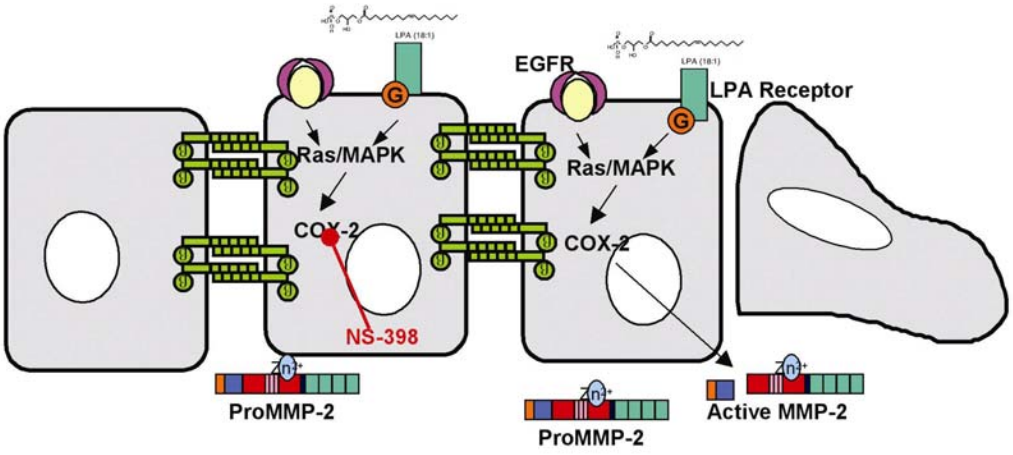
Chapter 4 Summary
LPA (18:1)
EGFR
LPA Receptor
G
Ras/MAPK
COX-2
NS-398
ProMMP-2
Active MMP-2

Figure 4.7: Chapter 4 summary of results

COX-2 protein expression is increased in the DOV13 ovarian cancer cell line via the EDG/LPA receptors and transactivation of EGFR. COX-2 then acts as a downstream mediator of LPA since COX-2-specific inhibitor NS-389 treatment results in decreased proMMP-2 activation, cell migration, and matrigel invasion.

Chapter 5: Lysophosphatidic acid regulation of matrix metalloproteinase-9-dependent E-cadherin cleavage and ectodomain shedding

Introduction and Rationale

. Although mutations in the E-cadherin gene are rare in ovarian tumors (Wong and Auersperg 2002), post-translational modification of E-cadherin function is suggested by data demonstrating sE-cad in ascites and cystic fluids from ovarian cancer patients (Darai and others 1998a; Sundfeldt and others 2001)(Chapter 3). Due to its elevated concentrations in ovarian cancer patients, including stage I patients, LPA is identified as an additional factor found in the ovarian tumor microenvironment that promotes ovarian cancer dissemination. Several studies have shown that LPA treatment increased proteolytic activity, motility, and invasion in ovarian cancer cells *in vitro* (Fishman and Borzorgi 2002; Fishman and others 2001; Li and others 2005; Pustilnik and others 1999; Ren and others 2006; So and others 2004), but the effects of LPA on cell-cell adhesion and E-cadherin are largely unexplored. LPA is associated with enhancing adherens junction dissolution and colony dispersal (Jourquin and others 2006) and with indirectly promoting an EMT via phosphorylation of Stat5a in a Rho-dependent manner (Benitah and others 2003). As MMPs are implicated in E-cadherin ectodomain shedding (Covington and others 2006; Damsky and others 1983; Lochter and others 1997; Maretzky and others 2005; Noe and others 2001) and LPA is linked to changes in MMP expression (Fishman and Borzorgi 2002; Fishman and others 2001; So and others 2004), the current study has been proposed to evaluate a potential functional link between LPA and decreased E-cadherin function. This dissertation now presents preliminary results showing that LPA increases E-cadherin ectodomain shedding in an MMP-9-dependent manner. Although EGF also promotes E-cadherin ectodomain shedding,

LPA-mediated ectodomain shedding is not dependent on EGFR transactivation. Together, these new data and the results presented in Chapter 3 illustrate the complexity of the ovarian cancer microenvironment and show how similar processes influencing ovarian cancer cell dissemination and metastasis can be regulated by unique effectors and pathways.

Results

LPA increases MMP-9-dependent E-cadherin cleavage and ectodomain shedding.

The ability of LPA to increase MMP expression and activation in ovarian cancer cells (Fishman and Borzorgi 2002; Fishman and others 2001; So and others 2004) identify it as a potential upstream regulator of MMP-dependent E-cadherin cleavage and ectodomain shedding. To evaluate the role of LPA in E-cadherin ectodomain shedding, OVCA429 and OVCA433 cells were treated with 10μM LPA for 24 hours under serum-free conditions. The resulting conditioned media were examined for the presence of the 80kDa E-cadherin ectodomain using immunoprecipitation and western blotting. LPA increased the amount of shed 80kDa ectodomain from both cell lines [**Fig 5.1**]. In addition, no changes were observed in surface and net E-cadherin expression following 24 hours of LPA treatment [**Fig 5.2**]. Surface E-cadherin expression also remained constant after LPA treatment for 48 and 72 hours (data not shown). To verify that MMPs cleaved E-cadherin to generate the shed ectodomain, both cell lines were cotreated with LPA and broad spectrum MMP inhibitor GM6001. GM6001 cotreatment resulted in reduced ectodomain shedding [**Fig 5.1**], suggesting LPA-mediated ectodomain shedding is MMP-dependent.

The proteinase profile of OVCA429 and OVCA429 cells in response to LPA treatment was unknown at the beginning of this investigation. In order to identify MMPs that may cleave E-cadherin, OVCA429 and OVCA433 cells were treated with 30 and 80 μM LPA under serum-free conditions for 24 hours. The resulting conditioned media was examined via gelatin zymography for changes in MMP-9 and MMP-2 expression [**Fig 5.3A**]. An LPA dose-dependent increase in MMP-9 expression was observed in OVCA429 cells, but a non-dose-dependent increase in MMP-9 expression was seen in OVCA433 cells. Although previously reported in the DOV13 ovarian cancer cell line (Fishman and others 2001), LPA treatment did not increase proMMP-2 activation in OVCA429 and OVCA433 cells. Due to these observations and our previous results in Chapter 3 showing integrin-mediated ectodomain shedding was MMP-9-dependent, OVCA429 cells were then cotreated with 10 μM LPA and a MMP-9 function-blocking antibody (anti-MMP-9) under serum-free conditions. LPA-mediated ectodomain shedding was reduced in the presence of anti-MMP-9 [**Fig 5.3B**]. Because the MMP-9 blocking antibody inhibits extracellular MMP-9 activity, these data also demonstrate MMP-9-dependent cleavage of surface-associated, rather than intracellular, E-cadherin. As reported in Chapter 3, exogenous MMP-9 also increased shedding of the E-cadherin ectodomain [**Fig 3.5B**].

Figure 5.1

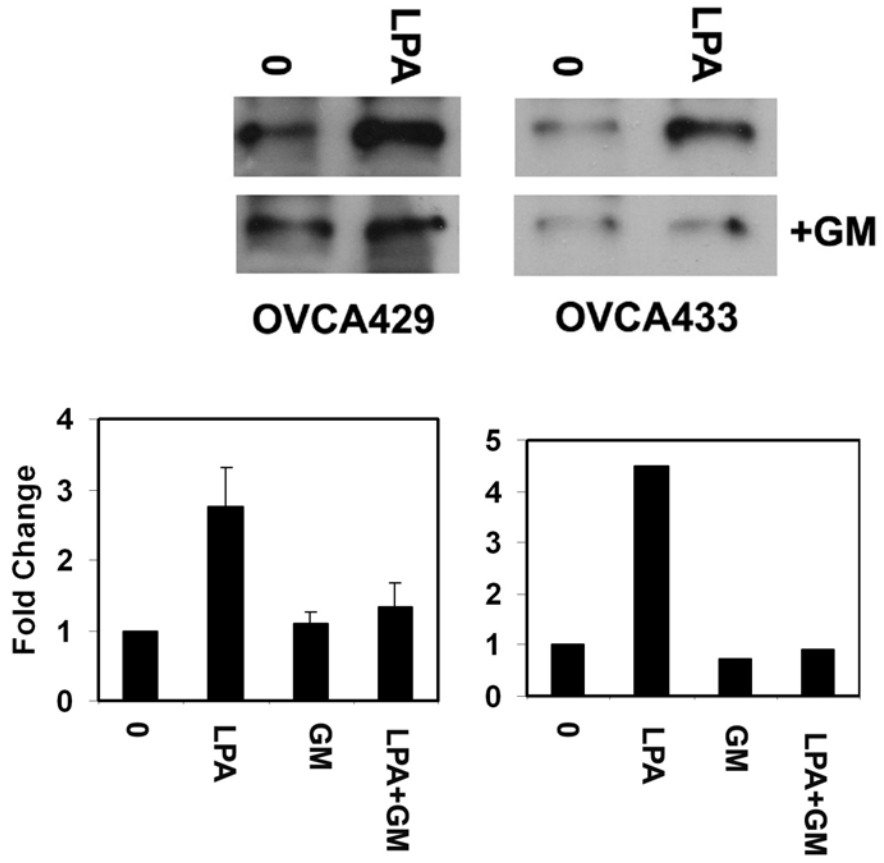
0
LPA
0
LPA
+GM
OVCA429
OVCA433
Fold Change
4
3
2
1
0
0
LPA
GM
LPA+GM
5
4
3
2
1
0
0
LPA
GM
LPA+GM

Figure 5.1: LPA promotes E-cadherin ectodomain shedding.

OVCA429 cells and OVCA433 cells were serum starved and preincubated with 50 μM GM6001 or equivalent DMSO prior to treatment with 10μM LPA for 24 hours. The 80kDa E-cadherin ectodomain was immunoprecipitated from the conditioned media, as described in Chapter 7. Immunoprecipitates were electrophoresed on a 9% SDS-PAGE gel, transferred to a PVDF membrane, and immunoblotted with anti-E-cadherin (HECD-1) (1:4000), followed by peroxidase-conjugated secondary antibody (1:5000) and enhanced chemiluminescence detection. A representative western blot and densitometric quantification of the 80kDa ectodomain were shown. Results were normalized against the densitometric reading for untreated cells (first lane, top band) and represent two independent experiments in the OVCA429 cells and one experiment in the OVCA433 cells. Immunoprecipitation (IP) controls are shown in Chapter 3 (Fig 3.2C).

Figure 5.2

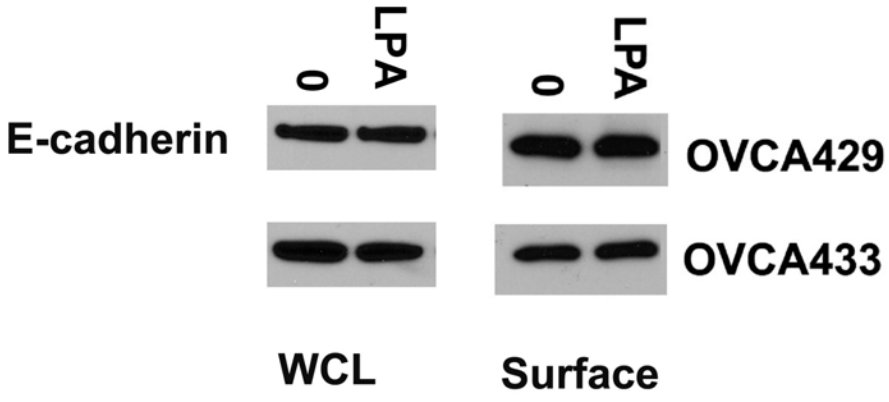

Figure 5.2: LPA treatment does not affect net or surface E-cadherin expression

OVCA429 and OVCA433 cells were incubated in serum-free media prior to treatment with 30μM LPA for 24 hours. Cells were processed for analysis of whole cell lysates and surface proteins, as indicated. Whole cell lysates (50μg OVCA433; 80μg OVCA429) were electrophoresed on a 9% SDS-PAGE gel, transferred to a PVDF membrane, and immunoblotted with anti-E-cadherin (HECD-1) (1:4000), followed by peroxidase-conjugated secondary antibody (1:5000) and enhanced chemiluminescence detection. Full length E-cadherin (120kDa) was detected. To evaluate the amount of E-cadherin present on the cell surface, cells were surface-biotinylated, lysed, and lysates (100μg OVCA433; 150μg OVCA429) incubated with NeutrAvidin. Following incubation, the NeutrAvidin-conjugated lysates and resulting supernatant were electrophoresed on a 9% SDS-PAGE gel, transferred to a PVDF membrane, and immunoblotted with anti-E-cadherin (HECD-1) (1:4000), followed by peroxidase-conjugated secondary antibody (1:5000) and enhanced chemiluminescence detection to examine the surface E-cadherin expression.

Figure 5.3

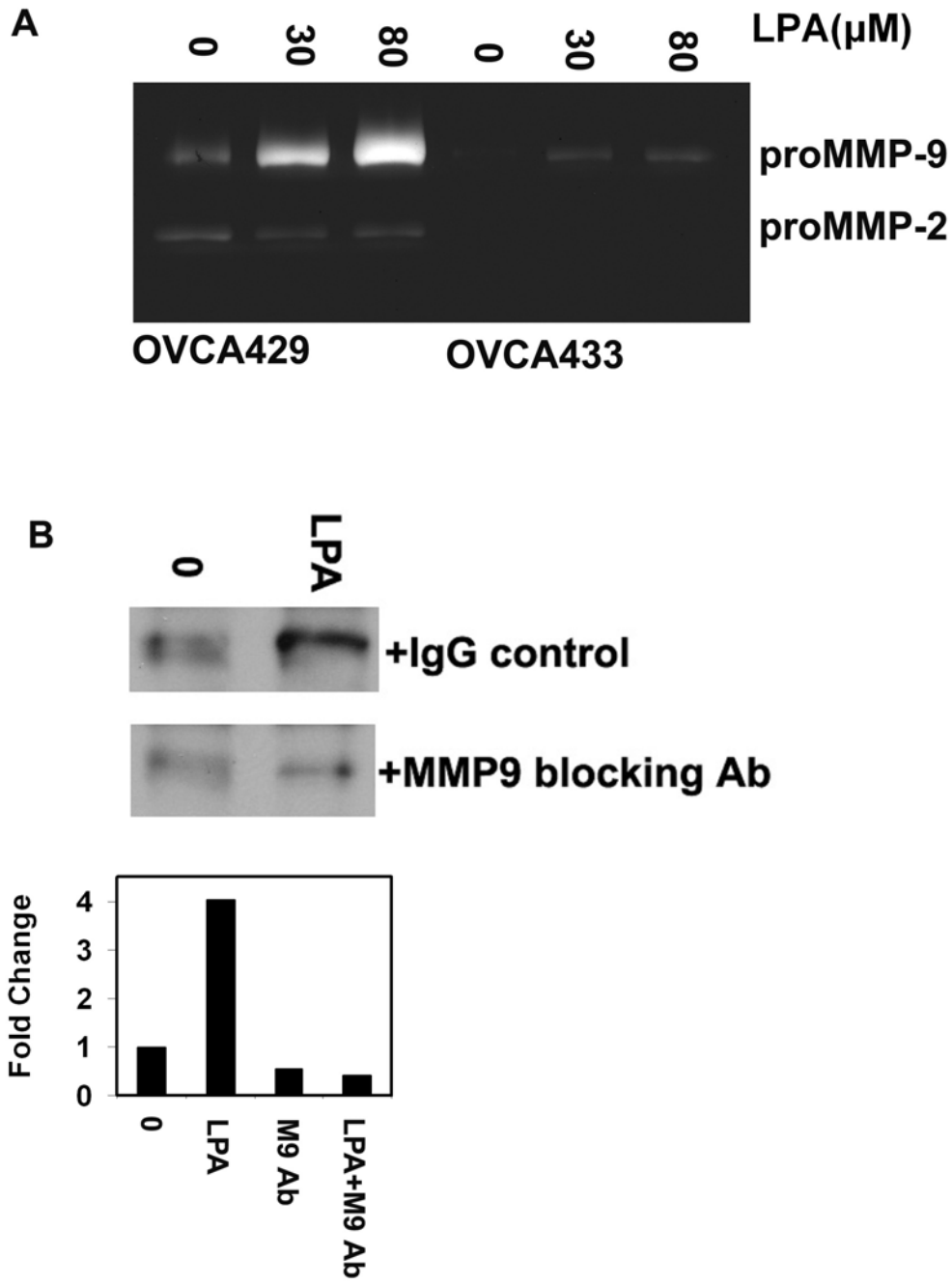
A
0
30
80
0
30
80
LPA(μM)
proMMP-9
proMMP-2
OVCA429
OVCA433
B
0
LPA
+IgG control
+MMP9 blocking Ab
Fold Change
4
3
2
1
0
0
LPA
M9 Ab
LPA+M9 Ab

Figure 5.3: MMP-9 promotes LPA-induced E-cadherin ectodomain shedding

A) OVCA429 and OVCA433 cells were serum starved prior to treatment with 30 or 80 μM LPA for 24 hours. The resulting conditioned media (30μl) were analyzed for MMP-9 and MMP-2 expression using gelatin zymography. Under serum-free conditions, the proenzyme form of MMP-9 was detected.

B) OVCA429 cells were serum starved and preincubated with anti-MMP-9 (10μg/ml) or control IgG prior to treatment with 10μM LPA for 24 hours. The 80kDa E-cadherin ectodomain was immunoprecipitated from the conditioned media, as described in Chapter 7. Immunoprecipitates were electrophoresed on a 9% SDS-PAGE gel, transferred to a PVDF membrane, and immunoblotted with anti-E-cadherin (HECD-1) (1:4000), followed by peroxidase-conjugated secondary antibody (1:5000) and enhanced chemiluminescence detection. A representative western blot and densitometric quantification of the 80kDa ectodomain were shown. Results were normalized against the densitometric reading for untreated cells (first lane, top band) and represent one experiment.

Characterization of LPA-mediated E-cadherin ectodomain shedding

EGF is an additional factor present in the ovarian cancer microenvironment known to upregulate MMP-9 expression in ovarian cancer cells (Alper and others 2001; Ellerbroek and others 1998), implicating it as a mediator of E-cadherin ectodomain shedding. EGF treatment (20ng/ml) under serum-free conditions also resulted in increased MMP-9 expression in OVCA433 cells and OVCA429 cells [**Fig 5.4A**](Ellerbroek and others 1998). ProMMP-2 activation did not occur after EGF treatment in either cell line. An increase in E-cadherin ectodomain shedding was also observed in OVCA429 cells after 8 hours of EGF treatment (20ng/ml) under serum-free conditions [**Fig 5.4A**]. Increased E-cadherin ectodomain shedding did not occur in OVCA433 cells following EGF treatment (data not shown). OVCA429 cells were also cotreated with EGF and GM6001 to verify that EGF-mediated ectodomain shedding was MMP-dependent [**Fig 5.4B**]. EGF-induced ectodomain shedding was reduced in the presence of GM6001, suggesting MMPs cleave E-cadherin. Due to technical issues with cell lines and western blotting, it could not be determined if EGF-mediated ectodomain shedding was MMP-9-dependent at this time. The G protein coupled receptors of the LPA receptor family have also been shown to transactivate the EGFR in EGF-free conditions in many different cell types (Daub and others 1997; Daub and others 1996; Gshwind and others 2002; Gshwind and others 2001; Kim and others 2000). Due to the high basal levels of phospho EGFR in OVCA429 and OVCA433 cells, it could not be determined if LPA transactivated the EGFR in these cell lines despite pretreatment of cells with an inhibitor of EGFR activity, AG1478, prior to LPA addition (data not shown). Instead OVCA429 cells were cotreated with LPA and AG1478 to determine if LPA-mediated ectodomain shedding was dependent on EGFR transactivation [**Fig**

5.4C]. LPA-mediated ectodomain shedding was not reduced in the presence of AG1478, implying that EGFR activity was unnecessary.

OVCA429 cells were also cotreated with pertussis toxin (PTX), an inhibitor of G protein coupled receptor activity. LPA-mediated ectodomain shedding was not reduced in the presence of PTX [**Fig 5.5A**], but previous studies reported that LPA can mediate its effects via both PTX-sensitive and –insensitive pathways (Daub and others 1997; Daub and others 1996; Gshwind and others 2002; Kim and others 2000; Laffargue and others 1999). To verify that LPA mediated-ectodomain shedding is regulated by the LPA receptor family, this experiment will be repeated in the presence of Ki16425, a LPA receptor antagonist that displays a preference for LPA1 and LPA3 receptors (Ohta and others 2003).

It was speculated in Chapter 3 that Src activity is necessary to partially disrupt cell-cell junctions to permit the access of MMP-9 to the E-cadherin cleavage site [**Fig 3.2D**]. Because LPA was also reported to transactivate Src family kinases (Luttrell and others 1996), OVCA429 cells were cotreated with Src kinase family inhibitor PP2 and LPA under serum-free conditions [**Fig 5.5B**]. LPA-mediated ectodomain shedding remained unchanged by PP2, suggesting Src activity was not required for LPA-mediated ectodomain shedding, as it was in integrin-mediated ectodomain shedding. Together these results and the results presented in Chapter 3 show that upstream regulation of E-cadherin ectodomain shedding by integrins, LPA, and EGF was far more complex than initially predicted.

Figure 5.4

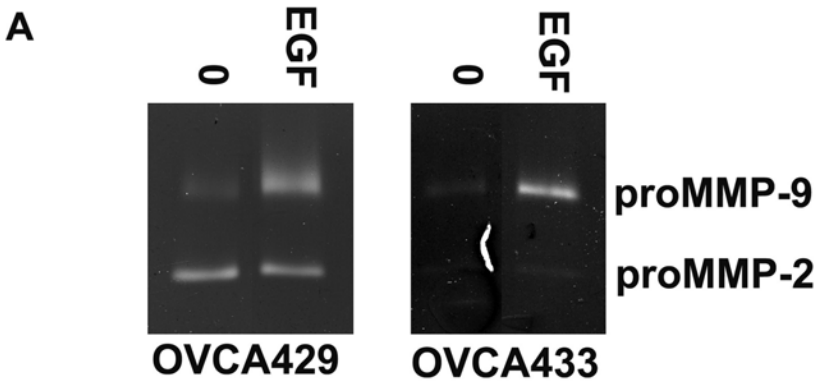

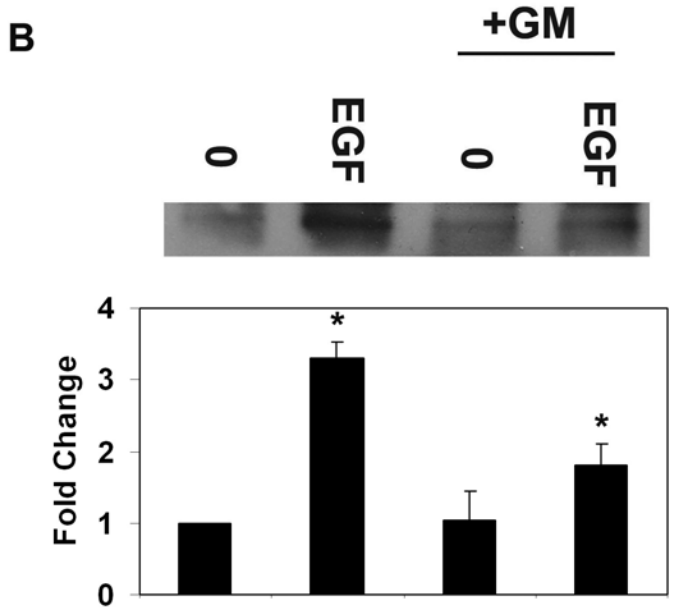

* P-value < 0.005

Figure 5.4

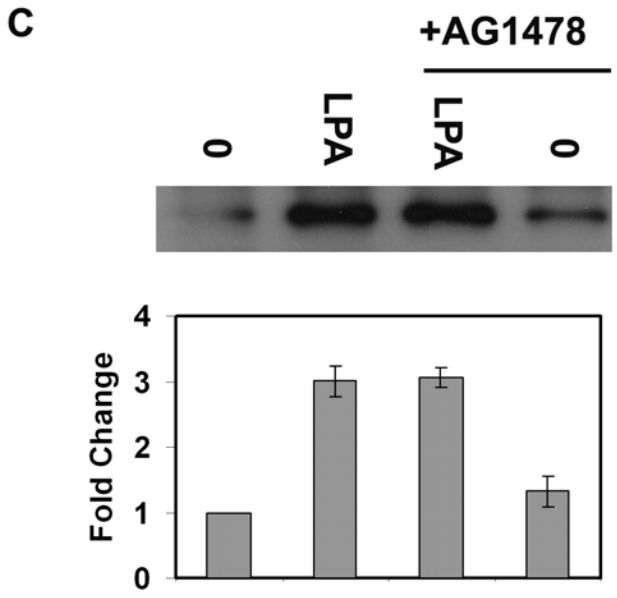

Figure 5.4: LPA-induced E-cadherin ectodomain shedding is not dependent on EGFR transactivation.

A) OVCA429 and OVCA433 cells were serum starved prior to treatment with 20ng/ml EGF for 8 hours. The resulting conditioned media (30µl) were analyzed for MMP-9 and MMP-2 expression using gelatin zymography. Under serum-free conditions, the proenzyme form of MMP-9 was detected.

B) OVCA429 cells were serum starved and preincubated with 50µM GM6001 prior to treatment with 20ng/ml EGF for 8 hours. The 80kDa E-cadherin ectodomain was immunoprecipitated from the conditioned media, as described in Chapter 7. Immunoprecipitates were electrophoresed on a 9% SDS-PAGE gel, transferred to a PVDF membrane, and immunoblotted with anti-E-cadherin (HECD-1) (1:4000), followed by peroxidase-conjugated secondary antibody (1:5000) and enhanced chemiluminescence detection. A representative western blot and densitometric quantification of the 80kDa ectodomain were shown. Results were normalized against the densitometric reading for untreated cells (first lane) and represent three independent experiments.

C) OVCA429 cells were serum starved and preincubated with 10µM AG1478 or equivalent DMSO prior to treatment with 10µM LPA for 24 hours. The 80kDa E-cadherin ectodomain was immunoprecipitated from the conditioned media, as described in Chapter 7. Immunoprecipitates were electrophoresed on a 9% SDS-PAGE gel, transferred to a PVDF membrane, and immunoblotted with anti-E-cadherin (HECD-1) (1:4000), followed by peroxidase-conjugated

secondary antibody (1:5000) and enhanced chemiluminescence detection. A representative western blot and densitometric quantification of the 80kDa ectodomain were shown. Results were normalized against the densitometric reading for untreated cells (first lane, top band) and represent two independent experiments.

Figure 5.5

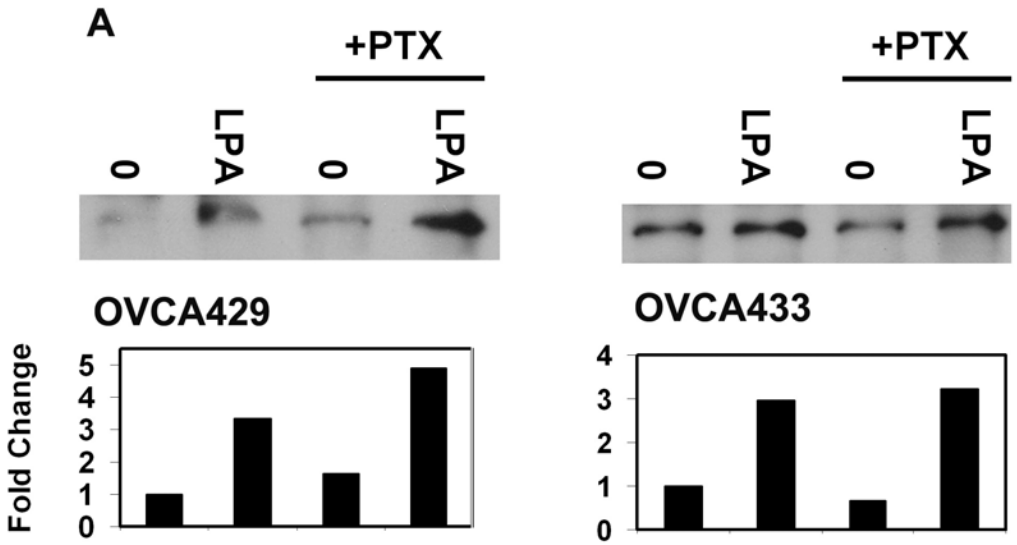
A
+PTX
+PTX
0
LPA
0
LPA
0
LPA
0
LPA
OVCA429
OVCA433
Fold Change
0
1
2
3
4
5
0
1
2
3
4

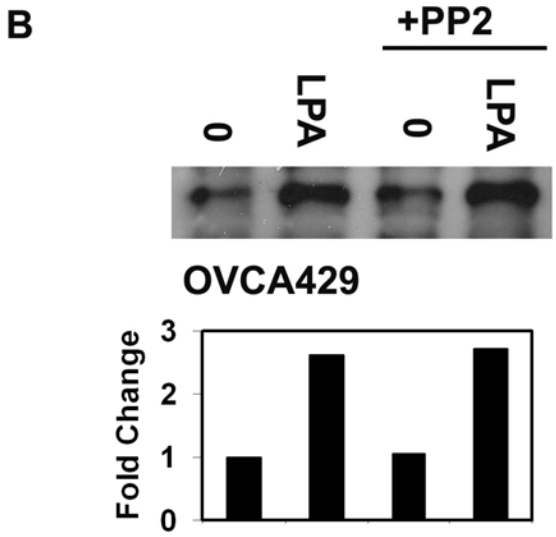
B
+PP2
0
LPA
0
LPA
OVCA429
Fold Change
0
1
2
3

Figure 5.5: LPA-induced E-cadherin ectodomain shedding is not pertussis toxin-dependent or Src kinase-dependent.

A) OVCA429 and OVCA433 cells were serum starved and preincubated with 100ng/ml PTX prior to treatment with 10μM LPA for 24 hours. The 80kDa E-cadherin ectodomain was immunoprecipitated from the conditioned media, as described in Chapter 7. Immunoprecipitates were electrophoresed on a 9% SDS-PAGE gel, transferred to a PVDF membrane, and immunoblotted with anti-E-cadherin (HECD-1) (1:4000), followed by peroxidase-conjugated secondary antibody (1:5000) and enhanced chemiluminescence detection. A representative western blot and densitometric quantification of the 80kDa ectodomain were shown. Results were normalized against the densitometric reading for untreated cells (first lane) and represent one experiment for each cell line.

B) OVCA429 cells were serum starved and preincubated with 10μM PP2 or equivalent DMSO prior to treatment with 10μM LPA for 24 hours. The 80kDa E-cadherin ectodomain was immunoprecipitated from the conditioned media, as described in Chapter 7. Immunoprecipitates were electrophoresed on a 9% SDS-PAGE gel, transferred to a PVDF membrane, and immunoblotted with anti-E-cadherin (HECD-1) (1:4000), followed by peroxidase-conjugated secondary antibody (1:5000) and enhanced chemiluminescence detection. A representative western blot and densitometric quantification of the 80kDa ectodomain were shown. Results were normalized against the densitometric reading for untreated cells (first lane) and represent one experiment for each cell line.

Discussion

Several proteinases have been reported to cleave E-cadherin (Covington and others 2006; Damsky and others 1983; Lochter and others 1997; Maretzky and others 2005; Noe and others 2001), but with the exception of integrin engagement (Chapter 3), the upstream regulators of the proteinase(s) that promote ectodomain shedding in ovarian cancer cells are largely unexplored. The preliminary data presented in this chapter support the hypothesis that LPA-regulated MMP-9-catalyzed E-cadherin ectodomain shedding may also potentiate metastatic dissemination of EOC, but via different pathways than integrin- or EGF-mediated E-cadherin ectodomain shedding [**Fig 5.6**].

Very few similarities are observed among integrin- and LPA-mediated ectodomain shedding. For example, endogenous MMP-9 appears to be the only common regulator of LPA- and integrin-mediated ectodomain shedding. Src activity is required to promote integrin-mediated E-cadherin ectodomain shedding, but it is not necessary for LPA-induced E-cadherin ectodomain shedding [**Fig 3.2D and 5.5B**]. It is currently unknown if Src activity is necessary for EGF-mediated ectodomain shedding. Although EGF increases ectodomain shedding, it is also surprisingly to find that crosstalk did not occur between EGFR and integrins or between EGFR and the LPA receptors [**Fig 3.2E and 5.4**] when both integrins and LPA have previously been reported to transactivate EGFR (Daub and others 1997; Daub and others 1996; Gshwind and others 2002; Gshwind and others 2001; Kim and others 2000; Yu and others 2000). The potential for crosstalk between integrins and the LPA receptors has not been considered in this investigation, although two recent reports suggest it may occur. Engagement of fibronectin-binding integrins increases nuclear localization of the receptor LPA1 (Waters and others 2006).

Nuclear localization of LPA1 is constitutive in some cell types, but is also increased upon LPA treatment. Nuclear LPA1 may also participate in intranuclear regulation of cell signaling to regulate COX-2 expression (Gobeil and others 2003; Waters and others 2006). LPA also enhances cell viability via Rho kinase (ROCK) in cells where fibronectin-binding integrin expression or fibronectin exposure is limited (Valenick and Schwarzbauer 2006). Although LPA-mediated ectodomain shedding is pertussis toxin insensitive, it can still be regulated via an LPA receptor (Daub and others 1997; Daub and others 1996; Gshwind and others 2002; Kim and others 2000; Laffargue and others 1999). This could be verified with the LPA receptor antagonist Ki16425, provided OVCA429 and OVCA433 cells express LPA1 and/or LPA3. The LPA receptor profile for these two cells lines is currently unknown, but ovarian cancer cells have previously been shown to generally express elevated levels of LPA3 and LPA2 and variable levels of LPA1 (Mills and others 2002b; Mills and Moolenaar 2003). It is essential to determine which LPA receptor mediates ectodomain shedding before crosstalk between integrins and LPA receptors can be evaluated in this system.

Unlike integrin signaling, LPA likely plays an earlier role in ovarian cancer metastasis, specifically in the promotion of primary tumor cell exfoliation and ascitic cell survival. Because LPA levels are elevated in the ascites of stage I ovarian cancer patients, LPA likely increases E-cadherin ectodomain shedding in the primary tumor, which feeds back to promote initial cell exfoliation from the primary tumor. In contrast, integrin signaling likely increases ectodomain shedding only in ascitic cells and peritoneal metastases after cells already separated from the primary tumor and encounter collagen fragments or the collagen-rich submesothelial ECM. This hypothesis is supported by the observation that two stage I ovarian cancer patients express the E-

cadherin ectodomain in ascites [**Fig 3.1B,C**]. In addition, based on results examining the role of fibronectin-binding integrins and LPA from Valenick and Schwarzbauer (Valenick and Schwarzbauer 2006), LPA may enhance survival of ascitic cells when their integrins are partially engaged by collagen fragments. LPA has also been shown to increase adhesion of ovarian cancer cells to type I collagen *in vitro* (Fishman and others 2001; Ren and others 2006), suggesting it may have the same effect after cells disrupted the mesothelial monolayer. Because LPA may increase ectodomain shedding early in ovarian cancer progression often before a diagnosis is sought, the identification of potential drug targets to prevent ectodomain shedding and its downstream effects is more complicated. In order to effectively prevent E-cadherin ectodomain shedding, a combinational therapy that inhibits MMP-9 in addition to several other effectors of ectodomain shedding would need to be administered to reduce ectodomain shedding and subsequent ovarian cancer metastases. The results presented in this chapter and in the previous chapters illustrate the complexities of microenvironmental regulation of ovarian cancer cell dissemination and metastasis and the difficulties of treating ovarian cancer metastasis.

Figure 5.6

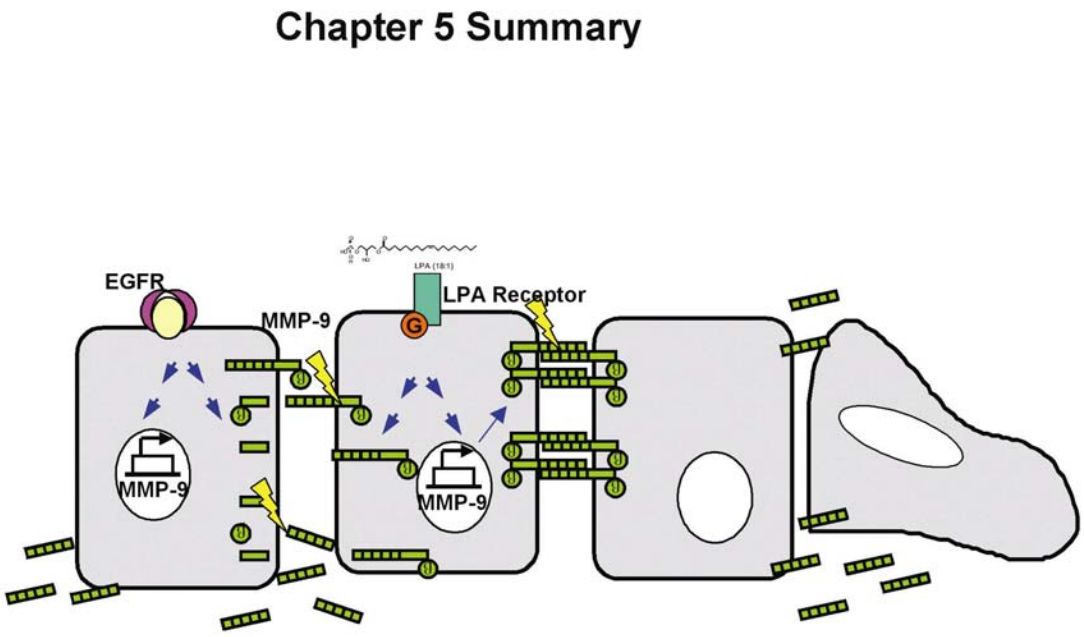

Figure 5.6: Chapter 5 summary of results

Additional factors in the tumor microenvironment, LPA and EGF, also increase MMP-dependent E-cadherin ectodomain shedding. These results illustrate the complexity of E-cadherin ectodomain shedding regulation because few common effectors were identified among the integrin-, LPA-, and EGF-mediated pathways and crosstalk between the LPA receptors and EGFR did not occur.

Chapter 6: Conclusions and Future Directions

Due to the lack of reliable early detection methods and the high percentage of ovarian cancer patients initially diagnosed with metastases present, it is imperative to understand the processes that govern ovarian cancer metastasis. This dissertation uncovers and dissects several novel mechanisms regulated by the ovarian tumor microenvironment that influence E-cadherin function, proteinase expression and activity, and subsequent increases in ovarian cancer cell dissemination and invasion. The results presented in the previous four chapters better illustrate the complexity of tumor microenvironment regulation of ovarian cancer metastasis and provide more insight about the events that may govern the following three sequential steps of ovarian cancer metastasis: primary tumor cell exfoliation, ascitic multi-cellular aggregate maintenance, and peritoneal cavity adherence and implantation.

These new results describe key events that may independently or jointly facilitate ovarian cancer metastasis at different points of the three sequential steps of metastasis. The steps where integrin engagement and LPA may regulate cell dissemination and metastasis are presented in the following model [**Fig 6.1**]. Collagen-binding integrin-mediated signaling is simply limited to when ovarian tumor cells encounter collagen; therefore, collagen-binding integrin engagement is restricted to ascitic tumor cells and invasive tumor cells adhering to the collagen-rich submesothelial ECM and integrin-mediated ectodomain shedding mainly occurs at these two stages. The shed ectodomain then may disrupt cell-cell adhesion in the ascitic cells to enhance the "seeding" of the peritoneal cavity or in the primary tumor to promote exfoliation of additional tumor cells. Increased E-cadherin internalization may then be necessary to break and

reform cell-cell junctions that facilitate adherence to peritoneal mesothelial cells. The resulting increase in β-catenin-mediated transcription and proteinase expression likely enhances invasion in the peritoneal cavity. While the effects mediated by integrin engagement are limited to collagen exposure, it is possible that LPA acts at all three sequential steps to enhance ovarian cancer metastasis as LPA is elevated in ovarian cancer patients stages I to IV. In contrast to integrin-mediated ectodomain shedding, LPA-mediated ectodomain shedding may additionally disrupt cell-cell adhesion in the primary tumor to promote the initial exfoliation of tumor cells, allowing the shed ectodomain to act in an autocrine fashion at this stage. LPA may also promote increased proMMP-9 expression and proMMP-2 activation to instigate invasion of the mesothelial monolayer, which may also promote exposure of the submesothelial ECM to encourage integrin engagement.

This dissertation also reveals that E-cadherin ectodomain shedding is mediated by three different upstream regulators: collagen-binding integrins, LPA, and EGF. Future experiments will likely test two possible scenarios addressing the combined effects of LPA, EGF, and integrin signaling on ectodomain shedding to gain a better understanding of microenvironment regulation of metastasis. First, integrin-, LPA-, and EGF-mediated ectodomain shedding may independently increase MMP-9 expression and ectodomain shedding, resulting in a larger net increase in the shed ectodomain and delayed E-cadherin replenishment. It is expected that cell dissemination will be amplified as the disruption of cell-cell junctions in the primary tumor and ascitic cell aggregates will be increased. An alternative possibility is unidentified additional regulation occurs to ensure integrins, LPA, and EGF each mediate ectodomain shedding at distinct steps of the ovarian cancer metastasis process to prevent a net loss of E-cadherin. For

example, downregulation or sensitization of the LPA receptors and/or EGFR upon increased signaling may downregulate LPA- and EGF-mediated ectodomain shedding, possibly limiting this event to the primary tumor cells. Integrin-mediated ectodomain shedding will then be restricted to ascitic tumor cells and tumor cells invading the mesothelial monolayer. Since this dissertation only fully investigates the disruption of cell-cell adhesion by the shed ectodomain, it will also be beneficial to further investigate the preliminary data presented in Chapter 3 to determine the effects of the shed ectodomain on ovarian cancer cell migration, invasion, and proteinase expression and peritoneal mesothelial cell wound closure and subsequent ovarian metastasis.

Based on the results from previous studies (Covington and others 2006; Damsky and others 1983; Hayashido and others 2005; Lochter and others 1997; Maretzky and others 2005; Noe and others 2001), it is also possible that other proteinases, including MMP-7 and MT1-MMP, may cleave E-cadherin to promote integrin- or LPA-mediated ectodomain shedding. Unfortunately, only the role of MMP-9 is considered because it has not been investigated in these other studies. Compared to MMP-7 and MT1-MMP, MMP-9 is likely the predominant MMP in the ovarian tumor microenvironment as it is secreted by tumor cells and stromal cells. E-cadherin is also cleaved by both endogenous and exogenous MMP-9. MMP-7 expression is limited to tumor cells (Ii 2006), suggesting MMP-7 levels are lower than MMP-9 levels in the tumor microenvironment, but it is also possible that MMP-7 plays a minor role in E-cadherin cleavage both directly and indirectly. Upon integrin engagement, MMP-7 may cleave E-cadherin to generate a small population of shed ectodomain. Alternatively, MMP-7 may participate in ectodomain shedding indirectly by activating proMMP-9 to cleave E-cadherin,

which occurs in the conditioned media from immortalized OSE cells (Wang and others 2005). The role of MT1-MMP in E-cadherin ectodomain shedding is not considered because MT1-MMP overexpression in OVCA433 cells caused cells to lift off tissue culture plates as cellular sheets (personal communication, Yueying Liu). Although the resulting conditioned media have not been examined for the shed ectodomain, these results suggest that when MT1-MMP is the predominant proteinase expressed in OVCA433 cells, it downregulates cell-matrix adhesion by an unknown mechanism, but does not affect cell-cell adhesion. It will be interesting to further investigate the roles of both MT1-MMP and MMP-7 in integrin- and LPA-mediated ectodomain shedding. Future studies will also address the role of ADAM10, uPA, and MMP-2 in E-cadherin cleavage and ectodomain shedding as preliminary investigations yielded inconclusive results (data not shown) and it would be informative to identify additional proteinases that enhance ectodomain shedding in ovarian cancer models.

The new data in this dissertation also show that integrin aggregation results in two different cellular observations involving E-cadherin, but unlike E-cadherin ectodomain shedding, less information has been uncovered regarding E-cadherin internalization. Future experiments will be planned to determine if E-cadherin is recycled back to the cell surface or degraded and resynthesized. Other than the unexpected ability to promote the upregulation of β-catenin-mediated transcription and proteinase expression, the purpose of E-cadherin internalization remains a mystery. It is interesting to speculate that E-cadherin internalization also regulates the breaking and re-forming of cell-cell junctions to support cell exfoliation from the primary tumor, maintenance of ascitic cellular aggregates, and adhesion of ovarian cancer cells to the peritoneal mesothelial cells. It will also be valuable to test the hypothesis that ectodomain shedding and E-

cadherin internalization are two separate events. This has been implied due to speculation in Chapter 3 suggesting E-cadherin cleavage occurs on the cell surface to facilitate ectodomain shedding. This hypothesis will be tested in the future since both observations may potentially lead to changes in β-catenin-mediated transcription (Chapter 2)(Maretzky and others 2005). Studies presented in Chapter 2 and 3 have also been designed to mimic ovarian cancer cells adhering to the collagen-rich submesothelial matrix; however, it would be extremely valuable to determine if integrin clustering also produces the same observations in ascitic multi-cellular aggregates or spheroids. It is best to continue this investigation in a 3D spheroid tissue culture model to gain a better physiological representation of ovarian cancer. This would also permit examination of interactions with peritoneal mesothelial cells in order to determine the purpose of E-cadherin internalization.

In conclusion, this dissertation identifies new additional details about the microenvironment regulation of the processes that may foster ovarian cancer cell dissemination and metastasis based on both *in vitro* data derived from 2D monolayer tissue culture models and patient data obtained from tumor and ascites samples. These results generate a strong foundation for the future studies of ovarian cancer metastasis in more physiologically relevant models, including 3D organotypic spheroid models, mouse models, and *drosophila* border cell migration models. The results presented in the four previous chapters may someday contribute to the development of more effective and targeted treatment for the thousands of stage III and IV ovarian cancer patients.

Figure 6.1

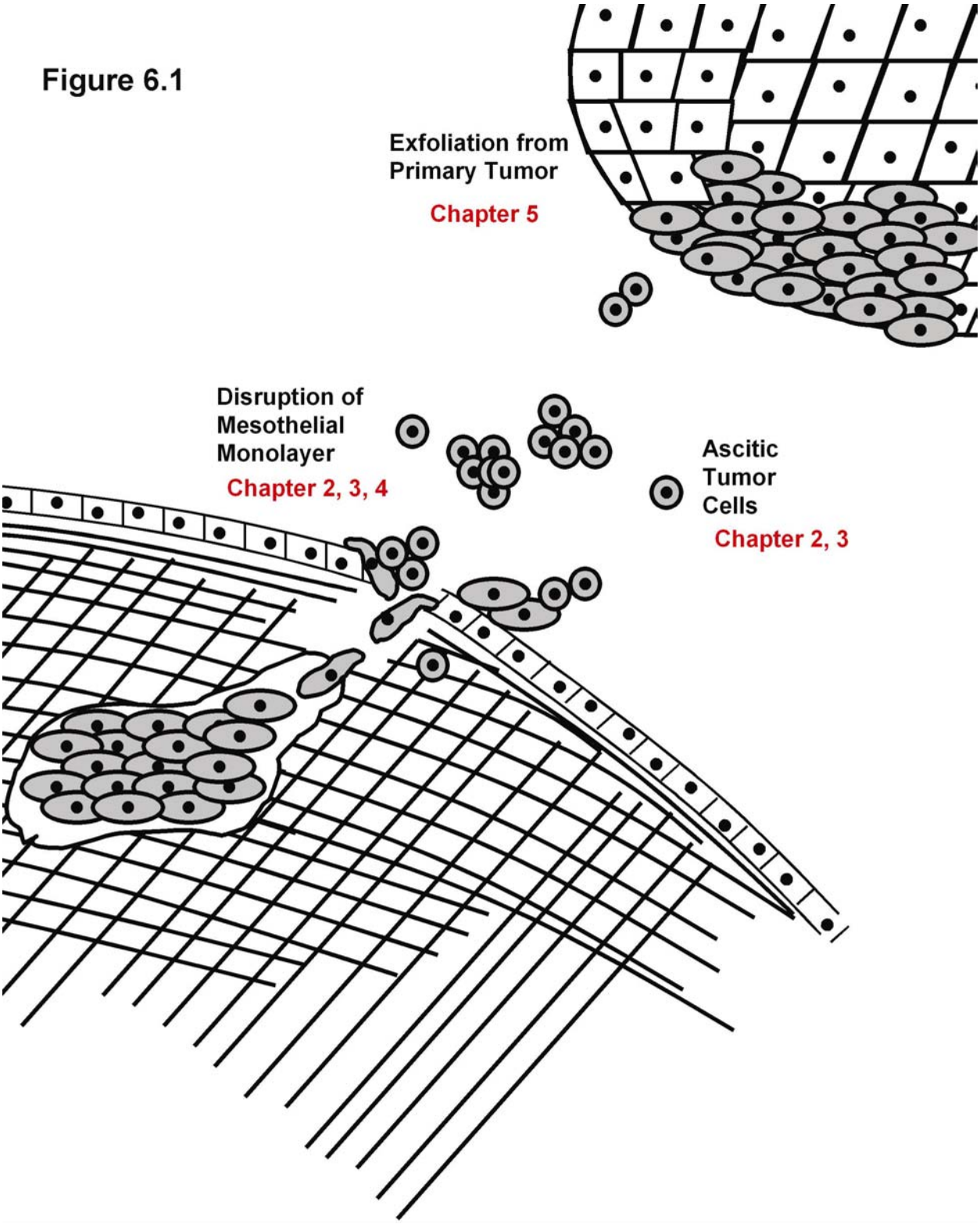
Exfoliation from
Primary Tumor
Chapter 5
Disruption of
Mesothelial
Monolayer
Chapter 2, 3, 4
Ascitic
Tumor
Cells
Chapter 2, 3

Figure 6.1: Summary of thesis results

This figure shows when the data in this dissertation may be relevant during the three steps necessary for ovarian cancer metastasis: exfoliation of primary tumor cells, maintenance of ascitic multi-cellular aggregates, and adherence and invasion of the peritoneal cavity. LPA may play a role at all three stages, but the effects of integrin engagement are limited to when cells encounter collagen. This likely occurs when ascitic cels are exposed to collagen fragments and when tumor cells disrupt the mesothelial monolayer and expose the collagen-rich submesothelial ECM. The results presented in Chapter 4 suggest COX-2 promotes aggressive and invasive behavior during and after disruption of the peritoneal mesothelial monolayer.

Chapter 7: Experimental Procedures and Reagents

I) Cell Lines and Patient Tumor and Ascites Samples

A) Cell Culture

DOV13 cells were used for experiments presented in Chapter 4 because a previous investigation showed LPA treatment resulted in increased proMMP-2 activation in this cell line (Fishman and others 2001). This serous type tumor-derived cell line expressed N-cadherin, but lacked E-cadherin and proMMP-9 expression. DOV13 cells were generously provided by Dr. Robert Bast (M.D. Anderson Cancer Center, Houston, TX), and were maintained in MEM (Gibco Invitrogen, Carlsbad, CA), 10% fetal bovine serum (Gibco Invitrogen), penicillin/streptomycin (Cellgro by Mediatech, Herndon, VA), amphotericin B (Cellgro by Mediatech), non-essential amino acids (Cellgro by Mediatech), sodium pyruvate (Cellgro by Mediatech), and insulin from bovine pancreas (10mg/L) (Sigma Aldrich, St. Louis, MO) at 37ºC in 5% CO_2.

OVCA433 and OVCA429 cells were chosen for experiments described in Chapters 2,3, and 5 due to their high levels of E-cadherin and proMMP-9 expression, identifying them a better model for the investigation of MMP-9-mediated E-cadherin cleavage and ectodomain shedding. Both cell lines displayed very low or absent levels of N-cadherin, which simplified the studies in Chapter 2 as N-cadherin also binds to β-catenin. These cell lines were derived from serous type tumors, which are most commonly observed in ovarian cancer patients. In addition, E-cadherin expression in these cells also identified them as an ovarian tumor relevant model as E-cadherin expression was often upregulated as ovarian cancer develops and progresses. OVCA429 and OVCA433 cells were generously provided by Dr. Robert Bast (M.D. Anderson Cancer Center,

Houston, TX) and were maintained in MEM, 10% fetal bovine serum, penicillin/ streptomycin, amphotericin B, non-essential amino acids, and sodium pyruvate at 37º in 5% CO_2.

A variety of other ovarian cancer cell lines were also used in Chapter 4 to screen for their ability to upregulate COX-2 expression in response to LPA. Immortalized human borderline ovarian epithelial cells (HuIOSBT-1.5, HuIOSBT-2.2, and HuIOSBT-3.3) were generated by Dr. Nelly Auersperg (University of British Columbia, Vancouver, B.C.) using SV40 and were maintained in a 1:1 mixture of media 199 (Sigma Aldrich) and MCDB105 (Sigma Aldrich), 5% fetal bovine serum, and 50μg/ml gentamicin (Sigma Aldrich). SKOV-3, OVCAR-3, and CaOV-3 cells were purchased from ATCC (Manassas, VA). SKOV-3 cells were maintained in McCoy's media (Cellgro by Mediatech), 10% fetal bovine serum, penicillin/streptomycin, amphotericin B, non-essential amino acids, and sodium pyruvate at 37ºC in 5% CO_2. OVCAR-3 cells were maintained in RPMI-1640 (ATCC), 20% fetal bovine serum, penicillin/streptomycin, amphotericin B, non-essential amino acids, sodium pyruvate, and insulin from bovine pancreas (10mg/L) at 37ºC in 5% CO_2. CaOV-3 cells were maintained in DMEM (ATCC), 10% fetal bovine serum, penicillin/streptomycin, non-essential amino acids, and sodium pyruvate. With the exception of CaOV-3 cells, all ovarian carcinoma cell lines described above were known to be ascites derived.

LP-9 cells were obtained from Coriell Cell Repositories (Camden, NJ). These normal human peritoneal mesothelial cells were isolated from an ovarian cancer patient. LP-9 cells were maintained in Ham's F12 medium/Medium 199 (1:1 mixture), penicillin/streptomycin, 2mM L-glutamine, 10% fetal bovine serum, 10ng/ml recombinant epidermal growth factor, and 0.4μg/ml hydrocortisone.

B) Ascites Samples

Ascites were collected from women undergoing surgical procedures at Prentice Women's Hospital (Chicago, IL) for gynecological indications with institutional review board-approved consent. Preoperative and intraoperative ascites were collected under sterile conditions and frozen at -20ºC. Samples were generously provided by Dr. David Fishman (now at New York University, New York, NY).

C) Immunohistochemistry (COX-2, E-cadherin, MMP-9)

Immunohistochemical analysis was performed retrospectively on tumor tissue microarrays prepared by the Pathology Core Facility of the Robert H. Lurie Comprehensive Cancer Center at Northwestern University assembled from tissue originally taken for routine diagnostic purposes. The microarray tissue specimens included human ovarian carcinomas and borderline tumors. Samples were cut 3 to 4 microns thick and deparaffinized. The cores were 1mm in diameter. The tissue microarray was divided into two blocks, one containing 106 cores and the other containing 87 cores. Antigen retrieval was accomplished by heat induction at 99ºC for approximately 45 minutes**.** Immunohistochemical staining with antibodies to COX-1 (Cayman Chemical; 1:50 dilution**)**, COX-2 (Cayman Chemical; 1:100 dilution) and cytokeratin-7 (DakoCytomation, Carpinteria, CA; 1:200 dilution) was performed according to standard procedures. Colon adenocarcinoma was used as a positive control for COX-1 and COX-2. Immunohistochemical staining with antibodies to MMP-9 (1:200 dilution) (Lab Vision, Fremont, CA) and E-cadherin (1:200 dilution) (clone NCH-38, Dako Cytomation, Carpinteria, CA) was performed according to standard procedures. Breast carcinoma and colon carcinoma were used

as positive controls MMP-9 and E-cadherin, respectively. Analysis of tissue sections was done by light microscopy by a pathologist (Dr. Brian Adley, Northwestern University) without prior knowledge of the clinical parameters. Scoring of COX-1, COX-2, E-cadherin, and MMP-9 was assigned according to the intensity of the staining and graded 0, 1+ (weak), 2+ (moderate), or 3+ (strong). Statistical analyses were performed by Dr. Alfred Rademaker of the Biostatistics Core Facility of the Robert H. Lurie Comprehensive Cancer Center.

II) Experimental Methods

A) Western Blot Analysis

Details on the cell and experimental conditions prior to western blot analysis were indicated in the figure legends. After experimental treatment, cells were lysed in mRIPA lysis buffer (50mM tris pH 7.5, 150mM NaCl, 0.1% SDS, 1% triton X-100, 5mM EDTA). Protein concentrations of the resulting lysates were determined using the BioRad protein assay. Lysates (concentration indicated in figure legend) were electrophoresed on an 8-12% SDS-polyacrylamide gel (Laemmli 1970), electroblotted to a PVDF membrane (Matsudaira 1987), and blocked in 5% milk/TBST (25mM tris pH 7.5, 150mM NaCl, 0.1% tween 20) or 3% bovine serum albumin (BSA)/TBST at room temperature for 1 to 3 hours. Blots were incubated overnight with 1:1000 dilution of the primary antibody. The immunoreactive bands were visualized using peroxidase-conjugated anti-mouse or rabbit IgG (1:5000 in 3% BSA/TBST) and enhanced chemiluminescence. To evaluate loading controls, blots were stripped of primary antibody using a low pH buffer (400mM glycine pH 2.5), blocked again in 3% BSA/TBST, and reprobed with primary antibody. Western blots were quantified using ImageJ (U.S. National Institutes of

Health, Bethesda, Maryland). P-values were determined using the T-test function (two sample, unequal variance, one tailed distribution) on Excel (Microsoft Corporation, Redmond, WA).

B) Gelatin Zymography

Details on the cell and experimental conditions were indicated in the figure legends. Serum-free conditioned media (25-30µl) was electrophoresed under non-reducing conditions on a 9% SDS-polyacrylamide gel containing approximately 0.1% gelatin (Heussen and Dowdle 1980). The gel was washed for 1-2 hours in 2.5% Triton X-100, incubated at 37ºC in 20mM Tris pH 8.3, 10mM $CaCl_2$, 1µM $ZnCl_2$ for 48 to 72 hours, and stained with Coomassie Blue. Enzyme activity was indicated by zones of gelatin clearance in the gel. Under serum-free conditions, MMP-9 was detected in the proenzyme form. Active MMP-9 is often not observed in conditioned media from cultured cells even though the cells may express potential proMMP-9 activators. It is possible that cell culture media may dilute physiologically relevant soluble activators of MMP-9, such as plasminogen and MMP-3, that are normally abundant in the serum or ascites (Fridman and others 2003).

C) MMP-2 ELISA

DOV13 cells were serum starved overnight, and pretreated with COX-2 inhibitor NS-398 (50-100µM) or DMSO vehicle control for 2 to 3 hours prior to incubation with 30µM LPA for 24 additional hours. Conditioned media was then analyzed with the Quantikine human/mouse

MMP-2 (total) immunoassay kit (R&D Systems, Minneapolis, MN) according to manufacturer's specifications. The data included normalized values from four separate experiments.

D) *In Vitro* Wound Scratch Assay

Cells were plated in 8 well plates, cultured to confluence, and serum starved overnight. One to two scratch wounds were made in each well using a micropipette tip and cells were treated as indicated in the figure legend. Two points were randomly selected and marked for each scratch, then photographed using a digital camera at 0, 24, and 48 hours. For assays using DOV13 cells (Chapter 4), five relative measurements were taken for each point for each experimental condition using the MetaMorph Imaging System (Universal Imaging Corporation, Downington, PA). For assays using OVCA433 cells and LP9 cells (Chapter 3), a picture of each scratch was printed out and five relative measurements of the scratch width were taken using a ruler. These resulting five measurements for each point were averaged and then normalized based on the initial measurement for that point at 0 hours. The normalized values were then averaged for each experimental condition.

E) Matrigel Invasion Assay (Chapter 4)

Matrigel (50µl of 0.1 mg/ml) was added to each chamber of the Falcon HTS Fluoroblok Insert System and left to dry overnight. DOV13 cells were serum starved overnight in serum-free MEM, trypsinized and resuspended in phenol red-free medium at a concentration of 500,000 cells/ml in the presence of NS-398 or DMSO as indicated. Cells (250,000 cells in 500µl) were

then added to the top chamber of the HTS Fluoroblok Insert System with serum-free, phenol red-free MEM (500µl) in the bottom chamber. After one hour, LPA (30µM) was added and chambers incubated for 48 hours prior to labeling with calcein AM (100µl, final concentration 5 µg/ml) for 30 minutes at 37^{o}C in 5% CO_2. Relative invasion was quantified by analysis of the fluorescent signal for the bottom chamber using a Wallac 1420 Victor2 multilabel plate reader (Perkin Elmer, Shelton, CT). Assays were performed in triplicate and analyzed relative to blank wells containing only medium.

F) Matrigel Invasion Assay (Chapter 2)

Matrigel (50µl of 0.1 mg/ml) was added to the top chamber of a Boyden chamber filter (8µm size) and left to dry for 1 hour at room temperature. OVCA433 cells were transiently transfected with either pFLAG-CMV-2 control vector (Flag) and pFLAG-CMV-2-ICAT vector (ICAT) using Fugene 6 Transfection Reagent according to the manufacturer's specifications. Twenty-four hours after transfection, OVCA433 cells were serum starved overnight, trypsinized, and resuspended in serum-free medium at a concentration of 500,000 cells/ml. Cells (250,000 cells in 500µl) were then added to the top chamber of the Boyden filter with serum-containing MEM (750µl) in the bottom chamber and allowed to invade for 24 hours. Non-invading cells were removed from the top chamber using a cotton swab, filters were stained with Diff-Quick Stain, and invading cells adherent to the bottom side of the filter were counted under the microscope (10X magnification). The results represent the total number of invading cells per filter and include three independent experiments done in triplicate.

G) E-cadherin ELISA

Ascites samples from 47 patients were diluted in phospho buffered saline (PBS) and were analyzed using a Human E-cadherin EIA Kit (Invitrogen Corporation, formerly Zymed Laboratories Inc.) according to manufacturer's specifications.

H) MMP-9 (total) ELISA

Ascites samples from 35 ovarian cancer patients and women with benign ovarian cysts were diluted 1:100 in phospho buffered saline (PBS) analyzed using a human MMP-9 (total) Immunoassay (R&D Systems) according to manufacturer's specifications.

I) Biotin Surface Labeling

Details on the cell and experimental conditions were indicated in the figure legends. Following experimental treatment, cells were incubated with Sulfo-NHS-LC-Biotin (1mg/ml) for 25 minutes on ice. Cells were washed three times in cold 100mM glycine in PBS and one time in cold PBS before lysis in mRIPA buffer (50mM tris pH 7.5, 150mM NaCl, 1% triton X-100, 5mM EDTA). Equivalent amounts (50-100µg) of lysate, as determined by the BioRad Protein Assay, were incubated with 25-30µl NeutrAvidin Protein overnight at 4° with gentle agitation. The supernatant was saved to analyze the levels of non-labeled/non-surface proteins in the lysates in some experiments. The NeutrAvidin-biotin labeled lysate complex was washed five times in mRIPA lysis buffer, resuspended in mRIPA lysis buffer plus sample dilution buffer with 2-mercaptoethanol and prepared for western blot analysis.

J) E-cadherin Ectodomain Immunoprecipitation

Cells were plated in 6 well plates at 60-70% confluence. Details on the cell and experimental conditions are described in the figure legends. At the appropriate time point, the total volume of conditioned media (1ml) was collected and centrifuged for 5 minutes. The conditioned media (1ml) was incubated with 2.5µg of anti-E-cadherin (HECD-1) for 3 hours at room temperature or overnight at 4°C and then with 20µl sepharose 4B FastFlow recombinant protein G for an additional hour at room temperature. The antibody-sepharose protein G complex was washed five to seven times in PBS, resuspended in mRIPA lysis buffer plus sample dilution buffer with 2-mercaptoethanol and prepared for western blot analysis.

K) Immunofluorescence (Chapter 3)

Cells were plated at 60-70% confluence on 22-mm^2 glass coverslips placed in 6 well tissue culture plates. Cells were cultured in serum-free MEM overnight and then treated with 12µg/ml hEcad-Fc, mouse IgG, or exogenous MMP-9 the next day for 24 to 48 hours. Cells were gently washed in PBS, fixed in ice-cold Methanol at -20°C for 5 minutes, gently washed in PBS, and blocked in PBS/1% BSA for 1 hour at room temperature followed by the addition of anti-E-cadherin (clone 4A2C7), anti-E-cadherin (clone HECD-1), or anti-β-catenin (1:300 dilution in PBS/1% BSA) for 90 minutes at 37°C. After two washes in PBS, coverslips were incubated with Alexa Fluor 488 goat anti-mouse IgG (1:500 dilution in PBS/1% BSA) in the dark at room temperature for 30 minutes. Coverslips were washed in PBS twice and in distilled water once, fixed using Vectashield Mounting Medium for Fluorescence with DAPI (Vector Laboratories, Burlingame, CA), and visualized using a Zeiss Axiovert 200 microscope.

L) Immunofluorescence (Chapter 2)

Cells were plated on 22-mm^2 glass coverslips coated with thin layer type I collagen placed in 6 well tissue culture plates. Control cells were plated on uncoated glass coverslips. Cells were gently washed in PBS, fixed in paraformaldehyde (10%) at room temperature for 10 minutes, washed in PBS, and blocked in PBS/1% BSA for 1 hour at room temperature followed by the addition of anti-E-cadherin (HECD-1 clone)(1:500 dilution in PBS/1% BSA) for 90 minutes at 37°C. After two washes in PBS, coverslips were incubated with Alexa Fluor 488 goat anti-mouse IgG (1:500 dilution in PBS/1% BSA) in the dark at room temperature for 30 minutes. Coverslips were washed in PBS twice and in distilled water once, fixed using gelvatol, and visualized using a fluorescence microscope.

M) Analysis of Internalized E-cadherin

OVCA433 cells were plated at 60-70% confluence in 6 well plates. The next day, cells were labeled with a cleavable form of biotin (Sulfo-NHS-SS-Biotin at 1mg/ml) for 25 minutes on ice. Cells were then washed three times in cold 100mM glycine in PBS and one time in cold PBS. Warm cell culture media (37ºC) was added to the cells with 20µl of magnetic beads coated with β1 integrin antibody. After a one hour incubation at 37ºC, cells were treated with MESNA (100mM in PBS) for 30 minutes and iodoacetamide (5mg/ml in PBS with 1%BSA) for 10 minutes at room temperature to strip off any biotin still remaining on the cell surface. The cells were then lysed and incubated with NeutrAvidin to isolate the labeled surface proteins that had been internalized following integrin engagement. The NeutrAvidin-biotin labeled lysate

complex was washed five times in mRIPA lysis buffer, resuspended in mRIPA lysis buffer plus sample dilution buffer with 2-mercaptoethanol and prepared for western blot analysis. In control experiments, the MESNA step was not included, allowing analysis of total labeled protein (internalized and cell surface pool). Cells were also kept on ice during the course of the experiment to determine the efficiency of surface stripping with MESNA.

N) TOPflash TCF Reporter Assay

OVCA433 cells were plated at 40-50% confluence in 6 well plates. Approximately 8 hours after plating, cells were cotransfected with a Renilla luciferase reporter construct (pRL-CMV) and either the firefly luciferase TOPflash TCF Reporter Plasmid or the FOPflash TCF mutant Reporter Plasmid using Fugene 6 Transfection Reagent according to the manufacturer's instructions. Approximately 18 hours after transfection, cells were cultured in low calcium (0.1mM $CaCl_2$) serum-containing MEM [S-MEM (Invitrogen), 10% fetal bovine serum, penicillin/ streptomycin, amphotericin B, non-essential amino acids, glutamine, and sodium pyruvate] for 1 hour before the addition of latex beads coated with TS2/β1 integrin antibody or control IgG for an additional 30 hours. Cells were then lysed in passive lysis buffer (Promega). Both Renilla and Firefly Luciferase readings were taken on a Veritas Microplate Luminometer (Turner Biosystems, Sunnyvale, CA) using the reagents and protocol provided by Promega in the Dual Luciferase Reporter Assay System. Firefly luciferase readings were first normalized to the reading for the corresponding Renilla luciferase reading to account for transfection efficiency. The adjusted TOPflash reading was then normalized to the corresponding adjusted FOPflash

reading to account for background reading of the TOPflash construct to yield the ratios presented in Figure 2.3C.

O) uPA Activity Assay

Details on the cell and experimental conditions were indicated in the figure legends. Net plasminogen activator activity in serum-free conditioned media was quantified using a coupled colorimetric assay to monitor plasminogen activation and the resulting plasmin hydrolysis of a colorimetric substrate (D-Val-Leu-Lys-*p*-nitroanilide; Sigma Alrich)(Stack 1990).

III) Materials: Source and Preparations

A) Magentic Bead-immobilized Antibody Preparation

Antibodies were passively absorbed onto Dynabeads M-450 Epoxy magnetic beads (Invitrogen Corporation, formerly Dynal Biotech ASA) using the procedure for coating of antibodies/proteins provided by the manufacturer described below. Beads were washed and resuspended in Buffer A (0.1M phosphate buffer pH 7.0-8.5) prior to overnight incubation with 100μg of antibody and BSA (0.1-0.5%) at room temperature with gentle agitation. The beads were then washed in Buffer B (isotonic phosphate buffered saline pH 7.2-7.6) three times and stored in Buffer B at 4°C.

B) Latex Bead-immobilized Antibody Preparation

Integrin subunit specific antibodies and purified IgG were passively absorbed onto 3.0 micron diameter latex beads (Polysciences, Inc.) using the reagents in The Glutaraldehyde Kit for Amino Beads and Blue Dyed Beads (Polysciences, Inc.) and the following modifications of the protocol described by Ellerbroek and colleagues (Ellerbroek and others 1999). Beads were resuspended in 8% glutaraldehyde in PBS and incubated at room temperature with gentle agitation for 4 to 6 hours. The beads were washed and resuspended in PBS with 100μg of the appropriate antibody overnight at room temperature with gentle agitation prior to incubations in 0.2M Ethanolamine in PBS for 45 minutes followed by incubation in BSA Solution for an additional 45 minutes at room temperature. The beads were then resuspended in Storage Buffer.

C) Antibody Purification (TS2/β1 integrin antibody)

TS2/16.2.1 hybridoma cells were obtained from ATCC (Manassas, VA) and maintained in RPMI-1640 (Invitrogen), 10% heat inactivated, low IgG fetal bovine serum (Invitrogen), sodium pyruvate, glutamine (Cellgro by Mediatech, Herndon, VA), and penicillin/streptomycin at 37ºC in 5% CO_2. The resulting conditioned media was filtered and loaded onto a HiTrap Protein G HP column (GE Healthcare, Piscataway, NJ) at 4°C using a Fast Protein Liquid Chromatography (FPLC) system. The column was washed with 100mM Tris pH 8. The antibody was eluted using 150mM Glycine pH 3. Fractions were collected and buffered in 1M Tris pH 8, 1mM $CaCl_2$. Antibody concentration was determined using the BioRad Protein Assay. Antibody specificity was determined by immunofluorescence microscopy.

D) Activation of Recombinant proMMP-9

Purified recombinant proMMP-9 was generously provided by Dr. Rafael Fridman (Wayne State University, Detroit, MI). It was activated by 1mM 4-aminophenylmercuric acetate (APMA) (Sigma Aldrich) at 37ºC for 1 to 3 hours and then dialyzed in collagenase buffer (50mM Tris, 150mM NaCl, 5mM $CaCl_2$, 0.02% Brij-35, pH 7.5) at 4ºC for 8 hours to overnight. The concentration of recombinant MMP-9 was determined using the BioRad Protein Assay. The presence of the active form of MMP-9 was determined using gelatin zymography.

E) Purification of Recombinant Cadherin Ectodomain-Fc Chimeric Protein (hEcad-Fc)

CHO cells stably expressing recombinant E-cadherin ectodomain-Fc chimeric protein were generously provided by Dr. Barry Gumbiner (University of Virginia, Charlottesville, VA) (Niessen and Gumbiner 2002) via Dr. Cara Gottardi (Northwestern University, Chicago, IL) and maintained in Ham's F12 media (Invitrogen), 10% low IgG FBS, and penicillin/streptomycin at 37ºC in 5% CO_2. The resulting condition media was filtered and loaded onto a column containing rProtein A Sepharose Fast Flow (GE Healthcare) at 4°C and was washed, eluted, and collected according to the manufacturer's specifications. Fractions containing protein, as determined by SDS-PAGE analysis, were combined then desalted and concentrated using Microcon centrifuge tubes YM-10. Concentration was determined using the BioRad Protein Assay.

F) LPA Preparation

LPA [1-Oleoyl-2-Hydroxy-sn-Glycero-3-Phosphate (sodium salt)] was purchased from Avanti (Alabaster, AL) in solution in chloroform. The chloroform was allowed to evaporate at room temperature and the LPA was reconstituted in PBS (Cellgro by Mediatech, Herndon, VA) at a concentration of 2mM. Aliqouts were then stored at –80°C.

G) Thin Layer Collagen Coating of Tissue Culture Plates

Collagen Type I Rat Tail (BD Biosciences) was dissolved in 0.02N acetic acid at a concentration of 100μg/ml and added to tissue culture plates. Plates were incubated at room temperature for 1 hour and then washed three times in PBS and one time in cell culture media before cells were plated.

H) Antibodies

Mouse Anti-E-cadherin (clone HECD-1) and Mouse Anti-E-cadherin (clone 4A2C7) were purchased from Invitrogen Corporation (Carlsbad, CA), formerly Zymed Laboratories Inc. Mouse anti-human integrin β1 (clone P5D2), mouse anti-human integrin α3 (clone P1B5), mouse anti-human integrin α2 (clone P1E6) monoclonal antibodies, and purified mouse IgG, were purchased from Chemicon International (Temecula, CA). Anti-MMP9 (Ab-1) mouse mAb (6-6B) was purchased from Calbiochem (San Diego, CA). COX-2 and COX-1 monoclonal antibodies as well as COX-2 (ovine) and COX-1 (ovine) electrophoresis standards were purchased from Cayman Chemical (Ann Arbor, MI). EGF receptor antibody and a PhosphoEGF Receptor Antibody Sampler Kit were purchased from Cell Signaling Technology (Beverly, MA)

and a mixture of the four phosphoEGFR antibodies (specific to residues Tyr845, Tyr992, Tyr1045, and Try1068) was used for detection of activated EGFR. Total ERK 1 and 2 antibodies were purchased from Santa Cruz Biotechnology Inc. (Santa Cruz, CA). Mouse monoclonal anti-Tubulin was purchased from Sigma-Aldrich (St. Louis, MO). Active B-catenin (clone 8E7) was purchased from Upstate (Lake Placid, NY). Purified Mouse Anti-β-catenin monoclonal antibody was purchased from BD Transduction Laboratories (San Jose, CA). Phospho GSK-3β (Ser9) Antibody and GSK-3β (27C10) Rabbit mAb were purchased from Cell Signaling Technology. Anti-Matrix Metalloproteinase-14 Hinge Region Antibody was purchased from Sigma-Aldrich. Monoclonal Anti-human MMP-7 Antibody (clone 111433) was purchased from R&D Systems (Minneapolis, MN). Cyclin D1 (HD11) Antibody was purchased from Santa Cruz Biotechnology, Inc. Peroxidase-conjugated anti-mouse IgG and Peroxidase-conjugated anti-Rabbit IgG were purchased from Sigma-Aldrich. Anti-rabbit IgG HRP-conjugated antibody was purchased from Cell Signaling. Alexa Fluor 488 goat anti-mouse IgG (H+L) was purchased from Molecular Probes (Eugene, OR)

I) Pharmacological inhibitors

GM6001 were purchased from Chemicon International. Cycloheximide in solution was purchased from Sigma-Aldrich. COX-2 inhibitor, NS-398, was purchased from Cayman Chemical and suspended in DMSO at a concentration of 50mM. Pertussis toxin was purchased from Biomol (Plymouth Meeting, PA) and was reconstituted in sterile water at a concentration of 100ng/µl. AG1478 was purchased from Calbiochem and suspended in DMSO at a concentration of 10mM. AG1478 In Solution was also purchased from Calbiochem. PD58059 was purchased

from Calbiochem and suspended in DMSO at a concentration of 50mM. MG-132 was purchased from Calbiochem and suspended in DMSO at a concentration of 20μg/μl. PP2 In Solution was purchased from Calbiochem

J) Plasmids

TOPflash (TCF Reporter Plasmid) and FOPflash (TCF Mutant Reporter Plasmid) were generously provided by Dr. Hans Clevers (Hubrecht Laboratory and Utrecht University, Utrecht, the Netherlands) via Dr. Cara Gottardi (Northwestern University, Chicago, IL). The Renilla luciferase vector, pRL-CMV, was purchased from Promega (Madison, WI). The pFLAG-CMV-2 control vector and pFLAG-CMV-2-ICAT vector were generously provided by Dr. Cara Gottardi (Gottardi and Gumbiner 2004b).

K) Other Reagents

EZ-link Sulfo-NHS-LC-Biotin and EZ-link Sulfo-NHS-SS-Biotin was purchased from Pierce (Rockford, IL) and resuspended in Dulbecco's phosphate buffered saline (DPBS) with calcium (Cellgro by Mediatech). Ultralink Immobilized NeutrAvidin Protein was also purchased from Pierce. Protein G-sepharose 4B FastFlow, recombinant protein G was purchased from Sigma-Aldrich. Matrigel was purchased from Becton Dickinson (San Jose, CA). Falcon HTS Fluoroblok Insert Systems (8μM pore size) were purchased from Becton Dickinson. Calcein AM was purchased from Molecular Probes. A Quantikine Human/Mouse MMP-2 (total) Immunoassay kit was purchased from R&D Systems. Collagen Type I Rat Tail was purchased from BD Biosciences (San Jose, CA). Iodoacetamide and MESNA (2-mercaptoethanesulfonic

acid) were purchased from Sigma-Aldrich. Polybead Amino 3.0 micron microspheres (2.59% solids-latex) and The Glutaraldehyde Kit for Amino Beads and Blue Dyed Beads were purchased from Polysciences, Inc (Warrington, PA). Epoxy magnetic beads were purchased from Invitrogen Corporation, formerly Dynal Biotech ASA (Oslo, Norway). FuGENE 6 Transfection Reagent was purchased from Roche Diagnostics (Mannheim, Germany). Dual-Luciferase Reporter Assay System was purchased from Promega. Human MMP-9 (total) Immunoassay kit was purchased from R&D Systems. Recombinant human EGF was provided as a supplement to keratinocyte SFM media from Invitrogen.

References

Afzal S, Lalani, E, Poulsom, R, Stubbs, A, Rowlinson, G, Sato, H, Seiki, M, Stamp, GWH. 1998. MT1-MMP and MMP-2 mRNA expression in human ovarian tumors: possible implications for the role of desmoplastic fibroblasts. Hum Pathol 29:155-165.

Akhmendkhanov A, Toniolo, P, Zeleniuch-Jacquotte, A, Kato, I, Koenig, KL, Shore, RE. 2001. Aspirin and risk of epithelial cancer. Prev Med 33:682-687.

Akutagawa N, Nishikawa, A, Iwasaki, M, Fujimoto, T, Teramoto, M, Kitajima, Y, Endo, T, Shibuya, M, Kudo, R. 2002. Expression of vascular endothelial growth factor and E-cadherin in human ovarian cancer: association with ascites fluid accumulation and peritoneal dissemination in mouse ascites model. Jpn J Cancer Res 93:644-651.

Ali-Fehmi R, Che, M, Khalifen, I, Malone, JM, Morris, R, Lawrence, WD, Munkarah, AR. 2003. The effect of cyclooxygenase-2 expression on tumor vascularity in advanced stage ovarian serous carcinoma. Cancer 98:1423-1429.

Almeida M, Han, L, Bellido, T, Manolagas, SC, Kousteni, S. 2005. Wnt proteins prevent apoptosis of both uncommitted osteoblast progenitors and differentiated osteoblasts by beta-catenin-dependent and -independent signaling cascades involving Src/ERK and phosphatidylinositol 3-kinase/AKT. J Biol Chem 280:41342-41351.

Alper O, Bergmann-Leitner, ES, Bennett, TA, Hacker, NF, Stromberg, K, Stetler-Stevenson, WG. 2001. Epidermal growth factor receptor signaling and the invasive phenotype of ovarian carcinoma cells. J Natl Cancer Inst 93(18):1375-84.

Alper O, DeSantis, ML, Stromberg, K, Hacker, NF, Cho-Chung, YS, Salomon, DS. 2000. Antisense suppression of epidermal growth factor receptor expression alters cellular proliferation, cell adhesion, and tumorigencity in ovarian cancer cells. Int J Cancer 88:566-574.

Altorki N, Keresztes, RS, Port, JL, Libby, DM, Korst, RJ, Flieder, DB, Ferrera, CA, Yankelevitz, DF, Subbaramaiah, K, Pasmantier, MW, Dannenberg, AJ. 2003. Celecoxib, a selective cyclooxygenase-2 inhibitor, enhances the response to preoperative paclitaxel and carboplatin in early-stage non-small-cell lung cancer. J Clin Oncol 21:2645-2650.

Araki Y, Okamura, S, Hussain, SP, Nagashima, M, He, P, Shiseki, M, Miura, K, Harris, CC. 2003. Regulation of cyclooxygenase-2 expression by the Wnt and ras pathways. Cancer Res 63:728-734.

Arias-Salgado E, Lizano, S, Sarkar, S, Brugge, JS, Ginsberg, MH, Shattil, SJ. 2003. Src kinase activation by direct interaction with the integrin beta cytoplasmic domain. Proc Natl Acad Sci U S A 100(23):13298-13302.

Attiga F, Fernandez, PM, Manyak, MJ, Patierno, SR. 2000. Effect of the cyclooxygenase-2 inhibitor NS398 on the secretion of matrix metalloproteinases (MMP-2 and MMP-9) and tissue inhibitors of metalloproteinase (TIMP-1 and TIMP-2) from human prostate tumor cells. Proc Am Assoc Cancer Res 41:131-132.

Auersperg N, Ota, T, Mitchell, GWE. 2002. Early events in ovarian epithelial carcinogenesis: progress and problems in experimental approaches. Int J Gynecol Cancer 12:691-703.

Auersperg N, Pan, J, Grove, BD, Peterson, T, Fisher, J, Maines-Bandiera, S, Somasiri, A, Roskelley, CD. 1999. E-cadherin induces mesenchymal-to-epithelial transition in human ovarian surface epithelium. Proc Natl Acad Sci U S A 96:6249-6254.

Avizienyte E, Frame, MC. 2005. Src and FAK signaling controls adhesion fate and the epithelial-to-mesenchymal transition. Curr Opin Cell Biol 17:542-547.

Avizienyte E, Wyke, AW, Jones, RJ, McLean, GW, Westhoff, MA, Brunton, VG, Frame, MC. 2002. Src-induced de-regulation of E-cadherin in colon cancer cells requires integrin signalling. Nat Cell Biol 4(8):632-8.

Azzam H, Thompson, EW. 1992. Collagen-induced activation of the Mr 72,000 type IV collagenase in normal and malignant fibroblastoid cells. Cancer Res 52:4540-4544.

Balzac F, Avolio, M, Degani, S, Kaverina, I, Torti, M, Silengo, L, Small, JV, Retta, SF. 2005. E-cadherin endocytosis regulates the activity of Rap1: a traffic light GTPase at the crossroads between cadherin and integrin function. J Cell Sci 118(Pt 20):4765-83.

Belotti D, Paganoni, P, Manenti, L, Garofalo, A, Marchini, S, Taraboletti, G, Giavazzi, R. 2003. Matrix metalloproteinases (MMP9 and MMP2) induce the release of vascular endothelial growth factor (VEGF) by ovarian carcinoma cells: implications for ascites formation. Cancer Res 63:5224-5229.

Benitah S, Valeron, PF, Rui, H, Lacal, JC. 2003. STAT5a activation mediates the epithelial to mesenchymal transition induced by oncogenic RhoA. Mol Biol Cell 14:40-53.

Billion K, Ibrahim, H, Mauch, C, Niessen, CM. 2006. Increased soluble E-cadherin in melanoma patients. Skin Pharmacol Physiol 19(2):65-70.

Birchmeier W, Behrens, J. 1994. Cadherin expression in carcinomas: role in the formation of cell junctions and the prevention of invasiveness. Biochim Biophys Acta 1198:11-26.

Boerboom D, Paquet M, Hsieh M, Liu J, Jamin SP, Behringer RR, Sirois J, Taketo MM, Richards JS. 2005. Misregulated Wnt/beta-catenin signaling leads to ovarian granulosa cell tumor development. Cancer Res 65(20):9206-15.

Boyd R, Balkwill, FR. 1999. MMP-2 release and activation in ovarian carcinoma: the role of fibroblasts. Br J Cancer 3/4:315-321.

Brabletz T, Jung, A, Spaderna, S, Hlubek, F, Kirchner, T. 2005. Migrating cancer stem cells-an integrated concept of malignant tumour progression. Nat Rev Cancer 5:744-749.

Brader K, Wolf, JK, Chakrabarty, S, Price, JE. 1998. Epidermal growth factor receptor (EGFR) antisense transfection reduces the expression of EGFR and suppresses the malignant phenotype of a human ovarian cancer cell line. Oncol Rep 5:1269-1274.

Brieher W, Yap, AS, Gumbiner, BM. 1996. Lateral dimerization is required for the homophilic binding activity of C-cadherin. J Cell Biol 135:487-496.

Bryant DM, Stow, JL. 2004. The ins and outs of E-cadherin trafficking. Trends Cell Biol 14(8):427-34.

Bryant, DM, Wylie, FG, Stow, JL. 2005. Regulation of endocytosis, nuclear translocation, and signaling of fibroblast growth factor receptor 1 by E-cadherin. Mol Cell Bio 16(1): 14-23.

Burleson K, Boente, MP, Pambuccian, SE, Skubitz, APN. 2006. Disaggregation and invasion of ovarian carcinoma ascites spheroids. J Translational Med 4(6):doi:10.1186/1479-5876-4-6.

Burleson K, Casey, RC, Skubitz, KM, Pambuccian, SE, Oegema, TR, Jr, Skubitz, APN. 2004. Ovarian carcinoma ascites spheroids adhere to extracellular matrix components and mesothelial cell monolayers. Gynecol Oncol 93:170-181.

Butler T, Zhu, C, Mueller, RA, Fuller, GC, Lemaire, WJ, Woessner, JF Jr. 1991. Inhibition of ovulation in the perfused rat ovary by the synthetic collagenase inhibitor SC44463. Biol Reprod 44:183-188.

Casslen B, Gustavsson, B, Astedt, B. 1991. Cell membrane receptors for urokinase plasminogen activator are increased in malignant ovarian tumours. Eur J Cancer 27:1445-1448.

Cavallaro U, Christofori, G. 2004. Cell adhesion and signaling by cadherins and Ig-CAMs in cancer. Nat Rev Cancer 4:118-130.

Chan A, Chu, KM, Lam, SK, Cheung, KL, Law, S, Kwok, KF, Wong, WM, Yuen, MF, Wong, BC. 2005. Early prediction of tumor recurrence after curative resection of gastric carcinoma by measuring soluble E-cadherin. Cancer 104(4):740-6.

Charalabopoulos K, Gogali, A, Dalavaga, Y, Daskalopoulos, G, Vassiliou, M, Bablekos, G, Karakosta, A, Constantopoulos, S. 2006. The clinical significance of soluble E-cadherin in nonsmall cell lung cancer. Exp Oncol 28(1):83-85.

Cheung L, Leung, PCK, Wong, AST. 2006. Gonadotropin-releasing hormone promotes ovarian cancer cell invasiveness through c-Jun NH_2-terminal kinase-mediated activation of matrix metalloproteinase (MMP)-2 and MMP-9. Cancer Res 66:10902-10910.

Chunthapong J, Seftor, EA, Khalkhali-Ellis, Z, Seftor, RE, Amir, S, Lubaroff, DM, Heidger, PM, Jr, Hendrix, MJ. 2004. Dual roles of E-cadherin in prostate cancer invasion. J Cell Biochem 91(4):649-61.

Clevers H. 2006. Wnt/beta-catenin signaling in development and disease. Cell 127:469-480.

Coffey R, Hawkey, CJ, Damstrup, L, Graves-Deal, R, Daniel, VC, Dempsey, PJ, Chinery, R, Kirkland, SC, DuBois, RN, Jetton, TL, Morrow, JD. 1997. Epidermal growth factor receptor activation induces nuclear targeting of cyclooxygenase-2, basolateral release of prostaglandins, and mitogenesis in polarizing colon cancer cells. Proc Natl Acad Sci U S A 94:657-662.

Coluccia A, Benati, D, Dekhil, H, De Filippo, A, Lan, C, Passerini, CG. 2006. SKI-606 decreases growth and motility of colorectal cancer cells by preventing pp60(c-Src)-dependent tyrosine phosphorylation of beta-catenin and its nuclear signaling. Cancer Res 66:2279-2286.

Coussens L, Tinkle, CL, Hanahan, D, Werb, Z. 2000. MMP-9 supplied by bone marrow-derived cells contributes to skin carcinogenesis. Cell 103:481-490.

Covington M, Bayliss, KJ, Burghardt, RC, Davis, GE, Parrish, AR. 2005. Ischemia-induced cleavage of cadherins in NRK cells: evidence for a role of metalloproteinases. Am J Physiol Renal Physiol 289:F280-F288.

Covington M, Burghardt, RC, Parrish, AR. 2006. Ischemia-induced cleavage of cadherins in NRK cells requires MT1-MMP (MMP-14). Am J Physiol Renal Physiol 290(1):F43-51.

Crawford H, Fingleton, B, Gustavson, MD, Kurpios, N, Wagenaar, RA, Hassell, JA, Matrisian, LM. 2001. The PEA3 subfamily of Ets transcription factors synergizes with beta-catenin-LEF-1 to activate matrilysin transcription in intestinal tumors. Mol Cell Biol 21:1370-1383.

Crawford H, Fingleton, BM, Rudolph-Owens, LA, Heppner Goss, KJ, Rubinfeld, B, Polakis, P, Matrisian, LM. 1999. The metalloproteinase matrilysin is a target of beta-catenin transactivation in intestinal tumors. Oncogene 18:2883-2891.

Daikoku T, Wang, D, Tranguchi, S, Morrow, JD, Orsulic, S, DuBois, RN, Dey, SK. 2005. Cyclooxygenase-1 is a potential target for prevention and treatment of ovarian epithelial cancer. Cancer Res 65:3735-3744.

Damsky C, Richa, J, Solter, D, Knudsen, K, Buck, CA. 1983. Identification and purification of a cell surface glycoprotein mediating intercellular adhesion in embryonic and adult tissue. Cell 34(2):455-66.

Danen E. 2005. Integrins: regulators of tissue function and cancer progression. Curr Pharm Des 11:881-891.

Darai E, Bringuier, A.F., Walker-Combrouze, F, Feldmann, G., Madelenat, P., Scoazec, J.Y. 1998a. Soluble adhesion molecules in serum and cyst fluid from patients with cystic tumours of the ovary. Hum Reprod 13(10):2831-5.

Darai E, Leblanc, M, Walker-Combrouze, F, Bringuier, AF, Madelenat, P, Scoazec, JY. 1998b. Expression of cadherins and CD44 isoforms in ovarian endometrial cysts. Hum Reprod 13(5):1346-52.

Daub H, Wallasch, C., Lankenau, A., Herrlich, A., Ullrich, A. 1997. Signal characteristics of G protein-transactivated EGF receptor. Embo J 16:7032-7044.

Daub H, Weiss, FU, Wallasch, C, Ullrich, A. 1996. Role of transactivation of the EGF receptor in signaling by G protein coupled receptors. Nature 379:557-560.

Davidson B, Berner A, Nesland JM, Risberg B, Berner HS, Trope CG, Kristensen GB, Bryne M, Ann Florenes V. 2000. E-cadherin and alpha-, beta-, and gamma-catenin protein expression is up-regulated in ovarian carcinoma cells in serous effusions. J Pathol 192(4):460-9.

Davidson B, Goldberg, I, Gotlieb, WH, Kopolovic, J , Ben-Baruch, G, Nesland, JM, Berner, A, Bryne, M , Reich, R. 1999. High levels of MMP2, MMP9, MT1-MMP and TIMP-2 mRNA correlate with poor survival in ovarian carcinoma. Clin Exp Metastasis 17:799-808.

Davidson B, Reich, R, Berner, A, Givant-Horwitz, V, Goldberg, I, Risberg, B, Kristensen, GB, Trope, CG, Bryne, M, Kopolovic, J, Nesland, JM. 2001. Ovarian carcinoma cells in serous effusions show altered MMP-2 and TIMP-2 mRNA levels. Eur J Cancer 37:2040-2049.

de Nictolis M, Garbisa, S, Lucarini, G, Goteri, G, Masiero, L, Ciavattini, A, Garzetti, GG, Stetler-Stevenson, WG, Fabris, G, Biagini, G, Prat, J. 1996. 72 kilodalton type IV collagenase, type IV collagen, and Ki 67 antigen in serous tumors of the ovary: a clinicopathologic, immunohistochemical, and serological study. Int J Gynecol Path 15:102-109.

DeClerck YA. 2000. Interactions between tumour cells and stromal cells and proteolytic modification of the extracellular matrix by metalloproteinases in cancer. Eur J Cancer 36:1258-1268.

DeFrias D, Okonkwo, AM, Keh, PC, Nayar, R. 2002. Cytopathology of the ovary. In: Stack M, Fishman, DA., editor. Cancer Treatment and Research: Ovarian Cancer. Boston: Kluwer Academic Publishers. p 185-212.

Demeter A, Sziller, I, Csapo, Z, Olah, J, Keszler, G, Jeney, A, Papp, Z, Staub, M. 2005. Molecular prognostic markers in recurrent and in non-recurrent epithelial ovarian cancer. Anticancer Res 25(4):2885-9.

Dempke W, Rie, C., Grothey, A., Schmoll, H-J. 2001. Cyclooxygenase-2: a novel target for cancer chemotherapy. J Cancer Res Clin Oncol 127:411-417.

Denkert C, Furstenberg, A, Daniel, PT, Koch, I, Kobel, M, Weichert, W, Siegert, A, Hauptmann, S. 2003. Induction of G0/G1 cell cycle arrest in ovarian carcinoma cells by the anti-inflammatory drug NS-398, but not COX-2 specific RNA interference. Oncogene 22:8653-8661.

Denkert C, Kobel, M., Pest, S., Koch, I., Berger, S., Schwabe, M., Siegert, A., Reles, A., Klosterhalfen, B., Hauptmann, S. 2002. Expression of cyclooxygenase 2 is an independent prognostic factor in human ovarian carcinoma. Am J Pathol 160:893-903.

Deryck L, De Wever, O, Stove, V, Vanhoecke, B, Delanghe, J, Depypere, H, Bracke, M. 2006a. Soluble N-cadherin in human biological fluids. Int J Cancer 119:2895-2900.

Deryck L, Morbidelli, L, Ziche, M, De Wever, O, Bracke, M, Van Aken, E. 2006b. Soluble N-cadherin fragment promotes angiogenesis. Clin Exp Metastasis 23:187-201.

Dihlmann S, von Knebel Doeberitz, M. 2005. Wnt/Beta-catenin pathway as a molecular target for future anti-cancer therapeutics. Int J Cancer 113:515-524.

Dinulescu D, Ince, TA, Quade, BJ, Shafer, SA, Crowley, D, Jacks, T. 2005. Role of K-ras and Pten in the development of mouse models of endometriosis and endometrioid ovarian cancer. Nat Med 11:63-70.

DiPersio CM, Shao, M., di Costanzo, L., Kriedberg, J.A., Hynes, R.O. 2000. Mouse keratinocytes immortalized with large T antigen acquire alpha3beta1 integrin-dependent secretion of MMP9/gelatinase B. J Cell Sci 113:2909-2921.

Dormond O, Bezzi, M, Mariotti, A, Ruegg, C. 2002. Prostaglandin E2 promotes integrin alphaV-beta3-dependent endothelial adhesion, rac-activation, and spreading through camp/PKA-dependent signaling. J Biol Chem 277:45838-45846.

Dormond O, Foletti, A, Paroz, C, Ruegg, C. 2001. NSAIDs inhibit alphaV-beta3 integrin-mediated and Cdc42/Rac-dependent endothelial cell spreading, migration, and angiogenesis. Nat Med 7:1041-1047.

Drew A, Blick, TJ, Lafleur, MA, Tim, ELM, Robbie, MJ, Rice, GE, Quinn, MA, Thompson, EW. 2004. Correlation of tumor- and stromal-derived MT1-MMP expression with progression of human ovarian tumors in SCID mice. Gynecol Oncol 95:437-448.

DuBois RN, Abramson, S.B., Crofford, L., Gupta, R., Simon, L.E., Van De Putte, L.B.A., Lipsky, P. 1998. Cyclooxygenase in biology and disease. FASEB 12:1063-1073.

Dwivedi D, Pino, G, Banh, A, Nathu, Z, Howchin, D, Margetts, P, Sivak, JG, West-Mays, JA. 2006. Matrix metalloproteinase inhibitors suppress transforming growth factor-beta-induced subcapsular cataract formation. Am J Path 168(1):69-79.

Egeblad M, Werb, Z. 2002. New functions for the matrix metalloproteinases in cancer progression. Nat Rev Cancer 2:161-174.

Eibl G, Bruemmer, D, Okada, Y, Duffy, JP, Law, RE, Reber, HA, Hines, OJ. 2003. PGE(2) is generated by specific COX-2 activity and increases VEGF production in COX-2-expressing human pancreatic cancer cells. Biochem Biophys Res Commun 306:888-897.

Elder D, Halton, DE, Crew, TE, Paraskeva, C. 2000. Apoptosis induction and cyclooxygenase-2 regulation in human colorectal adenoma and carcinoma cell lines by the cyclooxygenase-2-selective non-steroidal anti-inflammatory drug NS-398. Int J Cancer 86:553-560.

Elder D, Halton, DE, Playle, LC, Paraskeva, C. 2002. The MEK/ERK pathway mediates COX-2 selective NSAID-induced apoptosis and induced COX-2 protein expression in colorectal carcinoma cells. Int J Cancer 99:323-327.

Ellerbroek S, Fishman, DA, Kearns, AS, Bafetti, LM, Stack, MS. 1999. Ovarian carcinoma regulation of matrix metalloproteinase-2 and membrane type 1 matrix metalloproteinase through beta1 integrin. Cancer Res 59(7):1635-41.

Ellerbroek S, Halbleib, JM, Benavidez, M, Warmka, JK, Wattenberg, EV, Stack, MS, Hudson, LG. 2001a. Phosphatidylinositol 3-kinase activity in epidermal growth factor-stimulated matrix metalloproteinase-9 production and cell surface association. Cancer Res 61:1855-1861.

Ellerbroek S, Hudson, LG, Stack, MS. 1998. Proteinase requirements of epidermal growth factor-induced ovarian cancer cell invasion. Int J Cancer 78:331-337.

Ellerbroek S, Wu, YI, Overall, CM, Stack, MS. 2001b. Functional interplay between type I collagen and cell surface matrix metalloproteinase activity. J Biol Chem 276(27):24833-24842.

Faleiro-Rodrigues C, Macedo-Pinto, I, Pereira, D, Lopes, CS. 2004. Prognostic value of E-cadherin immunoexpression in patients with primary ovarian carcinomas. Annals of Oncology 15:1535-1542.

Fang X, Schummer, M., Mao, M., Yu, S., Tabassam, F.H., Swaby, R., Hasegawa, Y., Tanyi, J.L., LaPushin, R., Eder, A., Jaffe, R., Erickson, J., Mills, G.B. 2002a. Lysophosphatidic acid is a bioactive mediator in ovarian cancer. Biochim Biophys Acta 1582:257-264.

Fang X, Yu, S, Lu, Y, Bast, RC Jr, Woodgett, JR, Mills, GB. 2000. Phosphorylation and inactivation of glycogen synthase kinase 3 by protein kinase A. Proc Natl Acad Sci USA 97:11960-11965.

Fang X, Yu, S, Tanyi, JL, Lu, Y, Woodgett, JR, Mills, GB. 2002b. Convergence of multiple signaling cascades at glycogen synthase kinase 3: edg receptor-mediated phosphorylation and inactivation by lysophosphatidic acid through a protein kinaseC-dependent intracellular pathway. Mol Cell Biol 22:2099-2110.

Feeley K, Wells, M. 2001. Precursor lesions of ovarian epithelial malignancy. Histoplathology 38:87-95.

Fenwick S, Toogood, GJ, Lodge, JP, Hull, MA. 2003. The effect of selective cyclooxygenase-2 inhibitor rofecoxib on human colorectal cancer liver metastases. Gastroenterology 125:16-29.

Ferrandina G, Lauriola, L., Zannoni, G.F., Fagotti, A., Fanfani, F., Legge, F., Maggiano, N., Gessi, M., Mancuso, S., Ranelletti, F.O., Scambia, G. 2002a. Increased cyclooxygenase (COX-2) expression is associated with chemotherapy resistance and outcome in ovarian cancer patients. Ann Oncol 13:1205-1211.

Ferrandina G, Ranelletti, FO, Lauriola, L, Fanfani, F, Legge, F, Mottoleses, M, Nicotra, MR, Natali, PG, Zakut, VH, Scambia, G. 2002b. Cyclooxygenase-2 (COX-2), epidermal growth factor receptor (EGFR), and Her-2/neu expression in ovarian cancer. Gynecol Oncol 85:305-310.

Fishman D, Bafetti, LM, Banionis, S, Kearns, AS, Chilukuri, K, Stack, MS. 1997. Production of extracellular matrix-degrading proteinases by primary cultures of human epithelial ovarian carcinoma cells. Cancer 80(8):1457-1463.

Fishman D, Bafetti, LM, Stack, MS. 1996. Membrane-type matrix metalloproteinase expression and matrix metalloproteinase-2 activation in primary human ovarian epithelial carcinoma cells. Invasion Metastasis 16:150-159.

Fishman D, Borzorgi, K. 2002. The scientific basis of early detection of epithelial ovarian cancer: the national ovarian cancer early detection program (NOCEDP). In: Stack MS, Fishman, D.A., editor. Cancer Treatment and Research: Ovarian Cancer. Boston: Kluwer Academic Publishers. p 3-28.

Fishman D, Kearns, A, Chilukuri, K, Bafetti, LM, O'Toole, EA, Georgacopoulos, J, Ravosa, MJ, Stack, MS. 1998. Metastatic dissemination of human ovarian epithelial carcinoma is promoted by alpha2beta1-integrin-mediated interaction with type I collagen. Invasion Metastasis 18(1):15-26.

Fishman D, Liu, Y, Ellerbroek, SM, Stack, MS. 2001. Lysophosphatidic acid promotes matrix metalloproteinase (MMP) activation and MMP-dependent invasion in ovarian cancer cells. Cancer Res 61:3194-3199.

Foty R, Steinberg, MS. 2005. The differential adhesion hypothesis: a direct evaluation. Dev Biol 278:255-263.

Freedman RS, Deavers, M., Liu, J., Wang, E. 2004. Peritoneal inflammation: a microenvironment for epithelial ovarian cancer (EOC). J Transl Med 2:23.

Fridman R, Toth, M., Chvyrkova, I., Meroueh, S.O., Mobashery, S. 2003. Cell surface association of matrix metalloproteinase-9 (gelatinase B). Cancer Metastasis Rev 22:153-166.

Fujimoto J, Ichigo, S, Hirose, R, Sakaguchi, H, Tamaya, T. 1997. Expression of E-cadherin and alpha- and beta-catenin mRNAs in ovarian cancers. Cancer Lett 115(2):207-12.

Fujioka T, Takebayashi Y, Kihana T, Kusanagi Y, Hamada K, Ochi H, Uchida T, Fukumoto M, Ito M. 2001. Expression of E-cadherin and beta-catenin in primary and peritoneal metastatic ovarian carcinoma. Oncol Rep 8(2):249-55.

Fujita Y, Krause, G, Scheffner, M, Zechner, D, Leddy, HGM, Behrens, J, Sommer, T, Birchmeier, W. 2002. Hakai, a c-Cbl-like protein, ubiquitinates and induces endocytosis of the E-cadherin complex. Nat Cell Biol 4:222-231.

Gadducci A, Ferdeghini, M., Cosio, S., Annicchiarico, C., Ciampi, B., Bianchi, R., Genazzani, A.R. 1999. Preoperative serum E-cadherin assay in patients with ovarian carcinoma. Anticancer Res 19(1B):769-72.

Galvez B, Matias-Roman, S, Yanez-Mo, M, Sanchez-Madrid, F, Arroyo, AG. 2002. ECM regulates MT1-MMP localization with beta1 or alphavbeta3 integrins at distinct cell compartments modulating its internalization and activity on human endothelial cells. J Cell Biol 159:509-521.

Gamallo C, Palacios, J, Moreno, G, Calvo de Mora, J, Suarez, A, Armas, A. 1999. Beta-catenin expression pattern in stage I and II ovarian carcinomas: relationship with beta-catenin gene mutations, clinicopathological features, and clinical outcome. Am J Pathol 155:527-536.

Ghosh S, Brown, R., Jones, J.C., Ellerbroek, S.M., Stack, M.S. 2000. Urinary-type plasminogen activator (uPA) expression and uPA receptor localization are regulated by alpha-3 beta-1 integrin in oral keratinocytes. J Biol Chem 275(31):23869-236876.

Ghosh S, Wu, Y, Stack, M.S. 2002. Ovarian Cancer-Associated Proteinases. In: Stack MS, Fishman, D.A., editor. Cancer Treatment and Research: Ovarian Cancer. Boston: Kluwer Academic Publishers. p 331-354.

Gilles C, Polette, M., Seiki, M., Birembaut, P., Thompson, E.W. 1997. Implication of collagen type I-induced membrane type-1 matrix metalloproteinase expression and matrix metalloproteinase-2 activation in the metastatic progression of breast carcinoma. Lab Invest 76:651-660.

Gobeil F, Bernier, SG, Vasquez-Tello, A, Brault, S, Beauchamp, MH, Quinlou, C, Marrache, AM, Checchin, D, Sennlaub, F, Hou, X, Nader, M, Bkaily, G, Ribeiro-da-Silva, A, Goetzl, EJ, Chemtob, S. 2003. Modulation of pro-inflammatory gene expression by nuclear lysophosphatidic acid receptor type-1. J Biol Chem 278:38875-38883.

Goode N, Hughes, K, Woodgett, JR, Parker, PJ. 1992. Differential regulation of glycogen synthase kinase-3 beta by protein kinase C isotypes. J Biol Chem 267:16878-16882.

Gottardi C, Gumbiner, BM. 2004a. Distinct molecular forms of beta-catenin are targeted to adhesive or transcriptional complexes. J Cell Biol 167(2):339-49.

Gottardi C, Gumbiner, BM. 2004b. Role for ICAT in beta-catenin-dependent nuclear signaling and cadherin functions. Am J Physiol Cell Physiol 286(4):C747-56.

Gottardi C, Wong, E, Gumbiner, BM. 2001. E-cadherin suppresses cellular transformation by inhibiting beta-catenin signaling in an adhesion-independent manner. J Cell Biol 153(5):1049-60.

Grosch S, Tegeder, I, Niederberger, E, Brautigam, L, Geisslinger, G. 2001. COX-2 independent induction of cell cycle arrest and apoptosis in colon cancer cells by the selective COX-2 inhibitor celecoxib. FASEB J 15:2742-2744.

Gshwind A, Prenzel, N., Ullrich, A. 2002. Lysophosphatidic acid-induced squamous cell carcinoma cell proliferation and motility involves epidermal growth receptor signal transactivation. Cancer Res 62:6329-6336.

Gshwind A, Zwick, E, Prenzel, N, Leserer, M, Ullrich, A. 2001. Cell communication networks: epidermal growth factor receptor transactivation as the paradigm for interreceptor signal transmission. Oncogene 20:1594-1600.

Gumbiner B. 2000. Regulation of cadherin adhesive activity. J Cell Biol 148:399-404.

Guo W, Giancotti, F.G. 2004. Integrin signalling during tumour progression. Nat Rev Mol Cell Biol 5(10):816-826.

Gupta R, Tejada, LV, Tong, BJ, Das, SK, Morrow, JD, Dey, SK, DuBois, RN. 2003. Cyclooxygenase-1 is overexpressed and promotes angiogenic growth factor production in ovarian cancer. Cancer Res 63:906-911.

Haas TL, Davis, S.J., Madri, J.A. 1998. Three-dimensional type I collagen lattice induces coordinate expression of matrix metalloproteinases MT1-MMP and MMP-2 in microvascular endothelial cells. J Biol Chem 273:3604-3610.

Hagemann T, Wilson, J., Burke, F., Kulbe, H., Li, N.F., Pluddemann, A., Charles, K., Gordon, S., Balkwill, F.R. 2006. Ovarian cancer cells polarize macrophages toward a tumor-associated phenotype. J Immunol 176:5023-5032.

Hapke S, Kessler, H, Arroyo de Prada, N, Benge, A, Schmitt, M, Lengyel, E, Reuning, U. 2001. Integrin alpha-v-beta-3/vitronectin interaction affects expression of the urokinase system in huma ovarian cancer cells. J Biol Chem 276:26340-26348.

Harvey W, Amlot, PL. 1983. Collagen production by human mesothelial cell in vitro. J Pathol 139:337-347.

Hayashido Y, Hamana, T, Yoshioka, Y, Kitano, H, Koizumi, K-I, Okamoto, T. 2005. Plasminogen acitvator/plasmin system suppresses cell-cell adhesion of oral squamous cell carcinoma cells via proteolysis of E-cadherin. Int J Oncol 27:693-698.

Herrenknecht K, Kemler, R. 1993. Characterization of recombinant E-cadherin (uvomorulin) expressed in insect cells. J Cell Sci Suppl 17:147-154.

Heussen C, Dowdle, EB. 1980. Electrophoretic analysis of plasminogen activators in polyacrylamide gels containing sodium dodecyl sulfate and copolymerized substrates. Anal Biochem 102:196-202.

Hiendlmeyer E, Regus, S, Wasserman, S, Hlubek, F, Haynl, A, Dimmler, A, Koch, C, Knoll, C, van Best, M, Reuning, U, Brabletz, T, Kirchner, T, Jung, A. 2004. Beta-catenin up-regulates the expression of the urokinase plasminogen activator in human colorectal cancers. Cancer Res 64:1209-1214.

Hirao T, Nanba, D, Tanaka, M, Ishiguro, H, Kinugasa, Y, Doki, Y, Yano, M, Matsuura, N, Monden, M, Higashiyama, S. 2006. Overexpression of ADAM9 enhances growth factor-mediated recycling of E-cadherin in human colon cancer cell line HT29 cells. Exp Cell Res 312(3):331-9.

Hood J, Cheresh, DA. 2002. Role of integrins in cell invasion and migration. Nat Rev Cancer 2(2):91-100.

Hu YL, Tee, M.K., Goetzl, E.J., Auersperg, N., Mills, G.B., Ferrara, N., Jaffe, R.B. 2001. Lysophosphatidic acid induction of vascular endothelial growth factor expression in human ovarian cancer cells. J Natl Cancer Inst 93:762-768.

Huang L-W, Garrett, AP, Bell, DA, Welch, WR, Berkowitz, RS, Mok, SC. 2000. Differential expression of matrix metalloproteinase-9 and tissue inhibitor of metalloproteinase-1 protein and mRNA in epithelial ovarian tumors. Gynecol Oncol 77:369-376.

Huang S, Van Arsdall, M., Tedjarati, S., McCarty, M., Wu, W., Langley, R., Fidler, I.J. 2002. Contributions of stromal metalloproteinase-9 to angiogenesis and growth of human ovarian carcinoma in mice. J Natl Cancer Inst 94(15):1134-1142.

Hulboy D, Rudolph, LA, Matrisian, LM. 1997. Matrix metalloproteinases as mediators of reproductive function. Mol Human Reprod 3:27-45.

Ii M, Yamamoto, H, Adachi, Y, Maruyama, Y, Shinomura, Y. 2006. Role of matrix metalloproteinase-7 (matrilysin) in human cancer invasion, apoptosis, growth, and angiogenesis. Exp Biol Med 231:20-27.

Imai T, Horiuchi, A., Shiozawa, T., Osada, R., Kikuchi, N., Ohira, S., Oka, K., Konishi, I. 2004. Elevated expression of E-cadherin and alpha-, beta-, and gamma-catenins in metastatic lesions compared with primary epithelial ovarian carcinomas. Hum Pathol 35(12):1469-1476.

Irby RA, Yeatman, T.J. 2002. Increased Src activity disrupts cadherin/catenin-mediated homotypic adhesion in human colon cancer and transformed rodent cells. Cancer Res 62:2669-2674.

Ishizaki T, Katsumata, K., Tsuchida, A., Wada, T., Mori, Y., Hisada, M., Kawakita, H., Aoki, T. 2006. Etodolac, a selective cyclooxygenase-2 inhibitor, inhibits liver metastasis of colorectal cancer cells via the suppression of MMP9 activity. Int J Mol Med 17(2):357-62.

Ito K, Okamoto, I., Araki, N., Kawano, Y., Nakao, M., Fujiyama, S., Tomita, K., Mimori, T., Saya, H. 1999. Calcium influx triggers the sequential proteolysis of extracellular and cytoplasmic domains of E-cadherin, leading to loss of beta-catenin from cell-cell contacts. Oncogene 18:7080-7090.

Itoh Y, Seiki, M. 2006. MT1-MMP: A potent modifier of pericellular microenvironment. J Cell Physiol 206:1-8.

Iyer V, Pumiglia, K., DiPersio, C.M. 2005. alpha-3 beta-1 integrin upregulates MMP-9 mRNA stability in immortalized keratinocytes: a novel mechanism of integrin-mediated MMP gene expression. J Cell Sci 118:1185-1195.

Izumi G, Sakisaka, T, Baba, T, Tanaka, S, Morimoto, K, Takai, Y. 2004. Endocytosis of E-cadherin regulated by Rac and Cdc42 small G proteins through IQGAP1 and actin filaments. J Cell Biol 166(2):237-48.

Jemal A, Tiwari, RC, Murray, T, Ghafoor, A, Samuels, A, Ward, E, Feuer, EJ, Thun, MJ; American Cancer Society. 2004. Cancer Statistics, 2004. CA Cancer J 54:8-29.

Jourquin J, Yang, N, Kam, Y, Guess, C, Quaranta, V. 2006. Dispersal of epithelial cancer cell colonies by lysophosphatidic acid (LPA). J Cell Physiol 206:337-346.

Kamat AA, Fletcher, M., Gruman, L.M., Mueller, P., Lopez, A., Landen, C.N. Jr., Han, L., Gershenson, D.M., Sood, A.K. 2006. The clinical relevance of stromal matrix metalloproteinase expression in ovarian cancer. Clin Cancer Res 12(6):1707-1714.

Karbova E, Davidson, B., Metodiev, K., Trope, C.G., Nesland, J.M. 2002. Adenomatous polyposis coli (APC) protein expression in primary and metastatic serous ovarian carcinoma. Int J Surg Path 10(3):175-180.

Katori M, Majima, M.,. 2000. Cyclooxygenase-2: its rich diversity of roles and possible applications of its selective inhibitors. Inflammation Res 49:376-392.

Katsube Y, Berg, JW, Silverberg, SG. 1982. Epidemiologic pathology of ovarian tumors: a histopathologic review of primary ovarian neoplasms diagnosed in the Denver Standard Metropolitan Statistical Area, 1 July-31 December 1969 and 1 July-31 December 1979. Int J Gynecol Pathol 1(1):3-16.

Kim SN, Park, J.C., Lee, E.B., Kim, S.S., Yoo, Y.S. 2000. Characterisitics of epidermal growth factor receptor function in lysophosphatidic acid signaling in PC12 cells. J Cell Biochem 76:386-393.

Klimp A, Hollema, H, Kempinga, C, van der Zee, AGJ, de Vries, EGE, Daemen, T. 2001. Expression of cyclooxygenase-2 and inducible nitric oxide synthase in human ovarian tumors and tumor-associated macrophages. Cancer Res 61:7305-7309.

Koenig A, Mueller, C., Hasel, C., Adler, G., Menke,A. 2006. Collagen type I induces disruption of E-cadherin-mediated cell-cell contacts and promotes proliferation of pancreatic carcinoma cells. Cancer Res 66(9):4662-4671.

Kohn E. 1997. Angiogenesis in ovarian carcinoma: a formidable biomarker. Cancer (Phila.) 80:2219-2221.

Koonings P, Campbell, K, Mishell, DR, Jr, Grimes, DA. 1989. Relative frequency of primary ovarian neoplasms: a 10-year review. Obstet Gynecol 74(6):921-6.

Kuefer R, Hofer, M.D., Gshwend, J.E., Pienta, K.J., Sanda, M.G., Chinnaiyan, A.M., Rubin, M.A., Day, M.L. 2003. The role of an 80kDa fragment of E-cadherin in the metastatic progression of prostate cancer. Clin Cancer Res 9:6447-6452.

Kulkarni S, Rader, JS, Zhang, F, Liapis, H, Koki, AT, Masferrer, JL, Subbaramaiah, K, Dannenberg, AJ. 2001. Cyclooxygenase-2 is overexpressed in human cervical cancer. Clin Cancer Res 7:429-434.

Kuphal F, Behrens, J. 2006. E-cadherin modulates Wnt-dependent transcription in colorectal cancer cells but does not alter Wnt-independent gene expression in fibroblasts. Exp Cell Res 312:457-476.

Lacey J, Mink, PJ, Lubin, JH, Sherman, ME, Troisi, R, Hartge, P, Schatzkin, A, Schairer, C. 2002. Menopause hormone replacement therapy and risk of ovarian cancer. JAMA 288:334-341.

Laemmli UK. 1970. Cleavage of structural proteins during the assembly of the head of bacteriophage T4. Nature (London)(227):680-685.

Laffargue M, Raynal, P., Yart, A., Peres, C, Wetzker, R, Roche, S, Payastre, B, Chap, H. 1999. An epidermal growth factor receptor/Gab1 signaling pathway is required for activation of phosphoinositide 3-kinase by lysophosphatidic acid. J Biol Chem 274:32835-32841.

Landen CN, Mathur, S.P., Richardson, M.S., Creasman, W.T. 2003. Expression of cyclooxygenase-2 in cervical, endometrial, and ovarian malignancies. Am J Obstet Gynecol 188:1174-1176.

Le T, Joseph, SR, Yap, AS, Stow, JL. 2002. Protein kinase C regulates endocytosis and recycling of E-cadherin. Am J Physiol Cell Physiol 283(2):C489-99.

Le T, Yap, AS, Stow, JL. 1999. Recycling of E-cadherin: a potential mechanism for regulating cadherin dynamics. J Cell Biol 146(1):219-32.

Lee CM, Shvartsman H, Deavers MT, Wang SC, Xia W, Schmandt R, Bodurka DC, Atkinson EN, Malpica A, Gershenson DM and others. 2003. beta-catenin nuclear localization is associated with grade in ovarian serous carcinoma. Gynecol Oncol 88(3):363-8.

Lengyel E, Schmalfeldt, B, Konik, E, Spathe, K, Harting, K, Fenn, A, Berger, U, Fridman, R, Schmitt, M, Prechtel, D, Kuhn, W. 2001. Expression of latent matrix metalloproteinase 9 (MMP9) predicts survival in advanced ovarian cancer. Gynecol Oncol 82:291-298.

Lessan K, Aguiar, D.J., Oegema, T., Siebenson, Skubitz, A.P.N. 1999. CD44 and Beta-1 integrin mediate ovarian carcinoma cell adhesion to peritoneal mesothelial cells. Am J Pathol 154(5):1525-1537.

Lessan K, Skubitz, APN. 1998. Binding of an ovarian carcinoma cell line to peritoneal mesothelial cells *in vitro* is partially inhibited by an antibody against the beta-1 integrin subunit. FASEB J 12:A377.

Li H, Ye, X, Mahanivong, C, Bian, D, Chun, J, Huang, S. 2005. Signaling mechanisms responsible for lysophosphatidic acid-induced urokinase plasminogen activator expression in ovarian cancer cells. J Biol Chem 280:10564-10571.

Li M, Wang, X, Meintzer, MK, Laessiq, T, Birnbaum, MJ, Heidenreich, KA. 2000. Cyclic AMP promotes neuronal survival by phosphorylation of glycogen synthase kinase 3beta. Mol Cell Biol 20:9356-9363.

Li S, Miner, K., Fannin, R., Barrett, J.C., Davies, B.J. 2004. Cyclooxygenase-1 and 2 in normal and malignant ovarian epithelium. Gynecol Oncol 92:622-627.

Lim H, Paria, BC, Das, SK, Dinchuk, JE, Langenbach, R, Trzaskos, JM, Dey, SK. 1997. Multiple female reproductive failures in cyclooxygenase 2-deficient mice. Cell 91:197-208.

Liu J, Yang, G, Thompson-Lanza, JA, Glassman, A, Hayes, K, Patterson, A, Marquez, RT, Auersperg, N, Yu, Y, Hahn, WC, Mills, GB, Bast, RC, Jr. 2004. A genetically defined model for human ovarian cancer. Cancer Res 64:1655-1663.

Liu WF, Nelson, C.M., Pirone, D.M., Chen, C.S. 2006. E-cadherin engagement stimulates proliferation via Rac1. J Cell Biol 173(3):431-441.

Lochter A, Galosy, S, Muschler, J, Freedman, N, Werb, Z, Bissell, MJ. 1997. Matrix metalloproteinase stromelysin-1 triggers a cascade of molecular alterations that leads to stable epithelial-to-mesenchymal conversion and a premalignant phenotype in mammary epithelial cells. J Cell Biol 139(7):1861-72.

Luttrell L, Hawes, BE, van Biesen, T, Luttrell, DK, Lansing, TJ, Lefkowitz, RJ. 1996. Role of c-Src tyrosine kinase in G protein-coupled-receptor and G-beta-gamma subunit-mediated activation of mitogen-activated protein kinases. J Biol Chem 27:19443-19450.

Maeda M, Johnson, E, Mandal, SH, Lawson, KR, Keim, SA, Svoboda, RA, Caplan, S, Wahl, JK, 3rd, Wheelock, MJ, Johnson, KR. 2006. Expression of inappropriate cadherins by epithelial tumor cells promotes endocytosis and degradation of E-cadherin via competition for p120(ctn). Oncogene 25(33):4595-604.

Maines-Bandiera SL, Auersperg, N. 1997. Increased E-cadherin expression in ovarian surface epithelium: an early step in metaplasia and dysplasia? Int J Gynecol Path 16:250-255.

Makarla P, Saboorian, MH, Ashfaq, R, Toyooka, KO, Toyooka, S, Minna, JD, Gazdar, AF, Schorge, JO. 2005. Promoter hypermethylation profile of ovarian epithelial neoplasms. Clin Cancer Res 11:5365-5369.

Marambaud P, Shioi, J., Serban, G., Georgakopoulos, A., Sarner, S., Nagy, V., Baki, L., Wen, P., Efthimiopoulos, S., Shao, Z., Wisniewski, T., Robakis, N.K. 2002. A presenilin-1/gamma-secretase cleavage releases the E-cadherin intracellular domain and regulated disassembly of adherens junctions. EMBO J 21:1948-1956.

Maretzky T, Reiss, K, Ludwig, A, Buchholz, J, Scholz, F, Proksch, E, de Strooper, B, Hartmann, D, Saftig, P. 2005. ADAM10 mediates E-cadherin shedding and regulates epithelial cell-cell adhesion, migration, and beta-catenin translocation. Proc Natl Acad Sci U S A 102(26):9182-7.

Marques F, Fonsechi-Carvasan, GA, De Angelo Andrade, LAL, Bottcher-Luiz, F. 2004. Immunohistochemical patterns for alpha and beta-catenin, E- and N-cadherin expression in ovarian epithelial tumors. Gynecol Oncol 94:16-24.

Martin J, Yung, S., Robson, R.L., Steadman, R., Davies, M. 2000. Production and regulation of matrix metalloproteinases and their inhibitors by human peritoneal mesothelial cells. Perit Dial Int 20(5):524-533.

Matsudaira P. 1987. Sequence from picomole quantities of proteins electroblotted onto polyvinylidene difluoride membranes. J Biol Chem 262:10035-10038.

Matsumoto Y, Ishiko, O, Deguchi, M, Nakagawa, E, Ogita, S. 2001. Cyclooxygenase-2 expression in normal ovaries and epithelial ovarian neoplasms. Int J Mol Med 8:31-36.

McCawley L, Matrisian, LM. 2000. Matrix metalloproteinases: multifunctional contributors to tumor progression. Mol Med Today 6:149-156.

McCawley L, Matrisian, LM. 2001a. Matrix metalloproteinases: they're not just for matrix anymore! Curr Opin Cell Biol 13:534-540.

McCawley LJ, Matrisian, L.M. 2001b. Tumor progression: defining the soil around the tumor seed. Curr Biol 11:R25-R27.

Menke A, Philippi, C, Vogelmann, R, Seidel, B, Lutz, MP, Adler, G, Wedlich, D. 2001. Down-regulation of E-cadherin gene expression by collagen type I and type III in pancreatic cancer cell lines. Cancer Res 61:3508-3517.

Mills G. 2002a. Mechanisms underlying chemoprevention of ovarian cancer. Clin Cancer Res 8:7-10.

Mills GB, Eder, A., Fang, X., Hasegawa, Y., Mao, M., Lu, Y., Tanyi, J., Tabassam, F.H., Wiener, J., Lapushin, R., Yu, S., Parrott, J.A., Compton, T., Tribley, W., Fishman, D., Stack, M.S., Gaudette, D., Jaffe, R., Furui, T., Aoki, J., Erickson, J.R. 2002b. Critical role of lysophospholipids in the pathophysiology, diagnosis, and management of ovarian cancer. In: Stack MS, Fishman, D.A., editor. Cancer Treatment and Research: Ovarian Cancer. Boston: Kluwer Academic Publishers. p 259-284.

Mills GB, Moolenaar, W.H. 2003. The emerging role of lysophosphatidic acid in cancer. Nat Rev Cancer 3:582-591.

Miotti S, Tomassetti, A., Facetti, I., Sanna, E., Berno, V., Canevari, S. 2005. Simultaneous expression of caveolin-1 and E-cadherin in ovarian carcinoma cells stabilizes adherens junctions through inhibition of src-related kinases. Am J Pathol 167(5):1411-1427.

Miyamoto S, Akiyama, S.K., Yamada, K.M. 1995a. Synergistic roles for receptor occupancy and aggregation in integrin transmembrane function. Science 267:883-885.

Miyamoto S, Teramoto, H., Coso, O.A., Gutkind, J.S., Burbelo, P.D., Akiyama, S.K., Yamada, K.M. 1995b. Integrin function: molecular hierarchies of cytoskeletal and signaling molecules. J Cell Biol 131:791-805.

Molina M, Sitja-Arnau, M, Lemoine, MG, Frazier, ML, Sinicrope, FA. 1999. Increased cyclooxygenase-2 expression in human pancreatic carcinoma and cell lines: growth inhibition by nonsteroidal anti-inflammatory drugs. Cancer Res 59:4356-4362.

Montell D. 2003. Border-cell migration: the race is on. Nat Rev Mol Cell Bio 4:13-24.

Moolenaar WH, Kruijer, W., Tilly, B.C., Verlaan, I., Bierman, A.J., de Laat, S.W. 1986. Growth factor-like action of phosphatidic acid. Nature 323:171-173.

Morini M, Mottolese, M, Ferrari, N, Ghiorzo, F, Buglioni, S, Mortarini, Noonan, DM, Natali, PG, Albini, A. 2000. The alpha-3-beta-1 integrin is associated with mammary carcinoma cell metastasis, invasion, and gelatinase B (MMP-9) activity. Int J Cancer 87:336-342.

Moser T, Young, TN, Rodriguez, GC, PIzzo, SV, Bast, RC, Jr, Stack, MS. 1994. Secretion of extracellular matrix-degrading proteinases is increased in epithelial ovarian carcinoma. Int J Cancer 56:552-559.

Munkarah A, Genhai, Z, Morris, R, Baker, VV, Deppe, G, Diamond, MP, Saed, GM. 2003. Inhibition of paclitaxel-induced apoptosis by the specific COX-2 inhibitor, NS398, in epithelial ovarian cancer cells. Gynecol Oncol 88:429-433.

Munshi HG, Stack, M.S. 2006. Reciprocal interactions between adhesion receptor signaling and MMP9 regulation. Cancer Metastasis Rev 25:45-56.

Mutsaers SE. 2002. Mesothelial cells: their structure, function, and role in serosal repair. Respirology 7:171-191.

Nagar B, Overduin, M, Ikura, M, Rini, JM. 1996. Structural basis of calcium-induced E-cadherin rigidication and dimerization. Nature (London) 380:360-364.

Nagase H, Woessner, JF Jr. 1999. Matrix Metalloproteinases. J Biol Chem 274:21491-21494.

Naora H, Montell, DJ. 2005. Ovarian cancer metastasis: integrating insights from disparate model organisms. Nat Rev Cancer 5(5):355-66.

Nawrocki-Raby B, Gilles, C, Polette, M, Bruyneel, E, Laronze, JY, Bonnet, N, Foidart, JM, Mareel, M, Birembaut, P. 2003. Upregulation of MMPs by soluble E-cadherin in human lung tumor cells. Int J Cancer 105(6):790-5.

Naylor MS, Stamp, G.W., Davies, B.D., Balkwill, F.R. 1994. Expression and activity of MMPs and their regulators in ovarian cancer. Int J Cancer 58(1):50-56.

Nelson W, Nusse, R. 2004. Convergence of Wnt, Beta-catenin, and Cadherin Pathways. Science 303:1483-1487.

Niedbala M, Madiyalakan, R, Matta, K, Crickard, K, Sharma, M, Bernacki, RJ. 1987. Role of glycosidases in human ovarian carcinoma cell mediated degradation of subendothelial extracellular matrix. Cancer Res 47:4634-4641.

Niessen CM, Gumbiner, B.M. 2002. Cadherin-mediated cell sorting not determined by binding or adhesion specificity. J Cell Biol 156(2):389-399.

Noe V, Fingleton, B, Jacobs, K, Crawford, HC, Vermeulen, S, Steelant, W, Bruyneel, E, Matrisian, LM, Mareel, M. 2001. Release of an invasion promoter E-cadherin fragment by matrilysin and stromelysin-1. J Cell Sci 114(Pt 1):111-118.

Noe V, Willems, J, Vandekerckhove, J, Roy, FV, Bruyneel, E, Mareel, M. 1999. Inhibition of adhesion and induction of epithelial cell invasion by HAV-containing E-cadherin specific peptides. J Cell Sci 112(Pt 1):127-135.

Norman R. 2001. Reproductive consequences of COX-2 inhibition. Lancet 358:1287-1288.

Offner FA, Obrist, P. Stadlmann, S., Feichtinger, H., Klingler, P., Herold, M., Zwierzina, H. Hittmair, A., Mikuz, G., Abendstein, B., Zeimet, A., Marth, C. 1995. IL-6 secretion by human peritoneal mesothelial and ovarian cancer cells. Cytokine 7:542-547.

Ohno R, Yoshinaga, K, Fujita, T, Hasegawa, K, Iseki, H, Tsunozaki, H, Ichikawa, W, Nihei, Z, Sugihara, K. 2001. Depth of invasion parallels increased cyclooxygenase2 levels in patients with gastric carcinoma. Cancer 91:1876-1881.

Ohta H, Sato, K, Murata, N, Damirin, A. Malchinkhuu, E, Kon, J, Kimura, T, Tobo, M, Yamazaki, Y, Watanabe, T, Yagi, M, Sato, M, Suzuki, R, Murooka, H, Sakai, T, Nishitoba, T, Im, DS, Nochi, H, Tamoto, K, Tomura, H, Okajima, F. 2003. Ki16425, a subtype-selective antagonist for EDG-family lysophosphatidic acid receptors. Mol Pharmacol 64:994-1005.

Okegawa T, Li, Y, Pong, RC, Hsieh, JT. 2002. Cell adhesion proteins as tumor suppressors. J Urol 167(4):1836-43.

Okegawa TP, R-C, Li, Y., Hsieh, J-T. 2004. The role of cell adhesion molecules in cancer progression and its application in cancer therapy. Acta Biochimica Polonica 51:445-457.

Oloumi A, McPhee, T, Dedhar, S. 2004. Regulation of E-cadherin expression and beta-catenin/Tcf transcriptional activity by the integrin linked kinase. Biochim Biophys Acta 1691:1-15.

Overall C, Lopez-Otin, C. 2002. Strategies for MMP inhibition in cancer: innovations for the post-trial era. Nat Rev Cancer 2:657-672.

Ozalp S, Tanir HM, Yalcin OT, Kabukcuoglu S, Oner U, Uray M. 2003. Prognostic value of matrix metalloproteinase-9 (gelatinase-B) expression in epithelial ovarian tumors. Eur J Gynaecol Oncol 24(5):417-20.

Ozols R, Bookman, MA, Connolly, DC, Daly, MB, Godwin, AK, Schiler, RJ, Xu, X, Hamilton, TC. 2004. Focus on epithelial ovarian cancer. Cancer Cell 5:19-24.

Palacios F, Jogender, S., Fujita, Y., D'Souza-Schorey, C. 2005. Lysosomal targeting of E-cadherin: a unique mechanism for the down-regulation of cell-cell adhesion during epithelial to mesenchymal transitions. Mol Cell Biol 25(1):389-402.

Palacios F, Schweitzer, JK, Boshans, RL, D'Souza-Schorey, C. 2002. ARF6-GTP recruits Nm23-H1 to facilitate dynamin-mediated endocytosis during adherens junctions disassembly. Nat Cell Biol 4(12):929-36.

Palacios J, Gamallo, C. 1998. Mutations in the beta-catenin gene (CTNNB1) in endometrioid ovarian carcinomas. Cancer Res 58:1344-1347.

Pall M, Friden, BE, Brannstrom, M. 2001. Induction of delayed follicular rupture in the human by the selective COX-2 inhibitor rofecoxib: a randomized double-blind study. Hum Reprod 16:1323-1328.

Pan M, Chuang, LY, Hung, WC. 2001. Non-steroidal anti-inflammatory drugs inhibit matrix metalloproteinase-2 expression via repression of transcription in lung cancer cells. FEBS Lett 508:365-368.

Patel IS, Madan, P., Getsios, S., Betrand, M.A., MacCalman, C.D. 2003. Cadherin switching in ovarian cancer progression. Int J Cancer 106:172-177.

Paterson A, Parton, RG, Ferguson, C, Stow, JL, Yap, AS. 2003. Characterization of E-cadherin endocytosis in isolated MCF-7 and chinese hamster ovary cells: the initial fate of unbound E-cadherin. J Biol Chem 278(23):21050-7.

Pokutta S, Herrenknecht, R, Kemler, R, Engel, J. 1994. Conformational changes of the recombinant extracellular domain of E-cadherin upon calcium binding. Eur J Biochem 223:1019-1026.

Pon Y, Wong, AST. 2006. Gonadotropin-induced apoptosis in human ovarian surface epithelial cells is associated with cyclooxygenase-2 up-regulation via the beta-catenin/T-cell factor signaling pathway. Mol Endocrinol 12:3336-3350.

Prakasam A, Maruthamuthu, V, Leckband, DE. 2006. Similarities between heterophilic and homophilic cadherin adhesion. Proc Natl Acad Sci U S A 103:15434-15439.

Puls LE, Duniho, T., Hunter, J.E. IV, Kryscio, R., Blackhurst, D., Gallion, H. 1996. The prognostic implication of ascites in advanced-stage ovarian cancer. Gynecol Oncol 61:109-112.

Pustilnik T, Estrella, V, Wiener, JR, Mao, M, Eder, A, Watt, MAV, Bast, RC, Jr, Mills, GB. 1999. Lysophosphatidic acid induces urokinase secretion by ovarian cancer cells. Clin Cancer Res 5:3704-3710.

Radisky D, Bissell, MJ. 2006. Matrix metalloproteinase-induced genomic instability. Curr Opin Gen Dev 16:1-6.

Rask K, Nilsson, A, Brannstrom, M, Carlsson, P, Hellberg, P, Janson, PO, Hedin, L, Sundfeldt, K. 2003. Wnt-signalling pathway in ovarian epithelial tumours: increased expression of beta-catenin and GSK3beta. Br J Cancer 89(7):1298-304.

Rathi A, Virmani, AK, Schorge, JO, Elias, KJ, Maruyama, R, Minna, JD, Mok, SC, Girard, L, Fishman, DA, Gazdar, AF. 2002. Methylation profiles of sporadic ovarian tumors and nonmalignant ovaries from high risk women. Clin Cancer Res 8:3324-3331.

Reiser CO, Lanz, T, Hoffman, F., Hofer, G., Rupprecht, H.D., Goppelt-Struebe, M. 1998. Lysophosphatidic acid-mediated signal-transduction pathways involved in the induction of the early-response gene prostaglandin G/H synthase-2 and Egr-1: a critical role for the mitogen-activated protein kinase p38 and for Rho proteins. Biochem J 330:1107-1114.

Reiss K, Maretzky, T, Ludwig, A, Tousseyn, T, de Strooper, B, Hartmann, D, Saftig, P. 2005. ADAM10 cleavage of N-cadherin and regulation of cell-cell adhesion and beta-catenin nuclear signalling. EMBO J 24(4):742-52.

Ren J, Xiao, Y, Singh, LS, Zhao, X, Zhao, Z, Feng, L, Rose, TM, Prestwich, GD, Xu, Y. 2006. Lysophosphatidic acid is constitutively produced by human peritoneal mesothelial cells and enhances adhesion, migration, and invasion of ovarian cancer cells. Cancer Res 66:3006-3014.

Reuning U, Magdolen, V, Wilhelm, O, Fischer, K, Lutz, V, Graeff, H, Schmitt, M. 1998. Multifunctional potential of the plasminogen activation system in tumor invasion and metastasis. Int J Oncol 13:893-906.

Rimm D, Koslov, ER, Kebriaei, P, Cianci, CD, Morrow, JS. 1995. alpha1E-catenin is an actin-binding and -bundling protein mediating the attachment of F-actin to the membrane adhesion complex. Proc Natl Acad Sci U S A 92:8813-8817.

Rios-Doria J, Day, K.C, Kuefer, R., Rashid, M.G., Chinnaiyan, A.M., Rubin, M.A., Day, M.L. 2003. The role of calpain in the proteolytic cleavage of E-cadherin in prostate and mammary epithelial cells. J Biol Chem 278:1372-1379.

Rios-Doria J, Day, ML. 2005. Truncated E-cadherin potentiates cell death in prostate epithelial cells. Prostate 63(3):259-68.

Rodriguez-Burford C, Barnes, MN, Oelschlager, DK, Myers, RB, Talley, LI, Partridge, EE, Grizzle, WE. 2002. Effects of nonsteroidal anti-inflammatory agents (NSAIDs) on ovarian carcinoma cell lines: preclinical evaluation of NSAIDs as chemopreventive agents. Clin Cancer Res 8:202-209.

Roland I, Yang, WL, Yang, DH, Daly, MB, Ozols, RF, Hamilton, TC, Lynch, HT, Godwin, AK, Xu, XX. 2003. Loss of surface and cyst epithelial basement membranes and preneoplastic morphologic changes in prophylatic oophorectomies. Cancer 98:2607-2623.

Ryniers F, Stove, C, Goethals, M, Brackenier, L, Noe, V, Bracke, M, Vandekerckhove, J, Mareel, M, Bruyneel, E. 2002. Plasmin produces an E-cadherin fragment that stimulates cancer cell invasion. Biol Chem 383(1):159-65.

Saegusa M, Okayasu, I. 2001. Frequent nuclear beta-catenin accumulation and associated mutations in endometrioid-type endometrial and ovarian carcinomas with squamous differentiation. J Pathol 194:59-67.

Sagae S, Kobayashi, K, Nishioka, Y, Sugimura, M, Ishioka, S, Nagata, M, Terasawa, K, Tokino, T, Kudo, R. 1999. Mutational analysis of beta-catenin gene in Japanese ovarian carcinomas: frequent mutations in endometrioid carcinomas. Jpn J Cancer Research 90:510-515.

Sakata K, Shigemasa, K, Uebaba, Y, Nagai, N, Ohama, K. 2002. Expression of matrix metalloproteinases-2 and -9 by cells isolated from the peritoneal fluid of women with ovarian carcinoma. Acta Cytol 46(4):697-703.

Sawada K, Morishige, K, Tahara, M, Kawagishi, R, Ikebuchi, Y, Tasaka, K, Murata, Y. 2002. Alendronate inhibits lysophosphatidic acid-induced migration of human ovarian cancer cells by attenuating the activation of Rho. Cancer Res 62:6015-6020.

Schwartz B, Hong, G, Morrison, BH, Wu, W, Baudhuin, LM, Xiao, YJ, Mok, SC, Xu, Y. 2001. Lysophospolipids increase interleukin-8 expression in ovarian cancer cells. Gynecol Oncol 81:291-300.

Schwartz D, Wu, R, Kardia, SLR, Levin, AM, Huang, C-C, Shedden, KA, Kuick, R, Misek, DE, Hanash, SM, Taylor, JMG, Reed, H, Hendrix, N, Zhai, Y, Fearon, ER, Cho, KR. 2003. Novel candidate target of beta-catenin/T-cell factor signaling identified by gene expression profiling of ovarian endometrioid adenocarcinomas. Cancer Res 63:2913-2922.

Schwartz PE. 2002. Current Diagnosis and Treatment Modalities for Ovarian Cancer. In: Stack MS, Fishman, D.A., editor. Cancer Treatment and Research: Ovarian Cancer. Boston: Kluwer Academic Publishers. p 99-118.

Scully E, Young, RH, Clement, PB. 1998. Tumors of the ovary, maldeveloped gonads, fallopian tubes and broad ligament. Atlas of Tumor Pathology. 3rd series ed: AFIP.

Seltzer JL, Lee, A.Y., Akers, K.T., Sudbeck, B., Southon, E.A., Wayner, E.A., Eisen, A.Z. 1994. Activation of 72kDa type IV collagenase/gelatinase by normal fibroblasts in collagen lattices is mediated by integrin receptors but is not related to lattice contraction. Exp Cell Res 213:365-374.

Shariat SF, Matsumoto, K., Casella, R., Jian, W., Lerner, S.P. 2005. Urinary levels of soluble E-cadherin in the detection of transitional cell carcinoma of the urinary bladder. Eur Urol 48(1):69-76.

Sheng H, Shao, J, DuBois, RN. 2001. K-Ras-mediated increase in cyclooxygenase2 mRNA stability involves activation of the protein kinase B. Cancer Res 2670-2675.

Shih I, Kurman, RJ. 2004. Ovarian tumorigenesis: a proposed model based on morphological and moecular genetic analysis. Am J Pathol 164:1511-1518.

Shishodia S, Aggarwal, B.B. 2004. Cyclooxygenase (COX)-2 inhibitor celecoxib abrogates activation of cigarette smoke-induced nuclear factor (NF)-kappaB by suppressing activation of IkappaBalpha kinase in human non-small cell lung carcinoma: correlation with suppression of cyclin D1, COX-2, and matrix metalloproteinase-9. Cancer Res 64(14):5004-12.

Sillanpaa S, Anttila, MA, Voutilainen, KA, Ropponen, KM, Sironen, RK, Saarikoski, SV, Kosma, VM. 2006. Prognostic significance of matrix metalloproteinase-7 in epithelial ovarian cancer and its relation to beta-catenin expression. Int J Cancer 119:1792-1799.

Skubitz APN. 2002. Adhesion Molecules. In: Stack MS, Fishman, D.A., editor. Cancer Treatment and Research: Ovarian Cancer. Boston: Kluwer Academic Publishers. p 305-330.

Smith E, Daly, MB, Xu, XX. 2004. A mechanism for COX-2 inhibitor anti-inflammatory activity in chemoprevention of epithelial cancers. Cancer Epidemiol Biomark Prev 13:144-145.

So J, Navari, J, Wang, FQ, Fishman, DA. 2004. Lysophosphatidic acid enhances epithelial ovarian carcinoma invasion throuigh the increased expression of interleukin-8. Gynecol Oncol 95:314-322.

Srivastava A, Pandey, SK. 1998. Potential mechanism(s) involved in the regulation of glycogen synthesis. Mol Cell Biochem 182:135-141.

Stack MS, Ellerbroek, SM, Fishman, DA. 1998. The role of proteolytic enzymes in the pathology of ovarian carcinoma. Int J Oncology 12:569-576.

Stack S, Gonzalez-Gronow, M, Pizzo, SV. 1990. Regulation of plasminogen activation by components of the extracellular matrix. Biochemistry 22:4966-4970.

Steinhusen U, Weiske, J, Badock, V, Tauber, R, Bommert, K, Huber, O. 2001. Cleavage and shedding of E-cadherin after induction of apoptosis. J Biol Chem 276(7):4972-80.

Sternlicht M, Werb, Z. 2001. How matrix metalloproteinases regulate cell behavior. Annu Rev Cell Dev Biol 17:463-516.

Sundfeldt K, Ivarsson, K., Rask, K., Haeger, M., Hedin, L., Brannstrom, M. 2001. Higher levels of soluble E-cadherin in cyst fluid from malignant ovarian tumours than in benign cysts. Anticancer Res 21(1A):65-70.

Sundfeldt K, Piontkewitz, Y., Ivarsson, K., Nilsson, O., Hellberg, P., Brannstrom, M., Janson, P-O, Enerback, S., Hedin, L. 1997. E-cadherin expression in human epithelial ovarian cancer and normal ovary. Int J Cancer 74:275-280.

Sutphen R, Xu, Y, Wilbanks, GD, Fiorica, J, Grendys, EC Jr, LaPolla, JP, Arango, H, Hoffman, MS, Martino, M, Wakeley, K, Griffin, D, Blanco, RW, Cantor, AB, Xiao, YJ, Krischer, JP. 2004. Lysophospholipids are potential biomarkers of ovarian cancer. Cancer Epidemiol Biomark Prev 13:1185-1191.

Symowicz J, Adley, B.P., Woo, M.M.M., Auersperg, N., Hudson, L.G., Stack, M.S. 2005. Cyclooxygenase-2 functions as a mediator of lysophosphatidic acid to promote aggressive behavior in ovarian carcinoma cells. Cancer Res 65:2234-2242.

Symowicz J, Adley, BP, Gleason, KJ, Johnson, JJ, Ghosh, S, Fishman, DA, Hudson, LG, Stack, MS. 2007. Engagement of collagen-binding integrins promotes matrix metalloproteinase-9-dependent E-cadherin ectodomain shedding in ovarian cancer. Cancer Res 67:2030-2039.

Syrigos KN, Harrington, K.J., Karayiannakis, A.J., Baibas, N., Katirtzoglou, N., Roussou, P. 2004. Circulating soluble E-cadherin levels are of prognostic significance in patients with multiple myeloma. Anticancer Res 24(3b):2027-31.

Tago K, Nakamura, T, Nishita, M, Hyodo, J, Nagai, S, Murata, Y, Adachi, S, Ohwada, S, Morishita, Y, Shibuya, H, Akiyama, T. 2000. Inhibition of Wnt signaling by ICAT, a novel beta-catenin-interacting protein. Genes Dev 14:1741-1749.

Takahashi M, Tsunoda, T, Seiki, M, Nakamura, Y, Furukawa, Y. 2002. Identification of membrane-type matrix metalloproteinase-1 as a target of the beta-catenin/Tcf4 complex in human colorectal cancers. Oncogene 21:5861-5867.

Tavani A, Gallus, S, La Vecchia, C, Conti, E, Montella, M, Franceschi, S. 2001. Aspirin and ovarian cancer: an Italian case-control study. Ann Oncol 11:1171-1173.

Timoshenko A, Xu, G, Chakrabarti, S, Lala, PK, Charraborty, C. 2003. Role of prostaglandin E2 receptors in migration of murine and human breast cancer cells. Exp Cell Res 289:265-274.

Tomesek JJ, Halliday, N.L., Updike, D.L., Ahern-Moore, J.S., Vu, T.K., Liu, R.W., Howard, E.W. 1997. Gelatinase A activation is regulated by the organization of the polymerized actin cytoskeleton. J Biol Chem 272:7482-7787.

Torng P, Mao, TL, Chan, WY, Huang, SC, Lin, CT. 2004. Prognostic significance of stromal metalloproteinase-2 in ovarian adenocarcinoma and its relation to carcinoma progression. Gynecol Oncol 92:559-567.

Tsafriri A. 1995. Ovulation as a tissue remodeling process. Proteolysis and cumulus expansion. Adv Exp Med Biol 377:121-140.

Tsujii M, Kawano, S, DuBois, RN. 1997. Cyclooxygenase-2 expression in human colon cancer cells increases metastatic potential. Proc Natl Acad Sci U S A 94:3336-3340.

Vadlamudi R, Mandal, M, Adam, L, Steinbach, G, Mendelsohn, J, Kumar, R. 1999. Regulation of cyclooxygenase-2 pathway by HER2 receptor. Oncogene 18:305-314.

Valenick L, Schwarzbauer, JE. 2006. Ligand density and integrin repertoire regulate cellular response to LPA. Matrix Biology 25:223-231.

Van den Steen P, Dubois, B, Nelissen, I, Rudd, PM, Dwek, RA, Opdenakker, G. 2002. Biochemistry and Molecular Biology of Gelatinase B or matrix metalloproteinase-9 (MMP-9). Crit Rev Biochem Mol Biol 37:375-536.

van Noort M, van de Wetering, M, Clevers, H. 2002. Identification of two novel regulated serines in the N terminus of beta-catenin. Exp Cell Res 276:264-272.

Wagenaar-Miller R, Hanley, G, Shattuck-Brandt, R, DuBois, RN, Bell, RL, Matrisian, LM, Morgan, DW. 2003. Cooperative effects of matrix metalloproteinase and cyclooxygenase-2 inhibition on intestinal adenoma reduction. Br J Cancer 88:144-152.

Wang F, Smicun, Y, Calluzzo, N, Fishman, DA. 2006a. Inhibition of matrilysin expression by antisense or RNA interference decreases lysophosphatidic acid-induced epithelial ovarian cancer invasion. Mol Cancer Res 4:831-841.

Wang F, So, J, Reierstad, S, Fishman, DA. 2005. Matrilysin (MMP-7) promotes invasion of ovarian cancer cells by activation of progelatinase. Int J Cancer 114:19-31.

Wang S, Lien, HC, Xia, W, Chen, IF, Lo, HW, Wang, Z, Ali-Seyed, M, Lee, DF, Bartholomeusz, G, Ou-Yang, F, Giri, DK, Hung, MC. 2004. Binding at and transactivation of the COX-2 promoter by nuclear tyrosine kinase receptor ErbB-2. Cancer Cell 6:251-261.

Wang Y, Jin, G., Miao, H., Li, J., Y-S, Usami, S., Chien, S. 2006b. Integrins regulate VE-cadherin and catenins: Dependence of this regulation on Src, but not on Ras. Proc Natl Acad Sci USA 103(6):1774-1779.

Waters C, Saatian, B, Moughal, Zhao, Y, Tigyi, G, Natarajan, V, Pyne, S, Pyne, NJ. 2006. Integrin signaling regulates the nuclear localization and function of the lysophosphatidic acid receptor-1 (LPA_1) in mammalian cells. Biochem J 398:55-62.

Westermann AM, Havik, E., Postma, F.R., Beijnen, J.H., Dalesio, O., Moolenar, W.H., Rodenhuis, S. 1998. Malignant effusions contain lysophosphatidic acid (LPA)-like activity. Ann Oncol 9:437-442.

Wheelock M, Buck, CA, Bechtol, KB, Damsky, CH. 1987. Soluble 80-kd fragment of cell-CAM 120/80 disrupts cell-cell adhesion. J Cell Biochem 34(3):187-202.

Wilhelm O, Schmitt, M, Hohl, S, Senekowitsch, R, Graeff, H. 1995. Antisense inhibition of urokinase reduces spread of human ovarian cancer in mice. Clin Exp Metastasis 13:296-302.

Wolf K, Mazo, I, Leung, H, Engelke, K, von Andrian, UH, Friedl, P. 2003. Compensation mechanism in tumor cell migration: mesenchymal-amoeboid transition after blocking of pericellular proteolysis. J Cell Biol 160:267-277.

Wong AST, Auersperg, N. 2002. Normal Ovarian Surface Epithelium. In: Stack MS, Fishman, D.A., editor. Cancer Treatment and Research: Ovarian Cancer. Boston: Kluwer Academic Publishers. p 161-184.

Wong AST, Gumbiner, B.M. 2003. Adhesion-independent mechanism for suppression of tumor cell invasion by E-cadherin. J Cell Biol 161(6):1191-1203.

Wong AST, Maines-Bandiera, S.L., Rosen, B., Wheelock, M.J., Johnson, K.R., Leung, P.C.K., Roskelley, C.D., Auersperg, N. 1999. Constitutive and conditional cadherin expression in cultured human ovarian surface epithelium: influence of family history of ovarian cancer. Int J Cancer 81:180-188.

Wright K, Wilson, P, Morland, S, Campell, I, Walsh, M, Hurst, T, Ward, B, Cummings, M, Chenevix-Trench, M. 1999. Beta-catenin mutation and expression analysis in ovarian cancer: exon 3 mutations and nuclear translocation in 16% of endometrioid tumours. Int J Cancer 82:625-629.

Wu CY, Wang, C.J., Tseng, C.C., Chen, H.P., Wu, M.S., Lin, J.T., Inoue, H., Chen, G.H. 2005. Helicobacter pylori promote gastric cancer cells invasion through a NF-kappaB and COX-2-mediated pathway. World J Gastroenterol 11(21):3197-203.

Wu R, Zhai, Y, Fearon, ER, Cho, KR. 2001. Diverse mechanisms of beta-catenin deregulation in ovarian endometrioid adenocarcinomas. Cancer Res 61:8247-8255.

Xiao YJ, Schwartz, B., Washington, M., Kennedy, A., Webster, K., Belinson, J., Xu, Y. 2001. Electrospray ionization mass spectrometry analysis of lysophospholipids in human ascitic fluids: comparison of the lysophospholipid contents in malignant vs. nonmalignant ascitic fluids. Anals Biochem 290:302-313.

Xu Y, Fang, XF, Casey, G, Mills, GB. 1995a. Lysophospholipids activate ovarian and breast cancer cells. Biochem J 309:933-940.

Xu Y, Gaudette, D.C., Boynton, J.D., Frankel, A., Fang, X.J., Sharma, A., Hurteau, J., Casey, G., Goodbody, A., Mellors, A. 1995b. Characterization of an ovarian cancer activating factor in ascites from ovarian cancer patients. Clin Cancer Res 1:1223-1232.

Xu Y, Shen, Z., Wiper, D.W., Wu, M., Morton, R.E., Elson, P., Kennedy, A.W., Belinson, J., Markham, M., Casey, G. 1998. Lysophosphatidic acid as a potential biomarker for ovarian and other gynecologic cancers. JAMA 280:719-772.

Yamada KM, Miyamoto, S. 1995. Integrin transmembrane signaling and cytoskeletal control. Curr Opin Cell Biol 7:681-689.

Yamada S, Pokutta, S, Drees, F, Weis, WI, Nelson, WJ. 2005. Deconstructing the cadherin-catenin-actin complex. Cell 123:889-901.

Yano H, Mazaki, Y, Kurokawa, K, Hanks, SK, Matsuda, M, Sabe, H. 2004. Roles played by a subset of integrin signaling molecules in cadherin-based cell-cell adhesion. J Cell Biol 166:283-295.

Yoshida H, Cheng, W, Hung, J, Montell, D, Geisbrecht, E, Rosen, D, Liu, J, Naora, H. 2004. Lessons from border cell migration in the Drosophila ovary: A role for myosin IV in dissemination of human ovarian cancer. Proc Natl Acad Sci U S A 101:8144-8149.

Young TN, Rodriguez, G.C., Moser, T.L., Bast, R.C., Jr., PIzzo, S.V., Stack, M.S. 1994. Coordinate expression of urinary-type plasminogen activator and its receptor accompanies malignant transformation of the ovarian surface epithelium. Am J Obstet Gynecol 170:1285-1296.

Yu X, Miyamoto, S, Mekada, E. 2000. Integrin alpha-2 beta-1-dependent EGF receptor activation at cell-cell contacts. J Cell Sci 113:2139-2147.

Zhang W, Alt-Holland, A, Margulis, A, Shamis, Y, Fusenig, NE, Rodeck, U, Garlick, JA. 2006. E-cadherin loss promotes the initiation of squamous cell carcinoma invasion through modulation of integrin-mediated adhesion. J Cell Sci 119:283-291.

Zhou B, Deng, J, Xia, W, Xu, J, Li, YM, Gunduz, M, Hung, MC. 2004. Dual regulation of Snail by GSK-3beta-mediated phosphorylation in control of epithelial-mesencymal transition. Nat Cell Biol 6:931-940.

Zhu GG, Risteli, J., Puistola, U., Kauppila, A., Risteli, L. 1993. Progressive ovarian carcinoma induces synthesis of type I and type III procollagens in the tumor tissue and peritoneal cavity. Cancer Res 53:5028-5032.

Vita

Jaime Elizabeth Symowicz

Education

PhD in Cancer Biology, Integrated Graduate Program (IGP) in the Life Sciences, Northwestern University Feinberg School of Medicine, Chicago, IL, September 2001-January 2007. Degree conferred June 2007.

BS in Genetics, with honors, University of Wisconsin-Madison, September 1995-May 1999.

Experience

PhD Student
Lab of Dr. M. Sharon Stack, Department of Cell and Molecular Biology, Northwestern University, Chicago, IL, April 2002 to March 2007.
Thesis Project: Microenvironment regulation of proteinase expression and E-cadherin ectodomain generation in ovarian cancer

Research Technician
Lab of Dr. Benette Phillips, Department of OB/GYN, Northwestern University, Chicago, IL, August 1999-June 2001.
Project: Characterization of a novel regulatory site in the human papilloma virus (HPV18) upper regulatory region (URR) enhancer

Undergraduate Senior Honors Thesis
Lab of Dr. Linda A. Schuler, Department of Comparative Biosciences, University of Wisconsin-Madison, January 1998-August 1999.
Senior Thesis Project: Investigating the role of prolactin in human breast cancer using a prolactin knockout cell line

Student Help
Lab of Dr. William Engels, Department of Genetics, University of Wisconsin-Madison, May 1997-January 1998.
Research Area: Transposons and DNA Repair in Drosophila

Publications

Symowicz, J, Adley, BP, Gleason, KJ, Johnson, JJ, Ghosh, S, Fishman, DA, Hudson, LG, Stack, MS (2007) Engagement of collagen-binding integrins promotes matrix metalloproteinase-9-dependent E-cadherin ectodomain shedding in ovarian cancer. Cancer Research 67:2030-2039.

Symowicz, J, Adley, BP, Woo, MMM, Auersperg, N, Hudson, LG, Stack, MS (2005) Cyclooxygenase-2 functions as a mediator of lysophosphatidic acid to promote aggressive behavior in ovarian carcinoma cells. Cancer Research 65:2234-2242.

Schroeder, MD, **Symowicz, J**, Schuler, LA (2002) Prolactin modulates cell cycle regulators in mammary tumor epithelial cells. Molecular Endocrinology 16:45-57.

Woo, MM, Salamanca, CM, **Symowicz, J**, Oliveira, C, Ehlen, TG, Gilks, CB, Huntsman, D, Auersperg, N. Phenotypic and genotypic characterization of cultured serous borderline ovarian tumor cells reveals factors limiting invasiveness. *Manuscript submitted to Gynecologic Oncology 2007.*

Symowicz, J, Hudson, LG, Gottardi, CJ, Stack, MS. Engagement of collagen-binding integrins increases E-cadherin internalization and β-catenin-mediated transcription in ovarian cancer cells. *Manuscript in Preparation.*

Cowden Dahl, KD, **Symowicz, J**, Stack, MS, Hudson, LG. Matrix metalloproteinase-9 mediates epidermal growth factor disruption of E-cadherin in ovarian cancer cells. *Manuscript in Preparation.*

Posters

Symowicz, J and Stack, MS. Integrin-Cadherin Crosstalk and Proteinase Regulation in Ovarian Carcinoma.
Presented at:

AACR Workshop in Cancer Research: Pathobiology of Cancer, Snowmass, CO, July 17-24, 2005.
Gordon Research Conference: Cell Contact and Adhesion, Andover, NH, June 26-July 1, 2005.

Symowicz, J and Stack, MS. Clustering of collagen-binding integrins regulates surface E-cadherin expression and proteinase activity in ovarian carcinoma cells. Second National Meeting of the American Society for Matrix Biology, San Diego, CA, November 10-13, 2004.

Symowicz, J, Adley, BP, Woo, MMM, Auersperg, N, Hudson, LG, Stack, MS. Cyclooxygenase-2 functions as a downstream mediator of lysophosphatidic acid to promote pro-matrix metalloproteinase-2 activation and aggressive behavior in ovarian carcinoma cells.
Gordon Research Conference: Plasminogen Activation and Extracellular Proteolysis, Ventura, CA, February 8-13, 2004.

Symowicz, J., Miller, R.T., Phillips, B. Characterization of a novel regulatory site in the HPV18 URR enhancer.
Molecular Biology of Tumor Viruses Conference, Madison, WI, July 8-13, 2000.

Awards

NIH/NCI Carcinogenesis Training Grant, Northwestern University, 2004-2005 and 2003-2004.

Gramm Travel Fellowship Award from the Robert H. Lurie Comprehensive Cancer Center at Northwestern University, Spring 2005.

College of Agricultural and Life Sciences (CALS) Senior Honors Thesis Research Stipend, University of Wisconsin-Madison, 1998-1999.

Leadership

Graduate School Teaching Assistant
Cell Biology 405 (IGP), Northwestern University, Winter Quarter 2003.

Co-organizer of Tumor Cell Biology (TCB) Cancer Student Journal Club
Northwestern University, 2003-2004.